INVESTIGATION OF COLUMN CAPACITY OF SOFT STOREY BUILDING BY PUSHOVER ANALYSIS

MOHAMMAD NUR HOSSAIN

MASTER OF SCIENCE IN CIVIL ENGINEERING (STRUCTURAL)

Submitted to the

DEPARTMENT OF CIVIL ENGINEERING

BANGLADESH UNIVERSITY OF ENGINEERING AND TECHNOLOGY

DHAKA

INVESTIGATION OF COLUMN CAPACITY OF SOFT STOREY BUILDING BY PUSHOVER ANALYSIS

Submitted by

MOHAMMAD NUR HOSSAIN
Roll No. 1015042338

Submitted to the

DEPARTMENT OF CIVIL ENGINEERING
BANGLADESH UNIVERSITY OF ENGINEERING AND TECHNOLOGY

In partial fulfillment of requirements for the degree of

MASTER OF SCIENCE IN CIVIL ENGINEERING (STRUCTURAL)

DHAKA

JANUARY, 2018

THE THESIS TITLED "Investigation of column capacity of soft storey building by pushover analysis" submitted by Mohammad Nur Hossain, roll no: 1015042338, session: October/2015; has been accepted as satisfactory in partial fulfillment of the requirement for the degree of Master of Science in Civil Engineering (Structural) on 24 January 2018.

BOARD OF EXAMINERS

Dr. Khan Mahmud Amanat Professor Department of Civil Engineering BUET, Dhaka-1000	Chairman (Supervisor)
Dr. Ahsanul Kabir Professor and Head Department of Civil Engineering BUET, Dhaka-1000	Member (Ex-Officio)
Dr. Tahsin Reza Hossain Professor Department of Civil Engineering BUET, Dhaka-1000	Member
Dr. Mohammad Al Amin Siddique Asoc. Professor Department of Civil Engineering BUET, Dhaka-1000	Member
Dr. Sharmin Reza Chowdhury Professor Department of Civil Engineering AUST, Dhaka 1208	Member (External)

DECLARATION

It is hereby declared that except for the contents where specific references have been made to the work of others, the study contained in this thesis is the result of investigation carried out by the author under the guidance of thesis supervisor. No part of this thesis has been submitted to any other University or other educational establishment for a Degree, Diploma or other qualification (except for technical publication).

Signature of the Candidate

(Mohammad Nur Hossain)

CONTENTS

Abbreviation	Explanation
MI	Masonry Infill
ESFM	Equivalent Static Force Method
BFL	Bare Frame Linear
BFP	Bare Frame Push
SSFL	Soft Storey Frame Linear
SSFP	Soft Storey Frame Push
MF	Magnification Factor
DC	Demand Curve
CC	Capacity Curve

ACKNOWLEDGEMENT

The author wishes to convey his profound gratitude to Almighty Allah for His graciousness, unlimited kindness and blessings, and for allowing him to complete the thesis.

The author wishes to express his sincere appreciation and gratitude to his supervisor, Dr. Khan Mahmud Amanat, Professor, Department of Civil Engineering, BUET, Dhaka, for his continuous guidance, invaluable suggestions and continued encouragement throughout the progress of the research work.

A special debt of deep gratitude is offered to his parents and colleagues for their continuous encouragement and cooperation during this study. Last but not the least; the author is deeply indebted to his beloved wife for supporting him all the time with love and inspiration.

ABSTRACT

In Bangladesh, many high-rise buildings have open ground storey with masonry infill in the upper storeys. They are mainly constructed to accommodate parking, reception lobbies and other commercial spaces. Conventional practice is to design these buildings as moment resisting frame building considering masonry infill as non-structural element. Thus contribution of infill in the total structural response is neglected. In reality, masonry infill interacts with frame members and makes the structure stiffer than the bare frame except ground storey. The open ground storey building has stiffness irregularity as visualized during an earthquake. In this thesis, an extensive computational study has been conducted to monitor the response of the open ground storey column subjected to ground acceleration.

Numerical investigation of present study is meant to evaluate the soft storey effect on the ground storey column of a soft storey building subjected to earthquake loading. Dhaka city is selected as the investigation site of this study. The variable parameters in the investigation are number of bays, number of spans, and percentage of infill. Two 3D models are generated namely as bare frame model and soft storey frame model. The masonry infill is converted to equivalent diagonal strut within the panel. Conventional static linear analysis is carried out for basic loading (i.e., Dead load, Live load and Earthquake load) and load combination is done as per BNBC (Draft), 2015. Pushover analysis is performed to get nonlinear static response of the models. The effects of said parameters on the models are monitored in detail and evaluated in terms of top deflection, shear force and bending moment of ground storey column. Finally, nonlinear responses of soft storey building model are compared with nonlinear responses of bare frame model.

It has been found that the base shear, shear force and bending moment of soft ground storey column of soft storey model, as obtained by pushover analysis method, are considerably higher than the corresponding nonlinear values of bare frame model. This indicates that the ground storey columns of soft storey buildings are overstressed under earthquake loading; as such unexpected soft storey failure of such building occurs before reaching to its ultimate performance point of maximum earthquake.

Based on findings of the study, few suggestions are made to safeguard buildings with open ground storey from soft storey collapse. At design stage, magnification of design shear force and bending moment of ground storey column of soft storey building is to be done before designing the columns. This shall compensate the absence of infill wall and minimize the stiffness irregularity in vertical direction. It is expected that justified application of the suggestions would be useful for safeguarding buildings with open ground floor.

CHAPTER 1

INTRODUCTION

1.1 GENERAL

Earthquake engineering is a special domain of civil engineering. Structural engineers carried out extensive researches on building design to evaluate its capability to withstand earthquake. This has led to a good understanding of earthquake and the forces they exert on building. There are well established concepts concerning the earthquake resistance of building as determined by their ability to absorb energy input due to earth vibration. Performance based design is one of those concepts where building performance is assessed beyond its elastic limit. Besides, nonlinear behavior of building and structural element capability during earthquake is also studied in different range by the structural engineers.

Selection of appropriate configuration of the structural system, on which seismic performance of the building mainly depends, is one of the most important subjects in seismic design. Structural engineers developed appropriate configurations of structure in seismic design and many countries incorporated these in their design codes (IS-1893; NBC-105, 1995; NZS-3101, 1995; SNIP-II-7-81, 1996; NSR-98, 1998). This implies that the structural system is now designed as an effective earthquake resistant system integrating the behavior of whole building. Yet, soft storey phenomenon is identified as a weakness in building design which might bring considerable disaster to the urban community during a major earthquake. It is desirable that the seismically designed building system should be able to sustain an earthquake at any circumstances.

Buildings are classified as "soft storey" if that level is less than 70% as stiff as the storey immediately above it, or less than 80% as stiff as the average stiffness of the three storeys above it (ASCE 7-05, 2007 and BNBC, 2015 (Draft)). Here, stiffness refers to the buildings‘ ability or resistance to undergo lateral sway when subjected to seismic load. This type of buildings has masonry infill in the upper storeys whereas ground storey is kept open for services like car parking, lobby, reception corner, etc. Providing such facilities is essential from functional point of view. In soft storey building interaction of masonry infill on the upper storeys makes those storeys much stiffer than the open ground storey. It is well recognized (Smith and Coul, 1991; Smith, 1962) that infill wall contributes to the lateral load

resistance mechanism of the building that is seldom considered in the design practice. The infill wall braces the frame partly by its in-plane shear resistance and partly by its behavior as a diagonal bracing strut in the frame. Their presence in the structure reduces the sway against lateral load. Infill influence the natural period in two ways; (a) their mass contributes to the total weight of the building which tends to increase the period and (b) their in-plane rigidity increases the stiffness of the structure causing some reduction in the period of vibration. A pictorial view open ground storey of a soft storey building is given as Figure 1.1.

Figure 1.1 Typical soft storey building with open ground storey

Infill walls are generally considered as a nonstructural element as such their effects are not reflected in the conventional structural analysis. The actual behavior of structures is different than those assumed by conventional analysis methods. This understanding was further supplemented by the effects of Northridge and Bhuj earthquakes (Petak, 2009 and Sudhir, 2004). It is observed that some buildings of these areas became much stiffer than expected due to soft storey phenomena thus collapsed. Besides, upper storeys with infill walls of soft storey building move almost together as a single rigid block thus soft storey columns face maximum moment, shear and deflection. As such, a thorough investigation of column capacity of open soft storey (Figure 1.2) under seismic loading is necessary to outline the nonlinear design procedure of column.

Figure 1.2 Typical ground storey columns of a soft storey building

1.2 BACKGROUND HISTORY

Soft storey configuration is known in architectural terms as the open storey. This configuration has been encouraged in building design all around the world since the first half of the 20th Century. The origin of this architectural configuration is mainly derived from the first three points of the ―Five points for a new architecture" published by Swiss-French architect Le Corbusier (LC) in 1926. This hypothesizes were possible due to the development of new construction techniques such as the innovative "Reinforced Concrete Frame Structure"(RCFS) and building materials since 19th Century. On the other hand, most Ultimate Zone Rating (UZR), consciously or unconsciously, encourages the use of the soft storey configuration. But in seismic zones, from the beginning of the 20th Century this building configuration has been attributed to the generation of seismic vulnerability in modern buildings.

Concept of soft storey in the building design is first considered by Fintel and Khan (1969). This concept is an attempt to reduce acceleration in a building by allowing first-storey column to yield during an earthquake to avoid building collapse due to excessive drifts. Whereas, Arlekar et. al., (1997) highlighted the importance of explicitly recognizing the presence of the open first storey in the seismic analysis of buildings. The error involved in modeling such buildings as complete bare frames, neglecting the presence of infills in the

upper storeys, was bought out for consideration. Mezzi (2004) illustrated that soft storey is very dangerous from seismic point of view because the lateral response of these building is concentrated mostly at soft storey columns. A solution was proposed for the preservation of a particular architectonic double soft storey configuration. Haque and Amanat (2009) studied the strength and drift demand of columns of RC framed buildings with soft ground storey. According to their study, base shear of soft storey building becomes twice than the base shear of bare frame building. Mastrandrea and Piluso (2009) proposed a design methodology for development of collapse mechanism of soft storey buildings. Tesfamariam and Liu (2010) used special index for soft storey for seismic risk assessment of RC buildings. It can be concluded by saying that the researchers identified some weaknesses in the soft storey configuration. Besides, effects of soft storey building can be visualized from Figure 1.3.

Figure 1.3 Collapse of soft storey building due to column failure, Turkey earthquake, 1999

Nonlinear analysis of soft storey got momentum since 1998. Rodsin (1998) evaluated the potential seismic performance of building with soft storey in an area of low to moderate seismicity region by a displacement-based method involving a pushover analysis. Shaiful and

Amanat (2007) carried out nonlinear time history analysis of RC frames with brick masonry infill. A solution was proposed by them to magnify the bending moment and shear force of ground storey column by a defined factor. Different national building codes like Costa Rican seismic code (1986), Algerian seismic code (1988), Egyptian seismic code (1988), IS-(1893:2002), NZSS-3101 (1995), SNIP –II-7-81 (1996), Japanese seismic code (1998), Euro code (2003), etc. have included soft storey phenomenon in their codes and proposed specific guidelines for building design more particularly soft storey beams and columns.

Analysis of soft storey building is multi-dimensional where most of the researches have conducted building analysis considering elastic performance of the structure. Some researchers also investigated nonlinear performance of soft storey building to visualize its performance till collapse but these are not exhaustive. There is no deliberate guideline for nonlinear performance of soft storey building during earthquake. Most of the building codes follow some empirical factor or formula which is at some stage felt exaggerative. At the back drop, it is necessary to investigate the soft storey building particularly soft storey column by a nonlinear analysis method to outline the nonlinear behavior of building and propose expectable measures in different circumstances.

1.3 OBJECTIVES OF THE PRESENT STUDY

The objective of present investigation is to study the seismic vulnerability of open ground storey columns. This thesis has highlighted the importance of explicitly recognizing the presence of the open ground storey in the analysis of building. The error involved in modeling such building, as complete bare frame neglecting the presence of infills in the upper storey, is the main focus of the study. This study has made an endeavor to find out the challenges of present conventional building analysis and its impact on the soft ground storey building. However, specific objectives of this study are listed below:

- To study the behavior of ground storey column of soft storey building based on advance nonlinear analysis method.
- To identify the major challenges of present conventional building analysis system in designing the multi-storeyed building with soft ground storey.
- To suggest remedial measures in regards to the design of open ground storey column under seismic loading.

1.4 METHODOLOGY AND SCOPE OF THE STUDY

The present research topic is undertaken to study the behavior of ground storey columns of multi-storeyed RC building with open ground storey. The methodology and scope of the study are as follows:

- The study is done following BNBC, 2015 (Draft).
- 3D models of multi-storeyed building are developed by using 3D finite element method with beams and columns as frame elements, slabs as shell element and infill as uniaxial brace element to carry out a systematic numerical investigation.
- Ground floor of RC building is kept open to depict soft storey i.e., no infill is present there.
- Models are analyzed with and without infill walls to study the appropriate behavior of the building.
- Models are subjected to all type loads, i.e. live load, dead load, floor finish, partition wall and earthquake load.
- Seismic responses of the models are analyzed by equivalent static force method and non-linear pushover analysis method.
- Dhaka earthquake response spectrum is used for linear dynamic analysis of the models.
- Nonlinear material properties are incorporated in the frame elements during nonlinear analysis; infill is assumed as linearly elastic.
- This study has been concentrated on the behavior of ground storey columns only.

1.5 ORGANIZATION OF THE THESIS

The current chapter is Chapter 1, which introduces the reader with the thesis work. Theories related to soft storey, masonry infill, equivalent diagonal strut, loading, seismic behavior of building, etc. are described in Chapter 2. Conventional linear static analysis, nonlinear static pushover analysis, performance criteria and collapse modeling of structures are also illustrated in Chapter 2. Chapter 3 illustrates the methodology for modeling the building frame with and without infill by using engineering software. The analysis techniques are also discussed in this chapter. Chapter 4 is dedicated for parametric study of reference models.

Chapter 5 describes detail analysis and comparison of results. In chapter 6, some remedial measures are recommended that might be effective to reduce the open ground floor effect. The conclusions made from the study are presented in Chapter 7. This chapter also recommends future works or extension of this work.

2.1 INTRODUCTION

Bangladesh and its neighboring areas have experienced earthquakes greater than 7.00 magnitudes in Richter scale in the past. In the last decade, several earthquakes of 4.0 to 6.0 magnitudes in Richter scale were also recorded in south Asia including Bangladesh as shown in Figure 2.1(Ahmed, 2005). The history of this region indicates that there is a strong possibility of major earthquakes in near future.

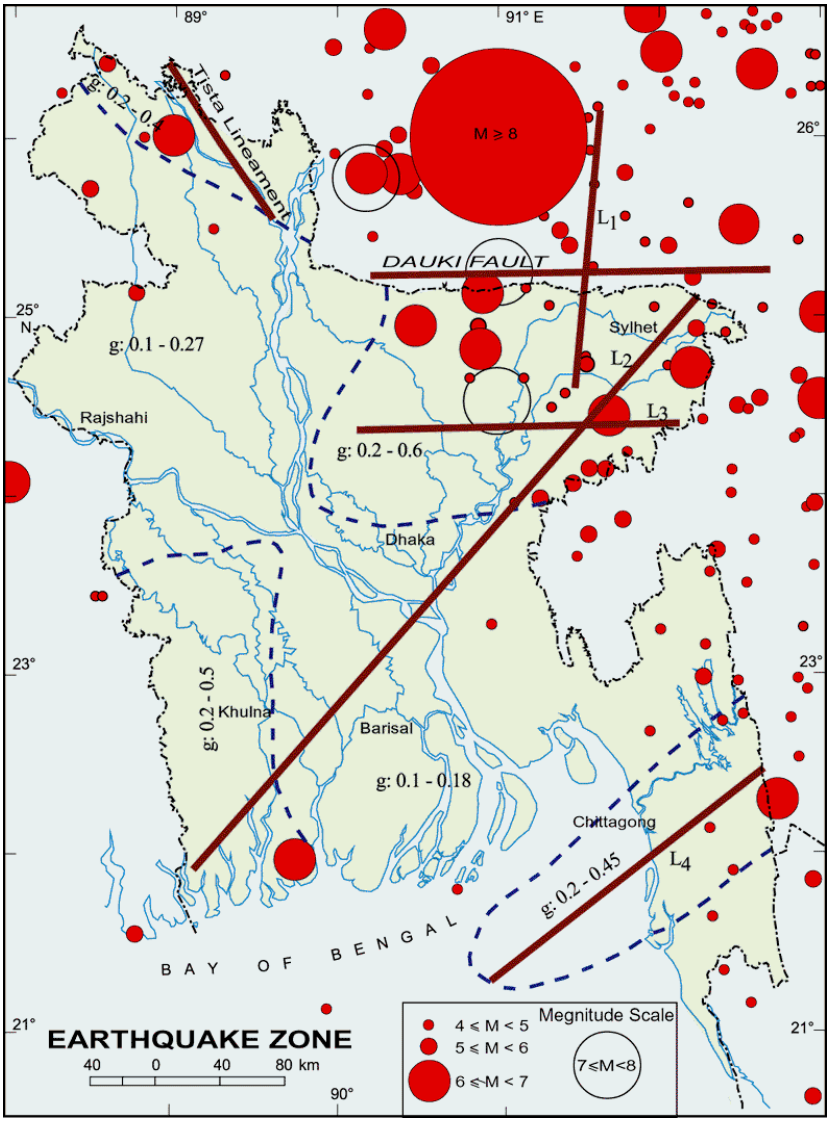

Figure 2.1 Seismic history map of Bangladesh (Source: Banglapedia)

Dhaka being a city of unplanned high rise buildings is likely to suffer most. Many of the buildings of Dhaka city generally possess open ground storey with brick infill in the upper

storeys as shown in Figure 2.2. Stiffness irregularity of these buildings leads to the formation of soft storey at ground storey level. Soft storey has long been recognized as an unfavorable feature for building structures especially during earthquakes. It causes negative effects such as stress concentration and alteration of dynamic properties of building. Most deflection occurs in the ground storey due to the stiffening effect of masonry infill in upper storeys. As a result, ground storey columns of soft storey building are over stressed resulting premature failure(ASCE 7-05,2006; FEMA P440A, 2009;BNBC, 2015 (Draft)).

Figure 2.2 A building with soft ground storey

2.2 DEFINITION OF SOFT STOREY BUILDING

When a sudden change in stiffness takes place along the building height, the storey at which this change of stiffness occurs is called a soft storey. According to BNBC2015 (draft) and ASCE 7-16, a soft storey is the one in which the lateral stiffness is less than 70% of that in the storey above or less than 80% of the average stiffness of the three storeys above. IBC 2000 defines an extreme soft storey as the one in which the lateral stiffness is less than 60 percent of that in the storey above or less than 70 percent of the three storeys above. The vertical geometric irregularity shall be considered to exist where the horizontal dimensions of the lateral-force-resisting system in any storey is more than 130 percent of that in an adjacent

storey. The most common form of vertical discontinuity arises due to unintended effect of infill components in the upper storeys. Usually in building analysis, only the bare frame effect is considered ignoring the effects of infill walls. Most building codes have no clear suggestion about the effect of infill walls on frames. In the Figure 2.3(a) it is shown that the total translational deflection of the building is equal to the summation of drift of each storey. On the other hand, the maximum deflection of soft storey building occurs in ground storey while upper floors move as a rigid body with negligible deflection as shown in figure 2.3(b).

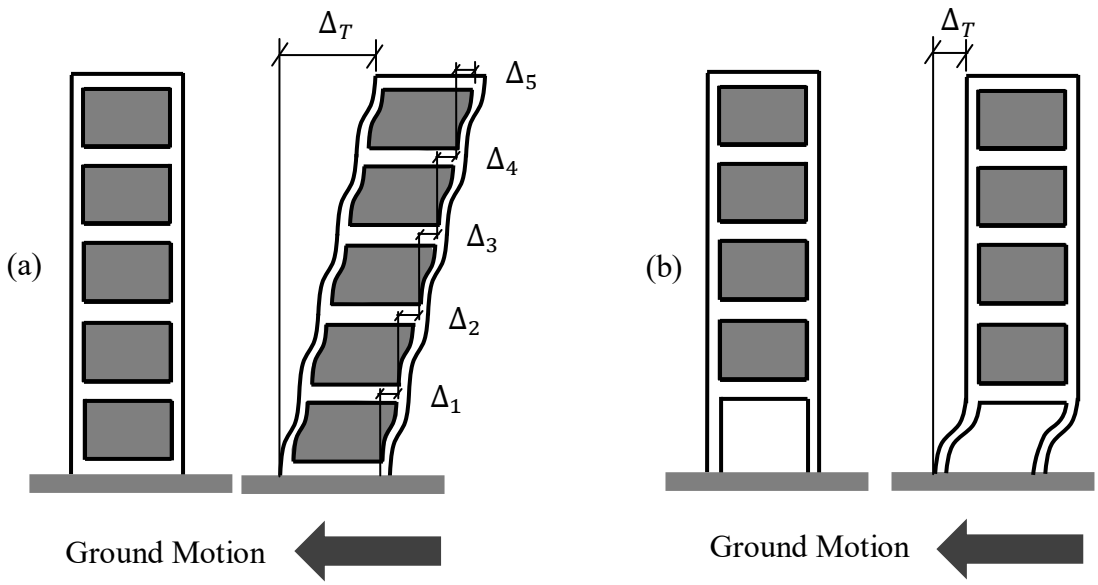

Figure 2.3 Distribution of displacement generated by an earthquake (a) a regular building; and (b) building with soft irregularity ground motion (Guevara and Perez, 2012)

2.3 RESPONSE OF COLUMNUNDER SEISMIC LOADING

A moment resisting frame building consists of vertical column and horizontal beam members (Figure 2.4). It resists vertical and lateral loads through beams and columns in the form of axial force, bending moment and shear forces. Beam and column sections are generally designed as under-reinforced sections thus they can be expected to undergo ductile behavior. Brittle shear failure of structural elements is prevented through capacity design procedures.

A reinforced concrete column is basically designed to carry the compressive load. The strength of columns is controlled by the strength of the material and the geometry of the cross section. Generally seismic design follows strong column-weak beam design philosophy and dictates the provision of ductility, adequate lateral-load resisting mechanism (e.g., special moment-resisting frames) and redundancy (alternative load paths) in the structural system. It

discourages irregularities in plan or elevation of the structures and does not allow presence of soft or weak storeys and short columns (Paulay and Priestley, 1991).

Figure 2.4 Typical RC moment resisting frame building

At element level, code requirements are mostly focused on proportioning and detailing of frame members (beam, column, and joint) to achieve certain amount of ductility in addition to the required strength. Such detailing requirements include provision of adequate and closely spaced transverse reinforcement with 135 degree end hooks, and continuity of longitudinal reinforcement in the regions that experience the most inelastic deformations and stress reversals during earthquakes (Paulay and Priestley, 1991).

The seismic details ensure that the structural members have the capacity to withstand high seismic activity. This lateral confinement substantially increases compressive strength and ductility of concrete (Mander et al., 1988). Properly confined concrete can remain intact and withstand large displacements even if it has cracked under flexural tension. During a seismic ground motion, a RC frame building undergoes transverse displacement as per the lateral force-displacement capacity of its structural elements (Figure 2.5).

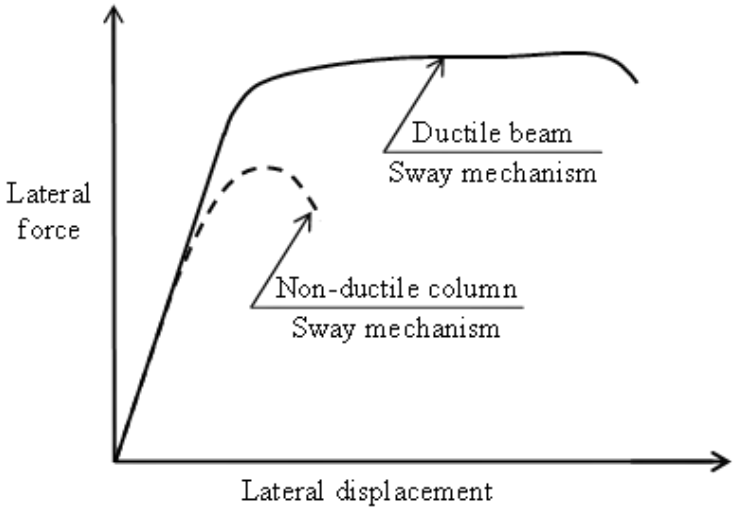

Figure 2.5 Typical lateral force and displacement capacity of structural elements

A RC frame building is design to take inelastic deformation by generating plastic hinges as per the locations shown in Figure 2.6(a). In inelastic deformation, this building deforms by forming plastic hinges initially in the beams and at the bottom of ground storey columns as shown in Figure 2.6(b).

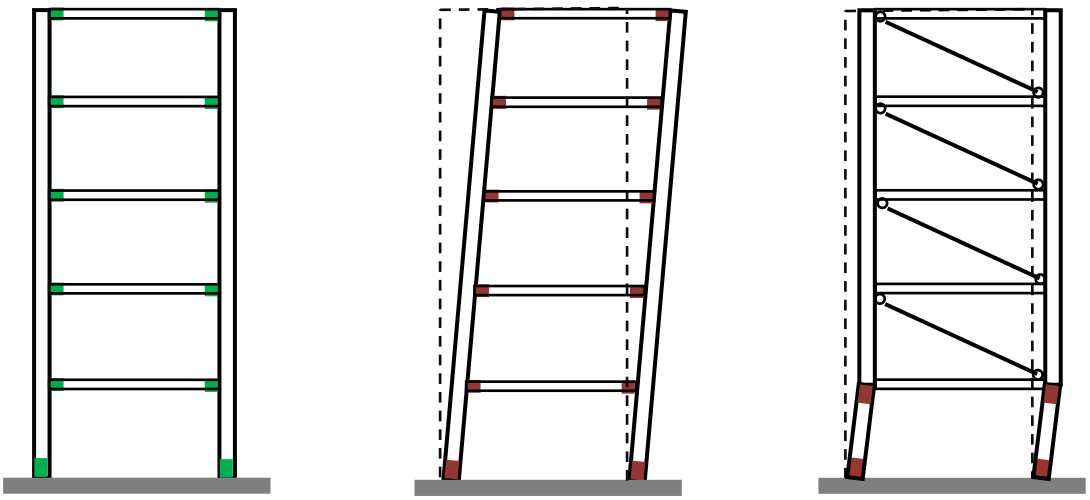

(a) Location of potential plastic hinges (b) Ductile beam sway mechanism (c) Non-ductile column sway mechanism

Figure 2.6 Typical sway mechanisms of beam and column of RC building frame

It is seen that the maximum deformation occurs in the ground storey columns of soft ground storey building thus failure occurs in those columns first. In soft storey building, after one or more columns fail, an alternate load path is needed to transfer the loads carried by failed member(s) to other structural members. If adjoining elements cannot resist and redistribute the additional loads, a series of failures will occur until entire or substantial part of the structure collapses.

Behavior of building is evaluated by determining load-deformation responses of the frame elements considering all potential failure mechanisms associated with axial, flexure and shear behavior. As columns are one of the critical vertical load carrying elements thus understanding their response to applied seismic loads is vital for overall assessment of the structural performance. Generally during earthquake, the longitudinal reinforcement in a shear-critical reinforced concrete column yields first, column continues to undergo further lateral drift (i.e. plastic deformation) until the shear demand on column exceeds its shear capacity. Thus shear failure of column occurs. In column investigation, an interaction diagram is useful to assess the interaction between a RC column axial and moment capacity prior to yielding of the longitudinal reinforcement. In nonlinear analysis, backbone curve of column elements is essential in determining capacity of columns.

2.4 MASONRY INFILL IN RC BUILDING

Masonry infill (MI) elements are used extensively as infill wall panels of RC buildings. MI fulfills architectural and other functional requirements such as forming a significant portion of building envelop, internal partition walls, temperature and sound barriers. It also provides adequate compartmentalization against fire hazard. Lack of knowledge on its performance under seismic loading has discouraged engineers from relying on the interaction of infill with the enclosing structural system. Therefore, it has become a common practice to ignore the participation of infill in resisting lateral loads. Researchers have shown that this interaction of MI and structural elements has beneficial effect on buildings during earthquake. Proper use of infill results in significant increases in the strength and stiffness of buildings subjected to seismic excitation (Klingner and Bertero 1978, Mehrabi et al. 1996, Bertero and Brokken, 1983).

MI walls confined by RC frames on all four sides play a vital role in resisting the lateral seismic loads on buildings. The behavior of masonry infilled frames has been extensively studied (Smith and Coul, 1991; Murty and Jain 2000; Moghaddam and Dowling, 1987; etc.) in attempts to develop a rational approach for design of such frames. It has been shown experimentally that MI walls have high initial lateral stiffness and low deformability (Moghaddam and Dowling, 1987). Thus introduction of MI in RC frames changes the lateral load transfer mechanism of the structure from predominant frame action Figure 2.7(a) to predominant truss action (Murty and Jain, 2000), as shown in Figure 2.7(b).

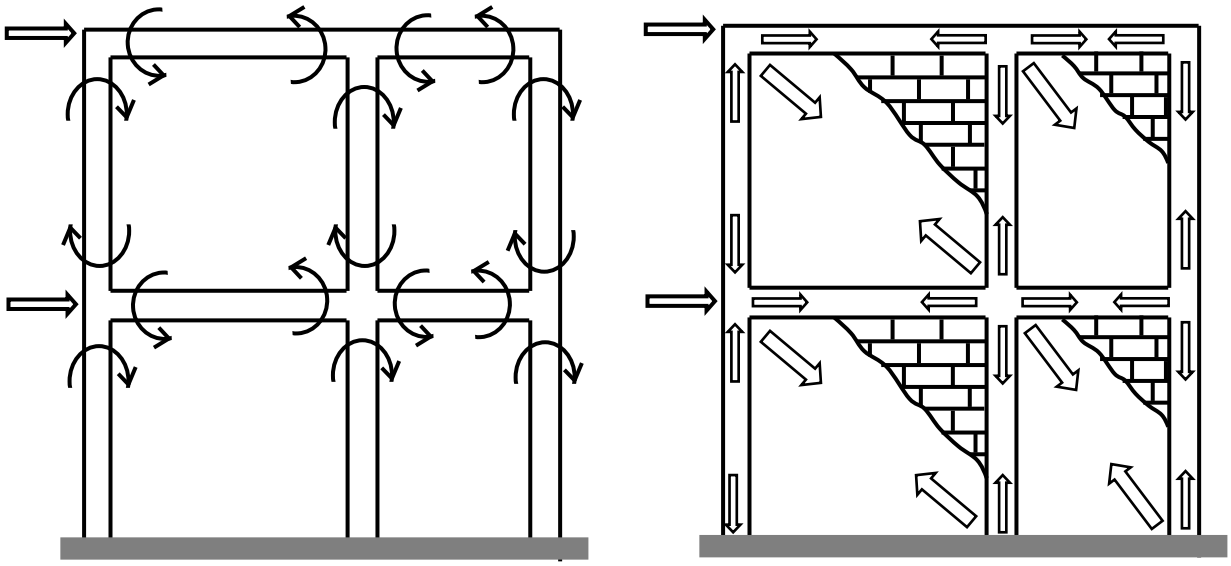

(a) Predominant frame action (b) Predominant truss action

Figure2.7 Change in lateral load transfer mechanism due to MI (Murty and Jain, 2000)

The high in-plane rigidity of the masonry wall significantly stiffens any relatively flexible frame. This results in a relatively stiff and tough bracing system. The wall braces the frame partly by its in-plane shear resistance and partly by its behavior as a diagonal bracing strut. It is experimentally shown that the relative strength of MI panel and mortar joints has a significant influence on determining the mode of failure of infill panels (Mosalam et al., 1997). Generally, the MI walls tend to widen from shearing action along crack surfaces (Figure 2.8). In case of solid infill, horizontal cracks appeared first at the center of infill, subsequently propagates diagonally towards the loaded corners.

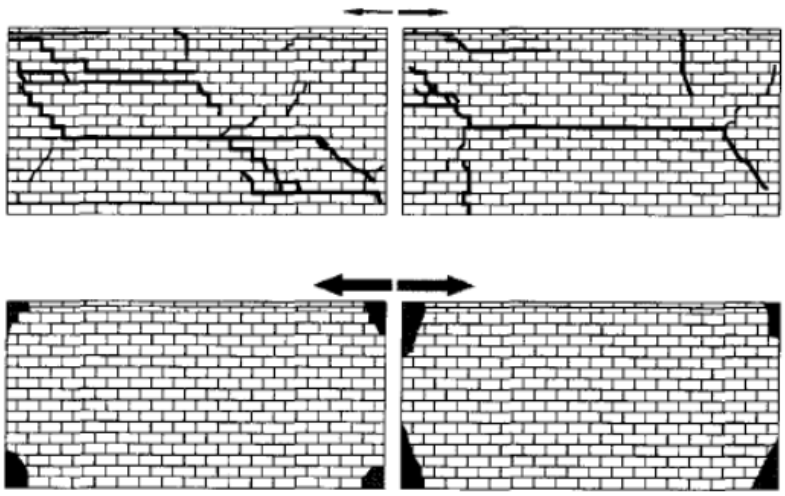

Figure 2.8 Modes of failure of infill walls (Mosalam et. Al.,1997)

According to Mosalam et. al. (1997), the solid infill causes the behavior of infilled frames to be brittle (i.e., sudden drop of load on crack initiation). The compressive stress of infill panel

predominates along diagonals (i.e., infill may be idealized using compression strut only). The stress-strain relation of infill wall along diagonals is almost linear within elastic limit indicates the validity of the equivalent strut analogy.

The nature of the forces in the RC frame can be understood by referring to the equivalent diagonal braced frame shown in Figure 2.9.The column facing the seismic load first is in tension and the other side of the building facing seismic load last is in compression. Since the infill bears on the frame not as exactly a concentrated force at the corners, but over the short lengths of the beam and column adjacent to each compression corner, the frame members are subjected also to transverse shear and a small amount of bending.

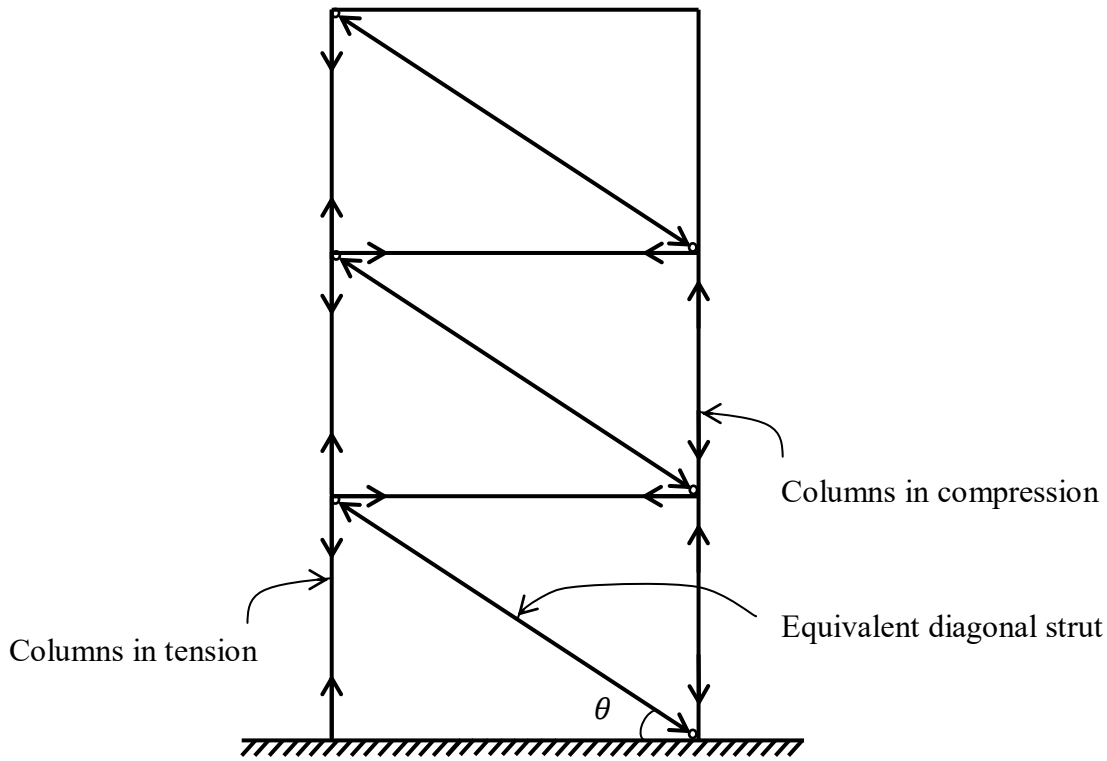

Figure2.9 Equivalent diagonal braced frame (Smith and Coull, 1991)

Saneinejad and Hobbs (1995) proposed a method of analyzing masonry infilled steel frames subjected to in-plane loading. Madan et al. (1997) further extended the work of Saneinejad and Hobbs (1995) by including a smooth hysteretic model for the equivalent diagonal strut. The proposed analytical development assumes that the contribution of masonry infill panel as shown in Figure 2.10(a) to the response of the infilled frame can be modeled by replacing the panel by a system of two diagonal masonry compression struts as shown in Figure 2.10(b).

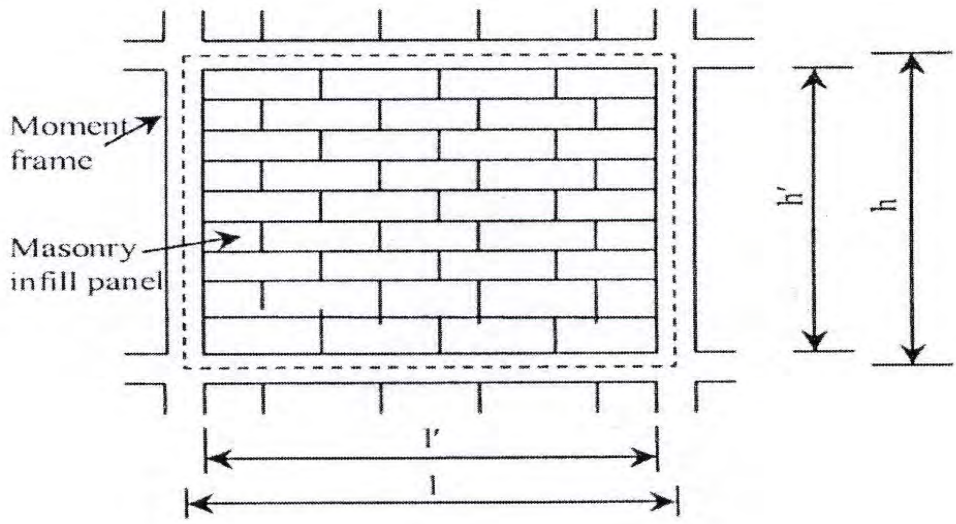

Figure 2.10(a) Masonry infill frame in masonry infill panel frame (Madan et. al, 1997)

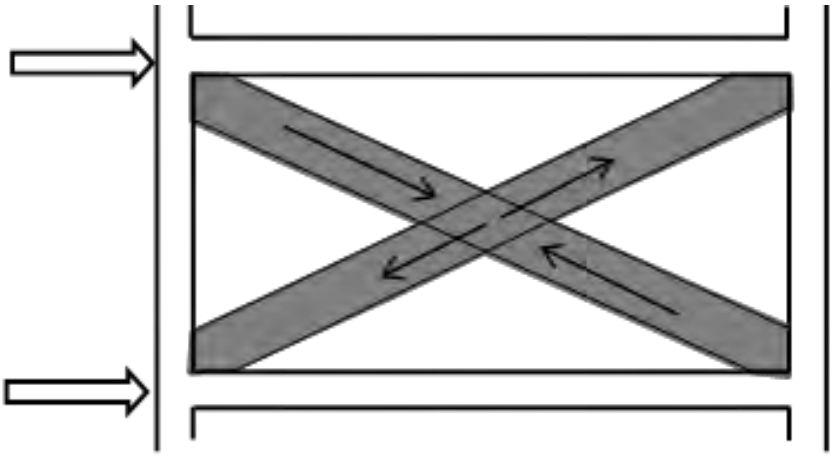

Figure 2.10(b) Infill wall is depicted by diagonal compressive strut (Madan et. al, 1997)

2.5 EQUIVALENT DIAGONAL STRUT APPROACH

Several methods since mid-50s of 20th century have been attempted for analysis and design of infill frame structures. Research on modeling of infill panel as an equivalent diagonal strut was first published by Holmes (1961). He assumed that the infill wall acts as a diagonal compression strut of the same thickness and elastic modulus as the infill with a width equal to one-third the diagonal length. He also concluded that, at the infill failure, the lateral deflection of the infill frame is small compared to the deflection of the corresponding bare frame. Smith (1962) conducted a series of tests on laterally loaded square mild steel frame models infill with micro-concrete. Monitoring the model deformations during the tests showed that the frame separated from the infill over three quarters of the length of each frame member. These observations led to the conclusion that, the wall could be replaced by an equivalent diagonal strut connecting the loaded corners.

Mainstone (1971) presented results of series of tests on model frames with infill of micro-concrete and model brickwork. He found that the factors such as initial lack of fit between infill and frame, variation in the elastic properties and strength of the infill can result in a wide variation in behavior even between nominally identical specimens. Mainstone (1971) also adopted the concept of replacing the infill with an equivalent pin jointed diagonal strut; although he believed that the concept can only be justified for behavior prior to first cracking of the infill. He plotted the aforementioned test results against the stiffness parameter, and empirically formulated three equivalent diagonal strut widths to evaluate the stiffness, first crack load, and ultimate composite strength of the infill frame.

Expressions used in this thesis have been adopted from Mainstone (1971) theory for its consistently accurate predictions of infill frame in-plane behavior when compared with experimental results of others. The equivalent strut width, , depends on the relative flexural stiffness of the infill to that of the columns of the confining frame. The relative infill to frame stiffness shall be evaluated using equation (2.1)

$$\mathrm{H} \quad \mathrm{H}\left[\frac{E_{\mathrm{m}} t \sin}{E_{\mathrm{c}}\ {}_{\mathrm{c}} h_{\mathrm{m}}}\right]^{/} \tag{2.1}$$

Where, His a dimensionless parameter is the height of the frame, t is the thickness of the masonry wall, is the angle made by the strut with the horizontal, $_{\mathrm{c}}$ and $_{\mathrm{c}}$ are the Young's modulus and moment of inertia of column respectively and $_{\mathrm{m}}$, t and h_{m} are the Young's modulus, thickness and height of masonry infill respectively. Mainstone (1971) considered the relative infill to frame flexibility in the evaluation of the equivalent strut width ( ) of the panel as shown in equation (2.2)

$$D(\quad) \tag{2.2}$$

Here, D is the diagonal length of infill. If there are openings and damaged infill in the MI panel then the equivalent width must be modified using the equation (2.3)

$$_{\mathrm{mod}} \qquad _{\mathrm{i}} \tag{2.3}$$

Where, ω_{mod}, $R_1$and $R_2$are the modified width of equivalent diagonal strut, reduction factor in plane evaluation due to presence of openings and reduction factor for in plane evaluation due to existing infill damage, respectively, $\zeta_i$is known as strength increase factor due to damage or decay of infill.

Liau and Kwan (1984) studied both experimentally and analytically the behavior of non-integral infill frames and presented few equations on equivalent strut width. Paulay and Preistley (1992) gave the width of diagonal strut as 0.25 times the diagonal length of the strut. Hendry (1998) has also presented equations on equivalent strut width that would represent the MI In Hendry's equation, $_h$ and $_L$ are the contact length between wall and column, and beam respectively at the time of initial failure of wall; and $_{inf}$ is the length of infill. The equations of these researchers are given in the Table 2.1 below:

Table 2.1 Equations for calculation of diagonal strut width for infill frame (Prachand, 2012)

Researchers	**Strut width (ω)**	**Remarks**
Holmes, 1961	$_m$	d is the length of diagonal
Mainstone, 1971	D H	H H $\left[\frac{E_m t \sin}{E_c \ _c h_m}\right]^{/}$
Liauw and Kwan, 1984	$\frac{h_m \cos}{\sqrt{(\ h_m)}}$	$\left[\frac{E_m t \sin}{E_c \ _c h_m}\right]^{/}$
Paulay and Priestley, 1992	$_m$	$_m$ is the length of diagonal
Hendry, 1998	$0.5(\ _h \ \ _L)^{/}$	$_h \ -\left[\frac{E_c \ _c h_m}{E_m t \sin}\right]^{/}$ $_L \ \left[\frac{E_c \ _b \ _{inf}}{E_m t \sin}\right]^{/}$

2.6 STRENGTH OF MASONRY INFILL WALLS

Infill wall of any RC building of Dhaka city consists of solid hand-made clay bricks and thin mortar layers. The bricks are arranged in an organized manner and bonded by cement mortars. The infill wall is located within beam-column panel to act as a partition wall. There are openings in infill wall to provide adequate door and windows. Compressive strength of the masonry prism, f_p', is determined from an equation recommended by Paulay and Priestlay (1992) as:

$$f_p' = \frac{f_{cb}'(f_{tb}' + \alpha f_j')}{U_u(f_{tb}' + \alpha f_{cb}')} \tag{2.4}$$

Where, $\alpha = \frac{j}{4.1 \times h_b}$ and $U_u = 1.5$

f'_{tb} , f'_{cb} , f'_j , h_b, j and U_u are the tension strength of the brick, compression strength of the brick, mortar compression strength, height of the solid brick (60 mm), mortar joint thickness (15 mm) and stress non-uniformity coefficient (Equal to 1.5) respectively

Based on a post-earthquake investigation of quality control for bricks by building and housing research center of Iran, an average of f'_{cb} is $7.36\ MPa$ and cement-sand ration of the mortar is 1: 5. The corresponding compression strength of the mortar is considered to be 4.9 MPa, which is derived from experimental results on the same cement-sand ratio, carried out by Moghaddam (2004). The tension strength of the solid bricks may be determined as (Paulay and Priestly,1992):

$$f'_{tb} = 0.1 \times f'_{cb} = 0.1 \times 7.36 = 0.736\ MPa$$

The compressive strength of a masonry prism is obtained as:

$$f'_b = \frac{7.36(0.736 + 0.061 \times 4.9)}{1.5(0.736 + 0.061 \times 7.36)} = 4.29\ MPa$$

2.6.1 **Shear Strength of Infill Walls**.

There are several potential failure modes for infill masonry walls (Paulay and Priestley, 1992) including:

a. Sliding shear failure of masonry walls horizontally.
b. Compression failure of diagonal strut.
c. Diagonal tensile cracking but it is not a general failure.
d. Tension failure mode (Flexural) which is not usually a critical failure mode.

Shear strength for the first and second critical types of failure mode are obtained for each infill panel, and the minimum value is considered to be the shear strength of the infill wall.

2.6.1.1 Shear Strength in Sliding Shear Failure.

The Mohr-Coulomb failure criteria can be applied to assess the maximum shear strength for this kind of failure mechanism.

$$\tau_f = \tau_0 + \mu\sigma_N \qquad (2.5)$$

Where, τ_0, μ and σ_N are the cohesive capacity of the mortar bed, sliding friction coefficient along the bed joint and vertical compression stress in the infill walls respectively.

Applying panel dimension, maximum horizontal shear Force V_f is assessed as follows:

$$V_f = \tau_0 t l_m + \mu N \quad (2.6)$$

Where, t, l_m and N are the infill wall thickness, length of infill panel and vertical load in infill walls respectively.

In FEMA 306 (1998), N is determined to be the vertical load applied by vertical shortening strain in the panel due to lateral drifts.

$$N = t\, l_m E_m r^2 \quad (2.7)$$

Where, E_m *and* r are the Young's modulus of the masonry and inter-storey drift angle respectively.

N is estimated directly as a summation of applied external vertical load on the panel and the vertical component of the diagonal compression force R_C by Mostafaei and Kabeya (2004), as shown in Fig.2.11.

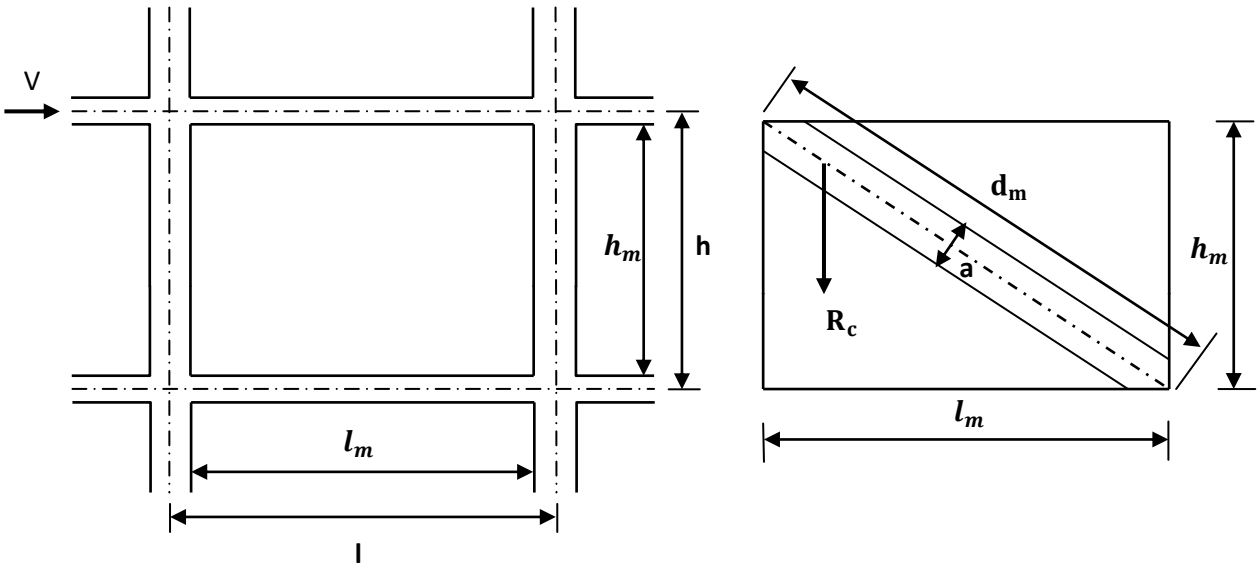

Figure 2.11 Infill masonry wall and the equivalent diagonal compression action parameters (Mostafaei and Kabeya, 2004)

The external vertical load is zero for the infill of the building, and only the vertical component of the strut compression force is considered. Therefore, maximum shear force can be calculated as:

$$V_f = R_c \cos\theta = \tau_0 t l_m + \mu R_c \sin\theta \quad (2.8)$$

$$\therefore\ V_f = \frac{\tau_0 t l_m}{(1 - \mu \tan\theta)}$$

Typical ranges of τ_0 are $1 \leq \tau_0 \leq 1.47\ MPa$, it may be assumed typically as $\tau_0 = 0.04 f_m'$. If we consider $f_m' = 4.29\ MPa$ than $\tau_0 = 0.04 \times 4.29 = 0.172\ MPa$ (Paulay and Priestly, 1992). μ is determined from the experimental results of Chen (2003) in the following equation:

$$\mu = 0.654 + 0.000515 f_j' \tag{2.9}$$

2.6.1.2 Shear Strength in Compression Failure.

Compression failure of infill walls occurred due to the compression failure of the equivalent diagonal strut. The shear force (Horizontal component of the diagonal strut capacity) can be calculated from an equation suggested by Stafford-Smith and Carter (1969), the equivalent strut width $\boldsymbol{a}$**,** is computed using a modification recommended by Mainstone (1974);

$$V_c = a\ t\ f_m'\ cos\ \theta \tag{2.10}$$

Where, f_m' = Masonry compression strength which for ungrouted clay brick masonry (Paulay and Priestley, 1992); $f_m' = f_b' = 4.29\ MPa$ and $a =$ equivalent strut width obtained from an equation suggested by Paulay and Priestley, 1992.

2.6.1.3 Diagonal Tensile Cracking.

Diagonal tensile cracking is not a general failure. Higher lateral forces can be supported by the other failure modes, Saneinejad and Hobbs (1995). However, it is regarded as a serviceability limit state, is defined as:

$$H_t = 2 \times \sqrt{2}\ t\ h_m\ f_t\ cos\ \theta\ sin\ \theta \tag{2.11}$$

Where, $f_t =$ Cracking capacity of masonry; $f_t = 0.166 \times \sqrt{f_b'} = 0.345\ MPa$

2.6.1.4 Maximum Shear Strength of Masonry Infill Walls.

The shear strengths obtained from the above failure modes, sliding shear failure and diagonal compression failure, may not exceed $0.814\ MPa$ as recommended by ACI 530-88. Therefore, the corresponding shear strengths cannot be beyond the following value;

$$\frac{V_{max}}{t \times l_m} = 0.814\ MPa \tag{2.12}$$

2.7 SEISMIC BEHAVIOR OF SOFT GROUND STOREY

The origin of soft storey configuration is mainly derived from an architecture manifesto named as ―Five points for a new architecture" published by Swiss-French architect Le Corbusier, 1926 (Guevara and Perez, 2012). Amongst these five points, first three points relevant to soft storey are listed below:

- Pilotis – Replacement of supporting walls by a grid of reinforced concrete columns that bears the structural load is the basis of the new aesthetic.
- The free designing of the ground plan - the absence of supporting walls - means the house is unrestrained in its internal use.
- The free design of the facade - separating the exterior of the building from its structural function - sets the frontage free from structural constraints.

These hypothesize were possible due to the development of new construction techniques and building materials, such as the "reinforced concrete frame structure"(RCFS) since the 19th century. Most nations statistics on high-rise building reflect frequent use of the open ground storey configuration in the metropolitan cities because the owners need not to pay tax for open storey but can derive economic benefit out of it. In seismic zones, from the beginning of the 20th century this building configuration has been attributed as one important factor to the generation of seismic vulnerability in modern buildings. In reconnaissance report on all major earthquakes it is found that the damage of soft storey buildings was very common in all the damaged sites In the ‘ s, a group of architects from California participated in significant studies with earthquake engineers, to promote the inclusion of soft storey in seismic codes for the design and construction of building. But it was not effective till the Michoacan, Mexico, earthquake of 1985. After this earthquake, 1988 UBC edition included for the first time two tables for defining some parameters for the identification of ―irregular" configurations, in plan and elevation (Guevara and Perez, 2012).Gradually different national codes have incorporated the soft storey phenomenon in their codes with necessary corrective measures.

In 21th century, soft storey building is frequently designed to fulfill the architectural or functional demands. This poses no problem in the usual course of vertical loading but in earthquake prone areas; this makes the structure potentially vulnerable to seismic load. Soft storey building with open ground storey is inherently possessing poor structural system with sudden drop in stiffness and strength in the ground storey. Current design practice neglects MI as structural element by considering building as bare frame (Figure 2.11(a) and (b)).

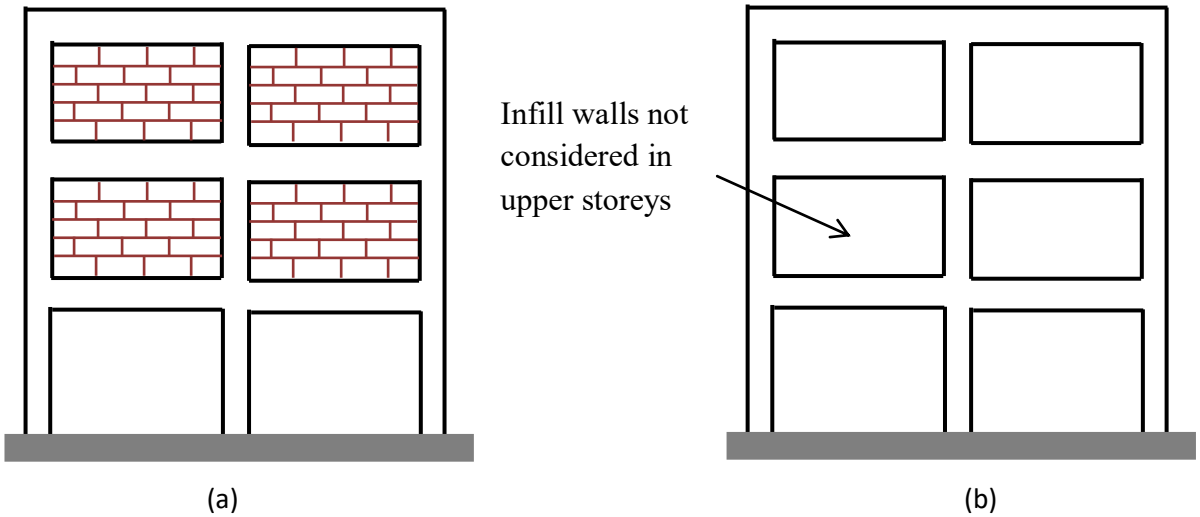

Figure 2.11 Buildings with open ground storey(a) actual building (b) building being assumed in current design practice

In a fully infilled frame, lateral displacements are uniformly distributed throughout the height as shown in Figure 2.12(a) and (b). On the other hand, in the case of open ground floor buildings, most of the lateral displacement is accumulated at the ground level itself because this floor is the most flexible due to absence of infill (Figure 2.12(c)).Similarly, the seismic storey shear forces and subsequently moments concentrate in the open ground storey, instead of gradually varying as in fully infilled frame (Figure 2.12(b) and (c)).

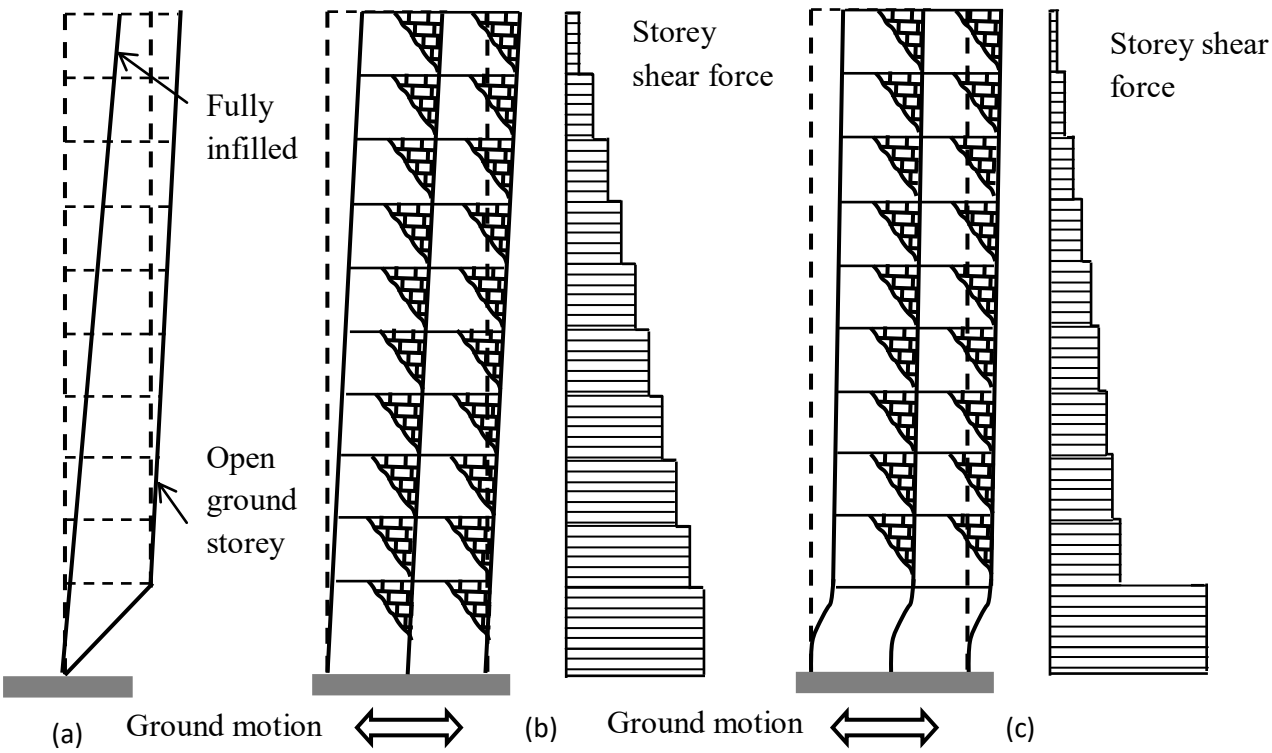

Figure 2.12 Effects of MI on first mode shape of ten storey building (a) Displacement profile (b) Fully infilled frame (c) Frame with open ground storey (Kaushik et.al., 2006)

The presence of walls in upper storeys makes them much stiffer than the open ground storey. Thus, upper storeys move almost together as a single block and most of the horizontal displacement of the building occurs in the soft ground storey itself. Therefore, buildings swing back-and-forth like inverted pendulums during earthquake shaking (Fig. 2.13).

Open ground-storey buildings have consistently performed poorly during earthquakes across the world, for example, during El Centro 1940, San Fernando 1971, 1999 Turkey, 1999 Taiwan, 2001 Bhuj (India), 2003 Algeria earthquakes, etc. a significant number of buildings with soft storey have collapsed. Alarming amount of damage to the buildings with open basements for parking has been reported during the Northridge Earthquake of January 17, 1994, as well as Great Hanstin Earthquake of Kobe 1995 (Haque, 2007).

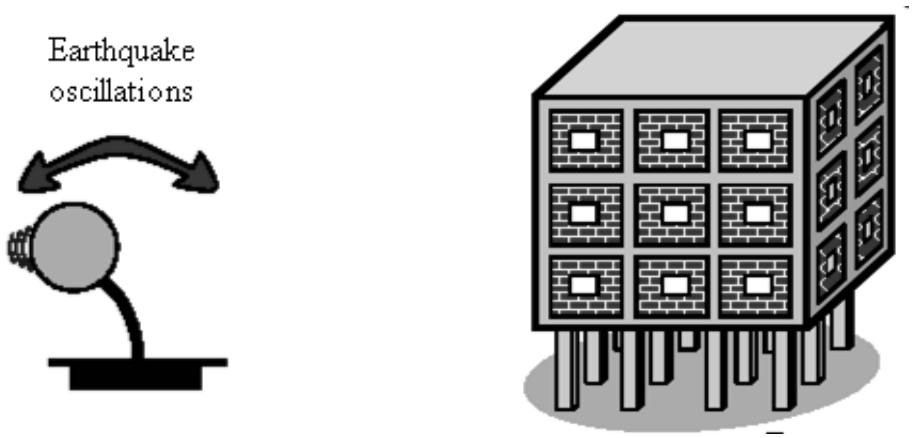

Figure 2.13 Soft storey building act as an inverted pendulum

2.8 MASONRY INFILL IN BUILDING CODES

Guidelines for the design and construction of building are defined as the building codes which ensure public safety from structural failure, loss of life and wealth. Because of the differences in magnitude of earthquake, geological formations, construction types, structure types, percentage of infill, economic development and other features, the seismic design aspects are different in different building codes.

A very few codes specifically recommend isolating the MI from the RC frames because the stiffness of MI does not play any role in the overall stiffness of the frame (NZS-3101 1995, SNIP-II-7-81 1996). As a result, MI walls are not considered in the analysis and design procedure of RC building. The isolation helps to prevent the problems associated with the brittle behavior and asymmetric placement of MI. Another group of national codes prefers to take advantage of certain characteristics of MI walls such as high initial lateral stiffness, cost-

effectiveness, and ease in construction. These codes require that the beneficial effects of MI are appropriately included in the analysis and design procedures as well as its detrimental effects are mitigated. In other words, these codes tend to maximize the role of MI as a first line of defense against seismic actions.

Most national codes recognize that the buildings with simple and regular geometry perform well during earthquakes, and unsymmetrical placement of MI walls may introduce irregularities into them. These codes permit static analysis methods for regular short buildings located in regions of low seismicity. However, for other buildings, dynamic analyses are recommended, in which it is generally expected but not specifically required that all components imparting mass and stiffness to the structure are adequately modeled. Most codes restrict the use of seismic design force obtained from dynamic analysis such that it does not differ greatly from a minimum value that is based on the code-prescribed empirical estimate of natural period. This restriction prevents the design of buildings for unreasonably low forces that may result from various uncertainties involved in a dynamic analysis.

Natural period of vibration is an important parameter in the building code equations for determining the design earthquake force by any kind of equivalent static force method. Natural periods of vibration of buildings depend upon their mass and lateral stiffness. Presence of non-isolated MI walls in buildings increases both the mass and stiffness of buildings; however, the contribution of latter is more significant. Consequently, the natural periods of an MI-RC frame are normally lower than that of the corresponding bare frame. Therefore, the seismic design forces for MI frames are generally higher than those for the bare frames. Although, all national codes explicitly specify empirical formulae for the fundamental natural period calculations of bare RC frames, only a few specify the formulae for MI-RC frames.

Several codes—IS-1893 (2002); NBC-105 (1995); NSR-98 (1998); Egyptian code (1988); Venezuelan code (1988); Algerian code (1988); ESCP-1 (1983)—suggest using an empirical formula given by Equation 2.4 to calculate the natural period of MI-RC frames, Ta in sec.

$$_{a} \quad \frac{h}{\sqrt{\ }} \tag{2.13}$$

Where, h is the height of the building (in meter) and d is the base dimension of building (in meter) at the plinth level along the considered direction of the lateral force. For T_a estimation,

French Code (AFPS - 90/1990) recommends following equation that is specified for masonry buildings:

$$T \quad \frac{h}{\sqrt{\ }}\sqrt{\frac{h}{\ \ h}} \tag{2.14}$$

In Eqn.2.4 and 2.5, total base width of buildings is used to calculate $_a$, which may not be appropriate. For example, d will be equal to the total base dimension for all the frames in Fig.2.13 irrespective of the distribution of MI in the frmae. However, for frame in Figure 2.13(c), it is more appropriate to consider as the effective base width, rather than total width d of the building. Therefore Eqn.2.4 and 2.5 may not estimate correct $_a$ values for different frames shown in Fig.2.14.

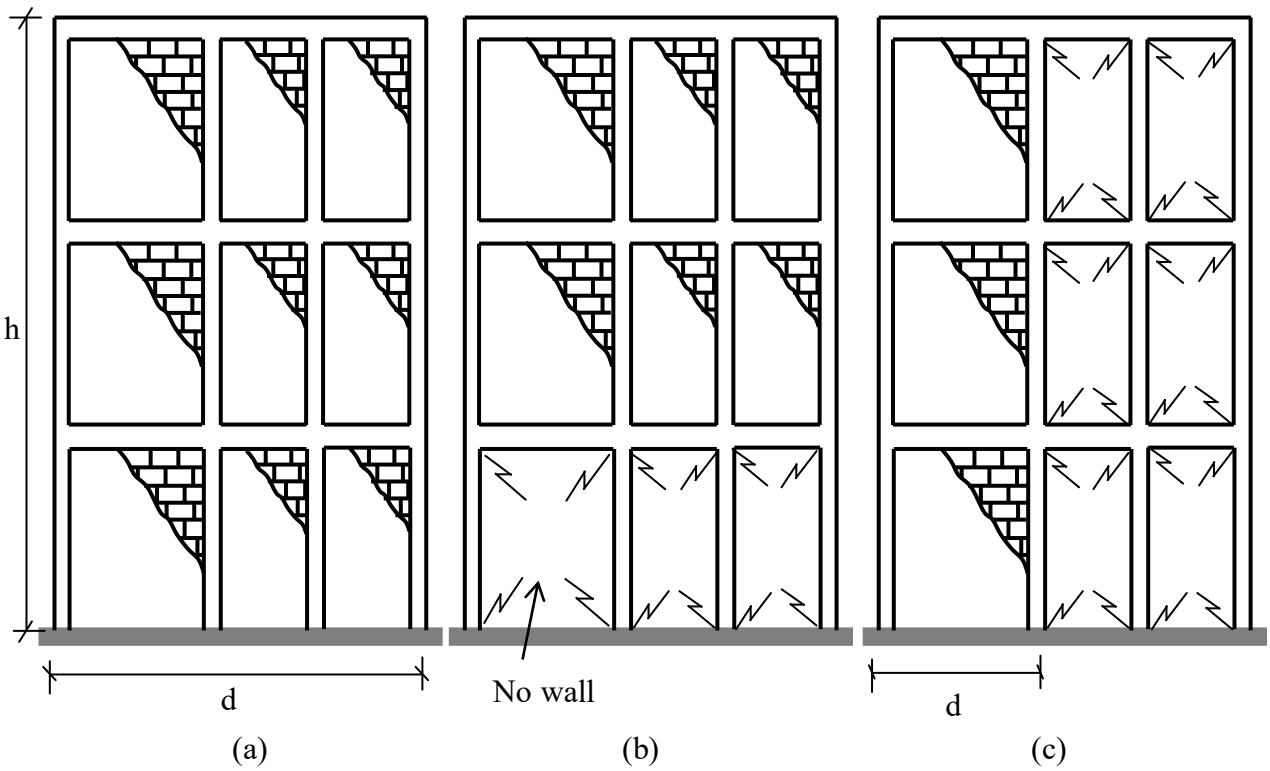

Figure 2.14 Different arrangements of masonry infill walls in RC frame

Vertical irregularities are introduced into MI-RC frames due to reduction or absence of MI in a particular storey compared to adjacent storeys. In general, this gives rise to mass, stiffness, and strength irregularities along height of buildings. A few national codes penalize beams and/or columns of the irregular storeys, as they are required to be designed for higher seismic forces to compensate for the reduction in the strength due to absence of MI in the irregular storeys.

The Indian seismic code (IS-1893:2002) requires members of the soft storey to be designed for 2.5 times the seismic storey shears and moments, obtained without considering the effects of MI in any storey. The factor of 2.5 is specified for all the buildings with soft storeys irrespective of the extent of irregularities; and the method is quite empirical. The other option is to provide symmetric RC shear walls, designed for 1.5 times the design storey shear force in both directions of the building as far away from the center of the building as feasible. On the other hand, Costa Rican code (1986) requires that all structural-resisting systems must be continuous from the foundation to the top of buildings, and stiffness of a storey must not be less than 50% of that of the storey below. BNBC (Draft), 2015 has also proposed design guideline for soft storey building which is almost similar to the Indian seismic code.

2.9 SEISMIC HAZARD AND DEMAND RESPONSE SPECTRUM

2.9.1 Seismic Hazard.

Seismic hazard at a site due to ground shaking is quantified to determine its impact on buildings. Three levels of seismic hazard are used to define ground shaking namely Serviceability Earthquake (SE), Design Earthquake (DE) and Maximum Earthquake (ME).SE is defined probabilistically as the level of ground shaking that has a 50 percent chance of being exceeded in a 50 years period. This level of earthquake ground shaking is typically about 0.5 time the level of ground shaking of the design earthquake. DE is defined probabilistically as the level of ground shaking that has a 10 percent chance of being exceeded in a 50 years period. ME is defined deterministically as the maximum level of earthquake ground shaking which may ever be expected at building sites within the known geologic framework. This level of ground shaking is typically expressed as 1.25 to 1.5 times the ground shaking of the design earthquake.

2.9.2 Primary Ground Shaking Criteria.

Primary ground shaking conditions are generally required for the design of all buildings. Primary conditions are known as site geology and soil characteristics, site seismicity characteristics, and site response spectra. In case of site geology and soil characteristics, each site is assigned a soil profile type based on properly substantiated geotechnical data using the site categorization procedure. Soil profile types are defined in the Table 2.2 but soil profile type S_F is defined as soils requiring site specified evaluation separately.

Table 2.2 Soil profile types (ATC 40, 1996)

Soil Profile Type	Soil Profile Name/ Generic Description	Average Soil Properties for Top 100 Feet of Soil Profile		
		Shear wave velocity: $\bar{V}_s$ (Feet/ second)	SPT, $\bar{N}$ (Blows/ foot)	Undrain Shear Strength $\bar{S}_u$ (psf)
S_A	Hard Rock	$\bar{V}_s > 5000$	Not Applicable	
S_B	Rock	$2500 < \bar{V}_s \leq 5000$	Not Applicable	
S_C	Very Dense Soil	$1200 < \bar{V}_s \leq 2500$	$\bar{N} > 50$	$\bar{S}_u > 2000$
S_D	Stiff Soil Profile	$600 < \bar{V}_s \leq 1200$	$15 \leq \bar{N} \leq 50$	$1000 < \bar{S}_u \leq 2000$
S_E	Soft Soil Profile	$\bar{V}_s < 600$	$\bar{N} < 15$	$\bar{S}_u < 1000$
S_F	Soil Requiring Site-specific Evaluation			

Seismicity characteristics for the site are based on the seismic zone, proximity of site to active seismic sources and site soil profile characteristics. Each site is assigned with a near source factor and seismic source type in accordance to the Table 2.3 and 2.4 (ICBO 1996).

Table 2.3 Near source factor, N_A and N_V

Seismic Source Type	Closest Distance to Known Seismic Source							
	≤ 2 km		5 km		10 km		≥ 15 km	
	N_A	N_V	N_A	N_V	N_A	N_V	N_A	N_V
A	1.5	2.0	1.2	1.6	1.0	1.2	1.0	1.0
B	1.3	1.6	1.0	1.2	1.0	1.0	1.0	1.0
C	1.0	1.0	1.0	1.0	1.0	1.0	1.0	1.0

Table 2.4 Seismic Source Type.

		Seismic Source Definition	
Source Type	Seismic Source Description	Maximum Moment Magnitude, M	Slip Rate SR (mm/ year)
A	Faults that are capable of producing large magnitude events and which have a high rate of seismic activity	$M \geq 7.0$	$SR \geq 5$
B	All faults other than types A and C	Not Applicable	Not Applicable
C	Faults that are not capable of producing large magnitude earthquakes and that have a relatively low rate of seismic activity	$M < 6.5$	$SR < 2$

2.9.3 Seismic Coefficients.

Building is assigned with a seismic coefficient C_A in accordance to the Table 2.5 (ICBO 1996) and a seismic coefficient C_V in accordance to the Table 2.6 (ICBO 1996) for each earthquake hazard level. The seismic coefficient C_A may be taken to be the default value of the Effective Peak Acceleration (EPA) of any selected site.

Table 2.5 Seismic coefficients C_A

	Shaking Intensity, ZEN[1,2]					
Soil Profile Type	$= 0.075$	$= 0.15$	$= 0.20$	$= 0.30$	$= 0.40$	≥ 0.40
S_B	0.08	0.15	0.20	0.30	0.40	1.0 (ZEN)
S_C	0.09	0.18	0.24	0.33	0.40	1.0 (ZEN)
S_D	0.12	0.22	0.28	0.36	0.44	1.1 (ZEN)
S_E	0.19	0.30	0.34	0.36	0.36	0.9 (ZEN)
S_F	Site-specific geotechnical investigation required to determine C_A					

1. The value of E used to determine the product, ZEN, should be taken to be equal to 0.5 for the Serviceability Earthquake, 1.0 for the Design Earthquake, and 1.5 for the Maximum Earthquake.
2. Seismic coefficient C_A should be determined by linear interpolation for values of the product ZEN other than those shown in the table.

Table 2.6 Seismic coefficients C_V

	Shaking Intensity, ZEN[1,2]					
Soil Profile Type	$= 0.075$	$= 0.15$	$= 0.20$	$= 0.30$	$= 0.40$	≥ 0.40
S_B	0.08	0.15	0.20	0.30	0.40	1.0 (ZEN)
S_C	0.13	0.25	0.32	0.45	0.56	1.4 (ZEN)
S_D	0.18	0.32	0.40	0.54	0.64	1.6 (ZEN)
S_E	0.26	0.50	0.64	0.84	0.96	2.4 (ZEN)
S_F	Site-specific geotechnical investigation required to determine C_V					

1. The value of E used to determine the product, ZEN, should be taken to be equal to 0.5 for the Serviceability Earthquake, 1.0 for the Design Earthquake, and 1.5 for the Maximum Earthquake.
2. Seismic coefficient C_V should be determined by linear interpolation for values of the product ZEN other than those shown in the table.

2.9.4 Site Response Spectrum and Demand Curve.

Elastic response spectrum of a site is based on estimates of C_A and C_V site seismic coefficients, spectral contour maps and site-specific hazard analysis studies. The elastic response spectrum using estimates of C_A and C_V is developed and shown in Figure 2.15. This figure shows acceleration vs. time period graph which depicts an elastic site response spectrum. An inelastic response spectrum for each earthquake hazard level is also calculated using the same procedure as stated above except the response modification coefficient. In this case, the response modification coefficient of structural system (R) is considered as one. In response spectrum, a factor of about 2.5 times C_A represents the average value of peak response of a 5 percent-damped short period system in the acceleration domain. The seismic coefficient C_V represents 5 percent-damped response of a 1-second system and when divided by period defines acceleration response in the velocity domain. The inelastic response spectrum is otherwise known as demand curve of any specific site and hazard level.

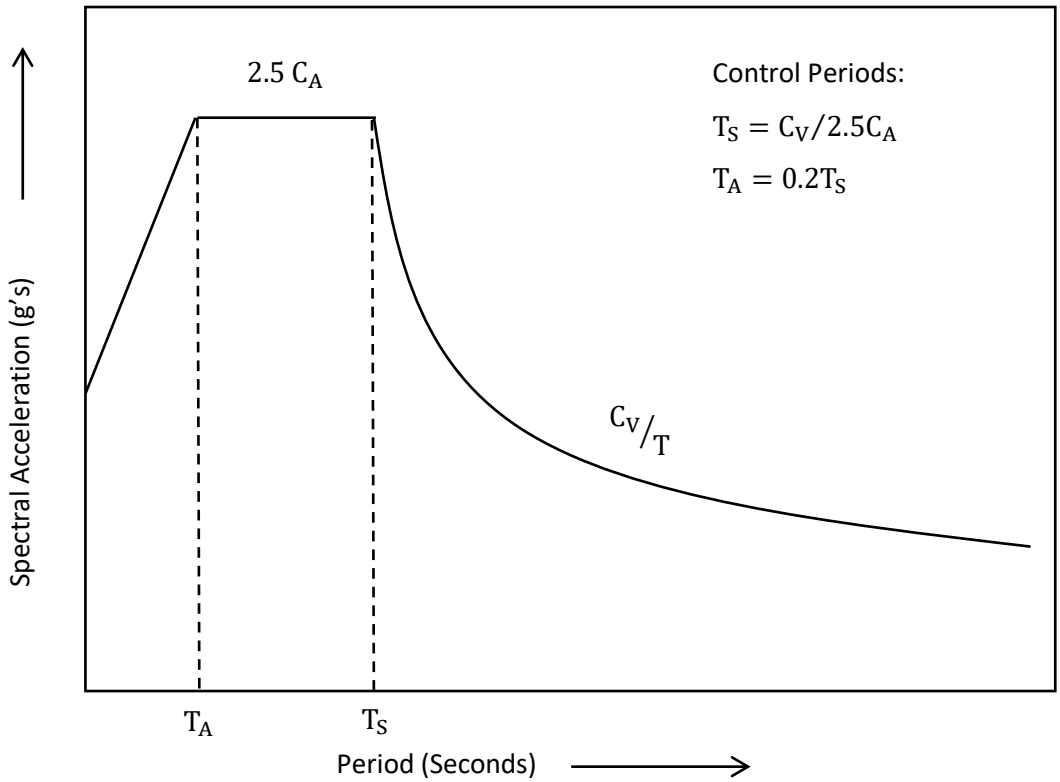

Figure 2.15 Response spectrum for an earthquake hazard level of interest

2.10 Structural Performance Levels and Ranges under Seismic Load

The Federal Emergency Management Agency in its report –Pre-standard and Commentary for the Seismic Rehabilitation of Building" FEMA-356, 2002) defines the structural performance level of a building into four discrete structural performance levels and two

intermediate structural performance ranges. The discrete structural performance levels are Immediate Occupancy (IO), Life Safety (LS), Collapse Prevention (CP) and Not Considered (NC). The intermediate structural performance ranges are the Damage Control Range (DCR) and the Limited Safety Range (LSR).

2.10.1 Immediate Occupancy Performance Level (S-1)

Structural Performance Level S-1, Immediate Occupancy, may be defined as the post-earthquake damage state of a structure that remains safe to occupy, essentially retains the pre-earthquake design strength and stiffness of the structure, and is in compliance with the acceptance criteria specified in this standard for this Structural Performance Levels defined in Table 4.1 to Table 4.3Structural Performance Level S-1, Immediate Occupancy, means the post-earthquake damage state in which only very limited structural damage has occurred. The basic vertical- and lateral-force-resisting systems of the building retain nearly all of their pre-earthquake strength and stiffness. The risk of life-threatening injury as a result of structural damage is very low, and although some minor structural repairs may be appropriate, these would generally not be required prior to re-occupancy.

2.10.2 Damage Control Performance Range (S-2)

Structural Performance Range S-2, Damage Control, may be defined as the continuous range of damage states between the Life Safety Structural Performance Level (S-3) and the Immediate Occupancy Level (S-1) defined in Table 4.1 to Table 4.3. Design for the Damage Control Structural Performance Range may be desirable to minimize repair time and operation interruption, as a partial means of protecting valuable equipment and contents, or to preserve important historic features when the cost of design for IO is excessive.

2.10.3 Life Safety Performance Level (S-3)

Structural Performance Level S-3, Life Safety, may be defined as the post-earthquake damage state that includes damage to structural components but retains a margin against onset of partial or total collapse in compliance with the acceptance criteria specified in FEMA (FEMA-356, 2002) for this Structural Performance Level defined in Table 4.1 to Table 4.3. Structural Performance Level S-3, Life Safety, means the post-earthquake damage state in which significant damage to the structure has occurred, but some margin against either partial or total structural collapse remains. Some structural elements and components are severely damaged, but this has not resulted in large falling debris hazards, either within or

outside the building. Injuries may occur during the earthquake; however, the overall risk of life-threatening injury as a result of structural damage is expected to be low.

2.10.4 Limited Safety Performance Range (S-4)

Structural Performance Range S-4, Limited Safety, may be defined as the continuous range of damage states between the Life Safety Structural Performance Level (S-3) and the Collapse Prevention Structural Performance Level (S-5) defined in Table 4.1 to Table 4.3.

2.10.5 Collapse Prevention Performance Level (S-5)

Structural Performance Level S-5, Collapse Prevention, may be defined as the post-earthquake damage state that includes damage to structural components such that the structure continues to support gravity loads but retains no margin against collapse in compliance with the acceptance criteria specified FEMA (FEMA-356, 2002). Structural Performance Level S-5, Collapse Prevention, means the post-earthquake damage state in which the building is on the verge of partial or total collapse. Substantial damage to the structure has occurred, potentially including significant degradation in the stiffness and strength of the lateral-force resisting system, large permanent lateral deformation of the structure, and degradation in vertical-load-carrying capacity. The structure may not be technically practical to repair and is not safe for re-occupancy.

Table 2.7 Damage Control and Building Performance Levels (FEMA-356, 2002)

	Target Building Performance Levels			
	Collapse Prevention Performance Level	Life Safety Performance Level	Immediate Occupancy Performance Level	Operational Performance Level
Overall Damage	Severe	Moderate	Light	Very Light
General	Little residual stiffness and strength, but loadbearing columns and walls function. Large permanent drifts. Some exits blocked. Infills and unbraced parapets failed or at incipient failure. Building is near collapse	Some residual strength and stiffness left in all storeys. Gravity-loadbearing elements function. No out-of-plane failure of walls or tipping of parapets. Some permanent drift. Damage to partitions. Building may be beyond economical repair.	No permanent drift. Structure substantially retains original strength and stiffness. Minor cracking of facades, partitions, and ceilings as well as structural elements. Elevators can be restarted. Fire protection operable.	No permanent drift. Structure substantially retains original strength and stiffness. Minor cracking of facades, partitions, and ceilings as well as structural elements. All systems important to normal operation are functional.
Nonstructural components	Extensive damage	Falling hazards mitigated but many mechanical, electrical and architectural systems are damaged.	Equipment and contents are generally secure, but may not operate due to mechanical failure or lack of utilities.	Negligible damage occurs. Power and other utilities as available, possibly from standby sources.

Table 2.8 Structural performance levels and damage–vertical elements (FEMA-356,2002)

	Structural Performance Levels			
		Collapse Prevention	Life Safety	Immediate Occupancy
Element	Type	S-5	S-3	S-1
Concrete Frame	Primary	Extensive cracking and hinge formation in ductile elements. Limited cracking and/or splice failure in some non-ductile columns. Severe damage in short columns	Extensive damage to beams. Spalling of cover and shear cracking < /8" width) for ductile columns. Minor spalling in non-ductile columns. Joint cracks < /8" wide	Minor hairline cracking. Limited yielding possible at a few locations. No crushing (strains below 0.003).
	Secondary	Extensive spalling in columns (limited shortening) and beams. Severe joint damage. Some reinforcing buckled	Extensive cracking and hinge formation in ductile elements. Limited cracking and/or splice failure in some non-ductile columns. Severe damage in short columns	Minor spalling in non-ductile columns and beams. Flexural cracking in beams and columns. Shear cracking in Joint < / " width.
	Drift	4% transient or permanent	2% transient; 1% permanent`	1% transient; negligible Permanent
Un-reinforced Masonry Infill Walls	Primary	Extensive cracking and crushing; portions of face course shed	Extensive cracking and some crushing but wall remains in place. No falling units. Extensive crushing and spalling of veneers at corners of openings.	Minor < /8" width cracking of masonry infill and veneers. Minor spalling in veneers at a few corner openings.
	Secondary	Extensive crushing and shattering; some walls dislodge.	Same as primary	Same as primary
	Drift	0.6% transient or permanent	0.5% transient; 0.3% permanent	0.1% transient; negligible permanent

2.10.6 Target Building Performance Levels

Building performance is a combination of the both structural and nonstructural components. Table 2.7 and Table 2.8 (FEMA-356, 2002) describe the approximate limiting levels of structural damage that may be expected of building evaluated to the levels defined for a target seismic demand. These tables represent the physical states of different performance levels.

2.11 Deformation and Force Controlled Actions.

All structural actions may be classified as either deformation controlled or force controlled using the component force versus deformation curves shown in Fig. 2.16 (ATC-40, 1996). The Type 1 curve is representative of ductile behavior where there is an elastic range (point 0 to point 1 on the curve) followed by a plastic range(points 1 to 3) with non-negligible residual

strength and ability to support gravity loads at point 3. The plastic range includes a strain hardening or softening range (points 1 to 2) and a strength-degraded range (points 2 to 3). Primary component actions exhibiting this behavior shall be classified as deformation-controlled if the strain-hardening or strain-softening range is such that e > 2g (shown in Fig. 2.16); otherwise, they shall be classified as force controlled. Secondary component actions exhibiting Type 1 behavior shall be classified as deformation-controlled for any e/g ratio. The Type 2 curve is representative of ductile behavior where there is an elastic range (point 0 to point 1 on the curve) and a plastic range (points 1 to 2) followed by loss of strength and loss of ability to support gravity loads beyond point 2. Primary and secondary component actions exhibiting this type of behavior shall be classified as deformation-controlled if the plastic range is such that e >2g; otherwise, they shall be classified as force controlled. The Type 3 curve is representative of a brittle or non-ductile behavior where there is an elastic range (point 0 to point 1 on the curve) followed by loss of strength and loss of ability to support gravity loads beyond point 1. Primary and secondary component actions displaying Type 3 behavior shall be classified as force controlled (FEMA-356, 2000).

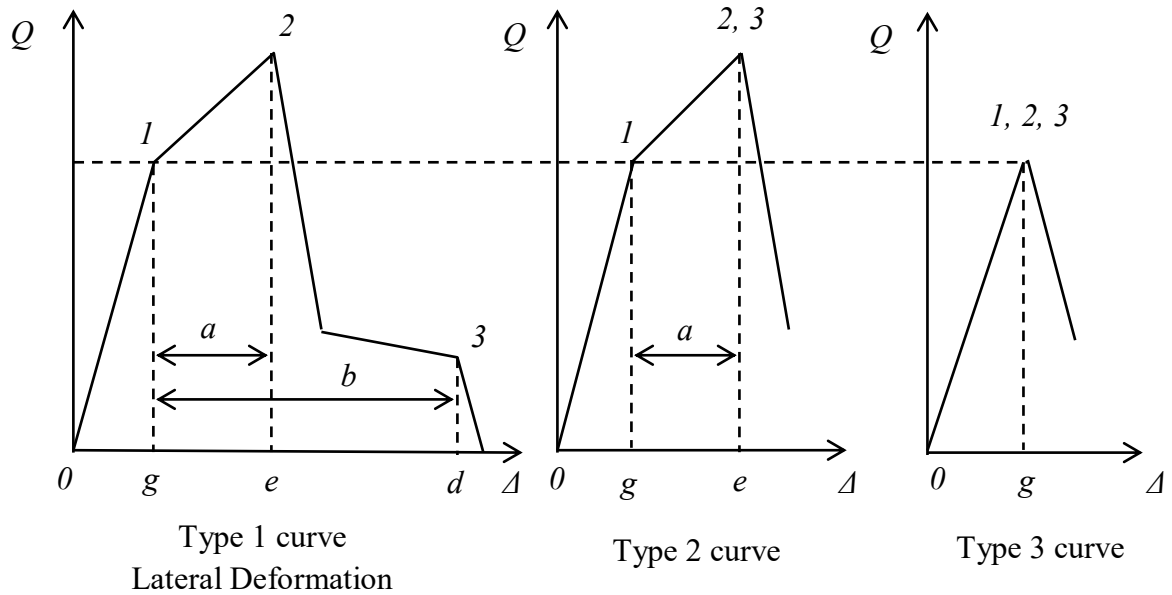

Figure 2.16 Different load-deformation curves

Acceptance criteria for primary components that exhibit Type 1 behavior are typically within the elastic or plastic ranges between points 0 and 2, depending on the performance level. Acceptance criteria for secondary elements that exhibit Type 1 behavior can be within any of the performance ranges. Acceptance criteria for primary and secondary components exhibiting Type 2 behavior will be within the elastic or plastic ranges, depending on the performance level. Acceptance criteria for primary and secondary components exhibiting

Type 3 behavior will always be within the elastic range. Table 2.9 provides some examples of possible deformation and force-controlled actions in common framing systems.

Table 2.9 Possible deformation and force controlled actions (FEMA-356, 2000)

Component	Deformation- Controlled Action	Force-Controlled Action
Moment Frames		
Beam	Moment (M)	Shear (V)
Columns	M	Axial load (P), V
Joints	-	V[1]
Braced Frames		
Braces	P	-
Beams	-	P
Columns	-	P
Shear Link	V	P, M

1. Shear may be a deformation-controlled action in steel moment frame connection
2. If the diaphragm carries lateral loads from vertical seismic resisting elements above the diaphragm level, then M and V shall be considered force-controlled actions.

2.12 ACCEPTABILITY LIMIT

A given component may have a combination of both force and deformation controlled actions. Each element must be checked to determine whether its individual components satisfy its acceptability requirement. Together with the global requirements, acceptability limits for individual components are the main criteria for assessing the calculated building response. Figure 2.17 shows a generalized load – deformation relation appropriate for most concrete components.

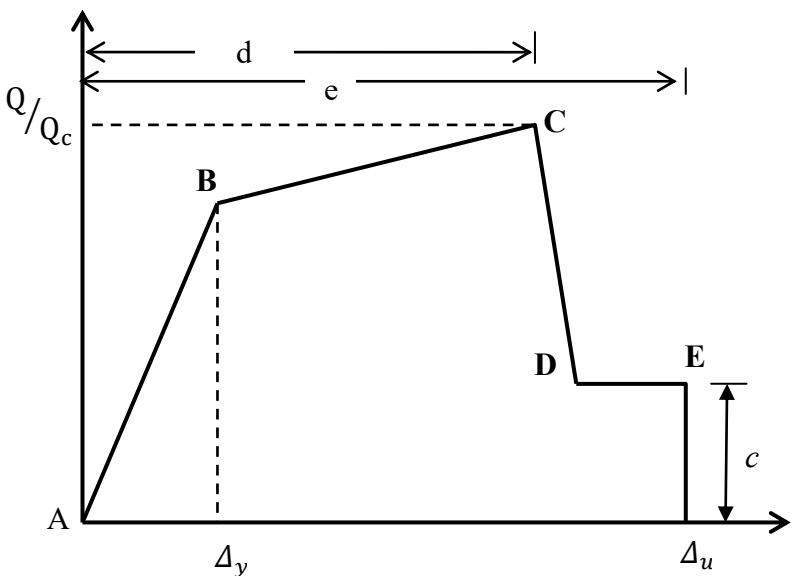

Figure 2.17 Load – deformation relation for concrete components (ATC-40, 1996)

The relation is described by linear response from A (unloaded component) to an effective yield point B, linear response at reduced stiffness from B to C, sudden deduction in lateral load resistance to D, response at reduced resistance to E, and final loss of resistance thereafter. Point A corresponds to the unloaded condition. Point B has resistance equal to the nominal yield strength. The slope from B to C, ignoring the effects of gravity loads acting through lateral displacements, is usually taken as between 5% and 10% of the initial slope. This strain hardening, which is observed for most reinforce concrete component, may have an important effect on the redistribution of internal forces among adjacent components. The abscissa at C significant strength degradation begins. The drop in resistance from C to D represents initial failure of the component. The residual resistance from D to E may be non-zero in some cases and may be effectively zero in others. Where specific information is not available, the residual resistance may be assumed to be equal to 20% of the nominal strength. Point E is a point defining the maximum deformation capacity. Table 2.10 and Table 2.11 give the acceptance criteria for nonlinear procedures for the structural elements.

Table 2.10 Numerical acceptance criteria for plastic hinge rotations in reinforced concrete beams, in radians (ATC-40, 1996)

			Performance Level[3]				
			Primary			Secondary	
Component Type			IO	LS	SS	LS	SS
1. Beams Controlled by Flexure[1]							
$\frac{\rho-\rho'}{\rho_{bal}}$	Transverse[2] Reinforcement	$\frac{V}{b_w d\sqrt{f'_c}}$ [4]					
≤ 0.0	C	≤ 3	0.005	0.020	0.025	0.020	0.050
≤ 0.0	C	≥ 6	0.005	0.010	0.020	0.020	0.040
≥ 0.5	C	≤ 3	0.005	0.010	0.020	0.020	0.030
≥ 0.5	C	≥ 6	0.005	0.005	0.015	0.015	0.020
≤ 0.0	NC	≤ 3	0.005	0.010	0.020	0.020	0.030
≤ 0.0	NC	≥ 6	0.000	0.005	0.010	0.010	0.015
≥ 0.5	NC	≤ 3	0.005	0.010	0.010	0.010	0.015
≥ 0.5	NC	≥ 6	0.000	0.005	0.005	0.005	0.010
2.Beams controlled by shear[1]							
Stirrup spacing$\leq d/2$			0.0	0.0	0.0	0.01	0.02
Stirrup spacing$> d/2$			0.0	0.0	0.0	0.005	0.01
3. Beams controlled by inadequate development or splicing along the span[1]							
Stirrup spacing$\leq d/2$			0.0	0.0	0.0	0.01	0.02
Stirrup spacing$> d/2$			0.0	0.0	0.0	0.005	0.01
4. Beams controlled by inadequate embedment into beam − column joint[1]							
			0.0	0.01	0.015	0.02	0.03

1. When more than one of the conditions 1, 2, 3 and 4 occur for a given component, use the minimum appropriate numerical value from the table.

2. Under the heading ~~tr~~ansverse reinforcement," _C' and _NC' are abbreviations for conforming and non-conforming details, respectively. A component is conforming if within the flexural plastic region: (1) closed stirrup are spaced at ≤d/3 and 2) for components of moderate and high ductility demand the strength provided by the stirrup (Vs) is at least three-fourths of the design shear. Otherwise, the component is considered non-conforming.

3. Linear interpolation between values listed in the table is permitted.

IO = Immediate Occupancy; LS = Life Safety; SS = Structural Stability

4. V = Design Shear

Table 2.11 Numerical Acceptance Criteria for Plastic Hinge Rotations in Reinforced Concrete Columns, in radians (ATC-40, 1996)

			Performance Level[3]				
			Primary			Secondary	
Component Type			IO	LS	SS	LS	SS
1. B**ColumnsControlledbyFlexure**[1]							
$\frac{P}{A_g f'_c}$ [5]	Transverse Reinforcement[2]	$\frac{V}{b_w d\sqrt{f'_c}}$ [4]					
≤ 0.1	C	≤ 3	0.005	0.010	0.020	0.015	0.030
≤ 0.1	C	≥ 6	0.005	0.010	0.015	0.010	0.025
≥ 0.4	C	≤ 3	0.000	0.005	0.015	0.010	0.025
≥ 0.4	C	≥ 6	0.000	0.005	0.010	0.010	0.015
≤ 0.1	NC	≤ 3	0.005	0.005	0.010	0.005	0.015
≤ 0.1	NC	≥ 6	0.005	0.005	0.005	0.005	0.005
≥ 0.4	NC	≤ 3	0.000	0.000	0.005	0.000	0.005
≥ 0.4	NC	≥ 6	0.000	0.000	0.000	0.000	0.000
2. Columnscontrolledbyshear[1,3]							
Hoop spacing≤ $d/2$ or $\frac{P}{A_g f'_c} \leq 0.1$			0.0	0.0	0.0	0.01	0.015
Other cases			0.00	0.00	0.00	0.00	0.00
3. **Columnscontrolledbyinadequatedevelopmentorsplicingalongtheclea height**[1,3]							
Hoop spacing≤ $d/2$			0.0	0.0	0.0	0.01	0.02
Hoop spacing> $d/2$			0.0	0.0	0.0	0.005	0.01
4. Columns with axial loads exceeding 0.70[1,3]							
Conforming reinforcement over the entire length			0.0	0.01	0.005	0.005	0.01
All other cases			0.0	0.0	0.0	0.0	0.0

1. When more than one of the conditions 1,2,3 and 4 occur for a given component, use the minimum appropriate numerical value from the table. See Chapter 9 for symbol definitions.

2. Under the heading ~~"tr~~ansverse reinforcement," _C' and _NC' are abbreviations for conforming and non-conforming details, respectively. A component is conforming if within the flexural plastic hinge region: (1) closed hoops are spaced at ≤d/3 and 2) for components of moderate and high ductility demand the strength provided by the stirrup (Vs) is at least three-fourths of the design shear. Otherwise, the component is considered non-conforming.

3. To qualify, (1) hoops must not be lap spliced in the cover concrete, and (2) hoops must have hooks embedded in the core or must have other details to ensure that hoops will be adequately anchored following spalling of cover concrete.

4. Linear interpolation between values listed in the table is permitted.
   IO = Immediate Occupancy; LS = Life Safety; SS = Structural Stability

5. P = Design axial load

6. V = Design shear force

2.13 STATIC LINEAR ANALYSIS

2.13.1 Loads

Full conventional static analyses of RC frames are carried out following different codes specifications. For the present study BNBC, 2015 (Draft) has been followed for analyzing the RC frames for four basic loads namely Dead Load (DL), Live Load (LL) and Earthquake (E) loads in the plane of the frame. These basic loads are combined as per the code as follows:

- DL
- DL LL
- DL E LL

2.13.1.1 Dead Load. Dead load is the vertical load due to the weight of permanent structural and nonstructural components of a building such as walls, floors, ceilings, permanent partitions and fixed service equipment etc.

2.13.1.2 Live Load. Live load is the load superimposed by the use or occupancy of the building not including the environmental loads such as wind load, rain load, earthquake load or dead load. The minimum floor live loads shall be the greatest actual imposed loads resulting from the intended use or occupancy of the floor.

2.13.1.3 Earthquake Load: Load effects of earthquake, or related internal moments and forces, Earthquake load is applied and analyzed in two methods. Equivalent static force method is used for static analysis and response spectrum method for dynamic analysis.

2.13.2 Equivalent Static Force Method

The Equivalent Static Force Method (ESFM) is a static analysis procedure which provides reasonable good results to the regular structure. It is a simplified technique to substitute the effect of dynamic loading of an expected earthquake by a static force distributed laterally on a structure for design purposes. The total applied seismic force V is generally evaluated in two horizontal directions parallel to main axes of the building. It assumes that the building responds in its fundamental lateral mode. For this to be true, the building must be fairly symmetric to avoid torsional movement under ground motion (BNBC, 2015(Draft)). The empirical relationship for base shear calculation is

$$V \quad \frac{C}{} \tag{2.15}$$

Where,

Seismic zone coefficient

= Structure importance coefficient

= Response modification coefficient for structural system

Total seismic load

C = Numerical coefficient given by the relation

$$C \quad \frac{}{T^{2/3}} \tag{2.16}$$

Fundamental period of vibration in sec

Site coefficient for soil characteristics

For regular concrete frames, period T may be approximated as

$$T \qquad (h_n)^{/} \tag{2.17}$$

Where, h_n = Height of structure above base in meter

The total base shear calculated by the Equation (2.6) at the base level is further distributed at different floor level basing on the guideline given in the BNBC, 2015 (Draft). This distributed base shear at different floor levels acts as the lateral forces due to earthquake at constant vertical load for design of the building. The equivalent static force method is used

for elastic analysis of building where the design spectral acceleration is reduced by the response modification factor R. The value of R varies with type of moment-resisting-frame-system. For example, the value of R for an intermediate moment-resisting-frame-system is 8.

2.14 NONLINEAR STATIC PUSHOVER ANALYSIS FOR RC FRAME

An elastic analysis gives a good indication of the elastic capacity of buildings and indicates where first yielding will occur, it cannot predict failure mechanisms and account for redistribution of forces during progressive yielding. Inelastic analyses procedures help to demonstrate how buildings really work by identifying modes of failure and potential for progressive collapse. The use of inelastic procedures for design and evaluation is an attempt to help engineers in better understanding as to how buildings will behave when subjected to major earthquakes, where it is assumed that the elastic capacity of the building will be exceeded. This resolves some of uncertainties associated with code and elastic procedures. Various analytical methods are available, both linear and non-linear for evaluation of concrete building. The best basic inelastic method is nonlinear time history analysis method. This method is too complicated and considered impractical for general use. The central focus of this thesis is to introduce the simplified non-linear procedure for the generation of the ¬pushover" or capacity curve of a structure This represents the plot of progressive lateral displacement as a function of the increasing level of force applied to the structure. Pushover analysis is a simplified static nonlinear analysis method which uses capacity curve and response spectrum to estimate maximum displacement of a building for a given earthquake.

Pushover analysis is an approximate non-linear analysis method in which the structure is subjected to monotonically increasing lateral forces with an invariant height-wise distribution. Pushover analysis consists of a series of sequential elastic analyses, superimposed to approximate a force-displacement curve of the structure. Initially, a two or three dimensional model which includes bilinear or tri-linear load deformation diagrams of all lateral force resisting elements is first created. A predefined lateral load is applied while the gravity load remains as constant. The lateral forces are increased until some members yield. The structural model is modified to account for the reduced stiffness of yielded members and lateral forces are again increased until additional members yield. The process is continued until a control displacement at the top of building reaches a certain level of deformation or structure becomes unstable. The roof displacement is plotted with base shear to get the global capacity curve as shown in Figure 2.15.

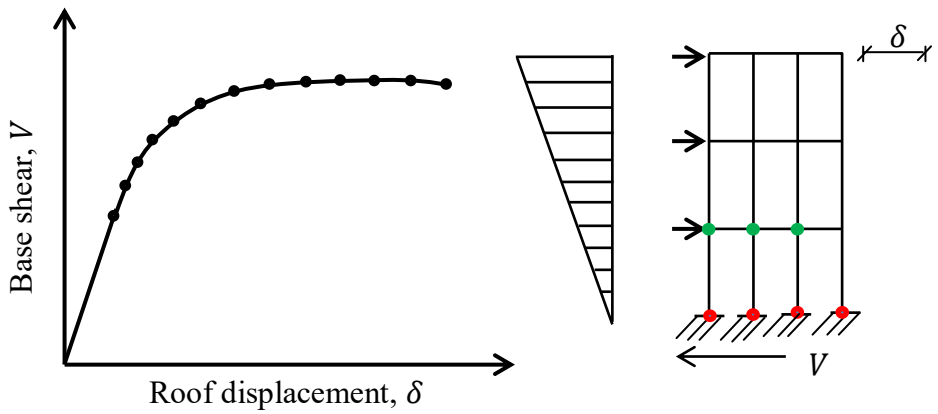

Figure2.18 Global capacity (pushover) curve of RC building (ATC 40, 1996)

Generally, pushover analysis is performed as displacement-controlled rather than force-controlled. In displacement-controlled procedure, specified drifts are sought (as in seismic loading) where the magnitude of applied load is not known in advance. The magnitude of load is increased or decreased as necessary until the control displacement reaches a specified displacement value. In displacement control method the target displacement is considered to be four percent. The internal forces and deformations computed at the target displacement are used as estimates of inelastic strength and deformation capability. The applied force and displacement once plotted forms the capacity curve. This curve has to be compared with available demand curve shown in Fig. 2.15. A graphical representation of pushover analysis is given as Figure 2.19.

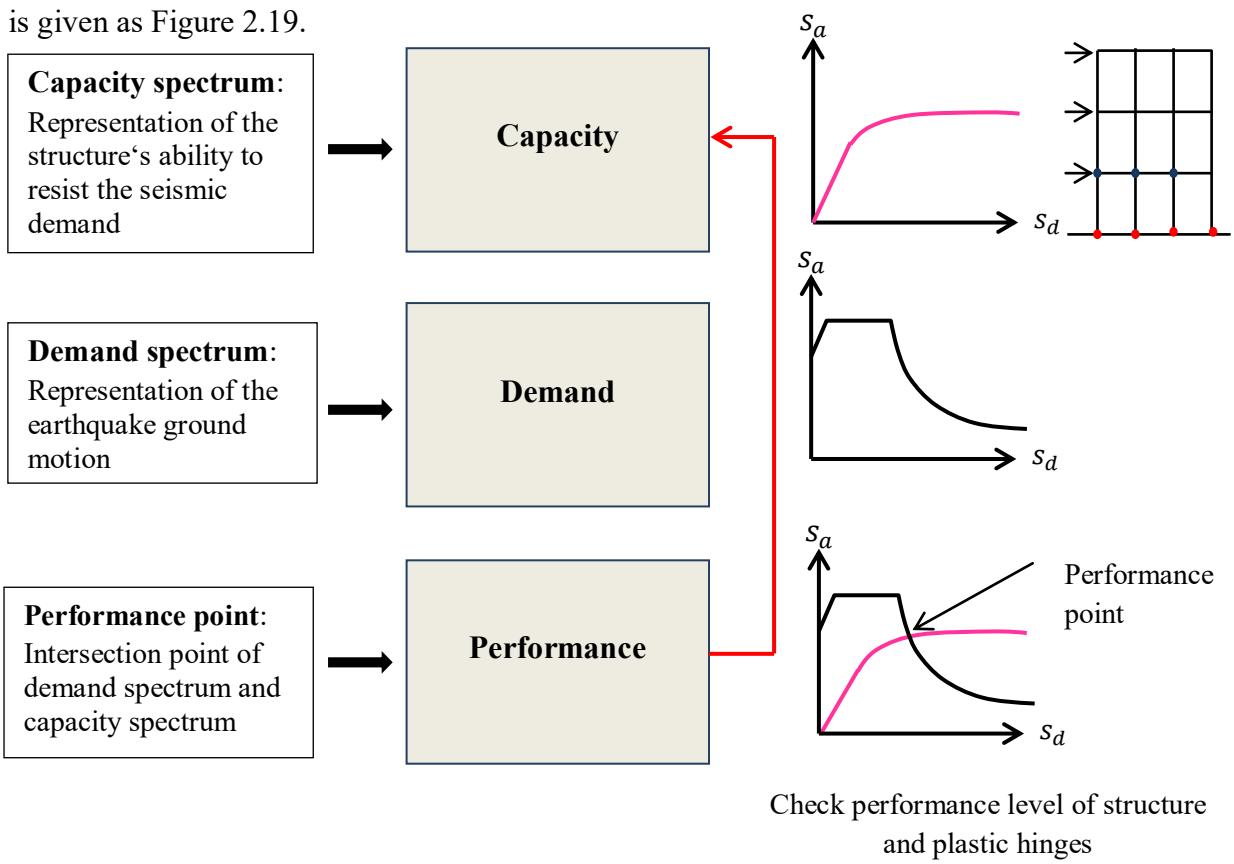

Figure 2.19 Pictorial view of pushover analysis procedure

The nonlinear static analysis procedure requires determination of three primary elements: capacity, demand and performance (ATC 40, 1996). It is to note that the intersection point of demand and capacity curve is known as the performance point. This point is the cardinal point which indicates the ultimate performance ability of any structure prior to collapse. Pushover analysis on a building is conducted to identify the performance point. Each performance point will have a corresponding special displacement.

2.15 COLLAPSE MODELING OF RC FRAME BUILDING

Soft storey building with open ground storey is considered to be vulnerable during earthquake. The rigid blocks at the upper storeys of soft storey building move as a body having limited energy absorption and displacement capacity. Thus ground storey column deflects maximum and reach inelastic limit early than expected. Collapse of the building is imminent when the energy absorption or displacement capacity of the ground storey column is exceeded by the energy or displacement demand. This concept is best illustrated using the ‗Capacity Spectrum Method' shown in Figure 8 where the seismic demand is represented in the form of an acceleration-displacement response spectrum (ADRS diagram). The structural capacity of the soft storey building is estimated by nonlinear pushover analysis and expressed in acceleration-displacement relationship (Wilson and Lam, 2006).The structure is considered to survive the design earthquake if the capacity curve intersects the demand curve and collapse if it fails to do so. In regions of high seismicity, the maximum displacement demand could exceed 200-300mm which translates to a drift in the order of 5-10% in a soft storey structure, which is significantly greater than the drift capacity of such structures even if the columns have been detailed for ductility (Paulay and Priestley, 1992). This is the reason soft storey structures behaved poorly and collapsed in larger earthquake events around the world. In high seismic regions, buildings are configured and detailed so that in an extreme event a rational yielding mechanism develops to dissipate the energy throughout the structure and increase the displacement capacity of the building. Ductile detailing in reinforced concrete columns includes closely spaced closed stirrups to confine the concrete, prevent longitudinal steel buckling and to increase the shear capacity of columns (Mander, 1988; Park, 1997; Paulay and Priestley, 1991; Watson *et al*, 1994; Priestley and Park, 1987; Bae et al, 2005, Priestley, 1994; Bayrak and Sheikh, 2001; Berry and Eberhard, 2005; Pujol et al, 2000; Saatcioglu and Ozcebe, 1992). The emphasis is on the prevention of brittle failure modes and the encouragement of ductile mechanisms through the formation of plastic hinges that can rotate without strength degradation to create the rational yielding mechanism.

Current detailing practice in the regions of lower seismicity typically allow widely spaced stirrups (typical stirrup spacing in the order of the minimum column dimension) resulting in concrete that is not effectively confined from crushing and spalling, longitudinal steel that is not prevented from buckling and columns that are weaker in shear. Design guidelines that have been developed in regions of high seismicity (ATC40, FEMA 273) recommend a very low drift capacity for columns that have such a low level of detailing. The application of such standards in the context of low-moderate seismicity regions results in most soft-storey structures being deemed to fail when subject to the earthquake event consistent with a return period in the order of 500 – 2500 years.

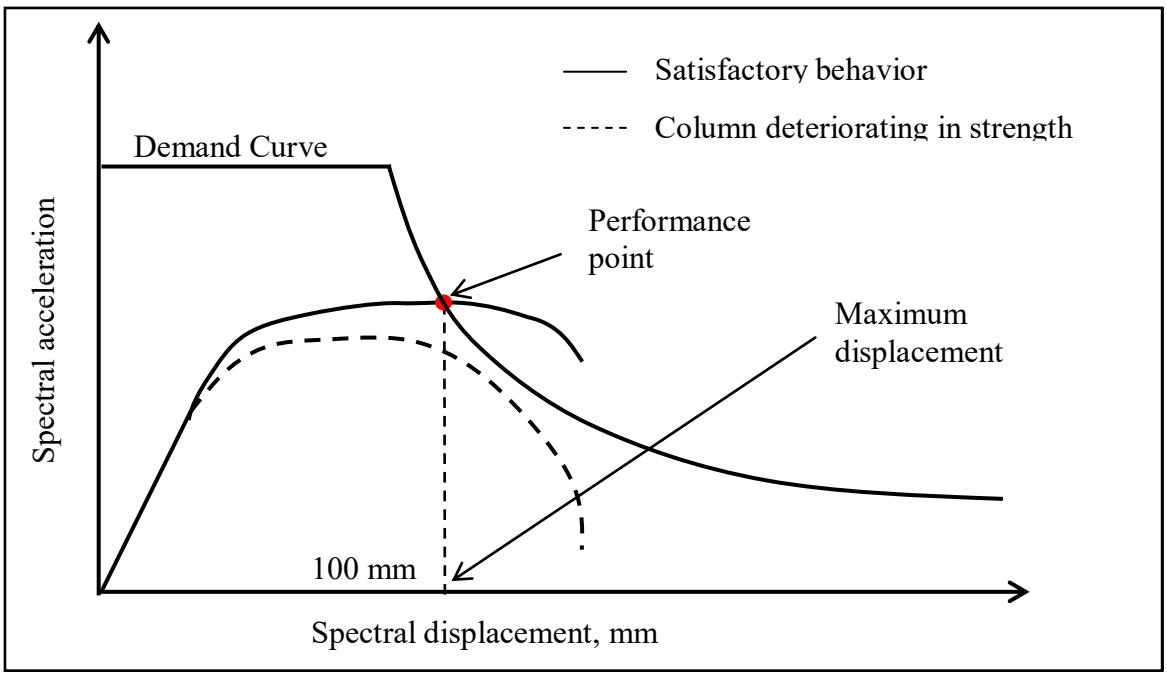

Figure 2.20 Schematic view of acceleration-displacement response spectrum diagram

2.16 PAST RESEARCH ON SOFT STOREY BUILDING

Experimental works on infill panel were conducted in mid of 20th century. Thomas (1953) and Wood (1958) studied on infill panel and found that the relatively weak infill can contribute significantly to the stiffness and strength of an otherwise flexible frame.

Smith (1962) conducted a series of tests on laterally loaded square mild steel frame model with micro-concrete infill. Monitoring the model deformations during the tests, he stated that the frame separates from infill over three quarters of the length of each frame member. These observations led to the conclusion that the infill wall can be replaced by an equivalent diagonal strut connecting the loaded corners.

Mainstone (1971) presented results of series of tests on model frame with infill of micro-concrete. He found that factors such as the initial lack of fit between the infill and the frame, variation in the elastic properties and strength of the infill can result in a wide variation in behavior between nominally identical specimens.

Costa Rican code (1986) has specific guidelines on soft storey buildings. The code proposed that all structural resisting system must be continuous from the foundation to the top of the building and stiffness of a storey must not be less than 50% of that of the storey below.

Mehrabi and Shing (1997) developed a cohesive dilatants interface model to simulate the behavior of mortar joints between masonry units as well as the behavior of frame to panel interface, and a smeared crack finite element formulation has been used to model concrete in the RC frame and masonry units in the infill panel.

Arlekar, Jain and Murty (1997) highlighted the importance of explicitly recognizing the presence of the open ground storey in the analysis of the building. The error involved in modeling such buildings as complete bare frames, neglecting the presence of in-fill in the upper storey, is brought out through the study of an example building with different analytical models.

Fardis and Panagiotakos (1997) studied through numerical analyses the effect of masonry infill on the global seismic response of reinforced concrete structures. Response spectra of elastic SDOF frames with nonlinear infill show that, despite their apparent stiffening effect on the system, infill reduces spectral displacement mainly through their high damping in the first large post-cracking excursion.

Ghosh and Amde (2002) verified the design of infilled frames to resist lateral load on buildings in terms of their failure modes, failure load and initial stiffness using procedures proposed by Riddington (1984) and Pook and Dawe (1986). This verification is made by comparing the results of the analytical procedures of the previous authors with those of a new finite element model for installed frames, which are verified using experimental results.

Mezzi (2004) illustrated soft storey to be very dangerous from seismic viewpoint as the lateral response of these buildings is characterized by a large rotation ductility demand concentrated at the extreme sections of the columns of the ground floors, while the

superstructure behaves like a quasi-rigid body. A solution was proposed for the preservation of a particular architectonic double soft storey configuration.

Huang (2005) studied the structural behaviors of low-to-midrise concrete buildings of various configurations with emphases on dynamic properties, internal energy, magnitude and distribution of seismic load. Several idealized models were made to represent different structural configurations including pure frame, frames with fully or partially infill panels, and frames with a soft storey at the bottom level. Comparison was made on the fundamental periods, base shear, and strain energy absorbed by the bottom level between these structures.

Rodsin (2005) evaluated the potential seismic performance of building with soft storey in an area of low to moderate seismicity regions (such as Australia) by a displacement-based method involving a push-over analysis.

Amanat and Hoque (2006) studied the fundamental periods of vibration of a series of regular RC framed buildings with MI using 3D FE modeling. It has been found that when the models do not include infill, as is done in conventional analysis, the period given by the analysis is significantly longer than the period predicted by the code equations justifying the imposition of upper limit on the period by the codes. It is also observed that the randomness in the distribution of infill does not cause much variation of the period if the total amount of infill panels is the same for all models.

Shaiful and Amanat (2007) carried out nonlinear time history analysis of RC frames with brick masonry infill. In their study, a solution was proposed to magnify the bending moment and shear force of soft ground storey column to compensate the soft storey effect.

Amanatand Haque (2009) further carried out extensive study on behavior of soft storey building as well as their seismic vulnerability. According to their study, the differences of moment and shear force of ground floor and 1st floor are very large due to the presence of soft ground floor. The study has also shown that base shear of RC framed building with open ground floor is approximately doubled in comparison to its base shear when calculated as bare frame.

Hasnain (2009) studied the phenomenon of soft storey building. He determined the effect of randomly distributed infill on seismic base shear for RC buildings with soft ground floor. His studied the soft storey effect with constant beam and column size, partition wall loads.

Quayum, Iasmin and Amanat (2009) analyzed RC frames with open ground storey. It was found that the structural responses i.e., base shear, column axial force, moment and natural period do not change appreciably by the ESFM for random infill distributions, while they increase enormously in the RSM analysis.

Tasmim and Amanat (2013) investigated RC frame structure having various percentages of masonry infill on upper floors with no infill and 20% infill on ground floor. The application of infill has been done randomly and the effect of seismic load has been investigated. From the investigation, it has been found that random (irregular) distribution of infill does not cause any significant variation in base shear for commonly occurring range of infill percentage on upper floors (40% and above). Actually it is the total amount of infill that affects the base shear as obtained by dynamic analysis. It has been also found that base shear ratio does not vary significantly with the span number or length, rather than it mainly depends on the number of floors. They suggested a simple expression for base shear ratio as a function of the number of floors which may be used to magnify base shear obtained by ESFM.

2.17 REMARKS

Soft storey building constructed without considering MI effect may get early damage during maximum earthquake and casualties could be fatal in a city like Dhaka. In seismic vulnerable zone, construction of building with soft ground storey is considered to be hazardous. This type of construction cannot be avoided because of lack of proper guidelines or restriction by the codes. As such developing an improved seismic design code for such building design would ensure a higher degree safety against seismic hazard.

Total seismic base shear as experienced by a building during an earthquake is dependent on its natural period; the seismic force distribution is dependent on the distribution of stiffness and mass along the height. In buildings with soft ground storey, the upper storey being stiff undergoes smaller inter-storey drift. But the inter-storey drift in the soft ground storey is large, which in turn, leads to concentration of forces at the connections of the storey above accompanied by large plastic deformations. In addition, the columns of the soft storeys dissipate most of the energy developed during the earthquake. In this process the plastic hinges are formed at the ends of columns, transforming into the soft storey mechanism. When this occurs in a lower storey, the collapse is unavoidable.

Conventional design of building is based on static linear analysis. The basic assumption in static linear analysis is that only the first mode of vibration of buildings governs the dynamics and the effects of higher modes are not significant; therefore, higher modes are not considered in the analysis. Thus, irrespective of whether the building is regular or irregular, static analysis is incapable of capturing the true dynamic behavior of soft storeyed building. As such high rise soft storey building is analyzed by any nonlinear method to visualize its nonlinear performance during seismic loading. In this study, pushover analysis is considered as the said nonlinear analysis method. Moreover, soft storey building is investigated by this method with different parameters to observe the behavior of soft ground storey columns.

CHAPTER 3

DEVELOPMENT AND ANALYSIS OF MODEL

3.1 INTRODUCTION

This chapter describes the development of finite element models of RC moment resisting frame building. In this study, two moment resisting frame models are considered namely bare frame and soft storey frame under different circumstances. Suitable software is used to create and analyze the models for static loading. Selection and development of structural elements, physical properties, loads, nonlinear hinges, deflection pattern, etc. are described in the subsequent paragraphs. Analysis techniques are also briefly illustrated in this chapter. Soft storey models are developed keeping the ground storey open to visualize the impact of soft storey phenomena on ground storey columns. Besides, a two storey building is manually calculated by nonlinear pushover analysis method to evaluate its nonlinear performance.

3.2 SOFTWARE USED FOR DEVELOPMENT OF MODEL

There are many finite element analysis tools or packages in the civil engineering field. They vary in degree of complexity, usability and versatility. Such packages are ABAQUAS, DIANA, ANSYS, ETABS, STRAND, ADINA, FEMSKI, SAP, STAAD, etc. Amongst these programs, ETABS has been proved to be relatively easy and appropriate for the study. ETABS model is object-based which consists of joint, frame, link and shell objects. These objects can be assigned as beams, columns, braces, floors, walls, loads, etc. The version of ETABS that has been used for this study is ETABS 2015 Ultimate. This version is capable of both linear and nonlinear analysis of any building model.

3.3 DEVELOPMENT OF RC MODELS

3D RC building models are developed in three steps by using the selected software. In first step, a series of joint, frame, link and shell elements are drawn to represent the building model using various drawing tools of the program. Structural properties and loads are assigned to the elements as second step. Finally meshing is done for floor element. Following elements are used for this research work:

- Element joints are automatically created at the corners or ends.
- Frame elements are used to model beams, columns and braces.
- Link element is used to model equivalent diagonal strut.
- Shell element is used to model slabs to develop floor and roof.

3.4 PARAMETERS OF REFERENCE MODELS

Two reference building models are developed namely bare frame and soft storey frame for parametric study and their geometric parameters, assigned loads and are shown in the Table 3.1. These reference buildings have six spans in direction and six bays in direction. Span length and bay width of the reference building models are considered basing on the common trend of high-rise buildings of Dhaka city.

Table 3.1 Parameters of reference building models

Parameter	Value	Reference
Span length (mm)	5500	
Bay width (mm)	5500	
Ground storey (mm)	4000	
Other storey (mm)	3000	
Beam exterior (mm)	575 × 300	
Beam interior (mm)	500 × 300	
Column exterior	500 ×500	
Column interior	600 × 600	
Diagonal strut (mm)	375 × 175	
Slab thickness (mm)	125	
Floor finish (KN/m²)	1.437	
Live load (KN/m²)	1.919	
Partition wall (KN/m²)	3.75	
Concrete compressive strength (MPa)	21	
Concrete compressive strength (MPa)	28	
Rebar yield strength (MPa)	415	
Poison ratio (Concrete)	0.2	
Infill percentage (%)	70	
Modulus of elasticity of infill material (MPa)	9350	BNBC (Draft), 2015
Concrete and rebar nonlinear hysteresis type	Takeda	Takeda, 1970
Concrete and rebar acceptance criteria of strain	-	BNBC (Draft), 2015

3.5 BARE FRAME (BF) MODEL FOR LINEAR ANALYSIS

The reference bare frame model for linear analysis is developed considering beams, columns and slab only. Initial dimensions of beam and column are calculated following standard design guidelines of BNBC (Draft), 2015. Later on a design check is conducted by the selected software to confirm its correctness and suitability for the study. The slab thickness is calculated by the traditional design procedure of RC slab as given in the section 6.2.5.3.3 of chapter 6 of BNBC (Draft), 2015. All the loads are calculated considering the load table of BNBC (Draft), 2015. Concrete compressive strength of slab and beam/column is considered as 21 MPa and 28 MPa respectively. Rebar is considered as 60 grade steel bar. Poisson ratio of concrete is considered as 0.2 for the study. The 3D and elevation views of bare frame and soft storey frame are given in Figure 3.1 to 3.2.

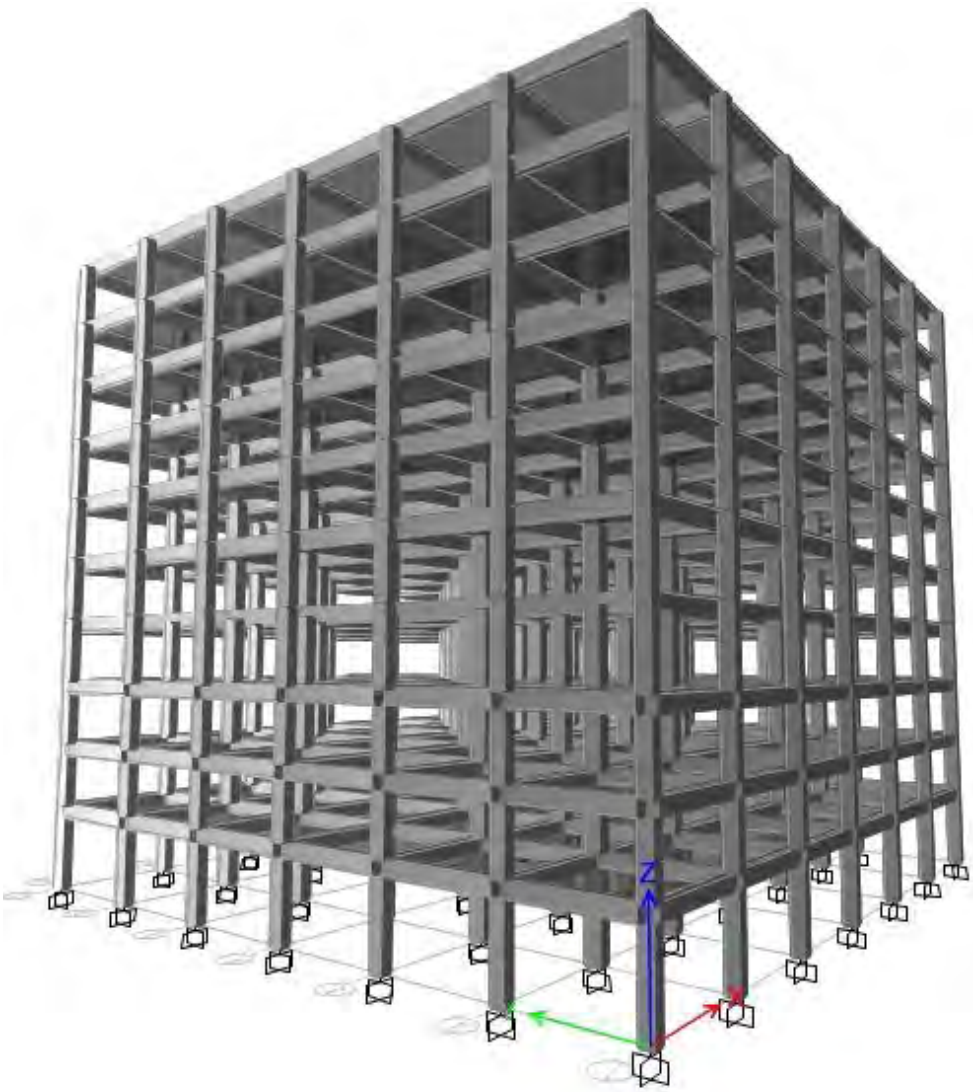

Figure 3.1 3D view of bare frame building model

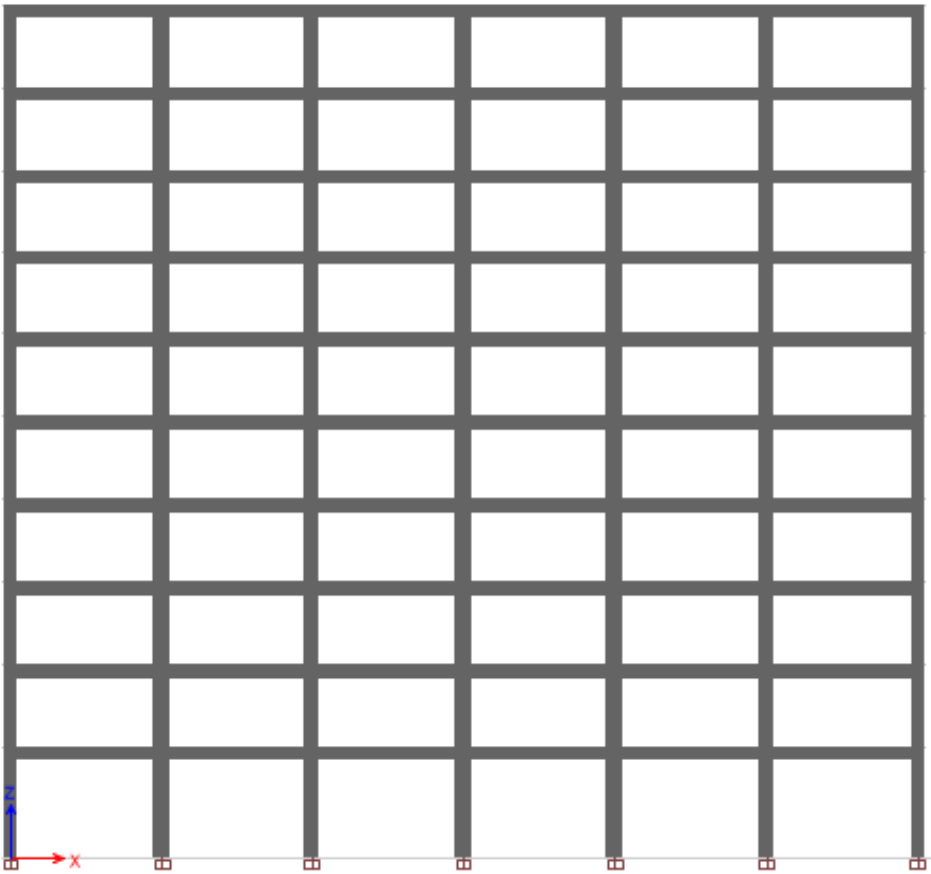

Figure 3.2 Elevation view of bare frame building model

3.6 SOFT STOREY FRAME (SSF) MODEL FOR LINEAR ANALYSIS

The reference soft storey frame model for linear analysis is similar to the bare frame model as described above except the inclusion of equivalent diagonal strut. MI of soft storey building is represented by equivalent diagonal strut. The engineering properties of MI are considered as per the guidelines of ATC 40, 1996. Each diagonal strut is developed considering the concentric strut analogy. The width of the diagonal strut is calculated following Mainstone (1971) equations and obtained dimension is given in the Table 3.1.The strut has the same thickness and modulus of elasticity as the infill panel it represents. The slab thickness is calculated according to the BNBC (Draft), 2015. All the loads are calculated considering the loading pattern of high-rise residential buildings of Dhaka city and following the load table of BNBC (Draft), 2015. Concrete compressive strength for slab and beam/column is considered as21MPa and 28MParespectively. Rebar is considered as usual 60 grade steel bar. Poisson ratio of concrete is considered as 0.2 for the study. Other details are given in the table 3.1.The 3D and elevation views of soft storey MI frame are given in Figure 3.3 to 3.4.

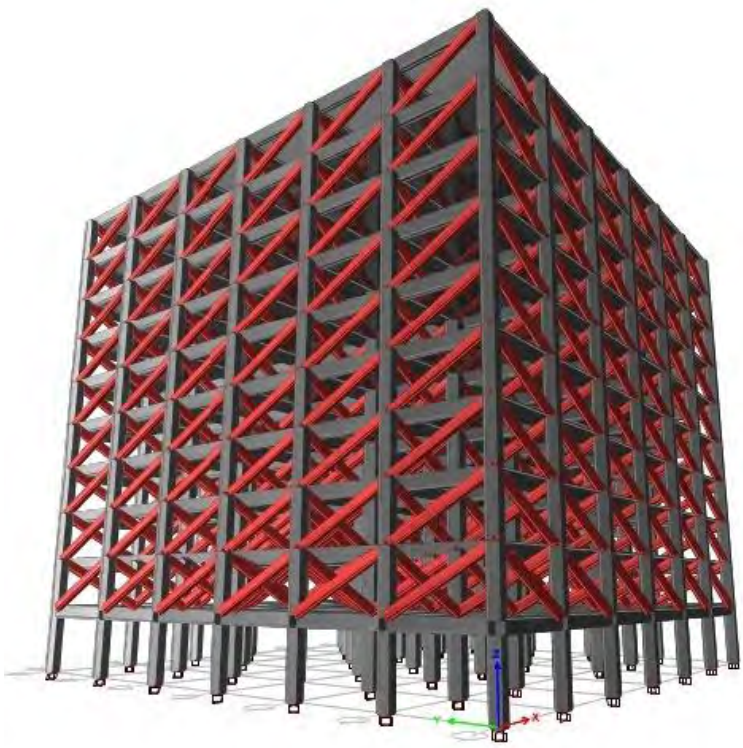

Figure 3.33D view of soft ground storey building model with MI

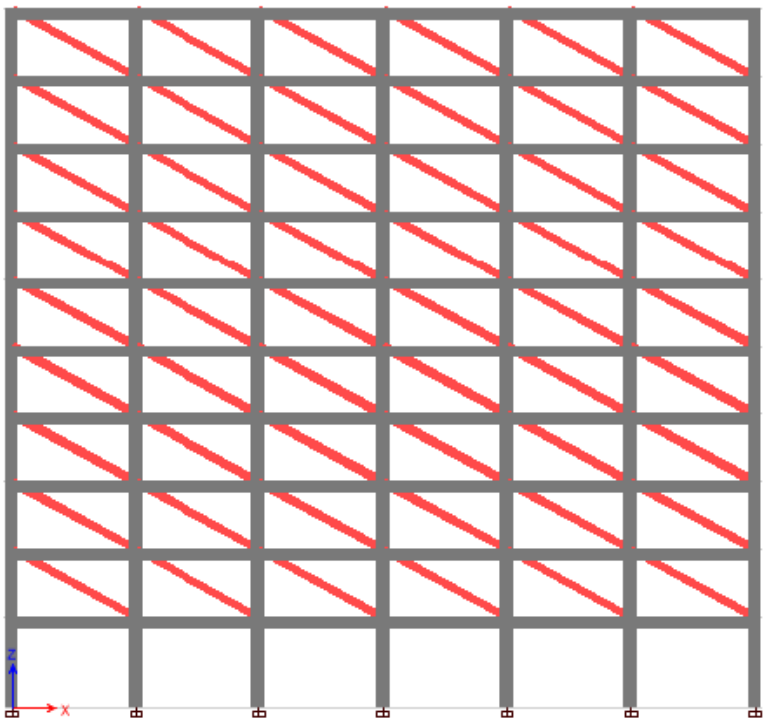

Figure 3.4 Elevation view of soft ground storey building model with MI

3.7 BARE FRAME (BF) MODEL FOR NONLINEAR ANALYSIS

The reference bare frame model is developed by incorporating plastic hinges to the beams and columns for nonlinear analysis. Nonlinear material properties are defined to the concrete section elements of this model. The hinges are assigned to the beams and columns as per the

guidelines of FEMA 356, 2000. All the loads, concrete strength, poissons ratio, etc are kept similar to above models. The moment type (M_3) plastic hinges are assigned to the beams and $P - M - M$ type plastic hinges are assigned to the columns.

3.8 SOFT STOREY FRAME (SSF) MODEL FOR NONLINEAR ANALYSIS

A reference soft storey frame model is developed by incorporating plastic hinges to the beams, columns and diagonal struts for nonlinear analysis. The moment type (M_3) plastic hinges are assigned to the beams, $P - M - M$ type plastic hinges are assigned to the columns and axial hinges are assigned to the diagonal struts. The hinge length for beam, column and diagonal strut is calculated following the formula given in the paragraph 3.14 below. The beam and column hinges are assigned automatically by using software where hinge length of diagonal struts is assigned manually. Hinge length always starts from the inner face of beam or column. The axial force in the diagonal start is calculated following procedures mentioned in paragraph 3.12. In case of assigning axial hinge to the diagonal strut, MI is checked for its in-plane and out-of-plane actions as described in the paragraph 3.14.

3.9 DESIGN CHECK OF REFERENCE MODELS

The reference building models discussed above are checked for their feasibility and accuracy as per the ACI standard using software. The models are found to be adequate and feasible. In the design check special attention was given to the ground storey columns and beams. The 3D view of the reference model is given as Figure 3.5.

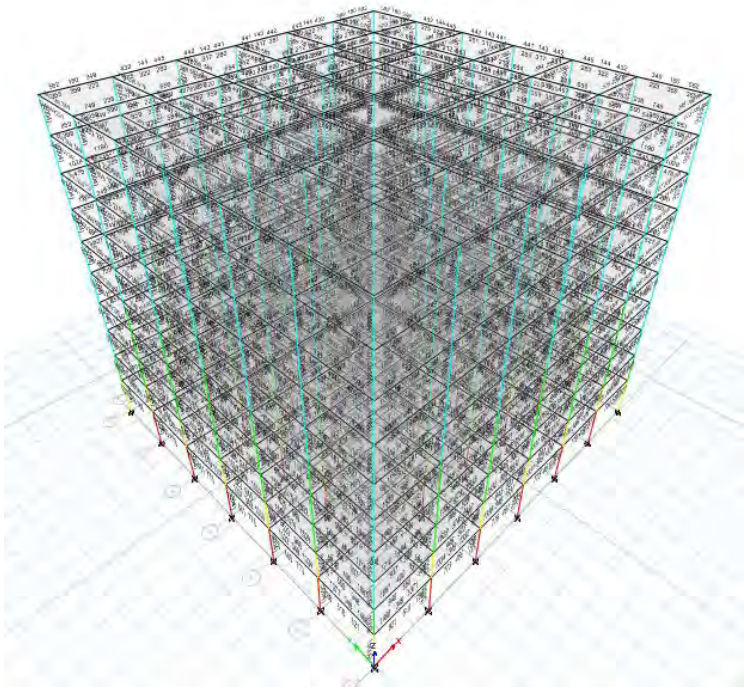

Figure 3.5 3D view of soft storey building after design check

3.10 MATERIAL PROPERTIES

Performance of structural concrete depends on the material characteristics and behavior under loads. In most cases the material property is better described by the stress - strain relationship under the type of stress to which the material is subjected in the structure. Material properties for the beam and column elements for the constituent models are described below.

3.10.1 Reinforced Concrete Element

Development of a material model for behavior of concrete is not an easy task. Concrete is a quasi-brittle material and has different behavior in compression and tension. The tensile strength of concrete is typically 8 to 15 percent of the compressive strength (Shah, et al., 1995). Figure 3.6 shows a typical stress-strain curve for normal weight concrete (Mander, 1988) to express its material property. The strength of concrete and reinforcement are taken as 8 MPa and MPa respectively. Modulus of elasticity, E_c for concrete of this study is obtained as 24855.58 MPa. In this thesis the stress-strain relation is used to model plasticity behavior of concrete under monotonic incremental loading beyond elastic limit. However in material modeling, the acceptance criteria of strain for compression are set Immediate Occupancy (IO), the Life Safety level (LS) and the Collapse Prevention (CP) level are three performance levels as mm/mm, mm/mm and mm/mm respectively. This stress-strain curve is applicable for all concrete element models in varying strength.

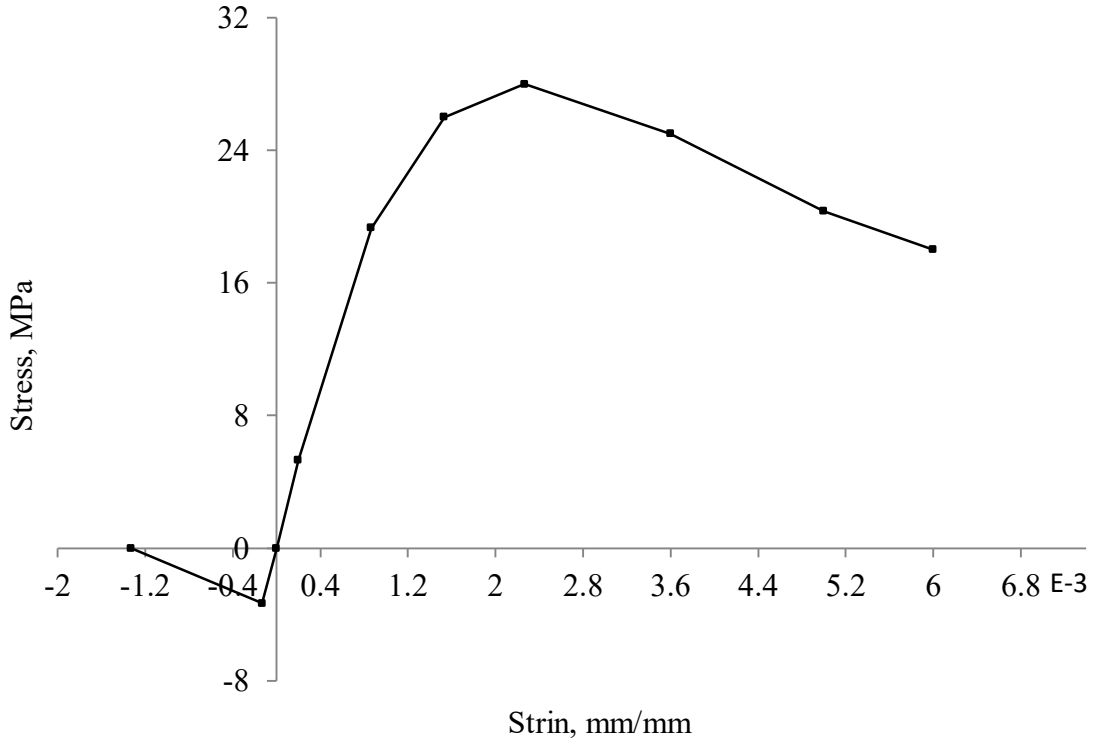

Figure 3.6 Typical concrete stress–strain curve (Mander, 1988)

3.10.2 Steel Reinforcement

Steel reinforcement in the reinforced concrete section enhances it strength enormously. Keeping this in mind, the frame elements are designed as section elements. It is also assumed that the reinforcement of section elements will be able to impart adequate ductility to the members due to ground acceleration.

3.10.3 Section Elements

Material properties are assigned to each beam/column/slab element to define the structural behavior of that element in the model. Sectional properties must be specified before assigning them as elements. A typical section stress–strain curve of a column element is given in Figure 3.7 below to depict its section property. Section properties are also specified in terms of its cross section, torsional constant, moment of inertia, mass and weight. The section properties are generally considered as unity for linear analysis. In nonlinear analysis, section properties like torsional constant and moment of inertia are modified due to the occurrence of permanent deformation in the section. In this study, torsional constant exterior beams and interior beams are considered as 0.01and 1.0 respectively. Moment of inertia of beam, column and slab sections is also modified as $_g$, $_g$ and $_g$, respectively.

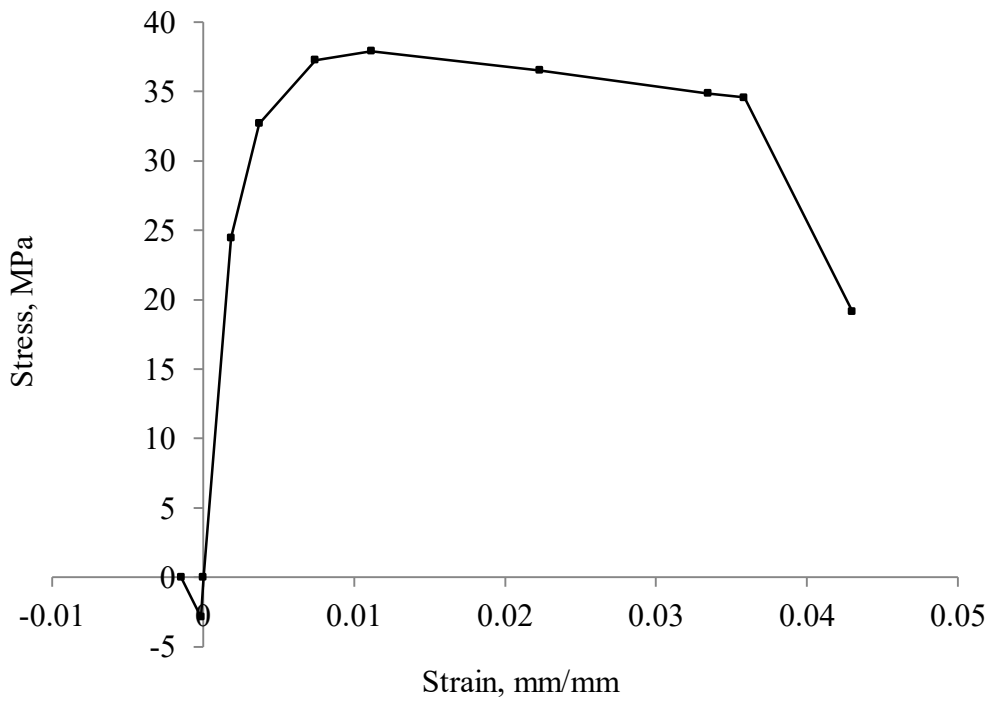

Figure 3.7 Typical frame section stress–strain curve (Mander, 1988)

3.11 MODELING OF MASONRY INFILL

MI panels of reference building models are modeled by replacing each panel with an equivalent diagonal masonry compression strut. By ignoring the tensile strength of the infill masonry, the strut provides a lateral load-resisting mechanism for the opposite lateral directions of loading. Figure 3.8 shows the analytical model and the strength envelope for masonry infill walls.

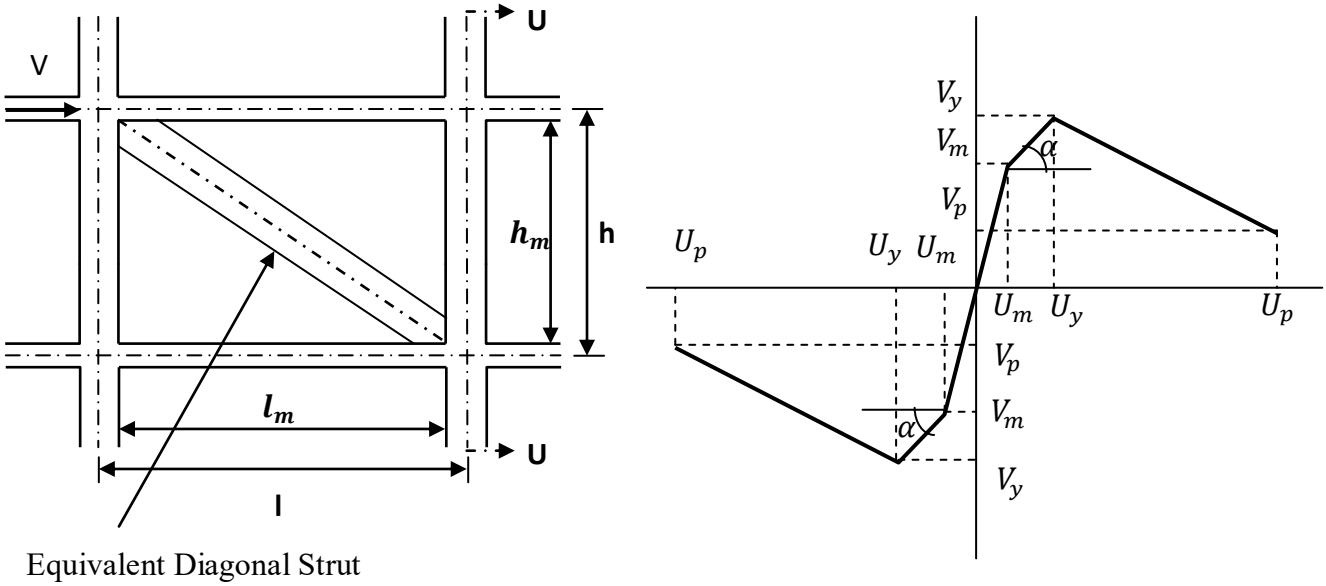

Fig. 3.8 Strength envelope for conventional masonry infill walls and analytical model (Mostafaei and Kabeya, 2004)

The main factors of the envelope model (Figure 3.8) are shear strengths at the assumed yielding point, V_y, at the maximum point, V_m, and the post-peak residual shear strength, V_p, and their corresponding displacements U_y, U_m and U_p respectively. In this figure α is the ratio of stiffness after yielding to that of the initial stiffness. To obtain the main parameters of the envelope curve, maximum lateral strength, V_m are estimated considering the two critical failure modes namely sliding shear and compression failures as mentioned in chapter 2. The other factors are approximated from the following equations. The maximum displacement at the maximum lateral force is estimated by given equation, Madan et al. (1997):

$$\mathrm{U_m} = \frac{\varepsilon'_{\mathrm{m}} \times \mathrm{d_m}}{\cos\theta} \tag{3.1}$$

Where, ε'_m is the masonry compression strain at the maximum compression stress; here, $\varepsilon'_m = 0.0018$, and d_m is the diagonal strut length. In any case, $\varepsilon'_m = \frac{U_m}{h_m} \leq 0.008$

3.12 DESIGN OF DIAGONAL STRUT

3.12.1 Length and Width of Diagonal Strut

The length of diagonal strut = $\sqrt{(4900^2 + 2600^2)} = 5547$ mm

The angle of diagonal strut with the beam = $\theta = \tan^{-1}\left(\frac{h_m}{l_m}\right) = \tan^{-1}\left(\frac{2600}{4900}\right) = 27.95$

$$\lambda H = \left[\frac{E_m\ t\ \sin 2\theta}{4\ E_c\ I_c\ h_m}\right]^{\frac{1}{4}} \times h = \left[\frac{3217.5 \times 230 \times \sin 55.9}{4 \times 24862 \times 1.08 \times 10^{10} \times 2600}\right]^{\frac{1}{4}} \times 3000 = 2.74$$

$a = 0.175 \times (2.74)^{-0.4} \times 5547 = 648.63$ mm

$a_{mod} = 0.7 \times 649 = 454$ mm

Here, thirty percent opening is considered in each masonry infill panel. This percentage may vary due to the size of door and windows.

The initial stiffness, k_0, is estimated by the following equation as suggested by Madan et al. (1997) :

$$K_0 = 2\frac{V_m}{U_m} \tag{3.2}$$

The lateral yielding force, V_y and displacement, U_y are calculated from the geometrical equation derived from Fig. 3.8.

$$V_y = \frac{(V_m - \alpha\ K_0\ U_m)}{(1 - \alpha)} \tag{3.3}$$

$$U_y = \frac{V_y}{K_0} \tag{3.4}$$

Here, the value of α is assumed to be equal to 0.2.

U_P and V_P are defined from the previews of experimental results of Mostafaei and Kabeya, 2004. The average value of drift ratio at the 80 percent post-peak point, defined as a point on the envelope curve, is about one percent for solid brick wall (Mostafaei and Kabeya, 2004). The U_P and V_P are determined considering that the line connecting the peak of the envelope and point (U_P, V_P) passes through the 80 percent post-peak point. Therefore, the equation of V_P as suggested by Mostafaei and Kabeya, 2004 is given below:

$$V_P = 0.3\ V_m \tag{3.5}$$

$$U_P = 3.5(0.01h_m - U_m) \tag{3.6}$$

3.12.2 Calculation of Lateral Force Capacity of Infill Wall

The lateral force capacity for infill wall in the compression failure mechanism is calculated as:

$$V_c = \frac{454 \times 230 \times 4.29 \times \cos 27.95}{1000} = 395.71\ \text{KN}$$

The lateral force capacity for infill wall in the slide shear failure mechanism is calculated as:

$$V_f = \frac{0.172 \times 230 \times 4900}{(1 - 0.66 \tan 27.95)1000} = 298.31\ \text{KN}$$

The maximum shear strength of infill wall according to ACI 530-88 is as follows:

$$V_{max} = \frac{0.814 \times 230 \times 4900}{1000} = 917.38\ \text{KN}$$

The selected of minimum shear strength from above three types of failure mechanisms is given below:

$$V_m = V_f = 298.31\ \text{KN}$$

From the equation 3.1;

$$U_m = \frac{0.0018 \times 5547}{\cos 27.95} = 11.3\ \text{mm}$$

The initial stiffness K_0, lateral yielding force, V_y and displacement, U_y can be estimated as:

$$K_0 = 2 \times \frac{298.31}{11.3} = 52.8\ \text{KN/mm}$$

$$V_y = \frac{(298.31 - 0.2 \times 52.8 \times 11.3)}{(1 - 0.2)} = 223.73\ \text{KN}$$

$$U_y = \frac{223.73}{52.8} = 4.24\ \text{mm}$$

The lateral post-peak ultimate force, V_P and ultimate displacement, U_P are as follows:

$$V_p = 0.3 \times V_m = 0.3 \times 298.31 = 89.5\ \text{KN}$$

$$U_P = 3.5(0.01 \times 2600 - 11.3) = 51.45 \text{ mm}$$

Finally, the strength envelope of the masonry infill walls of this study is given below:

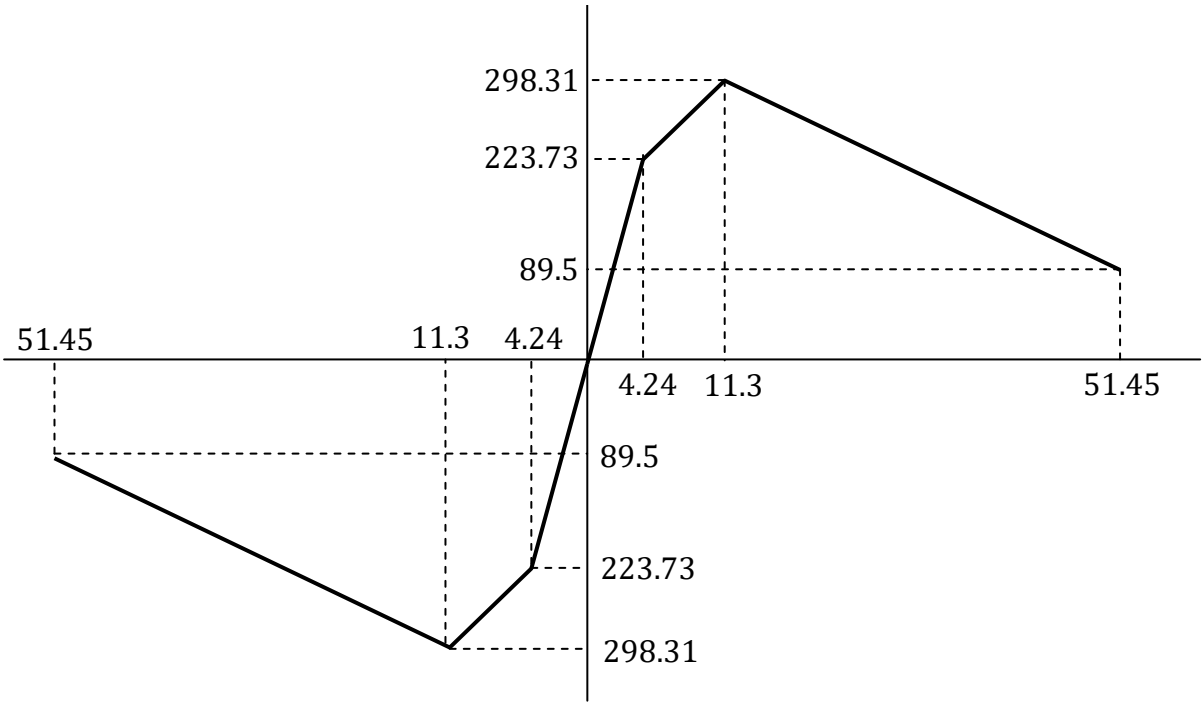

Fig. 3.9 Strength envelope of the masonry infill walls (Mostafaei and Kabeya, 2004)

3.12.3 Stress-strain Relation of Masonry Infill

The area of equivalent diagonal strut, $A_d = a \times t = 455 \times 230 = 104420 \text{ mm}^2$

Stresses of masonry infill at yield point, maximum point and collapse point are expressed as a_y, a_m and a_P respectively.

$$a_y = \frac{223.73 \times 1000}{104420 \times \cos 27.95} = 2.43 \text{ MPa}$$

$$a_m = \frac{298.31 \times 1000}{104420 \times \cos 27.95} = 3.23 \text{ MPa}$$

$$a_P = \frac{89.5 \times 1000}{104420 \times \cos 27.95} = 0.97 \text{ MPa}$$

Strains of masonry infill at yield point, maximum point and collapse point are expressed as $\varepsilon_y, \varepsilon_m$ and ε_P respectively

$$\varepsilon_y = \frac{4.24 \times \cos 27.95}{5547} = 0.0006 \text{ MPa}$$

$$\varepsilon_m = \frac{11.3 \times \cos 27.95}{5547} = 0.0018 \text{ MPa}$$

$$\varepsilon_P = \frac{51.45 \times \cos 27.95}{5547} = 0.008 \text{ MPa}$$

3.13 NONLINEAR PROPERTIES OF STRUCTURAL ELEMENTS

The ideal lateral load-deformation (backbone) curve of a building under monotonic lateral loading in pushover analysis reflects three clear features, namely linear behavior, nonlinear behavior and plastic behavior (Figure 3.9). These features may be used to identify three dominant ranges of structural behavior in the sequence in which they appear namely elastic behavior, early inelastic behavior and ductile inelastic behavior. The curve shows IO, LS and CP points by blue, light sky and light green colors respectively.

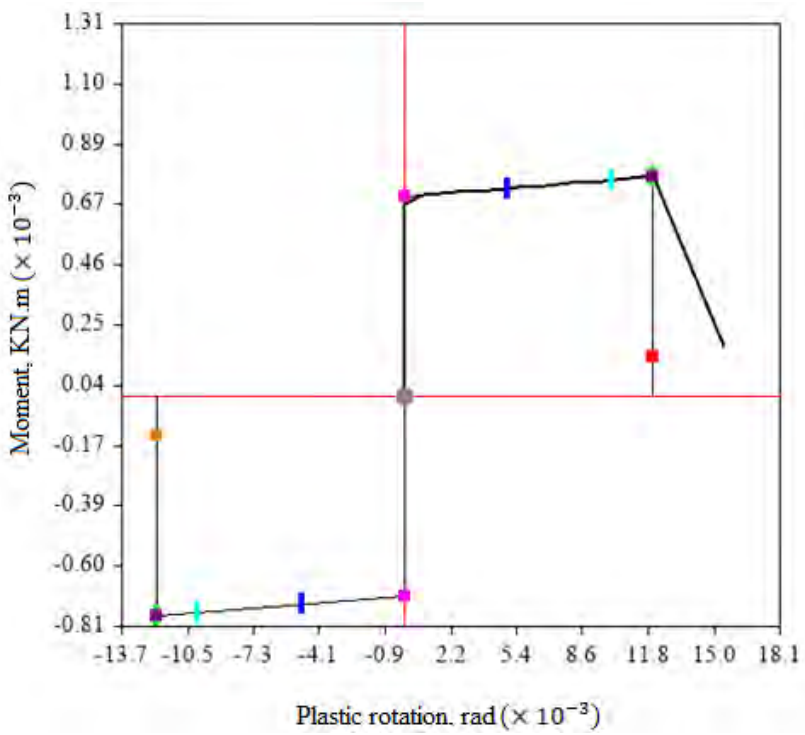

Figure Typical backbone curve of a RC interior column of reference building model

Nonlinear Hinges define the load-deformation behavior of elements‘ post-yield condition. Hinges are assigned to beam, column and strut elements of the reference building models to impart nonlinear properties to these elements. Hinges are defined in terms of their location, length and rotation pattern as given in Figure 3.8.

In frame element two hinges are assigned at both ends of each element. The length of plastic hinge is calculation by equation 3.1 or 3.2 (Paulay and Priesly, 1992).

l_p 8 l $_b f_y$ Mpa

l_p h h is the section depth 8

Here, l_p, $_b$ and f_y denote length of plastic hinge, diameter of rebar and modulus of elasticity of steel rebar respectively

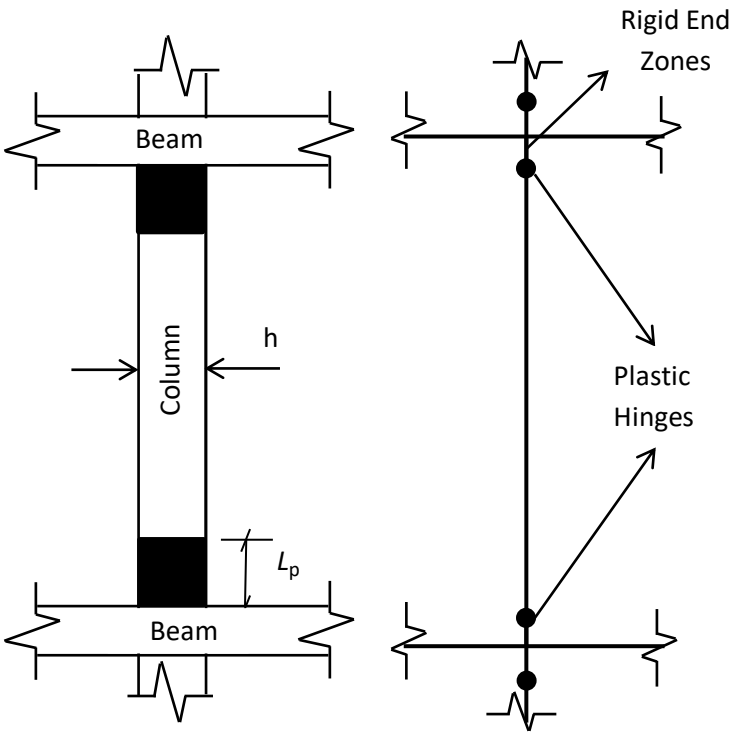

Figure Formation of plastic hinges in column element

3.14 NONLINEAR PROPERTIES OF MASONRY INFILL

3.14.1 Masonry Infill Properties and In-plane Action

Calculation of MI in-plane stiffness and strength based on nonlinear analysis of a composite frame with infill panels that account for the presence of openings and post-yield cracking of masonry is permitted by FEMA-356. The elastic in-plane stiffness of a solid unreinforced masonry infill plane prior to cracking is represented by an equivalent diagonal compression strut. The strut has the same thickness and modulus of elasticity as the infill panel it represents. Though there are different concepts of compression strut analogy but this study has considered the concentric strut analogy for the analysis.

The transfer of storey shear across a masonry infill panel confined within concrete frame is considered as a deformation-controlled action. Expected in-plane panel shear strength shall be determined as per the following requirements. Expected infill shear strength, V_{ine} , is calculated in accordance with the equation 3.9.

$$Q_{CE} = V_{ine} = A_{ni} V_{me} \quad (3.9)$$

Where, A_{ni}= Area of net mortared/ grouted section across infill panel, V_{me}= Effective shear strength of masonry infill

3.14.2 Nonlinear Procedure of Analysis

Each infill panel shall meet the requirement of deformation-controlled actions during nonlinear static analysis. Primary and secondary components shall have expected deformation capacities not less than maximum deformation demands calculated at the target displacement. Nonlinear lateral drift shall not exceed the values given in Table 3.2.

Table3.2 Nonlinear static procedure - simplified force-deflection relation for MI panel

$\beta = \frac{V_{fre}}{V_{ine}}$	$\frac{L_{inf}}{h_{inf}}$	c	d %	e %	Acceptance Criteria	
					LS (%)	CP (%)
$\beta < 0.7$	0.5	n.a.	0.5	n.a.	0.4	n.a.
	1.0	n.a.	0.4	n.a.	0.3	n.a.
	2.0	n.a.	0.3	n.a.	0.2	n.a.
$0.7 \leq \beta < 1.3$	0.5	n.a.	1.0	n.a.	0.8	n.a.
	1.0	n.a.	0.8	n.a.	0.6	n.a.
	2.0	n.a.	0.6	n.a.	0.4	n.a.
$\beta > 1.3$	0.5	n.a.	1.5	n.a.	1.1	n.a.
	1.0	n.a.	1.2	n.a.	0.9	n.a.
	2.0	n.a.	0.9	n.a.	0.7	n.a.

3.14.3 Masonry Infill Out-of-plane Action

Unreinforced infill panel is analyzed for out-of-plane seismic actions if its h_{inf}/t_{inf} ratio is more than those given in Table 3.3. It also needs to fulfill the conditions of arching action as given below. Otherwise the unreinforced infill panel is not analyzed for out-of-plane actions.

Table 3.3 Maximum h_{inf}/t_{inf} Ratios.

	Low Seismic Zone	Moderate Seismic Zone	High Seismic Zone
IO	14	13	8
LS	15	14	9
CP	16	15	10

Arching action shall be considered only if all of the following conditions exist. The conditions are as follows:

- The panel is in full contact with the surrounding frame components.
- The product of the elastic modulus and moment of inertia of the most flexible frame component exceeds a value of $3.6 \times 10^9\ \mathrm{lb} - \mathrm{in}^2$.
- The frame components have sufficient strength to resist thrusts from arching of an infill panel.
- The h_{inf}/t_{inf} ratio is less than or equal to 25.

The h_{inf}/t_{inf} ratio unreinforced infill frame of this study does not satisfy the table 3.3. On the other hand, this unreinforced infill frame meets the condition of arching action thus the frame may not be studied against out-of-plane seismic action. According to FEMA 356, 2000, the out-of-plane stiffness of infill panels shall be neglected in analytical models of the global structural system in the orthogonal direction.

3.15 HINGES FOR REFERENCE MODELS

3.15.1 Defining Hinges to Beam and Column

In nonlinear static pushover analysis, the reference models undergo nonlinear deformation causing permanent warp at the hinges of various section elements. In developing nonlinear properties of the models, hinges are to be defined and assigned to each section element. Hinge properties are calculated using table 9-6, 9-7 and 9-12 of ATC- 40, 1996. In this study, software used the hinge properties of table 10.6 and 10.7 of ASCE 41-13 manual. Hinge length of beam or column is calculated as half of the least dimension of its cross section.

In the reference models, beam hinges are defined following three steps. Firstly beams are selected than their hinge properties are incorporated and finally hinge lengths are assigned. Type of hinges defined in the beam and column elements are ‗Auto M_3‘ and ‗Auto $P - M - M'$respectively. In both the cases hinge lengths are defined manually. The hinge length calculation is as follows (if dimensions are measure from center to center of each element):

$$\text{Actual Hinge Length} = \frac{\text{Minimum Dimension of beam/column section}}{2} + \frac{\text{Column/beam width}}{2}$$

3.15.2 Define Hinges to Diagonal Strut

Diagonal strut represents MI panel of a RC building. In the software there is no provision to assign hinges to the diagonal strut thus it needs to be defined manually. In case of diagonal strut, axial hingePis selected as the diagonal strut hinge because it dominates the plastic deformation. Selecting the location of hinges for diagonal strut is influenced by MI in-plane and out-of-plane actions which have to be checked following FEMA 356, 2000. In this study, the MI of reference building models is affected by in-plane action only. Detail calculation of axial hinge of diagonal strut is given in the subsequent paragraphs.

The nonlinear static procedure-simplified force-deflection relation for MI panel of the reference models is calculated according to the section 3.12 as mentioned above. Terms c, d and e are explained in the figure 2.15 of chapter 2. According the guidelines of OPENSEES software, hinge length of diagonal strut can be considered as 10 percent of its total diagonal length. This diagonal length is basically calculated as clear length(l_1), excluding the internal diagonal length of beam-column joint as denoted by(l_2) in the Figure 3.10.

- Clear Hinge length, $\mathrm{l_{pc}} = 0.1 \times \sqrt{(4400^2 + 2600^2)} = 0.1 \times 5120 = 512$ mm

3.15.3 Hinge Properties of Diagonal Strut

In-plane strength and stiffness of MI panel are calculated considering the presence of openings and post-yield cracking of MI for nonlinear pushover analysis. MI is represented by equivalent diagonal strut. Their length, width and thickness are calculated according to the Mainstone (1971) guidelines. Strength and stiffness of MI panel of the reference models calculated following the guidelines of Mostafaei and Kabeya, 2004.

Collapse Prevention (CP) is not considered as the acceptance criteria of MI as it collapse before reaching the CP point. The selected software for this study does not run without any value of CP in the hinge property data proforma as shown in Table 3.4. As such, this study has considered CP value of column instead of MI panel because the beam-column frame takes the maximum load once MI cracked. In this situation the ground storey column takes the maximum load and reaches to CP point earlier than the beams and MI.

Table 3.4 Hinge property data for diagonal strut hinge - Axial P

Point	Force/SF	Displacement/SF	Remarks	Force - displacement Curve
E'	-62.72	-51.45	$SF = 1$	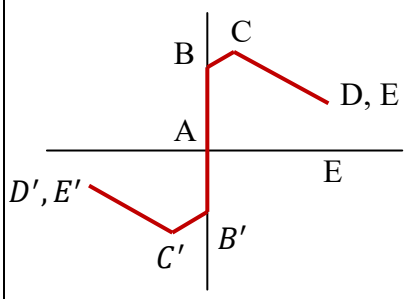
D'	-62.72	-51.45		
C'	-209.05	-11.3		
B'	-156.79	0		
A	0	0		
B	156.79	0		
C	209.05	11.3		
D	62.72	51.45		
E	62.72	51.45		

Acceptance Criteria (Plastic Displacement/SF)			Type: Force-Displacement Hysteresis Type and Parameter: Takeda
Limit	Positive	Negative	
IO	4	-4	
LS	8	-8	
CP	51.45	-51.45	

3.16 LOADS ON RC BUILDING MODELS

To find the linear and nonlinear behavior of multi-storeyed RC framed building models six basic load cases are considered namely dead load, live load, floor finish, partition wall, earthquake and pushover load. These loads are defined as load patterns in the software where floor finish and partition wall are shown as super dead loads. Earthquake load is defined as the seismic load. BNBC (Draft), 2015 is used for automatic generation of lateral load. Pushover load is defined as other type of load in the load pattern. For the present study, lateral loads are applied in the direction where x-axis depicts the horizontal plane and y-axis indicates elevation. These load cases are again combined according to BNBC (Draft), 2015.

3.16.1 Dead Load

Dead load (DL) is the vertical load due to the weight of permanent structural and non-structural components of a building. For the present study only self-weight of beams, columns and slabs are considered as dead load. Vertical loads applied on the structure are1.437KN/m and 3.75KN/m for Floor Finish (FF) and partition load (infill) respectively. In case of top floor, the vertical loads applied on the structure are 1.92 KN/m and 0.9 KN/m for FF and partition load (infill) respectively.

3.16.2 Live Load

Live Load (LL) considered in the analysis is the load due to movable service equipment, occupants, etc. Total live load applied on the structure is 1.916KN/ m for all the floors except roof top. Live load for the roof is considered as 1.2 KN/ m .

3.16.3 Earthquake Load

Earthquake (EQ) Load is calculated following the BNBC (Draft), 2015. The EQ load is incorporated in the software as user defined. This EQ load is applicable during linear analysis of the BF model only. Different parameters of EQ load for ESFM are listed below:

- Seismic zone coefficient
- Structure importance coefficient
- Response modification coefficient for structural system
- Site coefficient for soil characteristics

3.17 LOAD CASES

Load cases of the reference building models are defined in the selected software for this study. In this study the defined load cases are DL, LL, FF, partition wall, EQ and pushover load. These load cases are classified as linear or nonlinear depending on the analysis method used. Though pushover load does not fall in any type of load pattern thus it is defined as other type. Details of this load are than described in the load case clause of the software. On the other hand, a new load case namely Response Spectrum (RS) is defined in the load case clause to obtain response of the structure during linear analysis.

3.18 MODELING OF SUPPORTS

The reference models are supported at the base. The base supports are modeled considering restriction for all types of degrees of freedom on the bottom nodes. This is to represent that the columns of building models are fixed at the base. Since the fixity of base of the models is considered at ground level as such great beams are not considered in the ground storey.

3.19 LOAD COMBINATIONS

The load combination for this study is selected from BNBC (Draft), 2015. In case of seismic analysis, the total load is calculated as the summation of DL, LLand EQ loads.

These loads are defined as a load combination in the software. The present study followed CQC type of load combination to determine the combined effect.

3.20 ANALYSIS TECHNIQUES USED

3.20.1 Equivalent Static Force Method (ESFM)

The reference models have been analyzed by linear static analyses method. ESFM is a linear analysis method which is generally used for the design of RC building under seismic loading. Linear static load cases are considered for the linear static analysis. Geometric and material nonlinearity are not considered in the linear static analysis. The result of software is checked manually by ESFM. If the variation is zero than the design models are said to be correct.

3.20.2 Nonlinear Pushover Analysis Method

Nonlinear static analysis is used to analyze reference building models performance beyond elastic limit. Nonlinear static analysis of these models is carried out to study the performance of a RC building till collapse. This study has carried out pushover analysis of the selected models and results are compiled. These results are compared with the results obtained by linear analysis as stated above. In nonlinear analysis, material and geometric nonlinearities are imposed on all structural elements by placing nonlinear hinges in the selected locations.

Reference building models for nonlinear analysis used cracked cross-section properties in RC structural elements like beam, column, slab, etc. which significantly alters the natural period of the building. The cracked building is more flexible and hence is expected to have larger deformation and lesser base shear. The overall deformability of the building as estimated from pushover analysis will be affected only when the inelastic properties are changed. The pushover analysis conducted on the reference building models to derive the capacity curve of the frames.

3.21 DEVELOPMENT OF CAPACITY CURVE OF REFERENCE MODELS.

The 3D reference building models developed in this study are symmetrical in all regards. For simplification of the study, these symmetrical models are divided into number of independent frames oriented both in x and z directions. Amongst these individual frames, an interior frame is considered for the study because this frame is assumed to be most critically loaded. Ground storey columns are also considered to investigate the soft storey affect. The plan view of the reference building models with selected frame and column is given as Figure 3.13.

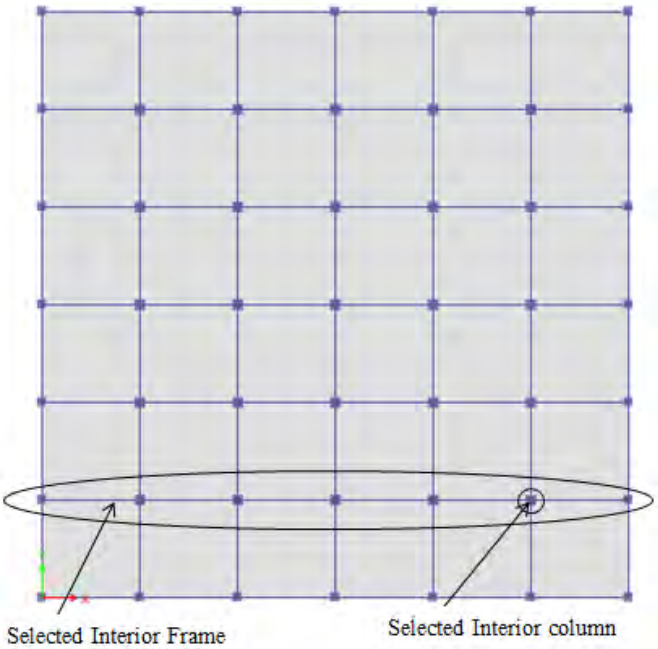

Figure 3.13 Selected interior frame and column (Plan view)

The pushover curve is derived from the software using Plot Type FEMA 440EL, Plot Axis Type S_a vs.S_v, spectrum source, etc. The values of spectral acceleration and spectral displacement are collected from the pushover curve and listed in the Table 3.5. Figure 3.14 depicts S_a and $S_v$graphs and represents pushover or capacity curve of both BF and SSF of reference models.

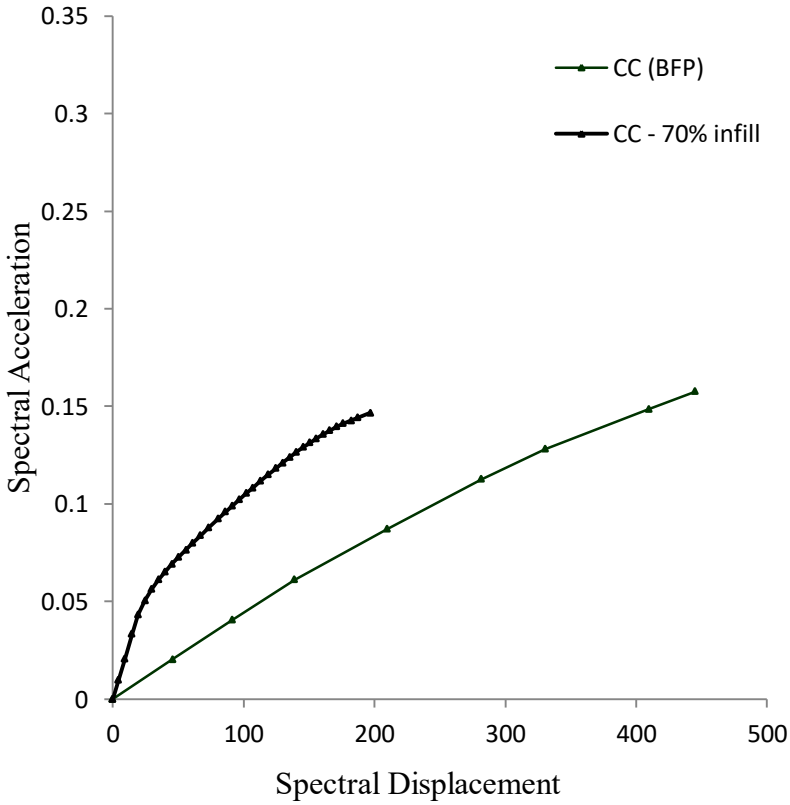

Figure3.14 Capacity (pushover) curve of reference building models

Table 3.5 Obtained data of S_a vs S_v (Frame 2 of BF and SSF of the reference models)

Bare Frame - Pushover Analysis			Soft Storey Frame - Pushover Analysis		
Steps	S_a	S_v		S_a	S_v
1	0	0	1	0	0
4	0.007377	13.8	4	0.025757	17
8	0.017214	32.3	8	0.041197	40.8
12	0.027053	50.8	12	0.055228	65
16	0.03689	69.2	16	0.06894	89.5
20	0.046727	87.7	20	0.079657	109
24	0.056564	106.2	24	0.091617	131
28	0.066401	124.6	28	0.103111	153.8
32	0.077012	144.8	32	0.114604	178.3
36	0.091442	174.8	36	0.126367	203.9
40	0.103006	200.6	40	0.138832	233
44	0.111291	219.3	44	0.149397	262.6
48	0.121465	242.7	48	0.15631	284.9
52	0.129937	262.4			
56	0.137352	282.6			
60	0.144718	303.8			
64	0.152482	330.4			
68	0.157757	349.3			
72	0.16291	368			
76	0.169367	391.4			
80	0.173376	406			

3.22 ESTABLISHING DEMAND CURVE OF THE REFERENCE MODELS

Three response spectrums are developed separately in this study for SE, DE and ME respectively. These demand spectrums are otherwise known as demand curves (Shown in Figure 3.15). Following controlling parameters are considered while calculating $C_A$and C_V values (Given in the Table 3.6) todevelop demand spectrum:

- Location of the site : Dhaka City
- Soil profile at the site : Soil type SD as per table 5.65, medium to stiff soil with shear wave velocity < VS≤ , ft/sec FEMA
- Earthquake source type : A – considering the great Indian Earthquake in Assam of 12 June, 1897
- Near Source Factor:> 15km

An elastic response spectrum for each earthquake hazard level of interest at a site is based on the site seismic coefficients CA and CV. The coefficient CA represents the effective peak acceleration (EPA) of the ground. A factor of about 2.5 times CA represents the average value of peak response of a 5% damped short period system in the acceleration domain. The seismic coefficient CV represents 5% damped response of a 1-second system and when divided by period defines acceleration response in velocity domain.

Table3.6 Calculation of C_A and C_V

Parameters	SE	DE	ME	Remarks
Seismic Zone Factor, Z	0.2	0.2	0.2	
Earthquake Hazard Level, E	0.5	1.0	1.5	
Near Source Factor, N	1.0	1.0	1.0	> 15 km
Shaking Intensity, Zen	0.134	0.134	0.134	$(2/3 * Z)$
For Soil Type S_D, $C_A$value	0.107	0.198	0.28	
For Soil Type S_D, $C_V$value	0.16	0.289	0.40	
Value of T_S	0.60	0.58	0.58	
Value of T_A	0.12	0.12	0.12	

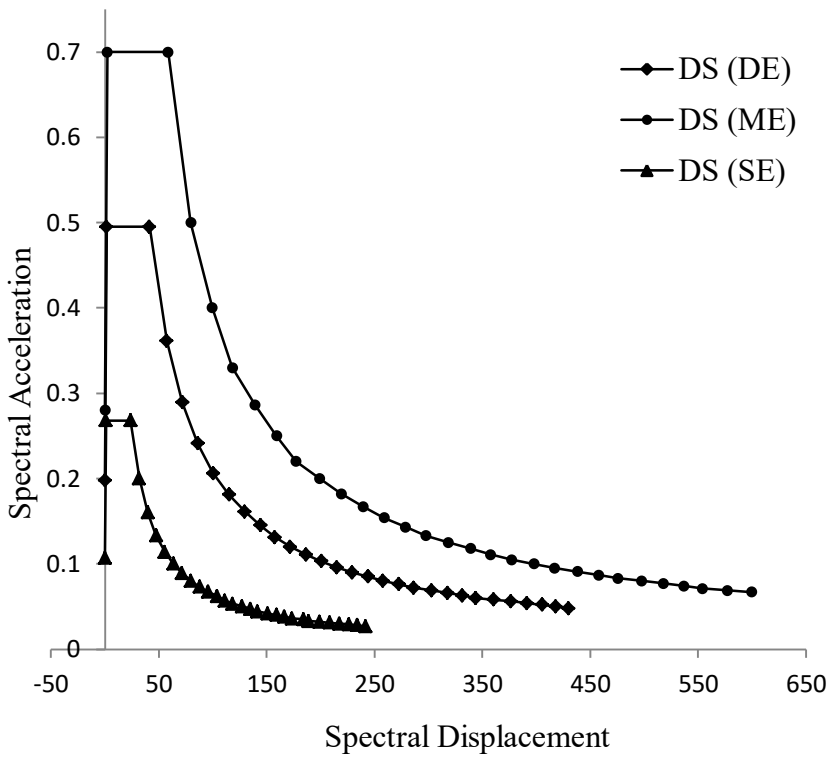

Figure3.15 Demand curves of reference model for SE, DE and ME

The calculated period and spectral acceleration are given in the Table 3.7. It is to note that the spectral displacements are found out for each time period using the relation $S_d = (T^2/4\pi^2)S_a$.

Table 3.7 Spectral acceleration and spectral velocity of different earthquakes for Dhaka city

Time	SE		DE		ME	
	S_a	S_v	S_a	S_v	S_a	S_v
0	0.107	0	0.198	0	0.28	0
0.12	0.268	0.959555	0.495	1.656128	0.7	2.341999
0.58	-	-	0.495	41.40319	0.7	58.54996
0.60	0.268	23.98888	-	-	-	-
0.8	0.2	31.82604	0.361	57.446	0.5	79.56509
1.0	0.16	39.78255	0.289	71.85723	0.4	99.45637
1.2	0.133	47.61971	0.241	86.28834	0.33	118.1542
1.4	0.114	55.55633	0.206	100.3913	0.286	139.3782
1.6	0.1	63.65208	0.181	115.2103	0.25	159.1302
1.8	0.089	71.6981	0.161	129.701	0.22	177.2312

Time	SE		DE		ME	
	S_a	S_v	S_a	S_v	S_a	S_v
2.0	0.08	79.56509	0.145	144.2117	0.2	198.9127
2.2	0.073	87.84981	0.131	157.6483	0.182	219.0228
2.4	0.067	95.9555	0.12	171.8606	0.167	239.1727
2.6	0.062	104.2104	0.111	186.5702	0.154	258.8451
2.8	0.057	111.1127	0.103	200.7825	0.143	278.7563
3.0	0.053	118.6017	0.096	214.8258	0.133	297.6232
3.2	0.05	127.3042	0.09	229.1475	0.125	318.2604
3.4	0.047	135.0916	0.085	244.3146	0.118	339.1661
3.6	0.044	141.785	0.08	257.7909	0.111	357.6849
3.8	0.042	150.7957	0.076	272.8685	0.105	376.9894
4.0	0.04	159.1302	0.072	286.4343	0.1	397.8255
4.2	0.038	166.669	0.069	302.6358	0.095	416.6725
4.4	0.036	173.2928	0.066	317.7034	0.091	438.0456
4.6	0.035	184.1435	0.063	331.4582	0.087	457.728
4.8	0.033	189.0467	0.06	343.7212	0.083	475.481
5.0	0.032	198.9127	0.058	360.5293	0.08	497.2818
5.2	0.031	208.4208	0.056	376.502	0.077	517.6903
5.4	0.03	217.5111	0.054	391.5199	0.074	536.5273
5.6	0.029	226.124	0.052	405.4637	0.071	553.6139
5.8	0.028	234.1999	0.05	418.214	0.069	577.1354
6.0	0.027	241.679	0.048	429.6515	0.067	599.7219

The data given in the Table 3.7 are plotted and three response spectrums generated as shown above. Since the models are stuided nonlinearly thus these curves are not reduced using the spectral reduction factors as per ATC 40, 1996.

3.23 DETERMINATION OF PERFORMANCE POINT OF REFERENCE MODELS

Performance Point (PP) of any building model is derived from the intersection point of the demand and capacity curves of that model. The capacity curves of the reference building models are plotted on the demand curves and three intersection points are found. The intersection point of capacity curve and demand curve of SE defines the PP of IO level. The intersection point of capacity curve and demand curve of DE defines the PP of LS level. Similarly intersection point of capacity curve and demand curve of ME defines the PP of CP level. Though three PPs are derived but PP at CP level is the most worrying factor for engineers as it defines full collapse of the building. This study decided to selection of PP at

CP level as the overall PP of all investigations. The performance points of different levels are shown in the Figure 3.16.

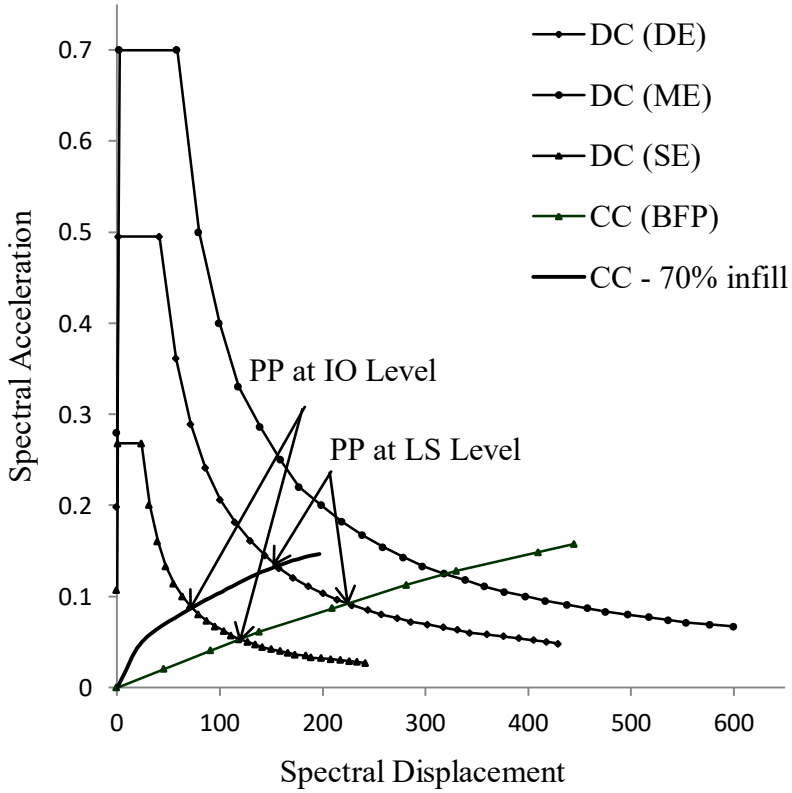

Figure3.16 Determination of performance point for SE, DE and ME

3.24 GENERATION OF RESULTS FROM THE SELECTED COLUMN

PP at CP level of reference building models is the initial finding of the study. This PP gives out the corresponding spectral displacement value. This spectral displacement is used to find out the moment and shear force of selected interior column using the software. This procedure is repeated for every model of this paper. In the next chapter these moment and shear force are evaluated in detail.

3.25 SWAY MECHANISM OF MODELS

The reference models are developed considering strength based design i.e., weak beam and strong column concept. To attain this concept, columns are designed as such they become relatively stiffer than the beams. In case of nonlinear analysis, it is expected the hinges form first in the beam element than the hinges are expected to form in the bottom of the ground storey columns. The sway mechanism of bare frame shows that the formation of hinges are homogenous and uniformly progressive with the increment of applied loads (Figure 3.17(a)

to 3.24 (a)). The situation is different in the case of soft storey. In soft storey frame hinges are formed in diagonal struts first then beams. The hinge forming pattern of soft storey frames is shown in Figure 3.17 (b) to 3.24 (b). Here maximum rotation occurs in the ground storey column. In pushover analysis, it is found that the soft storey frame and bare frame collapse in step 38 and step 47 respectively. As such, sway patterns of both the frames between step 38 to step 47 are compared in the above mentioned figures to evaluate effects on the frames.

STEP - 1

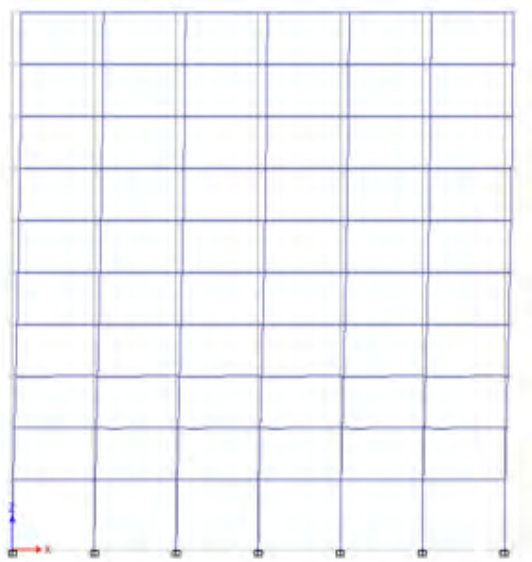

Figure 3.17(a) Bare Frame

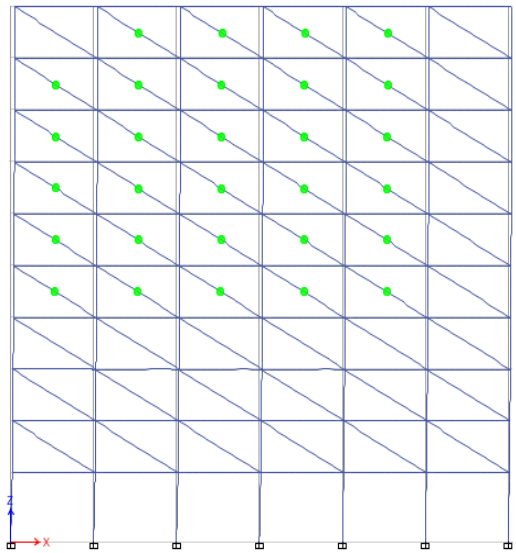

Figure 3.17(b) Infilled Frame

STEP - 2

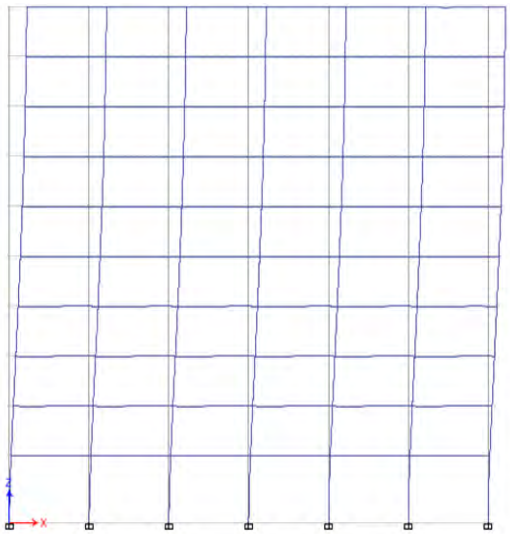

Figure 3.18(a) Bare Frame

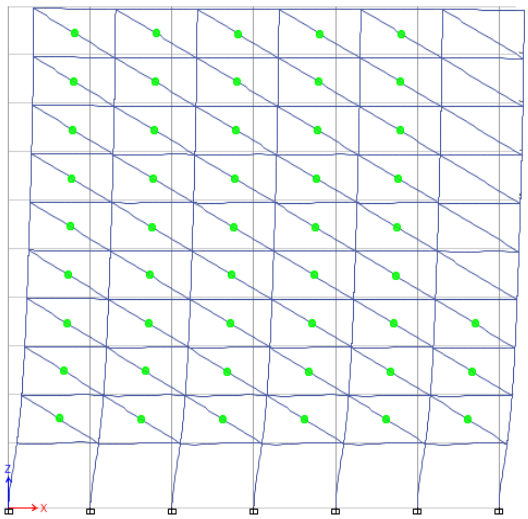

Figure 3.18(b) Infilled Frame

STEP - 3

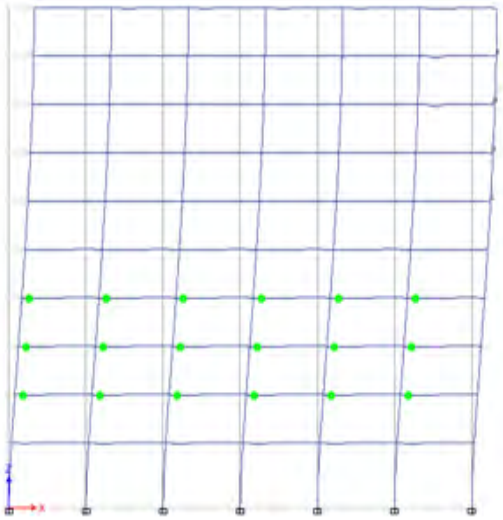

Figure 3.19(a) Bare Frame

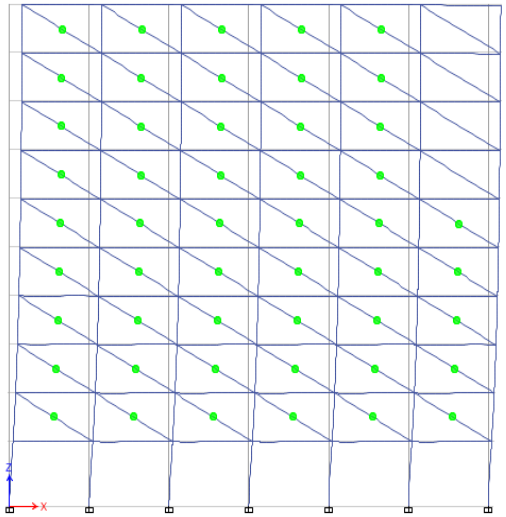

Figure 3.19(b) Infilled Frame

STEP - 4

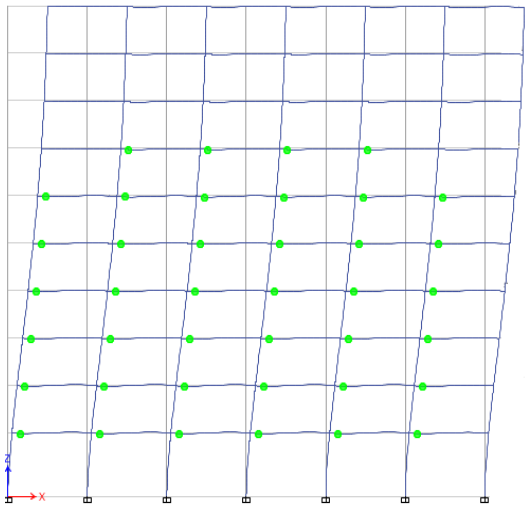

Figure 3.20(a) Bare Frame

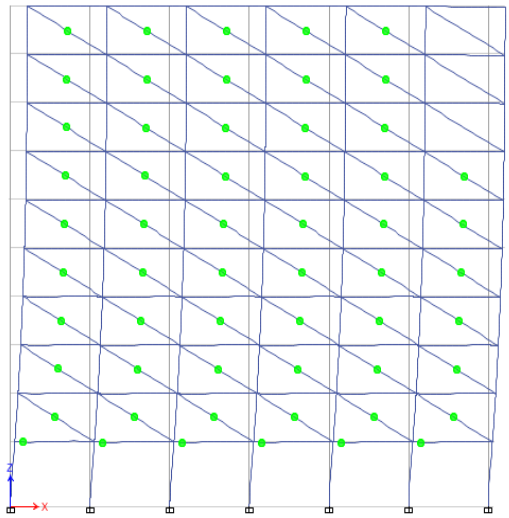

Figure 3.20(b) Infilled Frame

STEP - 5

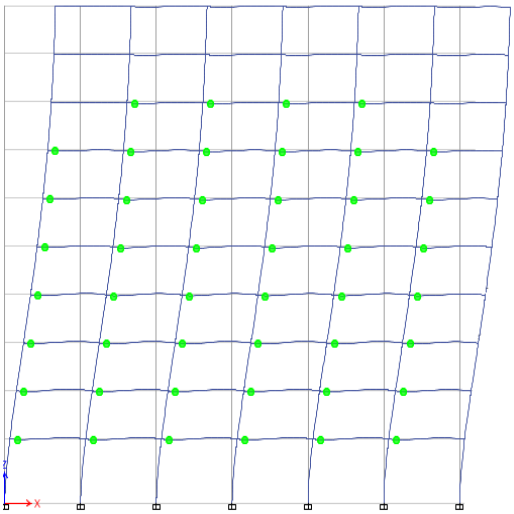

Figure 3.21(a) Bare Frame

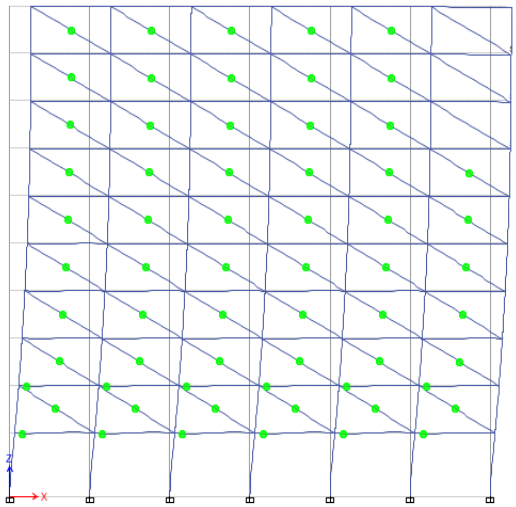

Figure 3.21(b) Infilled Frame

STEP - 6

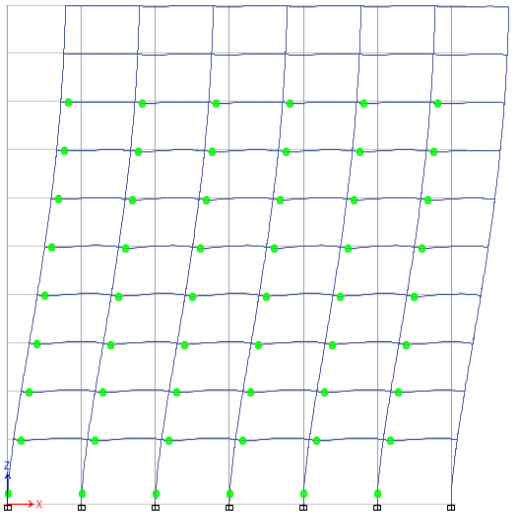

Figure 3.22(a) Bare Frame

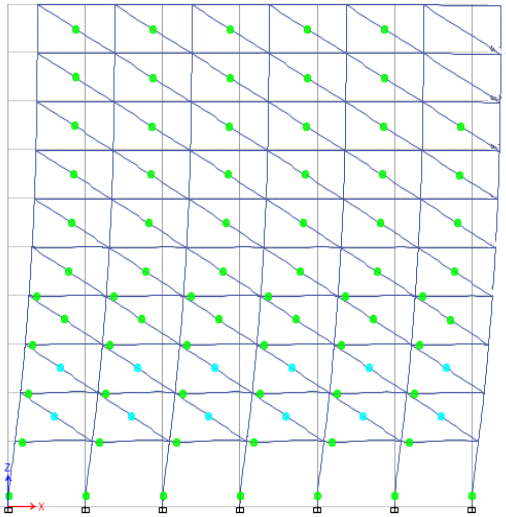

Figure 3.22(b) Infilled Frame

STEP - 7

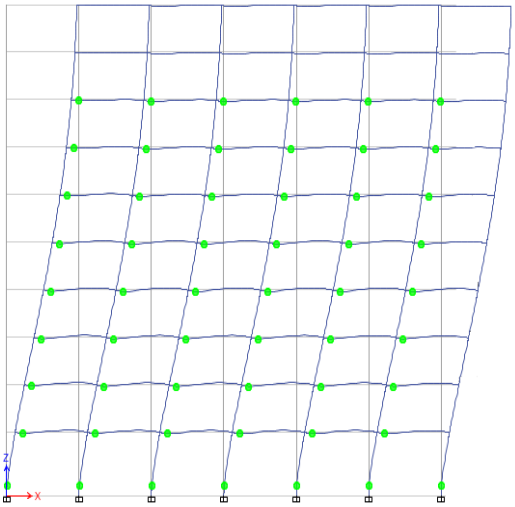

Figure 3.23(a) Bare Frame

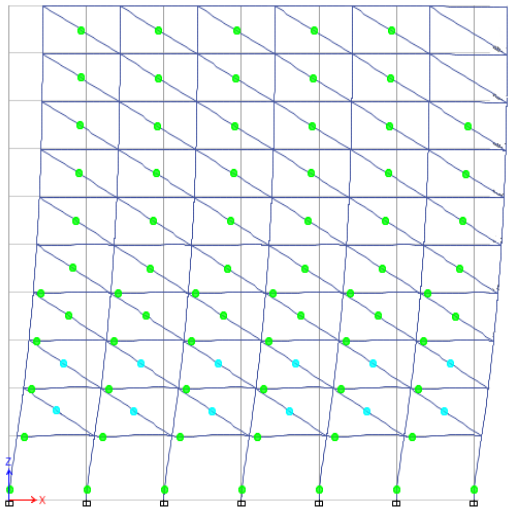

Figure 3.23(b) Infilled Frame

STEP - 8

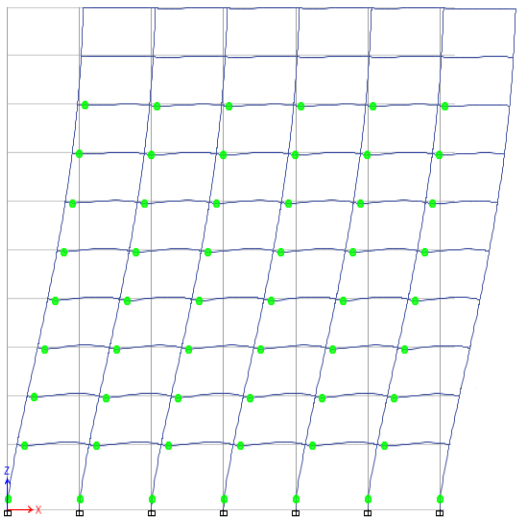

Figure 3.24(a) Bare Frame

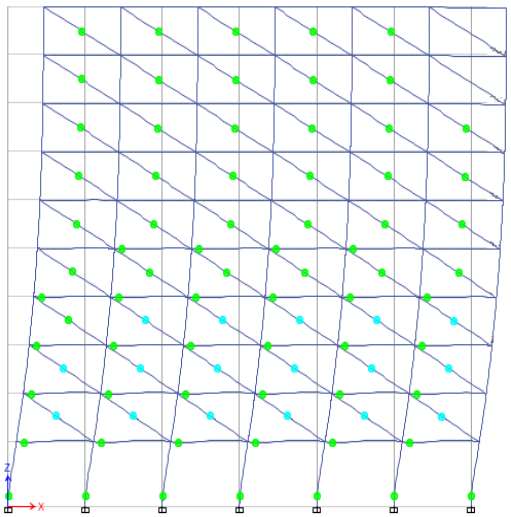

Figure 3.24(b) Infilled Frame

STEP - 9

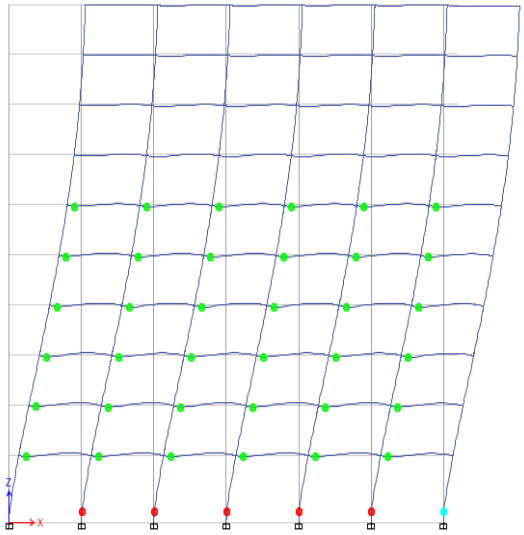

Figure 3.24(a) Bare Frame

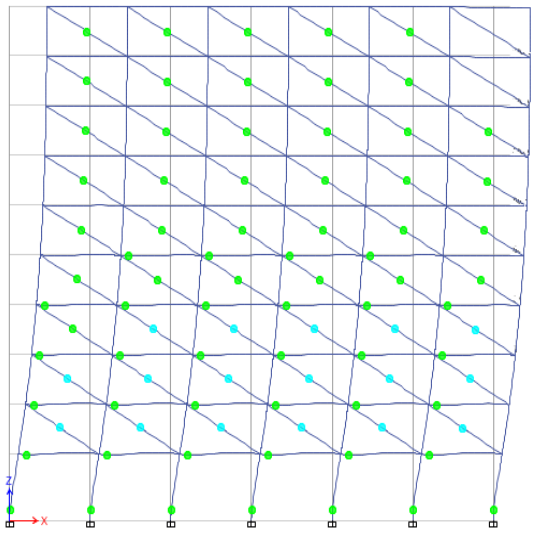

Figure 3.24(b) Infilled Frame

3.26 COLLAPSE PATTERN OF MODELS

Nonlinear deflection of the reference building models under loading is shown in the figures above. Though maximum deflection occurs in the base of the ground storey column yet total deflection of the building is proportionately distributed in the upper storeys. In this study, reference building models are analyzed for aforementioned lateral and vertical loads with all the parameters. Inelastic DC of SE, DE and ME are calculated for Dhaka city and plotted in the Fig. 3.25. The CCs of reference models are derived for each parameter. In the Figure below, the DC and CC of reference models are plotted for visualization of collapse pattern.

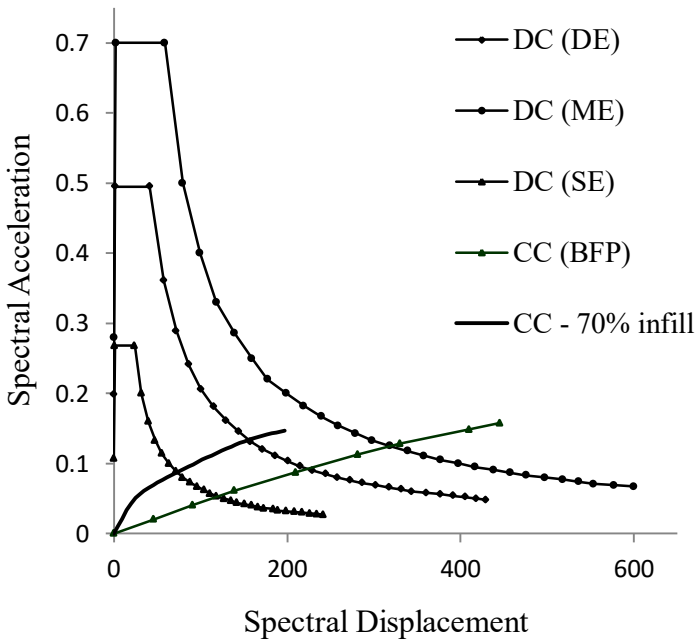

Figure 3.25 No collapse in ground storey column for 2 Bays

In all the cases, it is proved that the soft ground storey columns of the reference models for different parameters did not collapse during ME when the DC is developed in according to the BNBC (Draft), 2015 manual. Because, BNBC (Draft), 2015 has considered 80 percent value of C_A and C_V in developing the DCs. The ATC 40 manual allows this reduction of values to remain in safe side.

3.27 VERIFICATION OF PUSHOVER ANALYSISBY MANUAL CALCULATION

Non-linear Static Analysis (NSA), popularly known as pushover analysis, is used for its simplicity and rapidity. In pushover analysis, building is subjected to monotonically increasing static horizontal loads under constant gravity load. A two storey reinforced concrete moment resisting frame is considered for nonlinear static analysis under seismic loading to keep the numerical calculation simple. Detail calculation of this building is given as Appendix A to this paper. This manual calculation for larger building can be done by utilizing any existing engineering program like ANSYS, ETABS, SAP, etc. Initially Equivalent Static Force Method (ESFM) is used to find the base shear and its distribution along the height of the building. The building consider for the analysis is a symmetric structure with three bays and three spans both in x and y directions. The design data are given below:

a. Slab Thickness: mm
b. Beam: mm
c. Column: 250×300 mm
d. Floor Finish(FF): 1.437 KN/m
e. Live Load (LL): 1.915 KN/m
f. Partition Wall(PW): 3.83KN/m

Nonlinear deflection of the selected building is calculated by using the Newmark‘s constant average acceleration method. In this study, the analysis is done to determine the response u t of the frame (starting from rest) to the monotonic loading as mentioned above with Δt sec and Newton-Raphson iteration. The nonlinear deflections of the reference models are plotted against monotonic loads applied to the structure as lateral loads. The backbone curve of sample model is prepared basing on its load-deformation curve. The applied load in modified by the coefficient of backbone curve to incorporate effects of column or beam hinges rotation. The lateral pushover load and its corresponding displacement are calculated and converted to the modal acceleration and modal displacement by the formula as given in

the Figure 3.30 below. The modal acceleration and modal displacement are plotted to generate the capacity curve of two storey building. The design response spectrum of Dhaka City is converted into spectral acceleration and displacement graph.

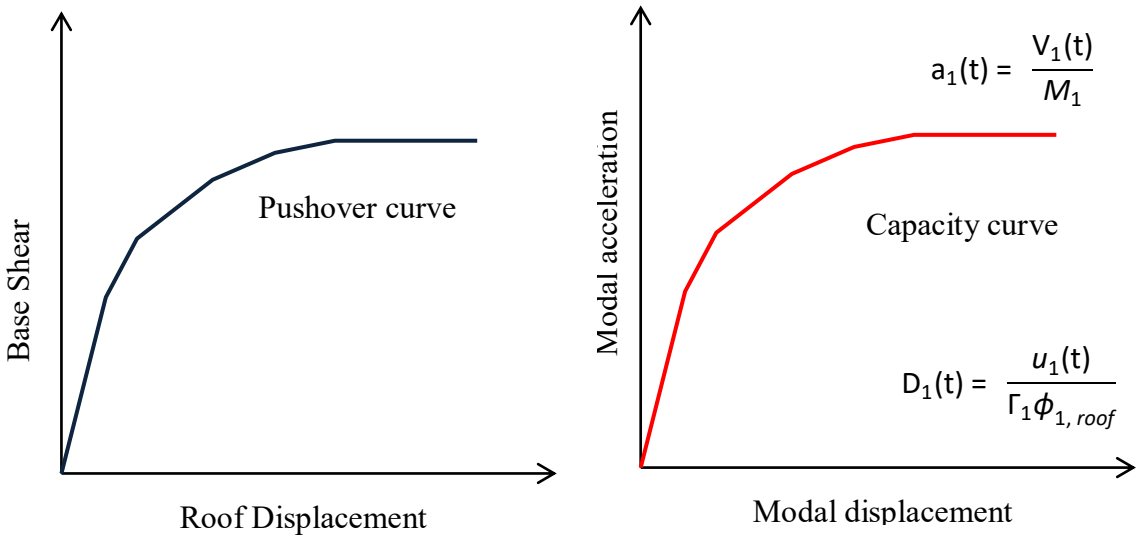

Figure Typical pushover and capacity curve ATC

Here, , and are known as spectral acceleration, base shear and normalized mass in the first mode shape. Again, , ,u *and* Dare commonly known as coefficient of Modal expansion of the influence vector, mode shape vector, roof top displacement in fundamental mode and spectral displacement of the building respectively. Manual calculation of two storey building is carried out in detail and attached to this research paper as Appendix A. The lateral deflection of the two storeys and its demand curve, capacity curve and their intersection point (Performance point) are shown in the Figure 3.31 below.

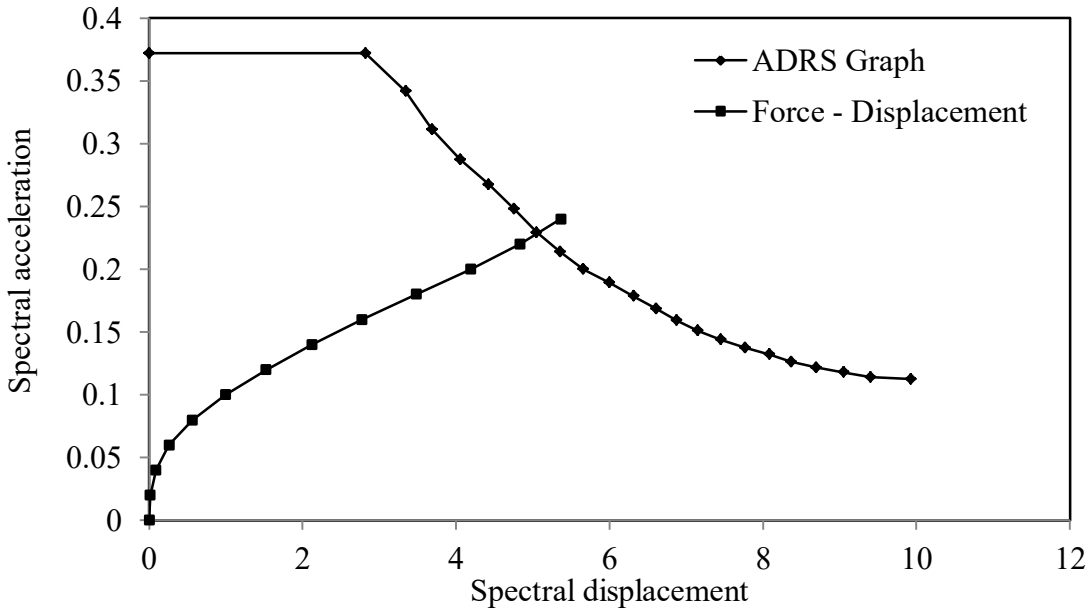

Figure Typical demand and capacity curve of a two storey building

3.28 REMARKS

This chapter describes the development procedure of reference models for present study starting from selection and assigning of software, elements, material properties, hinges and base support under vertical and design seismic loads to observe the effect of soft storey on ground storey column. The chapter has further described the analysis techniques, sequence of pushover analysis, static pushover analysis, sway and collapse mechanism of reference models. At the end, a two storey building is manually calculated by pushover analysis to develop the capacity curve and to verify the occurrence of performance point.

CHAPTER 4

PARAMETRIC STUDY

4.1 GENERAL

Two three dimensional (3D) reference building models are developed in the previous chapter to represent bare frame building and infill frame building with open ground storey. Procedure and methodology of developing 3D models are described in the same chapter. Models and their elements are suitably selected to reflect the properties of actual building. Load cases considered are described as per BNBC (Draft), 2015. Steel percentage in the column is kept within 2 to 4 percent. Masonry infill is placed as equivalent diagonal strut in the upper stories of the building model to develop soft storey effect. These models are analyzed by both ESFM and pushover analysis method with varying parameters under static earthquake loading. In ESFM earthquake acceleration data of Dhaka city is used for linear analysis of the models. Pushover analysis method is used as part of nonlinear static analysis. At the end, seismic behavior of soft ground storey columns of these models is compared. The comparison is done in terms of their bending moment and shear forces ability under different circumstances. Comparison is also made on their induced base shear and drift ability.

4.2 PARAMETERS OF INTEREST

A building frame subjected to an earthquake is primarily characterized by the development and distribution of base shear. Base shear of any building frame depends on its natural period. Mass and stiffness of the frame also define the natural period. Therefore any structural element that affects the stiffness and mass shall have influence on the natural period. Infill in a frame changes mass and stiffness thus it has direct influence on the natural period as well as base shear. There had been rigorous analysis on infill frame and effect of MI on natural period of building in terms of its quantity and distribution under earthquake loads. Amanat and Haque (2006) have analyzed building with different combination of infills and showed that randomness in the distribution of infill does not have significant effect on the period; instead it is the total amount of the infill that matters. It is observed that MI of residential buildings of Dhaka city is generally distributed in all stories. Thus the study has considered existence of infill in each storey of reference building models within beam-column panel in regular patter rather than the random fashion except the soft ground storey. This study has also considered 60 percent infill presence in each storey keeping in mind the existence opening in each masonry panel due door and windows.

All interior frames of a symmetric building take equal shear and moment under uniform vertical and horizontal loading. The fact is also true for the interior ground storey columns of each interior frame irrespective of their location within the frame. Thus each interior frame of the reference building models of this thesis takes equal shear and moment as they are symmetrical. As such, study of any interior frame of the reference building models will depict the most critical scenario of the building during earthquake. This study has considered first interior frame of the reference model as well as first right interior column of that frame for all parametric investigation. The parameters of this thesis are selected considering all possible variations that a RC moment resisting frame building may possess in any urban area. The parameters of interest of this study are given below:

- Percentage of infill.
- Number of bays.
- Number of spans.

4.3 PARAMETERS OF MODELS

The selected parameters and their values for this study are given in the table 4.1. The highlighted values of the table indicate the parameter of reference building models.

Table 4.1 Variable parameters of models

Parameter	Values
Percentage of infill	50, 60, **70**, 80, 100
Number of bay	2, 4, **6**, 8, 10
Number of span	2, 4, **6**, 8, 10
Type of frame	Bare Frame, Soft Storey Frame
Location of building	Dhaka city
Type of analysis	Equivalent static force method, pushover analysis method

4.4 PARAMETRIC STUDY

Selected interior frame of the reference building models is studied to examine the effects of selected parameters. Firstly, bare frame model is analyzed by ESFM and pushover analysis method. Secondly, soft storey frame of reference model is analyzed in similar pattern. In plane loads are applied to both the frames. This allows no chances of developing accidental torsion in the models. The infills are lateral load resisting elements and placed in ordered form to avoid development of unbalanced stress in the frame elements.

4.5 TERMINOLOGIES USED IN PARAMETRIC STUDY

4.5.1 Bare Frame Linear (BFL)

The multi-storey moment resisting frame with beam, column and slab elements is termed as Bare Frame (BF). This frame is termed as BFL when it is studied by ESFM for linear analysis under both vertical and seismic load.

4.5.2 Bare Frame Push (BFP)

The bare frame is termed as BFP when it is studied by pushover analysis method for nonlinear analysis. In this analysis geometric nonlinearity is imposed in beam and column elements by placing nonlinear hinges at the ends.

4.5.3 Soft Storey Frame Push (SSFP)

The multi-storey moment resisting frame with beam, column, slab and diagonal strut elements is termed as Soft Storey Frame (SSF). The SSF is termed as SSFP when it is analyzed by pushover analysis method for nonlinear analysis. In this analysis geometric nonlinearity is imposed in beam, column and diagonal strut elements by placing nonlinear hinges at the ends.

4.5.4 Nonlinear Magnification Factor of Bare Frame (MF_{BF})

The nonlinear magnification factor of bare frame is defined as the ratio between moment/shear force of BFP and moment/shear force of BFL. In short it is denoted as MF_{BF}.

4.5.5 Nonlinear Magnification Factor of Soft Storey Frame (MF_{SSF})

The nonlinear magnification factor of soft storey frame is defined as the ratio between moment/shear force of SSFP and moment/shear force of BFL. In short it is denoted as MF_{SSF}.

4.5.6 Design Magnification Factor (MF)

The design magnification factor is defined as the ratio between MF_{SSF} and MF_{BF}. In short it is denoted as MF. This magnification occurs in nonlinear state of the frame. But this study has found that this magnification is always constant from yield strength up to final collapse state. Thus MF which is obtained at performance point will be same at yield strength. Therefore, this magnification value can be used in the elastic design procedure.

4.6 INVESTIGATION OF REFERENCE BUILDING

The 3D models of reference building are investigated with the selected parameters. Initially bare frame model is investigated as a bare frame building by neglecting the effect of masonry infill. This bare frame model is analyzed by both ESFM and pushover analysis method to derive results of BFL, and BFP frames. It is to note that the aforementioned analyses are carried out on 3D model but results are calculated for the selected interior column of the selected interior frame.

The soft storey model is investigated as soft storey building with open ground storey. In this case masonry infill wall is considered as structural element. In soft storey building model masonry infill wall is considered as equivalent diagonal strut with hinge at ends. This diagonal strut is placed in all the beam-column panels except ground storey. Ground storey is kept open to get the soft storey effect. This model is now analyzed by pushover analysis method and results are derived and recorded for the selected interior column of the selected interior frame..

In model investigation, three frames result are obtained namely BFL, BFP and SSFP for any single parametric value. Basically moment and shear forces of selected interior column of above three frames are considered for the analysis and results are compared separately. In this study, moment and shear forces of BFP and SSFP are compared with the moment and shear forces of BFL separately. Besides, base shear and each storey deflection are calculated to see the variation between BFP and SSFP with respect to BFL.

4.6.1 Moment Diagram of Reference Building

A bending moment vs. height graph of reference building models (Figure 4.1) is plotted to depict the variation of moments of BFL, BFP and SSFP in relation to the height. In the graph it is observed that the negative moment of BFL is maximum at base which gradually decreases in the upper stories. Moment of BFP follows the pattern of BFL except ground and first storey. In ground storey BFP posses very high negative moment which remains fairly higher in first storey with respect to the moment of BFL. The moment diagram of SSFP is almost similar to the moment diagram of BFP except the ground storey. SSFP negative moment at the base is little higher than the moment of BFP. But moments of upper stories of SSFP, BFP and BFL are fairly similar. It is to note that the negative moments of BFP and SSFP of top three stories have reduced moderately as compared to the moments of BFL.

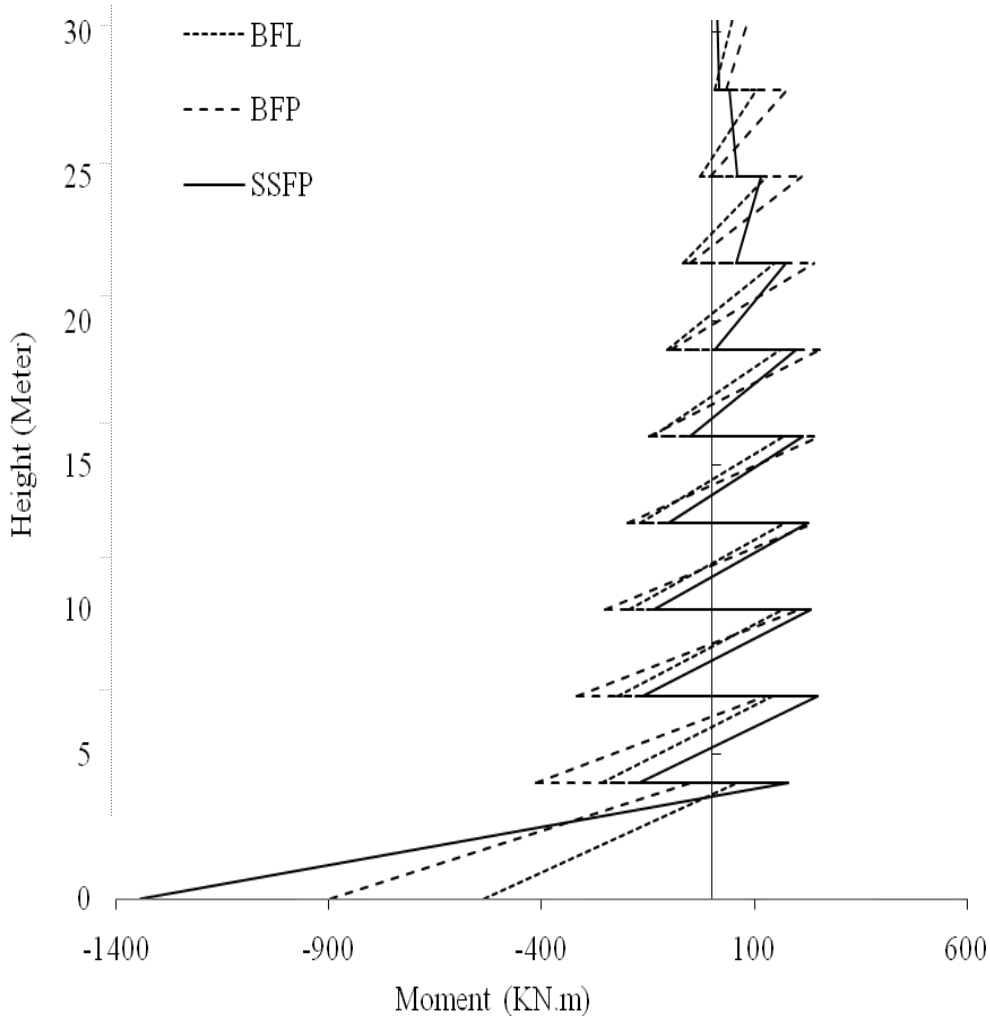

Figure 4.1 Bending moment diagram of an interior column of reference building model

4.6.2 Shear Force Diagram of Reference Building

A shear force vs. height graph of reference building models (Figure 4.2) is plotted to depict the variation of shear force of BFL, BFP and SSFP frames in relation to the height. In the graph it is observed that the shear force of BFL is maximum at base which gradually decreases in the upper stories. Shear force graph of BFP follows the pattern of BFL except bottom five stories. Shear force of BFP and SSFP sharply increased in the bottom stories. This increase is further higher for SSFP. In upper stories, graph of BFL, BFP and SSFP are closer and similar. However, shear force of upper stories of SSFP become considerably lesser then than the shear forces of BFL and BFP.

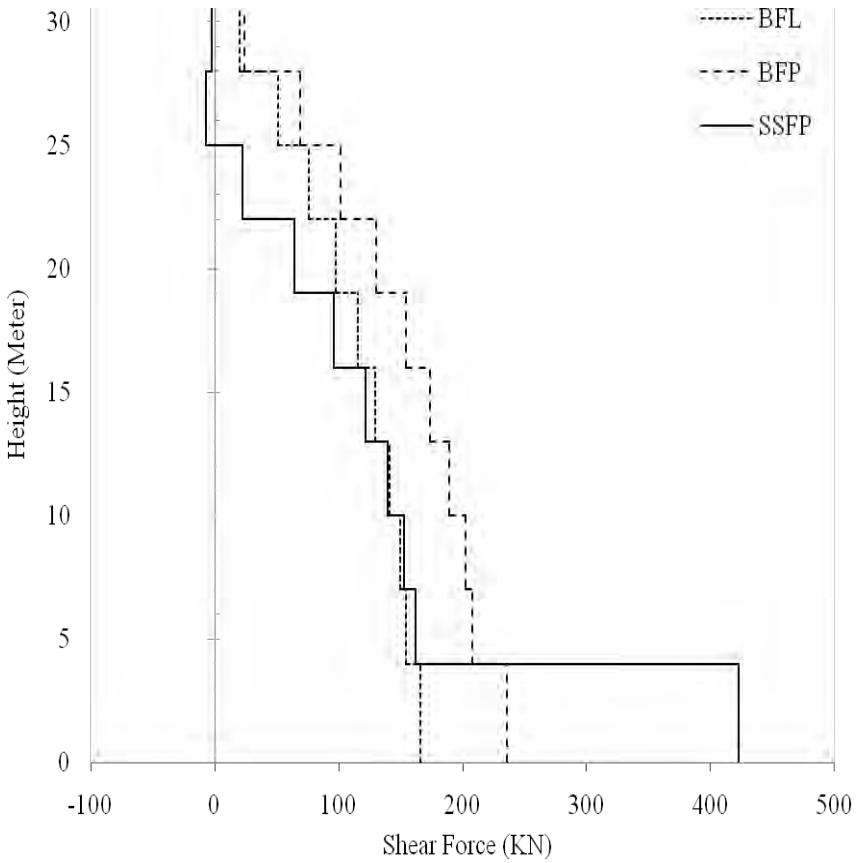

Figure 4.2 Shear Force diagram of columns of different stories of reference building model

4.7 EXTENT OF NONLINEAR INVESTIGATION

4.7.1 Selection of Performance Point.

The BF and SSF are analyzed by pushover method as part of nonlinear analysis. Two capacity curves are developed as outcome of pushover analysis. On the other hand, three site response spectra or demand curves are developed for Dhaka city considering three earthquake situations namely SE, DE and ME. The capacity and demand curves are plotted in Acceleration Displacement Response Spectrum (ADRS) format. There will be three intersection points between demand and capacity curves. First intersection point between capacity curve and SE demand curve will indicate IO performance level of building. Second intersection point between capacity curve and DE demand curve will indicate LS performance level of building. Third intersection point between capacity curve and ME demand curve will indication CP performance level. The building performance of BF and SSF are independent of each other as their capacity curves are different. In nonlinear analysis, CP performance level of a building is considered as the last limit of performance. This study has considered the third intersection point as the actual Performance Point (PP) of the

reference building models for nonlinear analysis. Under these circumstances BF and SSF will have two individual PPs.

4.7.2 Maximum Allowable Displacement and Results Compilation

Each performance point has a corresponding spectral displacement which is termed as the maximum allowable displacement for this study. This spectral displacement is the key factor in determining two pushover steps between which maximum allowable displacement is located using the selected software. Now moment and shear force of the reference models are derived for the aforementioned steps. Interpolation is done to find out the moment and shear force values of the selected column at maximum allowable displacement within the aforementioned steps.

4.8 REFERENCE BUILDING MODEL INVESTIGATION BY SELECTED PARAMETERS

Reference building models are investigated separately for five different variable parameters. The reference models are investigated with these variables in two spectrum firstly as bare frame and secondly as a soft storey building with open ground storey. For each parameter, this bare frame is analyzed by ESFM for linear analysis and pushover analysis method and soft storey building models is analyzed by pushover analysis method only. It is to note that the result of linear analysis of SSF is almost similar to the results of linear analysis of BF. Thus linear analysis of SSF is neglected in subsequent analysis. Each value of a parameter generates three shear force/bending moment diagrams for three different frames (BFL, BFP and SSFP). Therefore, seventy five moment diagrams are generated to investigate moment variation of ground storey column for all the selected parameters. Shear investigation of the same column requires additional seventy five shear force diagrams. This study has investigated 75 interior frames for the parametric investigation and results are recorded in the form of shear force or bending moment diagram. On the other hand, base shear and roof top drift of the selected interior frames are also recorded and results are given in the next chapter. Model investigated procedure for this study is described below.

4.8.1 Models Investigated by Variation of Number of Bays

Reference models are investigated by varying number of bays while keeping all other four parameter constant. Numbers of bays considered for the investigation are two, four, six, eight

and ten. Amongst these numbers, bay number six has been considered as standard bay number of the reference models. Reference models generate three bending moment/shear force diagrams for specified number of bays. Therefore, five bay numbers generate five sets of bending moment and shear force diagrams similar to the diagrams of Figure 4.1 and 4.2. Numerical values of bending moment and shear force of selected ground storey column are obtained by varying number of bays and results are given as Appendix B and C.

4.8.2 Models Investigated by Variation of Number of Spans

Reference models are investigated by varying number of spans while keeping all other four parameter constant. Number of spans considered for the investigation is two, four, six, eight and ten. Amongst these numbers, span number six has been considered as standard span number of the reference models. Reference models generate three bending moment/shear force diagrams for each number of spans. Therefore, five span numbers generate five sets of bending moment and shear force diagrams similar to the Figure 4.1 and 4.2. Bending moment and shear force diagrams of selected ground storey columns are obtained from these graphs and results are given as Appendix B and C.

4.8.3 Model Investigated by Variation of Percentage of Infill

Reference models are investigated by varying infill percentage while keeping all other parameters constant. Total five infill percentages are considered for the investigation those are 50%, 60%, 70%, 80% and 100%. Amongst these percentages, infill percentage 70% is considered as the standard infill percentage of the reference models. Reference models generate three bending moment/shear force diagrams namely BFL, BFP and SSFP for each infill percentage. Therefore, five percentages of infill will generate five sets of bending moment and shear force diagrams similar to Figure 4.1 and 4.2. Bending moment and shear force diagrams of ground storey columns are obtained from these graphs and results are given as Appendix B and C.

4.9 MODEL INVESTIGATED BY ANALYZING BASE SHEAR

For this study, investigation of base shear for two reference models (bare frame and soft storey frame) is done by varying the number of bays, spans, stories, span length and span to bay length ratio. Here, the base shear of BFP and SSFP are compared with base shear of BFL respectively to evaluate the rate of increase due to the nonlinear effect. Major concern of this

investigation is with the ground storey interior column. Analysis of base shear is mainly done to observe the effect of earthquake load on ground storey columns due to the soft storey configuration.

4.10 MODEL INVESTIGATED BY ANALYZING DRIFT VARIATION

The reference models are investigated by varying number of bays, spans, stories, span length and span to bay length ratio. In each case, their total drift is calculated and added up to the roof top. The results are recorded and discussed in the next chapter. In this study, drift ratio is calculated due to number of bays, number of stories and span to bay length ratio variations. In the parametric study, it is observed that the drift of reference building models is different for each parameter. Even the drift of BFP, SSFP and BFL are not same. This is due to the variation of mass, stiffness and applied loads both lateral and vertical. Moreover, it is found that the drift of reference soft storey building reduces despite being heavier than the bare frame. Thus a detail investigation is carried out on the drift pattern of models and results are analyzed in the next chapter.

4.11 REMARKS

Two models namely bare frame and soft storey frame are analyzed by each parameter for both linear and nonlinear analysis. The analyzed frames are known as BFL, BFP and SSFP. Thus total 75 building frame models are analyzed for five variables parameters. Investigation of these frames (i.e., BFL, BFP SSFP) is done and their bending moment and shear force diagrams are recorded. But only bending moment and shear force diagrams of selected ground storey columns are considered for this study. Investigation of reference building is also done with respect to the increment of base shear and drift pattern to observe the variation between bare frame and soft storey frame. Similarly, selected interior column of the selected interior frame is studied to witness the variation in strength of ground storey column at nonlinear state under seismic loading.

CHAPTER 5

RESULT ANALYSIS

5.1 GENERAL

Two reference building models have been analyzed by three different types of parameters as described in the previous chapter. Initially reference models are analyzed by varying percentage of infill. Reference models are also analyzed by varying number of bays and spans where masonry infill percentage is considered as 70 percent. Purpose of this analysis is to carry out deliberate investigation of ground storey column due to soft storey effect. The results obtained from the above investigation are compared and logical deductions are made in this chapter. This chapter initially describes the affect of soft storey building frame in terms of variation of bending moment and shear force of ground storey column due to variation of parameters. It also describes the magnification rate of bending moment or shear force of ground storey column of BFP and SSFP with respect to the corresponding bending moment or shear force of BFL. It illustrates the base shear variation and drift ability of the reference building frame models under different circumstances.

5.2 EFFECT ON STRENGTH OF SOFT GROUND STOREY COLUMN

The strength of ground storey column of a soft storey building is certainly affected by its configuration. Effect on bending moment of the selected ground storey column is numerically analyzed and results are discussed in the subsequent subparagraphs.

5.2.1 Effect on Column due to Variation of Percentage of Infill

Reference building models are analyzed by varying percentage of infill. A graph of spectral displacement vs. spectral acceleration is plotted for varying percentage of infill as shown in Figure 5.1. It is observed that the SSFP of 100 percent infill attracts higher spectral acceleration at smaller spectral displacement. The spectral acceleration decreases and spectral displacement increases at lower percentage of infill. This occurs due to the truss action of diagonal struts along the direction of the applied lateral load. On the other hand, collapse of building depends on infill percentage. If percentage of infill increases than building collapses earlier and vice versa. Finally, moments of ground storey column of the selected interior frame are plotted against percentage of infill to compare the effect of infill (Figure 5.2). Similarly, moments selected interior frame of BFP and BFL are also plotted in the same

figure. It is observed that the moment of ground storey column of BFL and BFP remains constant irrespective of variation of infill percentage. Contrarily, moment of SSFP sharply increases with the increase of percentage of MI.

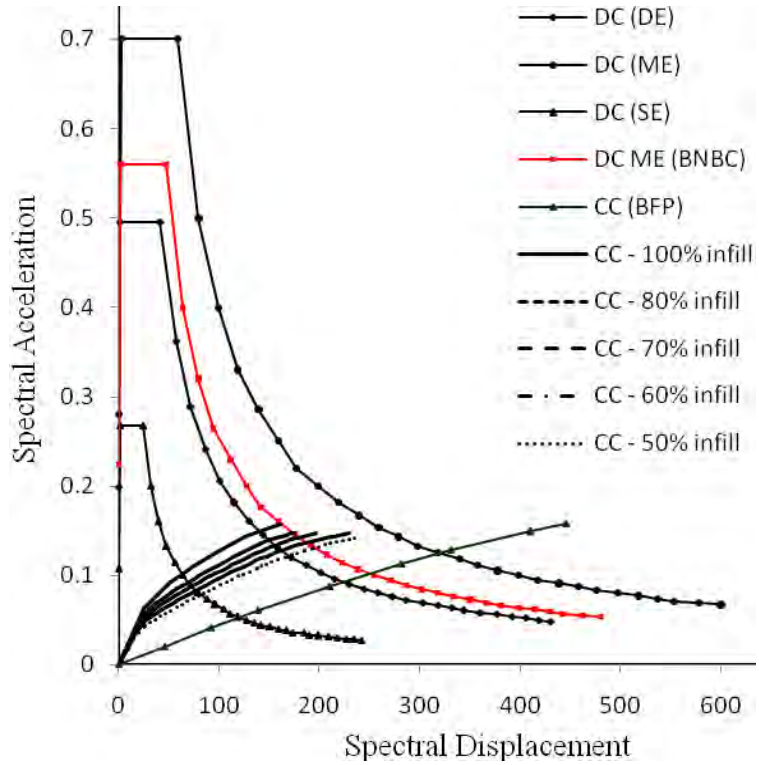

Figure 5.1 Spectral displacement vs. spectral acceleration of ground storey column graph

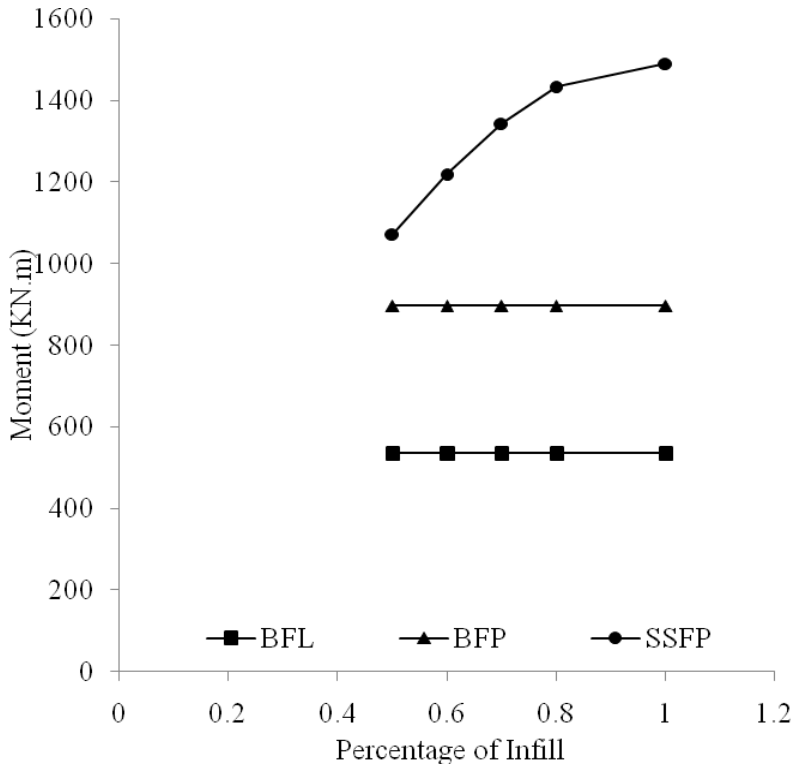

Figure 5.2 Percentage of infill vs. bending moment of ground storey column graph

5.2.2 Effect on Column due to Variation of Number of Bays

Reference building models are analyzed by varying number of bays. A graph on number of bays vs. bending moment of the selected interior ground storey column of selected frame is plotted to compare the results (Figure 5.3). It is observed that the moments of ground storey column almost remain constant despite variation of number of bays. This happens because increment of lateral load in the reference models is proportional to the increment of number of bays. Generally lateral load of a model increases with the increment of frame mass but it also decreases as the frame stiffness increases. According to approximate portal method, lateral load of a symmetric building frame is equally distributed to each interior frame. Exterior frame takes half of the lateral load of an interior frame. Besides, it is assumed that the lateral load induced by increment of a bay is carried by that bay only thus overall moment on individual bay remains constant. The bending moment lines of the selected column of all the three frames are almost straight lines. But there are huge differences in the moment magnitude of BFP and SSFP lines in comparison to the BFL line.

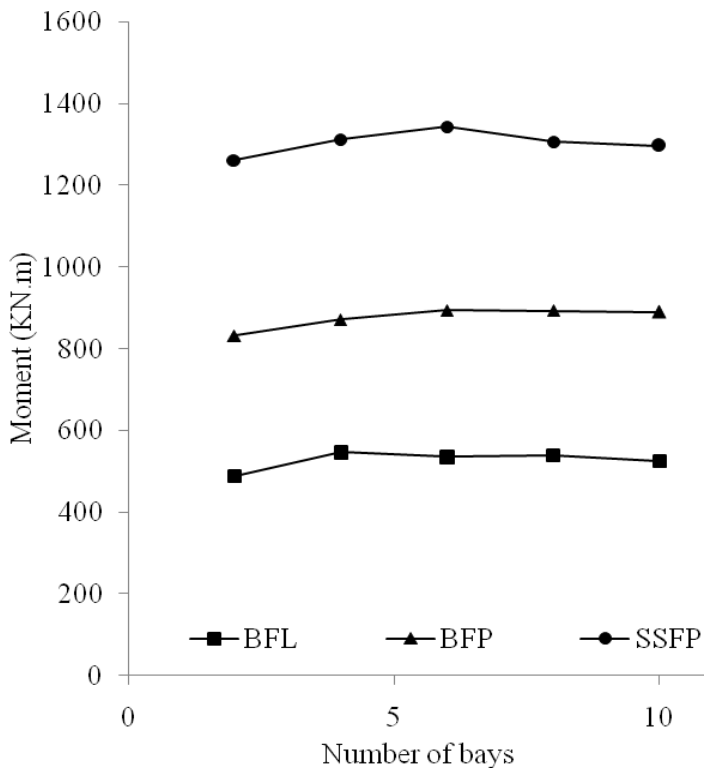

Figure 5.3 Number of bays vs. bending moment of ground storey column graph

It is also seen that the collapse point of all interior frames of reference models is not influenced by variation of number of bays. It is to note that the reference models for this

parametric study possess 70 percent infill. Thus the moments of soft ground storey column will increase for the same models of higher percentage of infill.

5.2.3 Effect on Column due to Variation of Number of Spans

Reference building models are studied by varying number of spans. A graph on number of spans vs. bending moment of selected ground storey column of selected interior frame is plotted to compare the results (Figure 5.4). It is observed that the moments of ground storey column of BFL and BFP are approximately constant. Contrarily, the moments of ground storey columns of SSFP have gradually increased due to variation of number of spans. According to approximate portal method, each interior frame is a summation of number of similar individual portal frame. Each portal frame again represents an individual span of an interior frame. Thus any lateral load applied to the interior frame is equally distributed to those portal frames. Though this method satisfies the behavior of BFL and BFP but the situation is different for SSFP where MI plays an important role in increasing said moments.

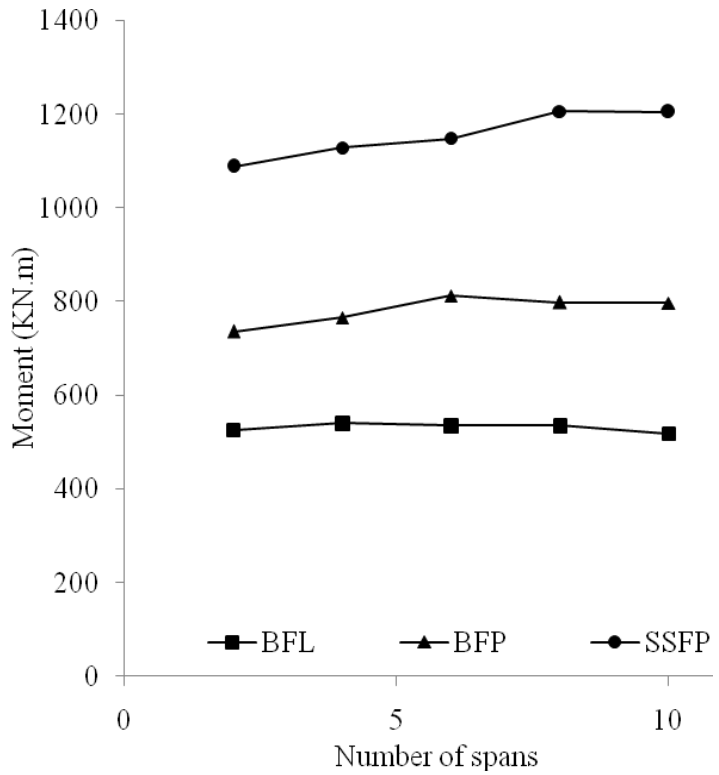

Figure 5.4 Number of spans vs. bending moment of ground storey column graph

It is observed that the frames with higher number of spans collapse earlier than the frame having lesser spans. It indicates that the large buildings with greater number of spans are more susceptible to early collapse. It can be said that the models collapse point is directly

influenced by variation of number of spans. There are huge differences in moment magnitude of ground storey columns of BFP and SSFP in comparison to the values of BFL. It is to note that the reference models for this parametric study possess 70 percent infill. Thus the moments of soft ground storey column will increase for higher percentage of infill.

5.3 MOMENT MAGNIFICATION FACTOR (MF) FOR SOFT STOREY COLUMN

Moment MF is used to compare the increment of moment of SSFP against the corresponding moment of BFP. Initially, magnification ratio of moment of ground storey column of BFP and SSFP is calculated with respect to the moment of BFL. Later on, the magnified ratio of the SSFP is compared with the magnified ratio of BFP. The obtained result is termed as design MF. This is referred here as an indicator of moment increment of ground storey column due to the soft storey effect. In subsequent subparagraphs this MF is discussed in relation to different parameters. Detail data of moment MF due to different parameters are attached to this paper as appendix D.

5.3.1 Moment MF for Variation of Percentage of Infill

Inelastic investigation of ground storey column of both bare frame and soft storey frame is carried out under seismic loading. A graph is plotted based on percentage of infill vs. moment MF of ground storey column of reference building models (Figure 5.5).

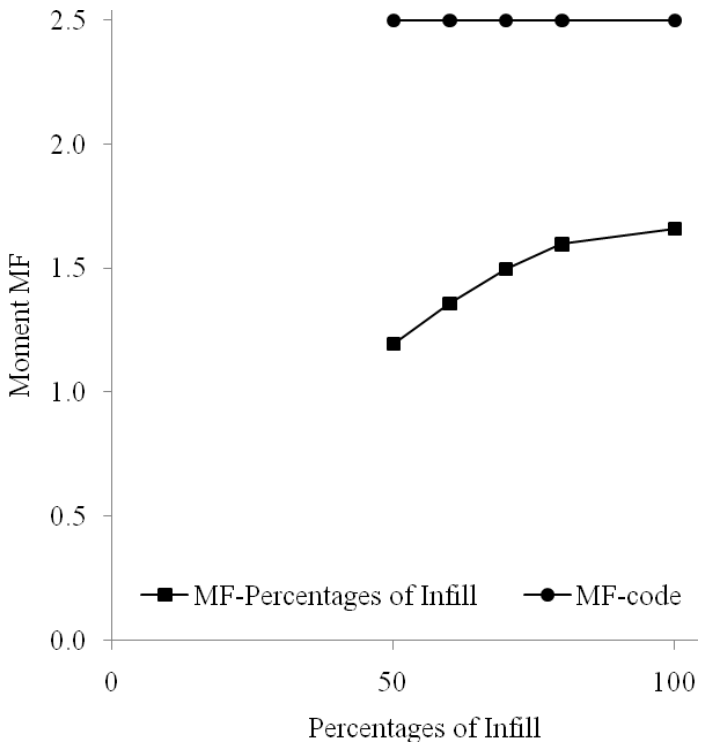

Figure 5.5 Percentage of infill vs. moment MF of ground storey column graph

The code specified MF (i.e., 2.5) for soft storey column is also plotted in the graph. The moment MF of soft ground storey column ranges from 1.20 to 1.66 due to variation of percentage of infill as observed in the graph. It is also observed that the MF of ground storey column increases with the increment of percentage of infill. Besides, this MF is quite smaller than the MF specified in the BNBC (Draft), 2015.

5.3.2 Moment MF for Variation of Number of Bays

Inelastic investigation of ground storey column of both BF and SSF is carried out under seismic loading. A graph is plotted based on number of bays vs. moment MF of ground storey column of selected interior frame (Figure 5.6). The code specified MF (i.e., 2.5) for soft storey column is also plotted in the graph. The moment MF of soft ground storey column ranges from 1.52 to 1.46 due to variation of number of spans as observed in the graph. The MF remains almost constant with the increment of number of bays. Thus moment of soft ground storey column is not affected by variation of number of bays. It is to note that the magnitude of moment MFs mentioned above will increase if the percentage of infill increases above 70 percent.

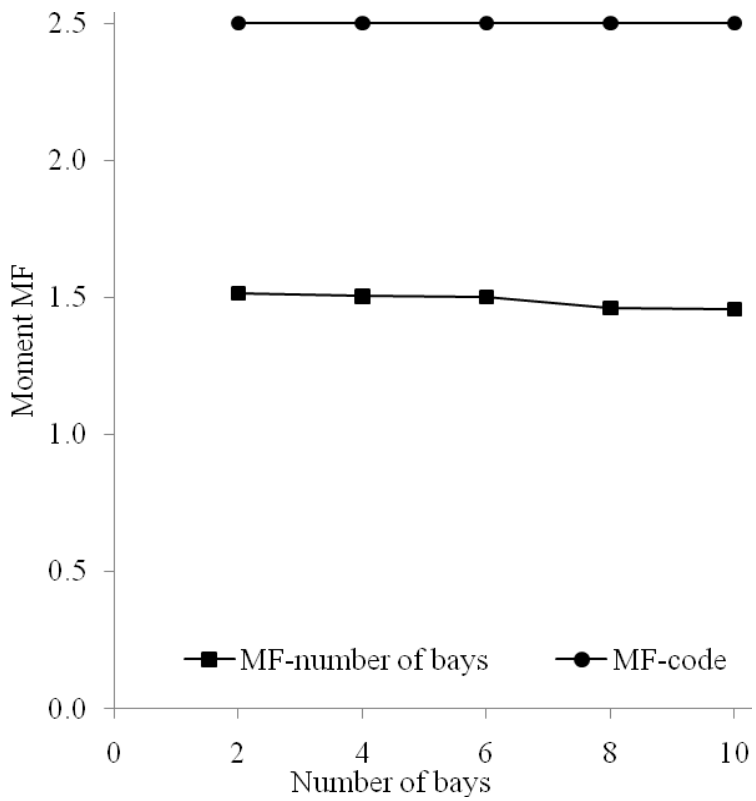

Figure 5.6 Number of bays vs. moment MF of ground storey column graph

5.3.3 Moment MF for Variation of Number of Spans

Inelastic investigation of ground storey column of both BF and SSF is carried out under seismic loading. A graph is plotted based on number of spans vs. moment MF of ground storey column of reference building models (Figure 5.7). The code specified MF (i.e., 2.5) for soft storey column is also plotted in the graph. The moment MF of soft ground storey column ranges from 1.48 to 1.51 due to variation of number of spans as observed in the graph. The MF remains almost constant with the increment of number of spans. Thus moment of soft ground storey column is not affected by variation of number of spans. It is to note that the magnitude of moment MFs mentioned above will increase if the percentage of infill increases above 70 percent.

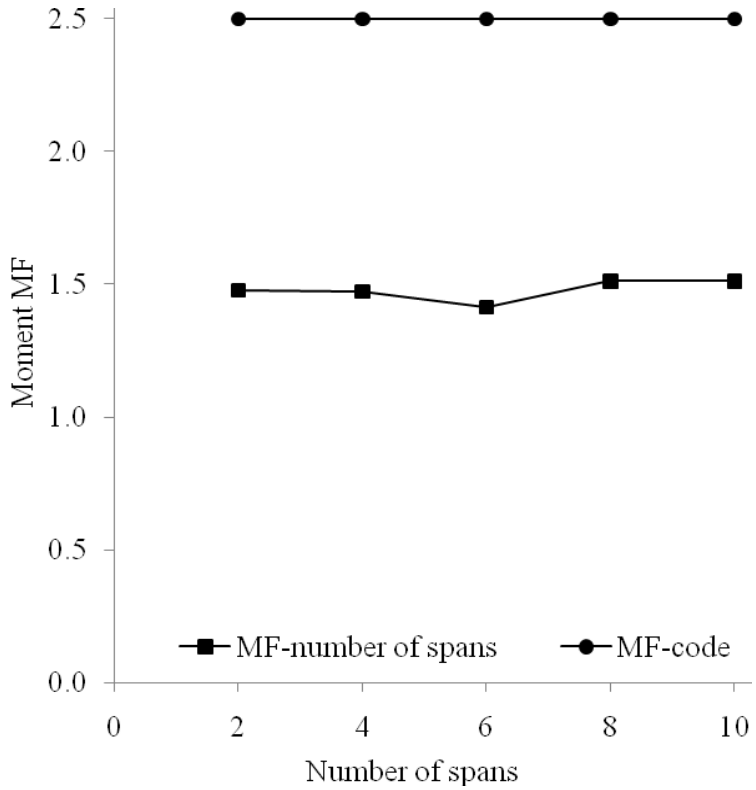

Figure 5.7 Number of spans vs. moment MF of ground storey column graph

5.4 EFFECT ON SHEAR FORCE OF SOFT GROUND STOREY COLUMN

The ground storey column of a soft storey building is certainly affected by the soft storey phenomenon. Effects of soft storey on the shear force magnitude of the selected columns are numerically analyzed and results are discussed in the subsequent subparagraphs. Initially effect on ground storey columns is analyzed by varying percentage of infill. They are also analyzed by varying number of bays and spans.

5.4.1 Effect on Column due to Variation of Percentage of Infill

Selected interior frame of the reference building models are analyzed by varying percentage of infill. A graph of shear force of ground storey column vs. percentage of infill is plotted for the selected interior frame to compare the results (Figure 5.8). It is observed that the shear force of ground storey column of BFL and BFP remains constant irrespective of variation of infill percentage. Contrarily, shear force of SSFP sharply increases with the increase of percentage of infill. This behavior of MI confirms its influence of structural behavior and demands attention during design.

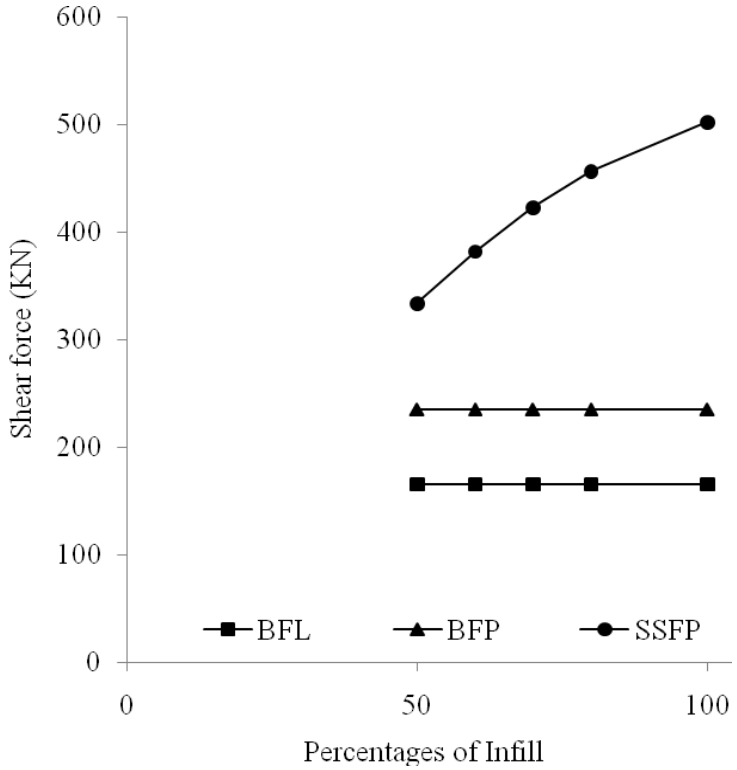

Figure 5.8 Percentage of infill vs. shear force of ground storey column graph

5.4.2 Effect on Column due to Variation of Number of Bays

Selected interior frames of reference building models are analyzed by varying number of bays. A graph on number of bays vs. shear force of the selected interior ground storey column of selected frame is plotted to compare the results (Figure 5.9). It is observed that the shear forces of ground storey column almost remain constant despite variation of number of bays. This happens because increment of lateral load in the reference models is proportional to the increment of number of bays. Generally lateral load of a model increases with the increment of frame mass but it also decreases as the frame stiffness increases. According to approximate portal method, lateral load of a symmetric building frame is equally distributed to each

interior frame. Exterior frame takes half of the lateral load of an interior frame. Besides, it is assumed that the lateral load induced by increment of a bay is carried by that bay only thus overall shear force on individual bay remains constant. The bending moments of the selected column of all the three frames are almost straight lines. But there are huge differences in the shear force magnitude of SSFP lines in comparison to the BFP and BFL lines. It is also seen that the collapse point of selected interior frames of reference models is not influenced by variation of number of bays. Besides, magnitude of shear force will increase if the percentage of infill increases above 70 percent.

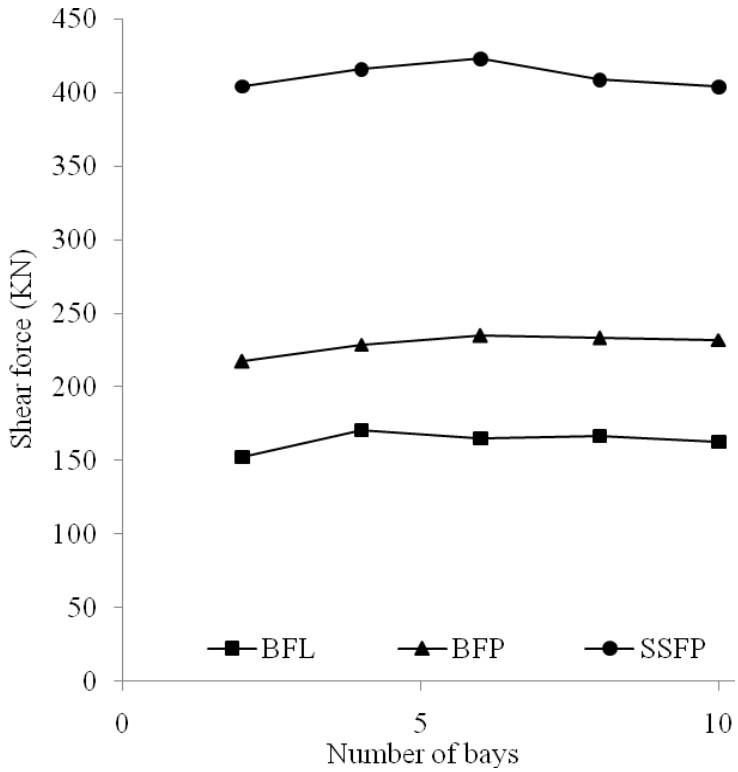

Figure 5.9 Number of bays vs. shear force of ground storey column graph

5.4.3 Effect on Column due to Variation of Number of Spans

Selected interior frames of the reference building models are studied by varying number of spans. A graph on number of spans vs. shear force of ground storey column of selected frame is plotted to compare the results (Figure 5.10). It is observed that the shear forces of ground storey column of BFL and BFP are approximately constant. Contrarily, the shear forces of ground storey columns of SSFP have gradually increased due to variation of number of spans. According to approximate portal method, each symmetric interior frame is a summation of number of similar individual portal frame. Each portal frame again represents an individual span of the interior frame. Thus any lateral load applied to the interior frame is

equally distributed to those portal frames. This method satisfies the behavior of BFL and BFP. But situation is different for SSFP where MI plays an important role in increasing shear force of the columns. It is also observed that the frame with greater number of spans collapses earlier than the frame having lesser spans. It indicates that the wide buildings are more susceptible to earlier collapse. Therefore, collapse point of any model is directly affected by variation of number of spans. However, there are huge differences in shear force magnitude of ground storey columns of SSFP in comparison to the BFP and BFL magnitudes. Besides, magnitude of shear force will increase if the percentage of infill increases above 70 percent.

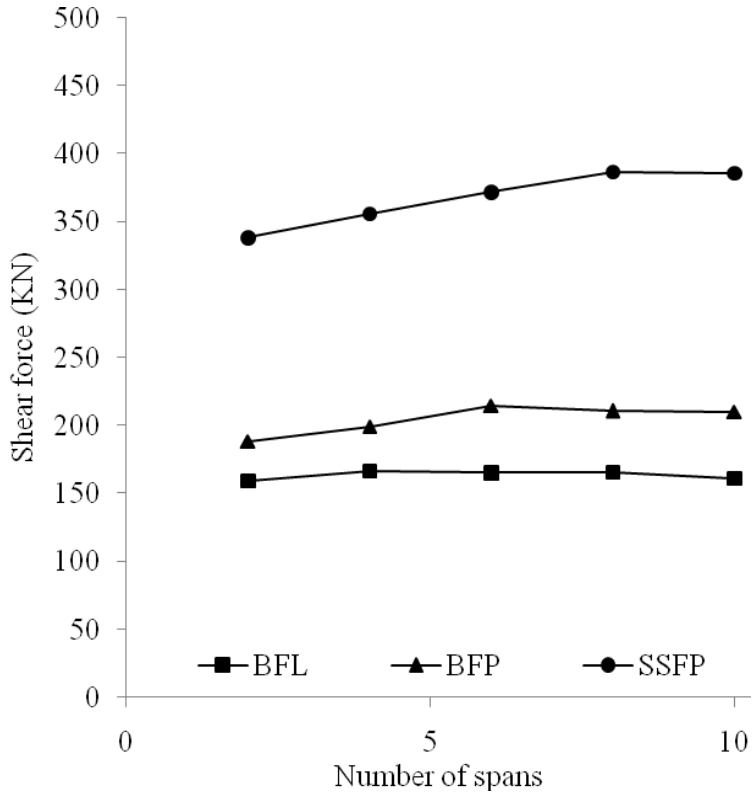

Figure 5.10 Number of spans vs. shear force of ground storey column graph

5.5 SHEAR FORCE MF FOR GROUND STOREY COLUMN

Shear force MF is used to compare the increment of shear force of SSFP in comparison to the corresponding shear force of BFP. This is referred here as an indicator of shear force increment of ground storey column due to the soft storey effect. In subsequent subparagraphs this MF is discussed in relation to different parameters. Detail data of shear force MF due to different parameters are attached to this paper as appendix E.

5.5.1 Shear Force MF for Variation of Percentage of Infill

Inelastic investigation of ground storey column of both bare frame and soft storey frame is carried out under seismic loading. A graph on percentage of infill vs. moment MF of ground storey column is plotted as shown in Figure 5.11. The code specified MF (i.e., 2.5) for soft storey column is also plotted in the graph. The moment MF of soft ground storey column ranges from 1.42 to 2.13 due to variation of percentage of infill as observed in the graph. It is observed that the MF of ground storey column increases with the increase of percentage of infill. Besides, this MF is quite lesser than the MF specified in the BNBC (Draft), 2015.

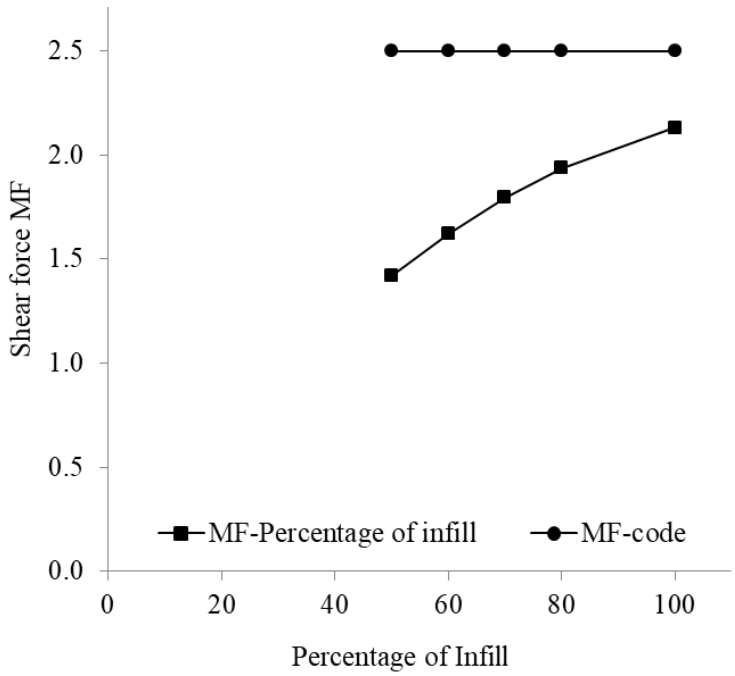

Figure 5.11 Percentage of infill vs. shear force MF of soft ground storey column graph

5.5.2 Shear Force MF for Variation of Number of Bays

Inelastic investigation of ground storey column of both bare frame and soft storey frame is carried out under seismic loading. A graph on number of bays vs. shear force MF of ground storey column is plotted as shown in Figure 5.12. The code specified MF (i.e., 2.5) for soft storey column is also plotted in the graph. The shear force MF of soft ground storey column ranges from 1.86 to 1.74 due to variation of number of bays as observed in the graph. The MF slightly decreases with the increase of number of bays. It is to note that the magnitude of moment MFs mentioned above will increase if the percentage of infill increases above 70 percent.

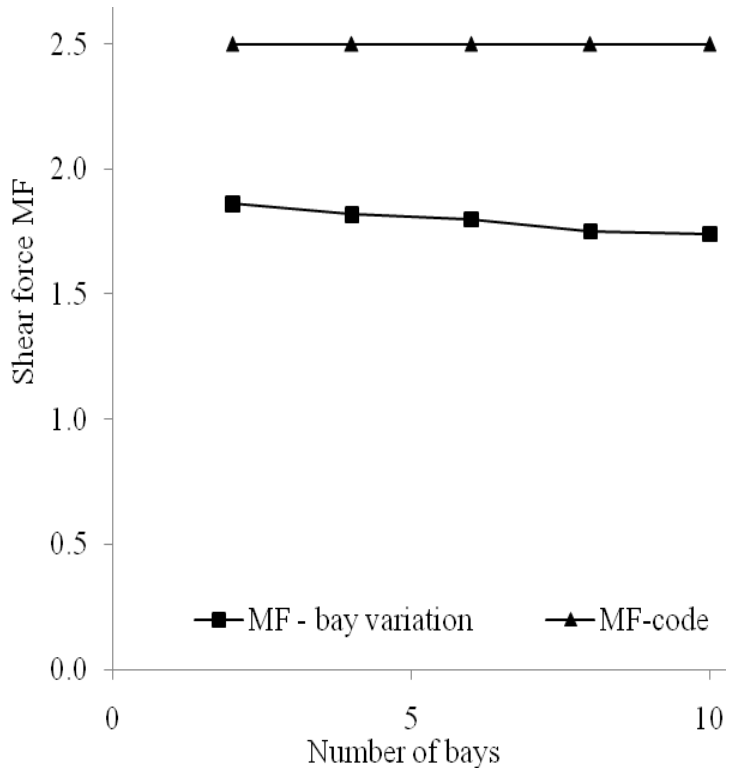

Figure 5.12 Number of bays vs. shear force MF of ground storey column graph

5.5.3 Shear Force MF for Variation of Numbers of Spans

A graph on number of bays and number of spans vs. moment MF of ground storey column is plotted as shown in Figure 5.13.

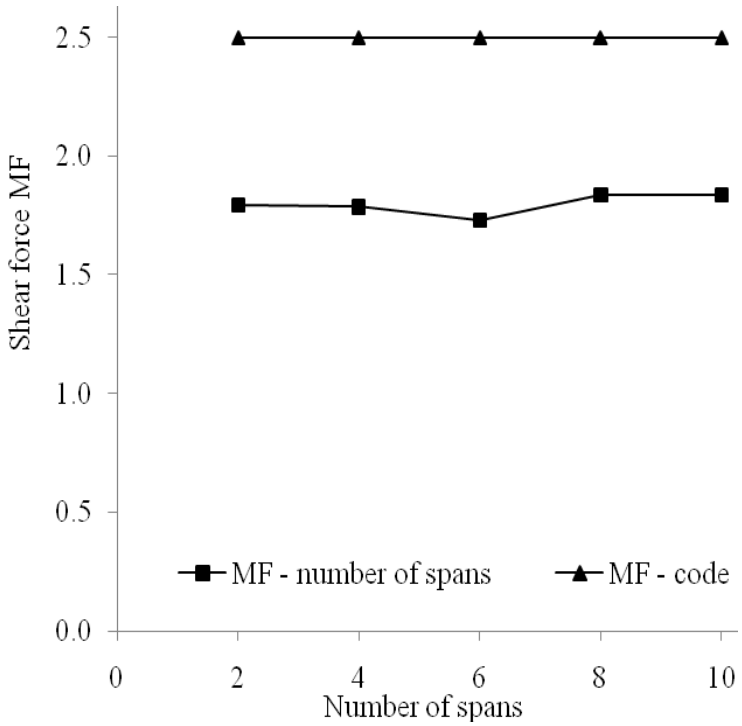

Figure 5.13 Number of spans vs. shear force MF of soft ground storey column graph

The code specified MF (i.e., 2.5) for soft storey column is also plotted in the graph. The moment MF of soft ground storey column ranges from 1.79 to 1.84 due to variation of number of spans as observed in the graph. The MF slightly increases with the increase of number of spans. It is to note that the magnitude of moment MFs mentioned above will increase if the percentage of infill increases above 70 percent.

5.6 BASE SHEAR COMPARISON BETWEEN BF AND SSF

5.6.1 Base Shear Comparison for Variation of Percentage of Infill

Base shear of ground storey column of BF and SSF, as obtained by pushover analysis, is compared with the base shear of BFL by varying percentage of infill. The ratio between nonlinear and linear base shear of the ground storey column is termed as the base shear MF. A bar chart is prepared with base shear MF of BF and SSF for different percentage of infill (Figure 5.14). It is observed that the base shear MF of ground storey column of both BF and SSF remains constant irrespective of any variation of percentage of infill. It is proved that the base shear of BF and SSF is magnified by 2.5 times prior to collapse.

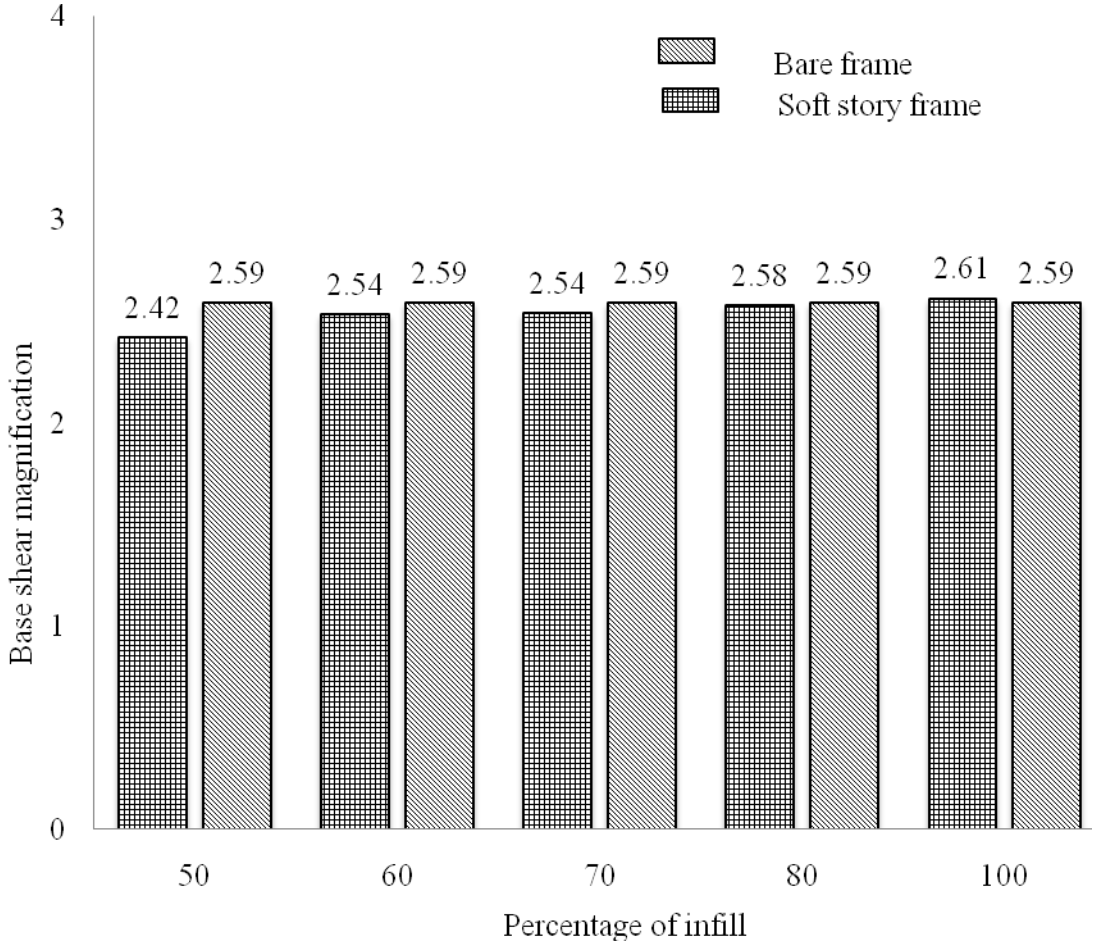

Figure 5.14 Percentage of infill vs. base shear MF of soft ground storey column chart

5.6.2 Base Shear Comparison for Variation of Number of Bays

Base shear of ground storey column of BF and SSF, as obtained by pushover analysis, is compared with the base shear of BFL by varying number of bays and spans. The ratio between nonlinear and linear base shear of the ground storey column is termed as the base shear MF. A bar chart is prepared with base shear MF of BF and SSF for different number of bays (Figure 5.15). It is observed that the base shear of ground storey column of BF, as obtained by pushover analysis, is approximately 2.90 to 2.32 times higher than the obtained base shear of same frame by linear analysis. Whereas, the base shear of soft ground storey column of SSF, as obtained by pushover analysis, is approximately 3.45 to 2.67 times higher the base shear of BFL.

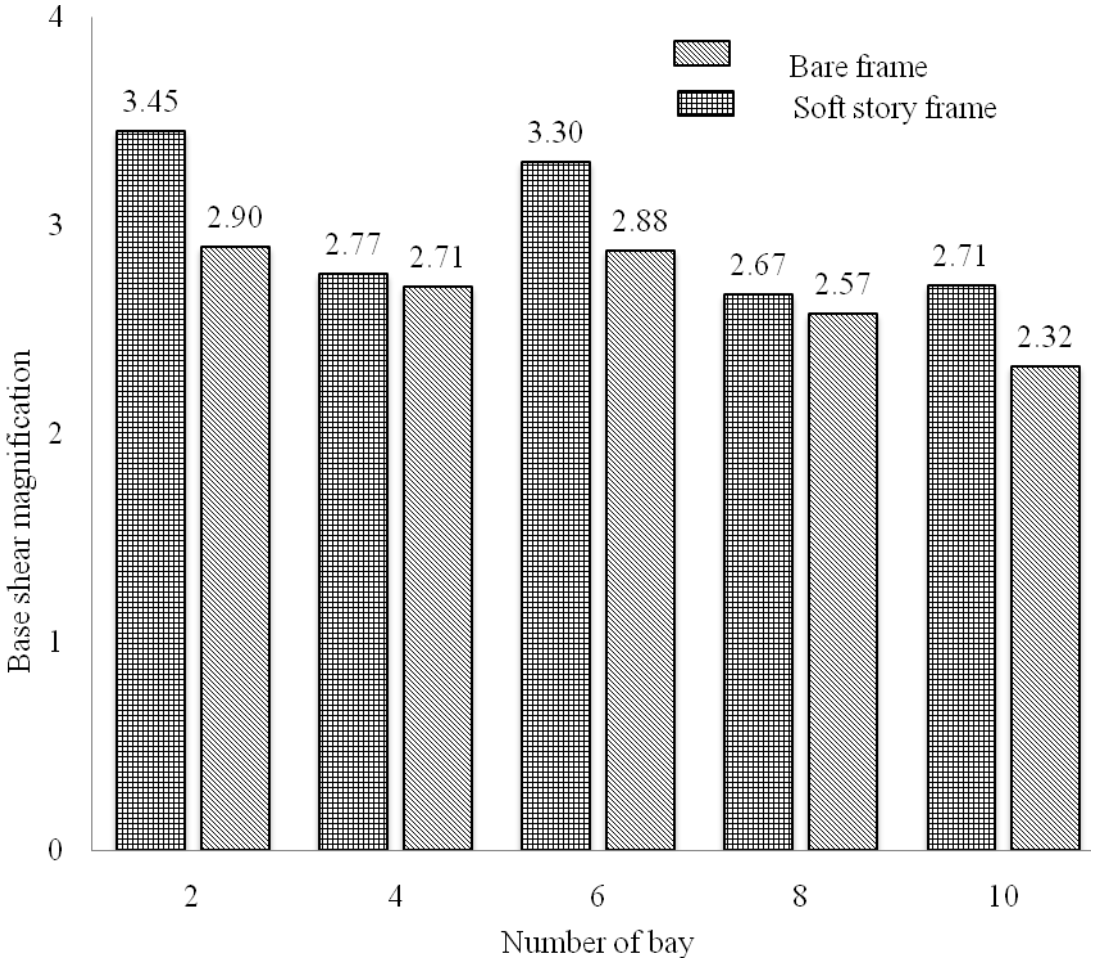

Figure 5.15 Number of bays vs. base shear MF of soft ground storey column chart

In reality, it is proved that addition shear force develops in soft storey column. This increase in shear force is due to the truss action of diagonal struts. Besides, the shear force of both BF and SSF reduces with the increase of number of bays.

5.6.3 Base Shear Comparison for Variation of Number of Spans

Base shear of ground storey column of BF and SSF, as obtained by pushover analysis, is compared with the base shear of BFL by varying number of bays and spans. The ratio between nonlinear and linear base shear of the ground storey column is termed as the base shear MF. A bar chart is prepared with base shear MF of BF and SSF for different number of bays (Figure 5.16). It is observed that the base shear of ground storey column of BF, as obtained by pushover analysis, is approximately 2.27 to 2.82 times higher than the obtained base shear of same frame by linear analysis. Whereas, the base shear of soft ground storey column of SSF, as obtained by pushover analysis, is approximately 3.23 to 2.42 times higher the base shear of BFL.

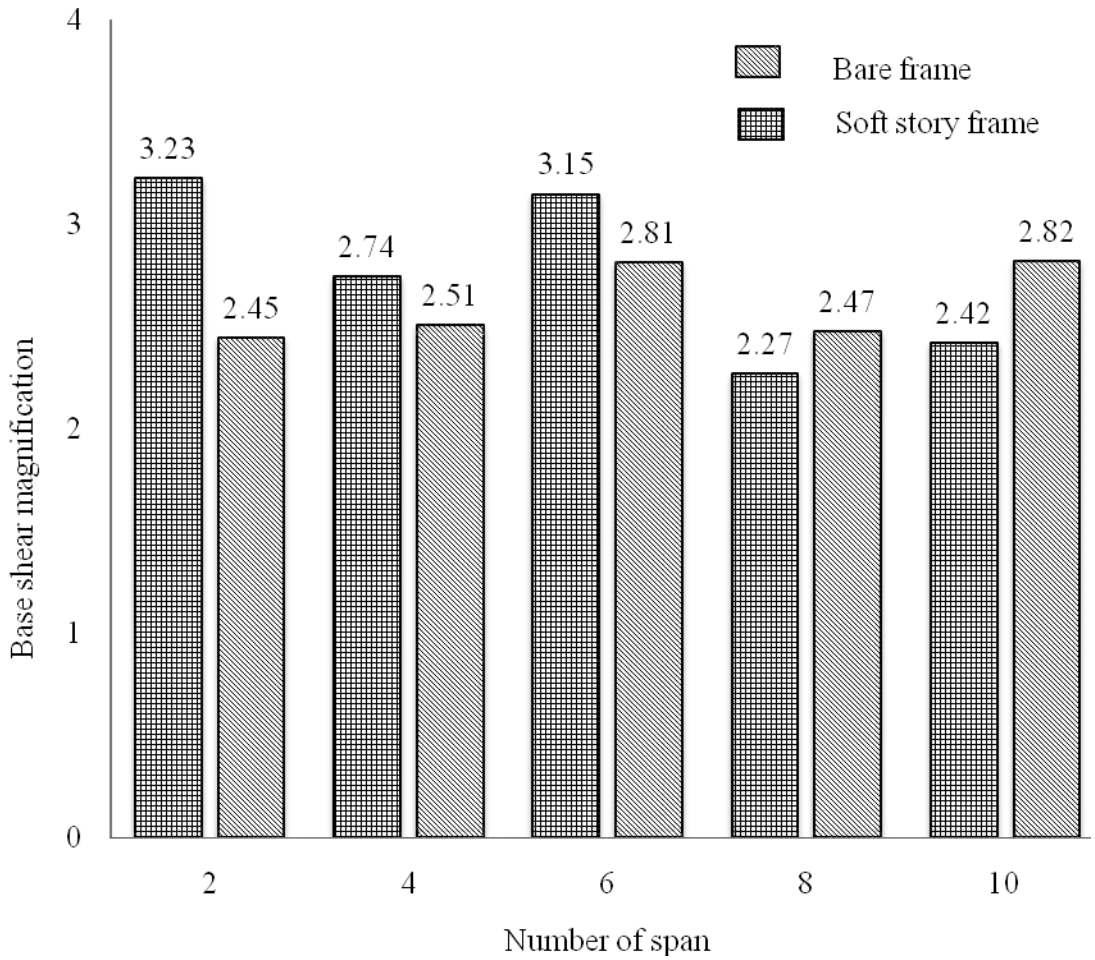

Figure 5.16 Number of spans vs. base shear MF of soft ground storey column chart

Here, the base shear MF increases with the increment of number of spans. Contrarily, the base shear MF of SSF decreases with the increment of number of spans. This decrease in the shear force MF of SSF is due to early collapse of ground storey columns with higher number

of spans. It is proved that the soft storey building is vulnerable to early failure at higher number of spans.

5.7 DRIFT PATTERN

According to BNBC (Draft), 2015, design storey drift of each storey of the reference building model shall not exceed the allowable drift i.e., 0.020 h_{sx}. Thus total drift of the reference building model is equal to the drift of each storey multiplied by number of stories. In pushover analysis top deflection of the building is considered for the study. Therefore, nonlinear effect of soft storey building on drift and performance point is studied considering the deflection of top right corner of the building as reference point. The numerical investigation has found that the deflection of BF at performance point is much higher than the code limit as shown in the table 5.1.

Table 5.1: Total drift of BF and SSF at performance point

Type of Parameter	Deflection at Performance Point		Deflection (Linear) (mm)	Allowable Deflection (Draft BNBC 2015) (mm)
	Bare Frame (BF) (mm)	Soft Storey (SSF) (mm)		
Bay Variation				
2 Bays	236.0	159.1	74.2	139.9
4 Bays	245.0	174.5	82.5	139.9
6 Bays	250.0	182.2	91.1	139.9
8 Bays	253.0	180.8	84.9	139.9
10 Bays	254.0	183.0	80.7	139.9
Span Variation (ATC 40)				
2 Spans	222.8	161.0	88.9	139.9
4 Spans	223.0	155.0	85.9	139.9
6 Spans	226.0	141.0	76.8	139.9
8 Spans	222.0	154	82.9	139.9
10 Spans	222.0	154	77.9	139.9
Percentage of Infill Variation				
50	251.0	161.2	83.5	139.9
60	251.0	174.4	83.5	139.9
70	251.0	182.2	83.5	139.9
80	251.0	185.5	83.5	139.9
100	251.0	194.2	83.5	139.9

The nonlinear deflection of SSF at performance point is considerably higher than the allowable nonlinear deflection by the code. This pattern of nonlinear drift of BF and SSF occurs due to rotational ability of each building.

5.8 REMARKS

Moment magnification occurs in soft ground storey column of SSF with respect to the moment of similar column of BF. This magnification starts from the yield point and remains almost constant till collapse. In the analysis above, it is found that the moment magnification pattern of number of bays and number of spans are almost similar. As such magnification graph of number of bays can be considered for both the parameters. Moment MF sharply increases with the increment of percentage of infill. This incensement proves that the presence of infill in the beam-column panel has direct influence on load bearing elements.

Shear force magnification also occurs in soft ground storey column of SSF with respect to the shear force of similar column of BF. This magnification starts from the yield point and remains almost constant till collapse. The shear force MF gradually decreases with the increment of number of bays. While, the shear force MF considerably decreases with the increment of number of spans. It is also observed that the shear force MF of ground storey column of both BF and SSF remains constant despite variation of percentage of infill.

In this study it is found that the moment MF ranges from 1.20 to 1.66 for all the parameters. This study has considered maximum MF as 1.70 for design of the soft ground storey column to remain in the safer side. Similarly, the shear force MF ranges from 1.42 to 2.13 for all the parameters. In this situation, the study has also considered maximum MF as 2.15 for the shear force design of ground storey column. Though the MF is almost constant for number of bays/spans but the MF sharply increases due to variation of percentage of infill.

It is observed that the BF and SSF can deflect greater than the deflection expected from them as per BNBC (Draft), 2015. It is also seen that the deflection BF and SSF gradually increases with the increment of number of bays. Deflection of BF and SSF almost remain constant due to variation of number of spans. Besides, the deflection of BF remains constant due to variation of percentage of infill. But the deflection of SSF gradually increases with the increment of percentage of infill.

CHAPTER 6

REMEDIAL MEASURES

6.1 INTRODUCTION

Results of the previous chapter support the fact that buildings with soft ground storey are moderately vulnerable to earthquake. Appropriate preventive measures should be taken to safeguard human lives and properties from any structural damage due to the soft storey affect. Measures must be taken at design phase, construction phase or afterwards. In design and construction phases, moment and shear force of ground storey columns may be magnified as per the suggestions below. These magnified moment and shear force will determine the size and reinforcement of the ground storey columns. Besides, retrofitting of soft ground storey columns is suggested for the constructed buildings. Some guidelines applicable for all the phases are presented below.

6.2 SUGGESTED REMEDIAL MEASURES

Building with open ground storey is an essential feature of modern apartment construction. As such suitable remedial measures against soft storey failure are required to ensure correct functioning of soft storey building. Keeping this in mind, following measures are suggested which may enhance safety of structures against any credible earthquakes.

6.2.1 Moment/Shear Force Magnification

Soft storey building is designed considering that the building will perform within its elastic limit. Yet, structural engineers accept limited nonlinear performance of building during earthquake. In the previous chapter it is proved by pushover analysis that the bare frame of a RC building performs well up to its performance point despite considerable increase in the column moments. It is also proved that the bare frame comfortably sustains all types of earthquake. In case of soft storey building the situation is different. Huge moment develops only in the soft ground storey column thus it collapses during maximum earthquake. Therefore, RC buildings with soft storey having minimum 50 percentage of infill, any number of spans and bays will collapse during maximum earthquake. To address this issue, some national codes including BNBC (Draft), 2015 have incorporated an empirical MF of 2.5 to increase the moment and shear force of soft ground storey column under any circumstances. In reality this factor varies with the variation of spans, bays and masonry

infill. Six moment and shear force MF graphs are developed in the previous chapter. Some suggestions are given in subsequent paragraphs for these graphs.

6.2.2 Moment/Shear Force MF for Soft Ground Storey Column

The Figure 6.1 shows the variation of MF of soft ground storey column due to variation of percentage of infill of reference building models.

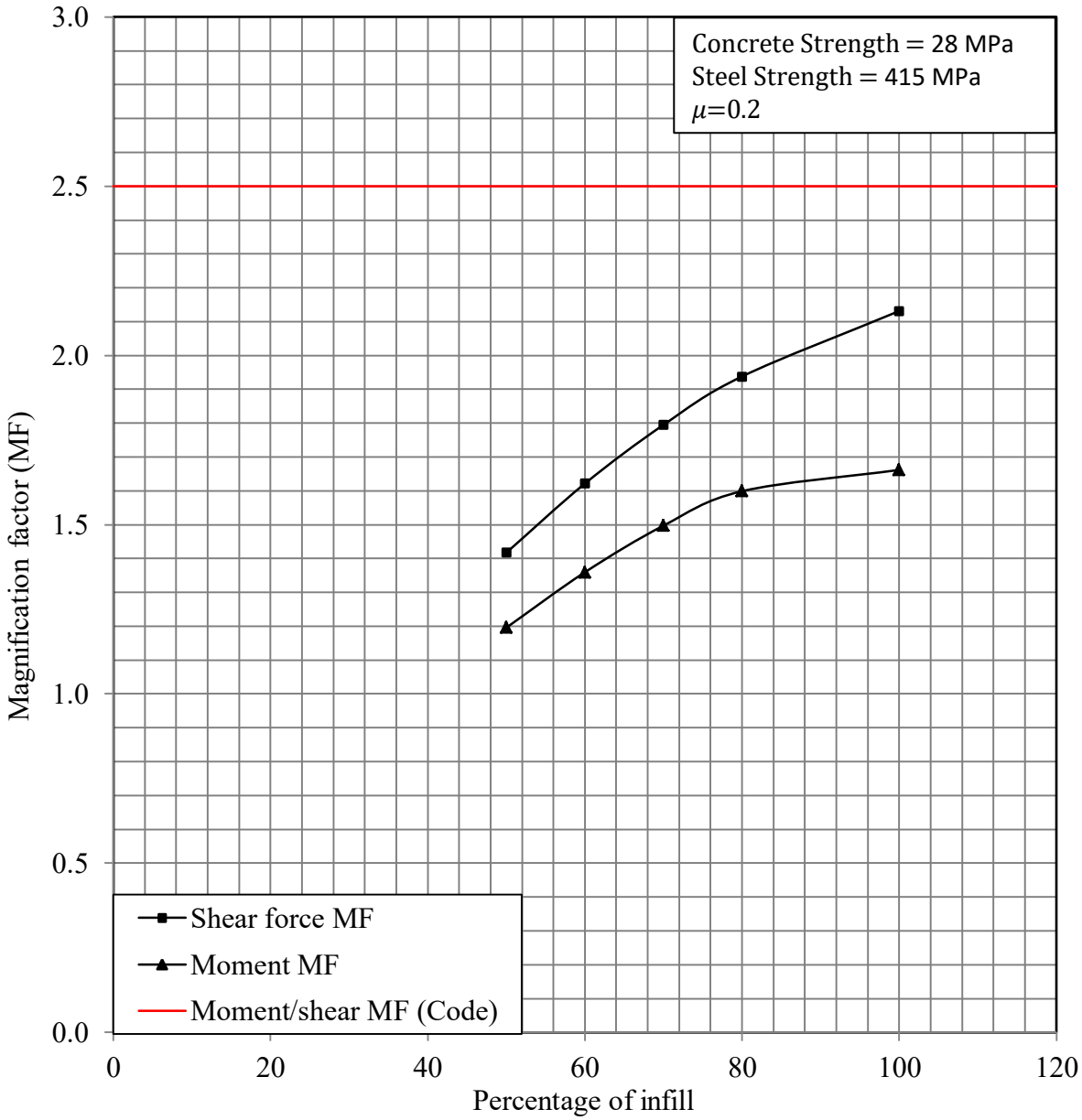

Fig.6.3 Percentage of infill vs. moment/shear force MF of soft ground storey column chart

The MF of soft storey column is also plotted in the graph as per BNBC (Draft), 2015 to understand the variation. The graph shows that the moment/shear force MF of soft storey building sharply increases due to the increment of percentage of infill.

6.2.3 Effect on Moment/Shear Force of Soft Ground Storey Column by Number of Bays

The Figure 6.2 shows the variation of MFs of soft ground storey column due to variation of number of bays. The MF of soft storey column is also plotted in the chart as per BNBC (Draft), 2015 to understand the variation. The graph shows that the moment of soft ground storey column is almost constant but shear force is very slowly decreased due to the increment of number of bays but this variation is only 5% which may be neglected. This graph is prepared for reference building models with 70 percent of infill. Therefore, the value of MF of soft storey column given in this graph will increase with the increment of percentage of infill above 70 percent and vice versa. It can be deduced that the moment and shear force MFs of ground storey column will remain constant irrespective of any variation in number of bays.

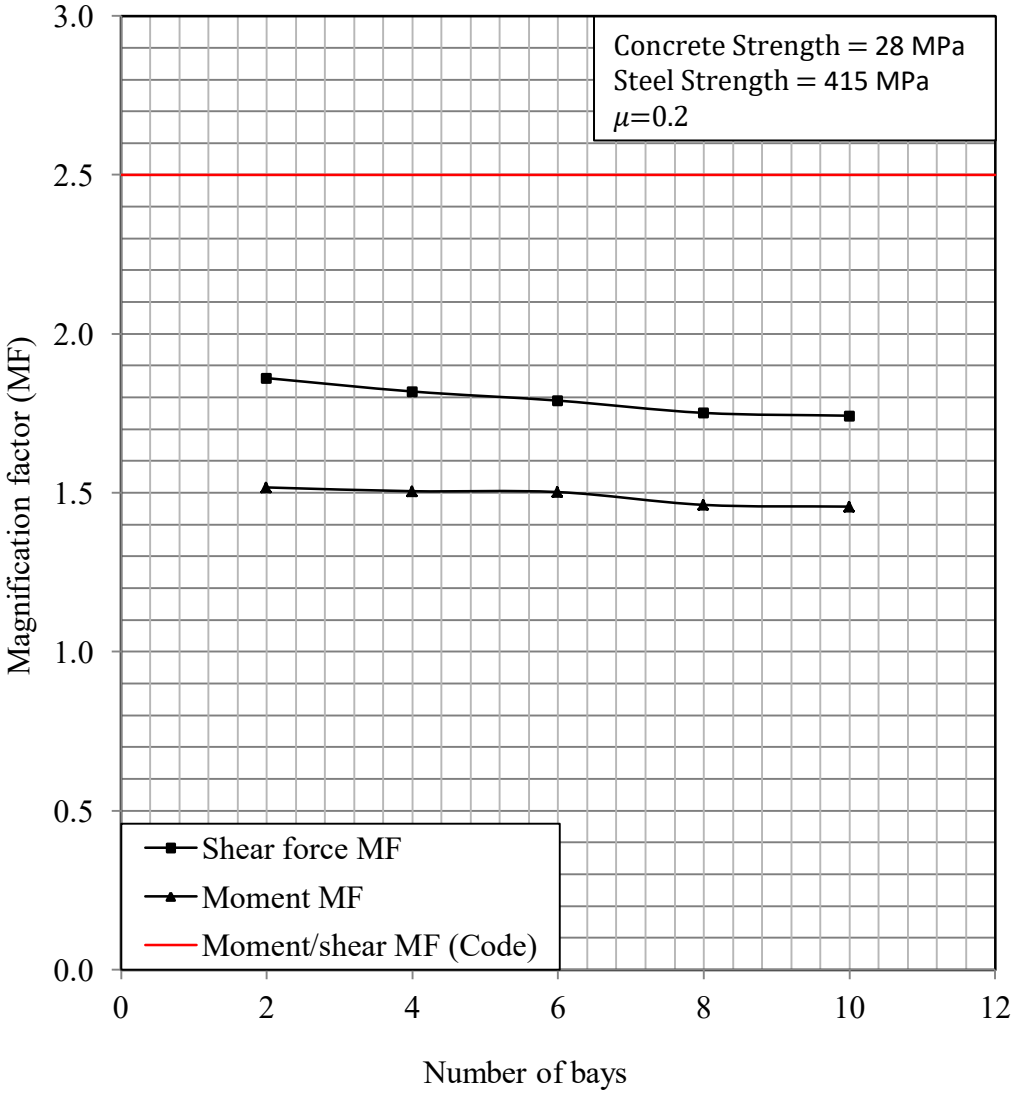

Fig.6.1 Number of bays vs. moment/shear force MF of soft ground storey column graph

6.2.4 Effect on Moment/Shear Force of Soft Ground Storey Column by Number of Spans

The Figure 6.2 shows the variation of MF of soft ground storey column due to variation of number of stories. The MF of soft storey column is also plotted in the chart as per BNBC (Draft), 2015 to understand the variation. The graph shows that the moment and shear force of soft ground storey column is almost constant for any number of spans. This graph is prepared for reference building models with 70 percent of infill. Therefore, the value of MF of soft storey column given in this graph will increase with the increment of percentage of infill above 70 percent and vice versa. It can be deduced that the moment MF of ground storey column will remain constant irrespective of any variation in number of spans.

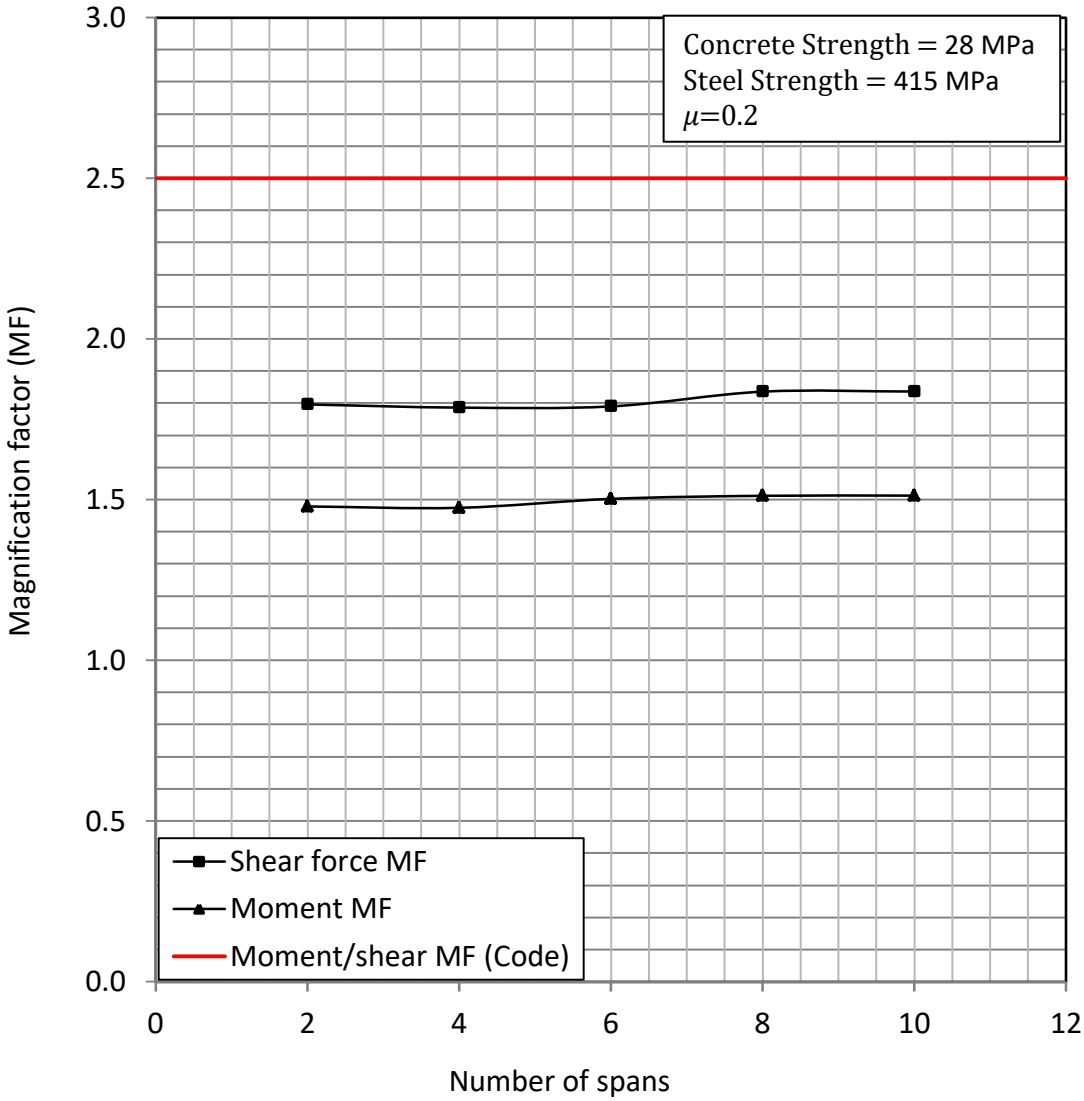

Fig.6.2 Number of spans vs. moment/shear force MF of soft ground storey column chart

6.3 EXAMPLE OF MOMENT AND SHEAR FORCE MAGNIFICATION OF A SOFT GROUND STOREY COLUMN OF A SAMPLE BUILDING

This paper has hypothetically considered a soft storey building with open ground storey as an example. The parameters of this building are given below:

- Number of bays: 4
- Number of spans: 6
- Percentage of infill: 80%

Selected soft storey building is initially analyzed by ESFM to derive the moment and shear force of ground storey column. According to the present design code, this building is considered as bare frame during seismic design. Soft storey effect of the building is not taken into consideration. This study has found that the moment and shear force of ground storey column are considerably higher than the values found by the ESFM. Thus soft ground storey column of this building collapses prior to reaching the performance point of bare frame. This study suggests moment or shear force magnification of ground storey columns as per the Magnification graph proposed by Figure 6.1. Steps involve in solving the problem are as follows:

- Determine the moment and shear force of ground storey column by ESFM.
- Determine the MF from the graph (Figure 6.1).
- Calculate the design moment of soft storey column.

6.3.1 Determination of Moment and Shear Force of Ground Storey Column by ESFM

The moment and shear force of ground storey column of soft storey building under seismic loading are calculated by ESFM and they are named as $_{\text{Static}}$ and $_{\text{static}}$.

6.3.2 Determination of MFs from Graph

The moment MFs for 80 percent infill (80%) are calculated from the Figures 6.1. The values are given below:

- MF of moment = 1.60
- MF of shear force = 1.95

6.3.3 Design Moment and Shear for Soft Ground Storey Column

The design ground storey column moment is M_{Static} and ground storey column shear force is V_{Static}. The ground storey column of the sample soft storey building should be design with this calculated moment and shear force.

6.4 APPROXIMATE METHOD FOR DETERMINING MF OF SOFT GROUND STOREY COLUMN

The sample example given above is a deliberate method of solving soft storey problem. There can be an approximate method where an approximate MF of both moment and share can be selected for a workable solution to the soft storey problem. In this study, the maximum MF for moment and shear force of soft storey building irrespective of their variable parameters can be considered as 1.50 and shear force 2.0 respectively.

6.5 OTHER REMEDIAL METHODS

6.5.1 Masonry Walls at the Open Ground Floor

Placement of masonry walls between the columns at the open ground storey in an organized manner will increase the stiffness of the storey. On the other hand, it will also facilitate the desire car parking. But, the builders and the users may want to have an uninterrupted open space instead of compartments as shown below.

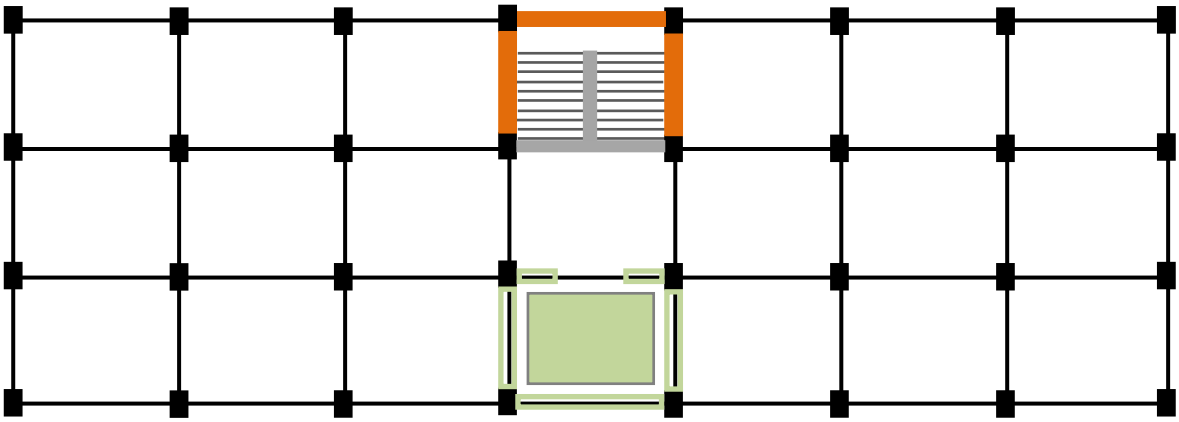

Figure 6.5 Retrofitting scheme of complete open ground storey(Murty, 2006)

6.5.2 Using of Glass as Partition Wall

Presence of infill makes the upper stories of any building much stiffer against lateral sway rendering the ground storey soft. Collapse of buildings due to soft ground storey can be avoided if the infill can be made structurally inactive. This can be achieved by replacing wall

by glass. In modern era, glasses are commonly used as partition wall. Since, glass decrease weight and are brittle as such they cannot absorb compression also. If the partition wall is brittle and RC frame solely behaves like a bare frame.

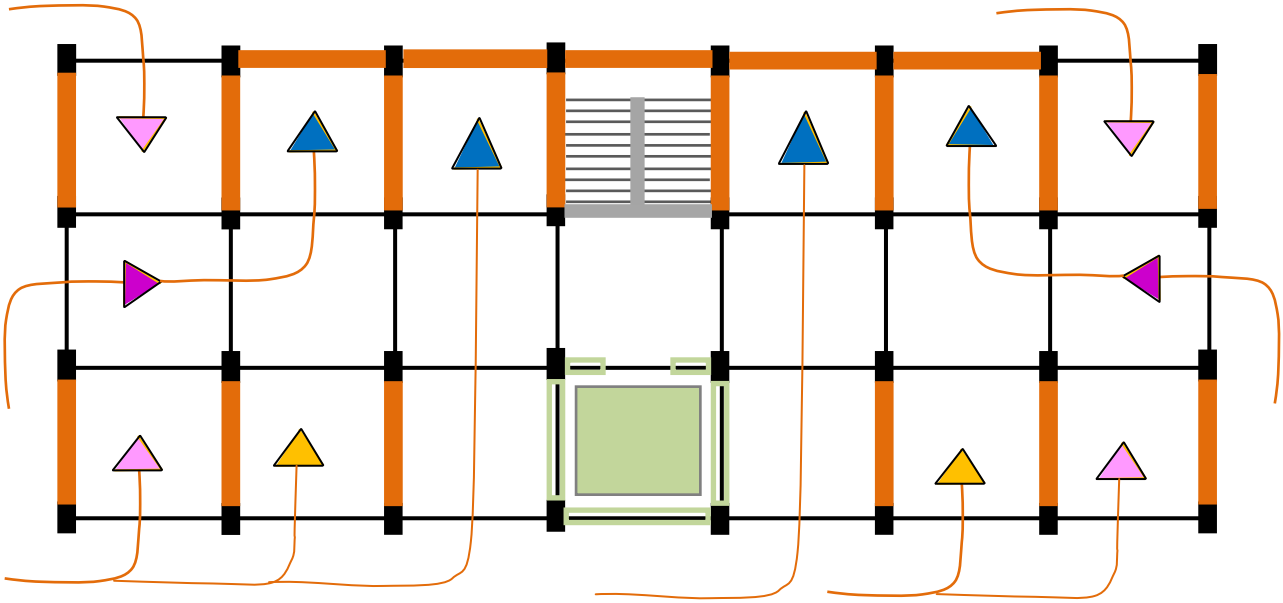

Figure 6.6 Retrofitting scheme of open ground storey; triangle indicates parking (Murty,2006)

6.6 ISOLATION OF MASONRY INFILL WALLS

MI of upper stories of a RC building with open ground storey causes the soft ground storey effect to occur. But collapse of soft ground storey column can be avoided by make the MI inactive. MI can be made inactive by avoiding interaction between beam-column panel and infill wall. If some gap is maintained between the frame element and infill wall than this infill wall can be made structurally inactive (Hoque, 2007). Such isolation of infill from the frame elements would thus prevent the rigid body like motion (pendulum effect) of the upper stories and the building frame would behave like an ordinary bare frame without any soft storey.

Isolated MI wall does not affect the frame performance and frame displacements are not restrained. Another advantage of the isolated MI is that the walls remain undamaged, thereby reducing post-earthquake repair costs. Under this circumstances, controlling weather conditions inside the building entails the gaps to be sealed with an elastic compressible material (like cork sheet).But it should be kept in mind that the above suggestions for providing gap needs further study before it is implemented in practice. It is certain that

providing gap shall render infill structurally inactive. However an additional problem may arise regarding the stability of the wall itself during earthquake shaking.

6.7 REMARKS

Since soft storey building is very common in Bangladesh thus some practical remedial measures for this type of building are discussed in this chapter. Suggestions proposed above are based on the present analysis where main focus is given to increase the shear force and bending moment of ground storey columns. These increased shear force and bending moment will be used for designing the open ground storey columns only. Following these suggestions, engineers will be able to design soft storey building without affecting the conventional construction practice and performance of this building will be enhanced to the desired level.

The other means of eradicating soft storey effect is to reduce the effect of MI by alternative construction material like glass. If high rise building uses glass as the partition wall in the upper stories than the soft storey effect can be negotiated.

CHAPTER 7

CONCLUSIONS AND RECOMMENDATIONS

7.1 GENERAL

Extensive numerical investigations of RC soft storey building with open ground storey have been carried out to identify their possible vulnerabilities during earthquake. Nonlinear material property of concrete has been incorporated to the frame members to observe the nonlinear global and local responses of buildings due to extreme earthquake loading. Selected parameters of this study are number of bays, number of spans, and percentage of infill. ESFM and nonlinear pushover analysis method are used for linear and nonlinear analyses of the building. Different codes restrictions are also studied and present building design practice is discussed. The present study supports the fact that conventional multistoried residential buildings with open ground storey are at risk under seismic loading. Besides, open ground storey is an important functional requirement of almost all the urban multi-storey buildings and cannot be avoided. Poor performance of such RC building during a strong earthquake is established by this study and remedial measures are suggested to improve their performance. These remedial measures can be applied to soft storey columns to render the building safe.

7.2 FINDINGS IN BRIEF

The findings of the study presented in the previous chapters are summarized below:

- Pushover analysis demonstrates the affect of MI on moment and shear force of soft ground storey columns of a building. The moment and shear force of these columns increase moderately when building undergoes nonlinear deformation due to earthquake. This paper has studied the said soft storey affect on those columns and suggested to increase their moment and shear force during design. The increase of moment and shear force can be obtained by using MF graph (Figure 6.1) as given in the previous chapter.

- Moment magnification of soft ground storey column remains almost constant due to variation of number of bays and spans as shown in graphs (Figure 6.2 to 6.3) of the previous chapter. But MF of the same column varies nonlinearly for variation of percentage of infill as shown in MF graph (Figure 6.1). According to

these graphs, moment MF of RC building with soft ground storey varies 1.2 to 1.66 for different percentage of infill. On the other hand, BNBC (Draft), 2015 specified moment MF of soft storey column as 2.5 which is much higher than the MF obtained by nonlinear pushover analysis. So it needs rethinking or further study. This paper suggests that the moment MF of soft ground storey column should be 1.5 instead of 2.5. Besides, deliberate calculation of moment MF can be done using Figure 6.1.

- Shear force magnification of soft ground storey column remains almost constant due to variation of number of bays and spans as shown in graphs (Figure 6.2 to 6.3) of the previous chapter. But MF of the same column varies nonlinearly for variation of percentage of infill as shown in Figure 6.1. According to the graph, shear force MF of RC building with soft ground storey varies form 1.42 to 2.13 for different percentage of infill as shown in the figure. On the other hand, BNBC (Draft), 2015 specified shear force MF of soft storey columns as 2.5 which is quite higher than the MF obtained by nonlinear pushover analysis. So it needs rethinking or further study. This paper suggests that the shear force MF of soft ground storey column should be 2.0 instead of 2.5. Besides, deliberate calculation of shear force MF can be done using Figure 6.1.

- Base shear of ground storey column of BF and SSF remains constant due to variation of percentage of infill. But the base shear of ground storey column BF and SSF decreases with the increase of number of bays or spans. Moreover, base shear of SSF noticeably reduces with respect to base shear of BF at higher number of spans. This occurs because soft ground storey column collapses earlier than limit set by the reference building model. This proved the requirement of shear force magnification of ground storey column of SSF.

- It is observed during study that the bare frame and soft storey buildings can deflect much higher than the limit suggested by the Bangladesh national building code.

Findings of the study can help us to produce safe design of buildings with open ground storey.

7.3 SUGGESTIONS FOR SAFEGUARDING BUILDINGS WITH SOFT GROUND STOREY

The behavior of RC framed buildings with open ground storey subjected to ground motion has been presented in Chapter 5. Based on these findings some suggestions are made and elaborately discussed in Chapter 6. Major focus of this study is to safeguard the soft storey building by increasing strength of ground storey columns as proposed in the previous chapter. The basic moment prior to magnification should be calculated according to conventional ESFM and then multiplied by the proposed factor to get the design moment for the ground storey column. Same procedure is also followed for shear force calculation. Columns designed following this process will be able to withstand the maximum earthquake force due to ground shaking. Besides, seismic detailing of column reinforcement has to be ensured in accordance with BNBC (Draft), 2015 to gain ductile behavior of column. In any case, shear damage must be avoided in columns by providing ties at close spacing along with the longitudinal reinforcements as per the code specification. The ends of the ties must be bent as 135° hooks.

7.4 FUTURE DIRECTIONS

The study presented in the investigation has been carried out for framed structures having regular geometry. The total structure was symmetric with fixed number of stories and span length. Presence of opening for placement of window, doors etc. and placement of utility materials like electricity, water or sewerage pipe was not considered here in the present study. Earthquake may come in any direction, but the structures were analyzed for in plane earthquake effects only.

The findings of the present investigation should be interpreted with the frame work of the above limitations. It can therefore be said that more work needs to be done on this topic to overcome such limitations. Some recommendations are listed below that may be carried out for further advancement of the research.

- Irregular shape building should be analyzed considering the combined earthquake loading from both the axes.

- Frames with lift core wall, small shear wall, etc. can be studied to see the stiffness phenomena of ground storey to eradicate soft storey status of ground storey.

- Building with different material properties like concrete compressive strength and steel tensile strength should be studied.
- A real building with stair case, door, window, opening for utility services, etc. need to be analyzed to see that actual impact of earthquake.

ACI Committee 318, (2002) Building Code Requirement for Structural Concrete, American Concrete Institute, Detroit.

Ahmed, M Z , –Four Possibility of Using HYDE Systems for Seismic Safety of Soft-Storey Buildings in Bangladesh", First Bangladesh Earthquake Symposium, Dhaka, Bangladesh.

Algerian Seismic Code 88 –Algerian Earthquake Resistant Regulations", Ministry of Town planning and Construction, Algiers, Algeria.

Amanat, K M and Hoque, E –A Rationale for Determining the natural period of RC Building Frames Having Infill" *Engineering Structures*, Vol.28, pp. 495-502.

ASCE 41-13, 2013 Publication Anticipated Seismic Evaluation and Upgrade of Existing Buildings, American Society of Civil Engineers, Reston, Virginia. Public Comment Edition available through the American Society of Civil Engineers.

ATC (1996) *Seismic Evaluation and and Retrofit of Concrete Building (Volume 1).* Report (ATC-40), Applied Technology Council, California, USA.

Arefin , –Seismic *Performance of Soft Storey Structures Retrofitted with FRP and AP "* M.Sc. Engg. Thesis, Department of Civil Engineering, Bangladesh University of Engineering and Technology.

Bertero, V , and Brokken, S , 8 –Infills in Seismic Resistant Building," *Journal of the Structural Engineering*, ASCE, Vol. 109, No 6, June, pp 1337-1361

BNBC, (2006) Housing and Building Research Institute and Bangladesh Standards and Testing Institution, Bangladesh National Building Code

Draft BNBC, (2015), Housing and Building Research Institute and Bangladesh Standards and Testing Institution, Bangladesh National Building Code.

Chopra A. K., (1989) Dynamics of structures; Theory and Applications to Earthquake Engineering, 4th Edition, Prentice Hall, New York, NY

Clough, R. W., and Penzien, J., (1993), Dynamics of Structures, 2nd Edition, McGraaw-Hill, Inc, New York, NY

Computer and Structures Inc. ETABS. Ultimate 15.0, California, USA.

Costa Rican Seismic Code, 8 –Seismic Code of Costa Rica", Federal College of Engineers and Architects of Costa Rica, San Jose, Costa Rica.

Egyptian Seismic Code, 88 –Regulations for Earthquake Resistant Design of Buildings in Egypt", Egyptian Society for Earthquake Engineering, Cairo, Egypt.

ESCP- , 8 –Code of Practice for Loading, Ethiopia", Ministry of Urban Development and Housing, Addis Ababa, Ethiopia.

Eurocode 8, (2003) European Committee of Standardization, Design of Structures for Earthquake Resistance—Part 1: General Rules, Seismic Actions and Rules for Buildings, 1998-1, Brussels, Belgium.

EERI, Annotated Slide Collection, CD Publication, Earthquake Engineering Research Institute, 2000, Oakland, CA.

EERI, –Annotated Images from the Bhuj, India Earthquake of January 26", CD Earthquake Engineering Research Institute, Oakland, CA

FEMA273, NEHRP Guideline for the Seismic Rehabilitation of Buildings, Washington DC, Federal Emergency Management Agency, USA, 1997.

FEMA 440, 2005, Improvements of Nonlinear Static Seismic Analysis Procedures, Federal Emergency Management Agency, Washington, D.C.

Fardis, M N , and Panagiotakos, T B , –Seismic design and response of bare and masonry-infilled reinforced concrete buildings, Part II: Infilled structures", *J. Earthquake Eng.*, Vol. 1, No. 3, 1997, pp. 475–503.

Faysal , –*Performance Point Evaluation of Masonry Infill RC Soft Storey Buildings Un e r e ismic o Using Pushover An l s is"* B.Sc. Engg. Thesis, Department of Civil Engineering, Bangladesh University of Engineering and Technology.

FEMA-356 (2000) Prestandard and commentary for the seismic rehabilitation of buildings. Building Seismic Safety Council, Washington (DC)

FEMA 356, 273. (2002) Pre-*standard and Commentary for the Seismic Rehabilitation of Buildings*, Federal Emergency Management Agency, Washington D.C., USA.

Ghosh, A K , Amde, A M –Finite Element Analysis of Infilled Frames ” *J. Struct. Engg*., ASCE, 128(7), 881-889.

Guevara, L T , and Perez –Soft Story and Weak Story in Earthquake Resistant Design: A Multidisciplinary Approach” t h World Conference on Earthquake Engineering, Venezuela.

Haque S , –*Behavior of Multistoried RC Framed Buildings with Open Ground Floor Un e r e ismic o ing”* M.Sc. Engg. Thesis, Department of Civil Engineering, Bangladesh University of Engineering and Technology.

Haque, S, Amanat, K M , –Seismic Vulnerability of Columns of RC Framed Buildings with Soft Ground Floor,” *International Journal Of Mathematical Models And Methods In Applied Sciences,* NAUN, Issue 3, Vol. 2, ISSN: 1998-0140, 2008.

Haque, S and Amanat, K M , –Strength and Drift Demand of Columns of RC Framed Buildings with Soft Ground Story,” Journal of Civil Engineering, The Institution of Engineers, Bangladesh. Vol. CE 37, pp. 99-110. 2009.

Holmes, M., (1961) "Steel Frames with-Brickwork and Concrete Infilling" Proceedings of the Institution of Civil Engineers, Vol. 19, pp. 473-47S.

IBC, (2000), Building Officials and Code Administrators International, International Conference of Building Officials and Southern Building, Code Congress International, U.S.A., International Building Code.

IS-1893, (2002) Bureau of Indian Standards, Indian Standard Criteria for Earthquake Resistant Design of Structures—Part 1: General Provisions and Buildings (Fifth Revision), New Delhi, India.

Mallick, D V and Severn R T —The Behavior of Infilled Frames under Static Loading " Proc Instn Civ Engrs n d Edn , 8 , pp –656.

Mainstone, R J , —On the Stiffness and Strengths of Infilled Frames " Proceedings of the Institution of Civil Engineers, Supplement IV, pp 57-90.

Mander, J.B., Priestley, M.J.N, and Park, R. "Theoretical stress-strain model for confined concrete," *Journal of Structural Engineering*, American Society of Civil Engineers, Vol.114, No. 8, 1988, pp. 1804-1825.

Mehrabi, A B , Shing, P B , Schuller, M P , and Noland, J N , —Experimental Evaluation of Masonry-Infilled RC Frames", *Journal of Structural Engineering*, ASCE, Vol. 122, No. 3, March, pp 228-237.

Mezzi, M , —Architectural and Structural Configurations of Buildings with Innovative Aseismic Systems", Proceedings of the t h World Conference on Earthquake Engineering, August 2004, (Paper No. 1318), Vancouver, B.C., Canada.

Moghaddam, H. A., and Dowling, P J , 8 —The State of the Art in Infilled Frames", Imperial College of Science and Technology, Civil Eng. Department, London, U.K, ESEE Research Report No. 87-2.

Murty, C V R , and Jain, S K , —Beneficial influence of masonry infills on seismic performance of RC frame buildings", Proceedings, t h World Conference on Earthquake Engineering, New Zealand, Paper No. 1790.

NBC- , —Nepal National Building Code for Seismic Design of Buildings in Nepal", Ministry of Housing and Physical Planning, Department of Buildings, Kathmandu, Nepal.

NSR- 8, 8 —Colombian Standards for Seismic Resistant Design and Construction", Bogota, Colombia

NZS-3101, Code of Practice for the Design of Concrete Structures, Part 1, Standards Association of New Zealand, Wellington, New Zealand, 1995.

Paulay T., and Priestley, M. J. N. (1992). Seismic Design of Reinforced Concrete and Masonry Buildings, John Wiley & Sons, Inc., New York, NY

Park, H., and Eom, T., (2004) ―Energy Dissipation Capacity of Flexure-dominated Reinforced Concrete Members, 13th World Conference on Earthquake Engineering, Canada, Paper No. 3481.

illi m Pet k, " he Northri ge E r thqu ke U A n its Economic n oc i l mp c ts." Euro Conference on Global Change and Catastrophe Risk Management, IIASA, Luxemburg, Austria (July 2000)

Pradhan, P M ―Equivalent Strut Width for Partial Infilled Frames" *Journal of Civil Engineering Research* 2012, 2(5): 42-48.

Quayyum, S, Nazmul, I.M., Iasmin, M.M , Amanat, K M , ―Effects of Randomly Distributed Infill on the Columns of Reinforced Concrete Frames with Soft Ground Storey," *International Journal of Structural Stability and Dynamics (IJSSD)*, Volume: 10, Issue: 3, pp. 555-569.

Sachanski, S ―*Analysis of the Earthquake Resistance of Frame Buildings Taking into Consideration the Carrying Capacity of the Filling Masonry*," Proc n d World Conf on Earthquake Engrg., Tokyo, 3, 2127-2141.

Saneinejad, A , and Hobbs, B , ―Inelastic Design of Infilled Frames" *ASCE Journal of Structural Engineering*, Vol. 121, No. 4, April, pp. 634-643.

Shah, S. P., Swartz, S. E., and Ouyang, C., (1995), Fracture Mechanics of Concrete, John Wiley & Sons, Inc., New York.

Shaiful I , ―*Nonlinear Time History Analysis of Reinforced Concrete Frames with Brick s onr nfill "* M.Sc. Engg. Thesis, Department of Civil Engineering, Bangladesh University of Engineering and Technology.

Smith, B S , ―Lateral stiffness of infilled frames" *ASCE Journal of Structural Division*, Vol. 88, No. ST6, pp. 183-199.

Smith, B S , ―Behavior of Square Infilled Frames" Proceedings of the American Society of Civil Engineers, Vol. 92, pp.381-403.

Smith, B S , and Carter, C , –A Method of Analysis for infilled Frames" Proceedings of the Inst. of Civil Engineers, Vol. 44, pp.31-48.

Smith, B. S. and Coull, (1991), An Infilled-Frame Structures, Tall Building Structures Analysis and Design, John Wiley & Sons, inc. 168-174.

SNIP-II-7-81, Building Code on Construction in Seismic Areas, The Ministry for Construction of Russia, Moscow, Russia, 1996.

Stafford-Smith, B and C Carter, –*A etho of An l s is for nfill Fr me s."* Proceedings of the institution of Civil Engineers, vol. 44, 1969.

Takeda, T., Sozen, M A and Nielsen, N N , —Reinforced Concrete Response to Simulated Earthquake", J Structure Engg Div , ASCE, Vol , No , , pp -2573.

Taskin A , –*Behaviour of Randomly Infilled RC Frames with Soft Ground Floor Subjected to e ismic o ing"* M.Sc. Engg. Thesis, Department of Civil Engineering, Bangladesh University of Engineering and Technology.

Tasmim R , –*Effect on Base Shear Under Seismic Load for Masonry Infilled RC Soft tor Buil ings "* B.Sc.Engg. Thesis, Department of Civil Engineering, Bangladesh University of Engineering and Technology.

Tasmim, R and Amanat, K M , –A Rational Estimation of Earthquake Base Shear for Buildings with Soft Ground Floor," Journal of Civil Engineering, The Institution of Engineers, Bangladesh. Vol. CE 41, pp. 71-80, June 2013.

Wood, R H , 8 –The Stability of Tall Buildings " Proceedings of the Institution of Civil Engineers, Vol. 11, pp. 69-102.

APPENDIX A

PUSHOVER ANALYSIS OF A TWO STOREY BUILDING

A.1 General

Static pushover analysis has rigorous theoretical foundation. It is based on the assumption that the response of the structure can be related to the equivalent single degree-of-freedom (SDOF) system. This implies that the response is controlled by a single mode and the shape of this mode remains constant throughout the time history response. Clearly, both assumptions are incorrect, but studies by several investigators have indicated that these assumptions lead to rather good predictions of the maximum seismic response of multi degree-of-freedom (MDOF) structures, provided their response is dominated by a single mode.

The formulation of the equivalent SDOF system is not unique, but the basic underlying assumption common to all approaches is that the deflected shape of the MDOF system can be represented by a shape vector$\{\Phi\}$that remain constant throughout the time history, regardless of the level of deformation. Accepting this assumption and defining the relative displacement vectorXof an MDOF system as$\mathrm{X} = \{\Phi\}x_r$ where $\{x_r = \text{roof displacement}\}$, governing differential equation of an MDOF system can be written as

$$\mathrm{M}\{\Phi\}\ddot{x}_r + \mathrm{C}\{\Phi\}\dot{x}_r + \mathrm{Q} = -\mathrm{M}\{1\} \tag{A.1}$$

Where M and C are the mass and damping matrices, Q denotes the storey force vector, and $\ddot{x}_g$ is the ground acceleration.

If we define the reference SDOF displacement x^*; $x^* = \frac{\{\Phi\}^T\mathrm{M}\{\Phi\}}{\{\Phi\}^T\mathrm{M}\{1\}}x_r$ (A.2)

From equation (A.1) and (A.2) we get the following differential equation for the response of the equivalent SDOF system:

$$\mathrm{M}^*\{\Phi\}\ddot{x}^*{}_r + \mathrm{C}^*\{\Phi\}\dot{x}^*{}_r + \mathrm{Q}^* = -\mathrm{M}^*\{1\}\ddot{x}_g \tag{A.3}$$

$\mathrm{M}^*, \mathrm{C}^*$ *and* Q^*denote the properties of the equivalent SDOF system and are given by

$$\mathrm{M}^* = \{\Phi\}^T\mathrm{M}\{1\} \tag{A.4}$$

$$Q^* = \{\Phi\}^T Q \tag{A.5}$$

$$C^* = \{\Phi\}^T C\{\Phi\} \frac{\{\Phi\}^T M\{1\}}{\{\Phi\}^T M\{\Phi\}} \tag{A.6}$$

Presuming that the shape vector $\{\Phi\}$ is known, the force-deformation characteristics of the equivalent SDOF system (as shown in Figure A.1) can be determined the Newmark nonlinear average acceleration method which usually produces a base shear vs. roof displacement diagram. In order to identify nominal global strength and displacement quantities, the force – displacement diagram needs to be represented by a bilinear relationship that defines ‗yield‘ strength and effective ‗elastic‘ stiffness, $K_e = {V_y}/{\delta_{r,y}}$ and a hardening stiffness, $K_s = \alpha K_e$ for the structure. For this study the elastic stiffness and hardening stiffness are considered as per the table 3-2 of FEMA P440A.

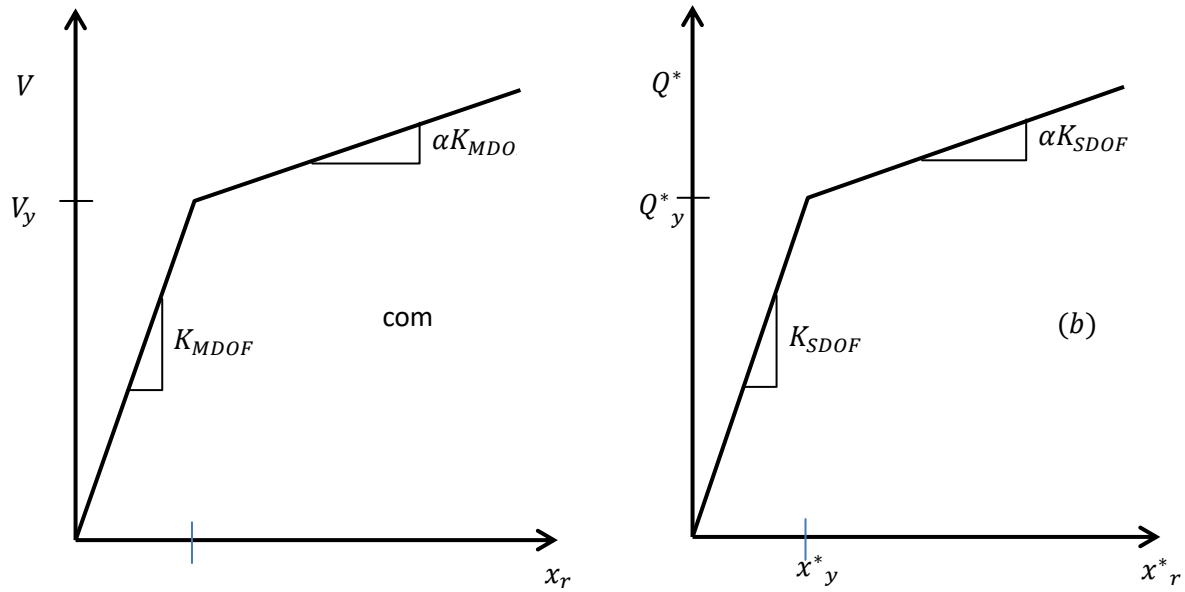

Figure A.1 Force-displacement relation of MDOF and equivalent SDOF system

The yield value of the base shear (V_y) and the corresponding roof displacement ($\delta_{r,y}$) from figure A.2 are used together with equation (A.2) and (A.5) to compute the force displacement relationship for the equivalent SDOF system as follows:

$$x_y{}^* = \frac{\{\Phi\}^T M\{\Phi\}}{\{\Phi\}^T M\{1\}} x_{r,y} \text{and } Q^*{}_y = \{\Phi\}^T Q_y \tag{A.7}$$

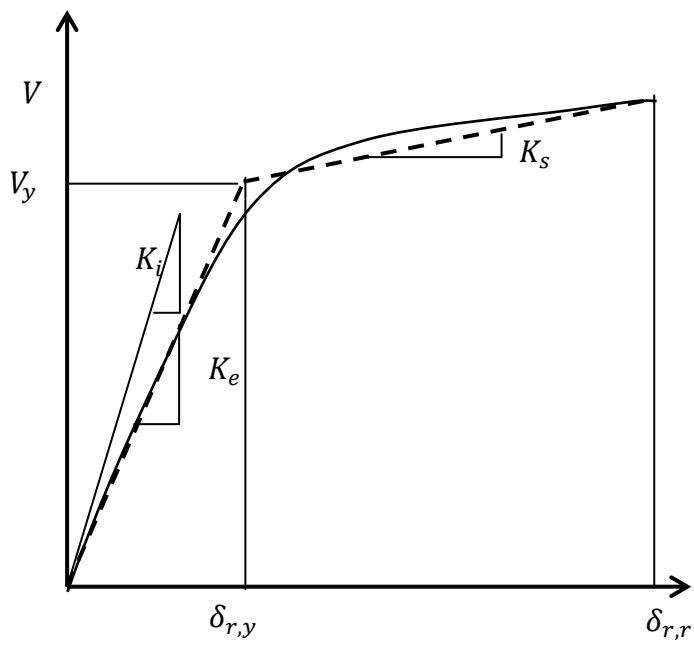

Figure A 2 Base Shear vs. displacement characteristics of MDOF system

Where,Q_y is the storey force vector at yield, i.e., $V_y = \{1\}Q_y$, The initial period of the equivalent SDOF system T_{eq} can be computed as

$$T_{eq} = 2\pi \left[\frac{x_y{}^* M^*}{Q^*{}_y}\right]^{\frac{1}{2}} \tag{A.8}$$

The strain hardening ratio ($\propto$) of the V - x_r relationship of equivalent SDOF structure defines the strain hardening ratio. The basic properties of the equivalent SDOF system are now known. The fundamental question in the execution of the pushover analysis is the magnitude of the target displacement at which seismic performance evaluation of structure is to be performed.

A.2 Pushover Analysis of a Two Storey Building

A two storey building subjected to earthquake loading is recommended to be analyzed by dynamic loading. Dynamic loading is defined as any load of which the magnitude and direction, or position varies with time. Building response to a dynamic load, i.e., the resulting deflections and stresses, is also dynamic or time varying. Essential physical properties of any linearly elastic structural system subjected to dynamic loads are mass, elastic properties (flexibility, stiffness), energy loss mechanism or damping, external source of excitation or loading. In the simplest modal of a SDOF system, each of these properties is assumed to be concentrated in a single physical element. A structural response under dynamic loading is

evaluated by the deterministic approach. The dynamic loading applied was a pushover backbone curve. The entire building is discretized following the lumped-mass procedure. Mass of a beam concentrated in a series of discrete points or lumps. Displacement and accelerations are defined only at these discrete points. But, the lumped mass procedure is effective when large portion of total mass is concentrated in a few discrete points. This can be achieved by converting the structure of MDOF to the equivalent structure of SDOF. Following paragraph will enumerate the procedure to convert the portal frame to equivalent structure of SDOF system (Figure A.3). The portal frame is discretized in following lumped structure:

a. Weight of each beam = $3.79 \times 20 = 75.8$ kips

b. Mass of each beam = $m = \frac{75.8}{32.2} = 2.35 \ \mathrm{kips} - \mathrm{s}^2/\mathrm{ft}$

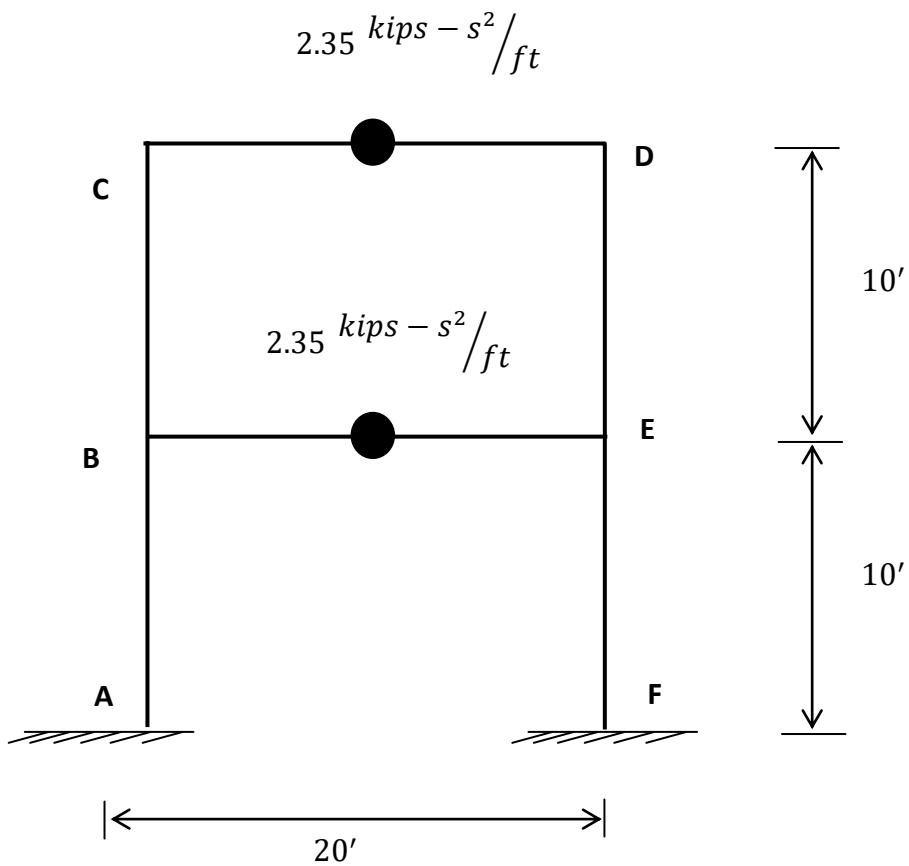

Figure A.3 Portal Frame with lumped at the center of gravity of the frame

c. Mass Matrix; $[M] = \begin{bmatrix} 2.35 & 0 \\ 0 & 2.35 \end{bmatrix}$ or $[M] = \begin{bmatrix} 2.35 & 0 & 0 & 0 & 0 & 0 \\ 0 & 2.35 & 0 & 0 & 0 & 0 \\ 0 & 0 & 0 & 0 & 0 & 0 \\ 0 & 0 & 0 & 0 & 0 & 0 \\ 0 & 0 & 0 & 0 & 0 & 0 \\ 0 & 0 & 0 & 0 & 0 & 0 \end{bmatrix}$

A.3 Determination of Stiffness Matrix

The 2D portal frame has six Degrees of Freedom (DOF) and amongst them two is translational and four are rotational DOFs. The horizontal displacements at ground storey and 1st storey level are defined as translational DOFs and named as u_1, u_2 respectively. The rotations at node B, D, C & E are defined as rotational DOFs and denoted by u_3, u_4, u_5, u_6 respectively. Determination of stiffness coefficient of these six DOFs and arranging in matrix form will generate the stiffness matrix of the frame. Calculation of stiffness coefficient is given below with figures:

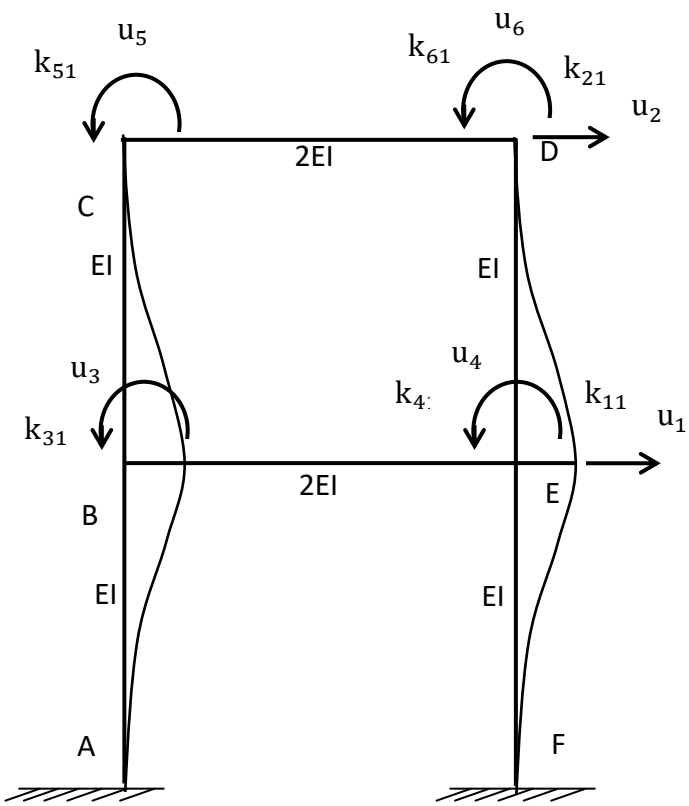

Case: 1

$k_{11} = \frac{48EI}{L^3}$

$k_{21} = \frac{-24EI}{L^3}$

$k_{31} = 0$

$k_{41} = 0$

$k_{51} = \frac{-6EI}{L^2}$

$k_{61} = \frac{-6EI}{L^2}$

FigureA.4 Portal Frame with one unit displacement of u_1

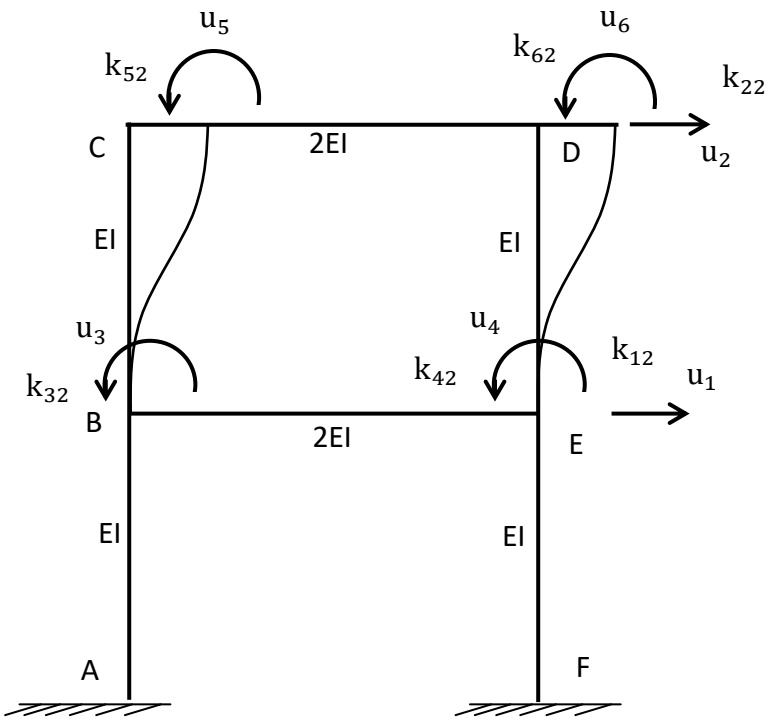

Case: 2

$$k_{12} = \frac{-24EI}{L^3}$$

$$k_{22} = \frac{24EI}{L^3}$$

$$k_{32} = \frac{6EI}{L^2}$$

$$k_{42} = \frac{6EI}{L^2}$$

$$k_{52} = \frac{6EI}{L^2}$$

$$k_{62} = \frac{6EI}{L^2}$$

Figure A.5 Portal Frame with one unit displacement of u_2

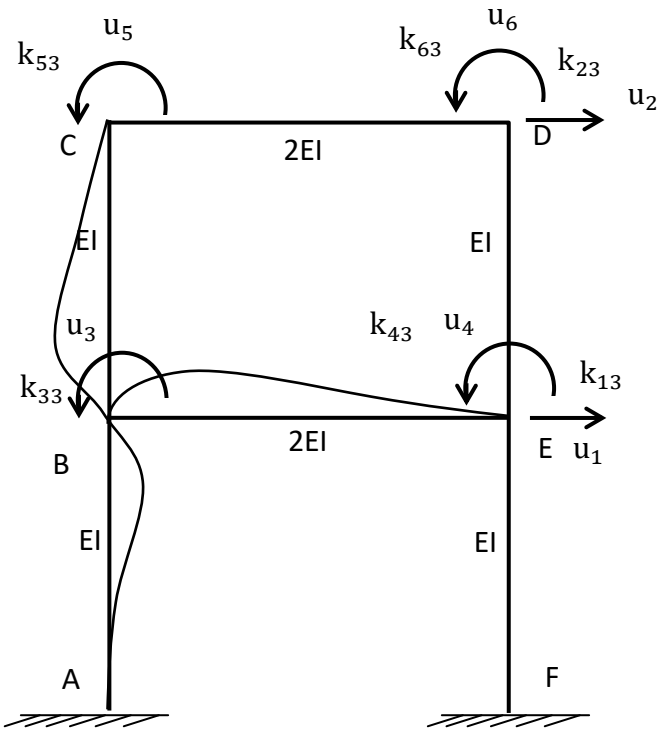

Case: 3

$$k_{13} = 0$$

$$k_{23} = \frac{6EI}{L^2}$$

$$k_{33} = \frac{12EI}{L}$$

$$k_{43} = \frac{2EI}{L}$$

$$k_{53} = \frac{2EI}{L}$$

$$k_{63} = 0$$

Figure A.6 Portal Frame with one unit rotation of u_3

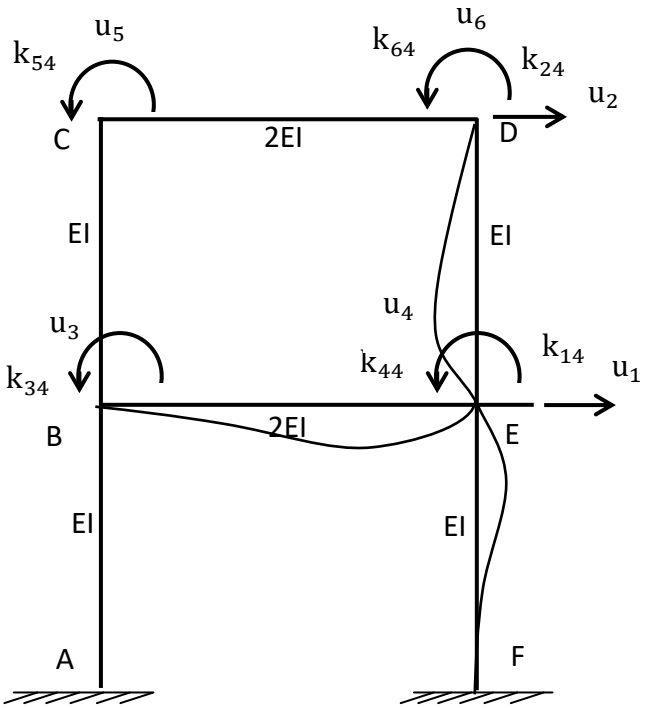

Case: 4

$k_{14} = 0$

$k_{24} = \frac{6EI}{L^2}$

$k_{34} = \frac{2EI}{L}$

$k_{44} = \frac{12EI}{L}$

$k_{54} = 0$

$k_{64} = \frac{2EI}{L}$

Figure A.7 Portal Frame with one unit rotation of u_4

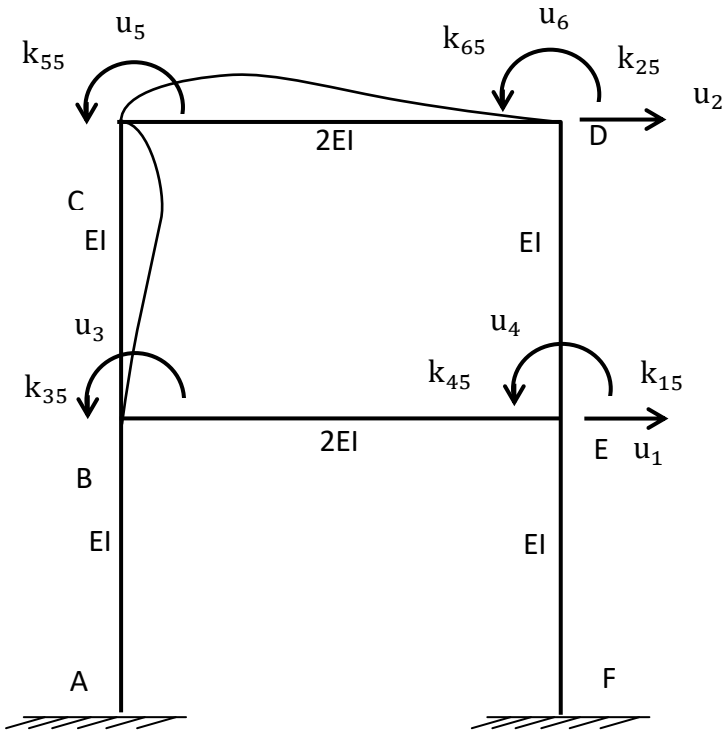

Case: 5

$k_{15} = \frac{-6EI}{L^2}$

$k_{25} = \frac{6EI}{L^2}$

$k_{35} = \frac{2EI}{L}$

$k_{45} = 0$

$k_{55} = \frac{8EI}{L}$

$k_{65} = \frac{2EI}{L}$

Figure A.8 Portal Frame with one unit rotation of u_5

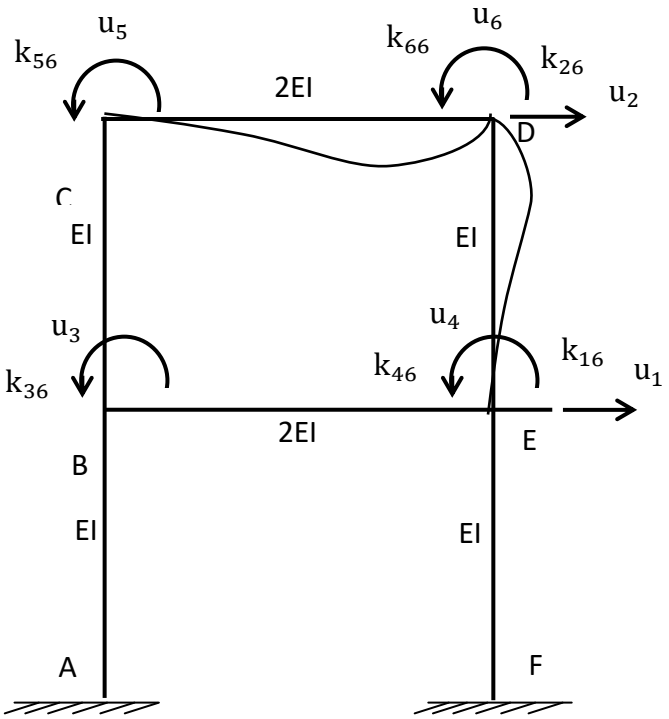

Case: 6

$$k_{16} = \frac{-6EI}{L^2}$$

$$k_{26} = \frac{6EI}{L^2}$$

$$k_{36} = 0$$

$$k_{46} = \frac{2EI}{L}$$

$$k_{56} = \frac{2EI}{L}$$

$$k_{66} = \frac{8EI}{L}$$

Figure A.9 Portal Frame with one unit rotation of u_6

The Stiffness matrix of this frame is, $[k] = \begin{bmatrix} \frac{48EI}{L^3} & \frac{-24EI}{L^3} & 0 & 0 & \frac{-6EI}{L^2} & \frac{-6EI}{L^2} \\ \frac{-24EI}{L^3} & \frac{24EI}{L^3} & \frac{6EI}{L^2} & \frac{6EI}{L^2} & \frac{6EI}{L^2} & \frac{6EI}{L^2} \\ 0 & \frac{6EI}{L^2} & \frac{12EI}{L} & \frac{2EI}{L} & \frac{2EI}{L} & 0 \\ 0 & \frac{6EI}{L^2} & \frac{2EI}{L} & \frac{12EI}{L} & 0 & \frac{2EI}{L} \\ \frac{-6EI}{L^2} & \frac{6EI}{L^2} & \frac{2EI}{L} & 0 & \frac{8EI}{L} & \frac{2EI}{L} \\ \frac{-6EI}{L^2} & \frac{6EI}{L^2} & 0 & \frac{2EI}{L} & \frac{2EI}{L} & \frac{8EI}{L} \end{bmatrix}$

$$= \begin{bmatrix} \frac{48EI}{L^3} & \frac{-24EI}{L^3} & 0 & 0 & \frac{-6EI}{L^2} & \frac{-6EI}{L^2} \\ \frac{-24EI}{L^3} & \frac{24EI}{L^3} & \frac{6EI}{L^2} & \frac{6EI}{L^2} & \frac{6EI}{L^2} & \frac{6EI}{L^2} \\ 0 & \frac{6EI}{L^2} & \frac{12EI}{L} & \frac{2EI}{L} & \frac{2EI}{L} & 0 \\ 0 & \frac{6EI}{L^2} & \frac{2EI}{L} & \frac{12EI}{L} & 0 & \frac{2EI}{L} \\ \frac{-6EI}{L^2} & \frac{6EI}{L^2} & \frac{2EI}{L} & 0 & \frac{8EI}{L} & \frac{2EI}{L} \\ \frac{-6EI}{L^2} & \frac{6EI}{L^2} & 0 & \frac{2EI}{L} & \frac{2EI}{L} & \frac{8EI}{L} \end{bmatrix}$$

The stiffness matrices can be separately written as follows:

$$k_{tt} = \frac{2EI}{L^3}\begin{bmatrix} 24 & -12 \\ -12 & 12 \end{bmatrix}$$

$$[k_{\theta\theta}] = \frac{2EI}{L^3}\begin{bmatrix} 6L^2 & L^2 & L^2 & 0 \\ L^2 & 6L^2 & 0 & L^2 \\ L^2 & 0 & 4L^2 & L^2 \\ 0 & L^2 & L^2 & 4L^2 \end{bmatrix}$$

$$[K_{\theta t}] = \frac{2EI}{L^3}\begin{bmatrix} 0 & 3L \\ 0 & 3L \\ -3L & 3L \\ -3L & 3L \end{bmatrix}$$

$$[K_{t\theta}] = \frac{2EI}{L^3}\begin{bmatrix} 0 & 0 & -3L & -3L \\ 3L & 3L & 3L & 3L \end{bmatrix}$$

Stiffness Coefficient, $k = \begin{bmatrix} k_{tt} & K_{t\theta} \\ K_{\theta t} & k_{\theta\theta} \end{bmatrix}$ (A.9)

Effective Stiffness, $\hat{k} = k_{tt} - K_{t\theta} k_{\theta\theta}{}^{-1} K_{\theta t}$ (A.10)

The translational stiffness is calculated considering rigid beams neglecting rotational component as $EI_{beam} = \propto$. In this study the values of E and I are considered as E = 3000 ksi and I = 1000 in^4. These values are kept constant during the numerical calculation. The moment of inertia is calculated based on the actual column dimension. The column dimension is calculated based on conventional method of building analysis as described by the ACI Code 311.

A.4 Determination of Mode Shape Function and Damping Matrix

Let us consider the value as EI $= 0.7\left(57000\sqrt{4000}\right) \times \left(\frac{10\times10^3}{12}\right)$

$$= 0.7 \times 3605 \times 833 = 2.1 \times 10^6 kip$$

Therefore, the translational stiffness, $k_{tt} = \frac{2EI}{L^3}\begin{bmatrix} 24 & -12 \\ -12 & 12 \end{bmatrix} = \begin{bmatrix} 58.41 & -29.21 \\ -29.21 & 29.21 \end{bmatrix}$

Determination of Steady-state Response of the Two Storey Frame (Figure A.10):

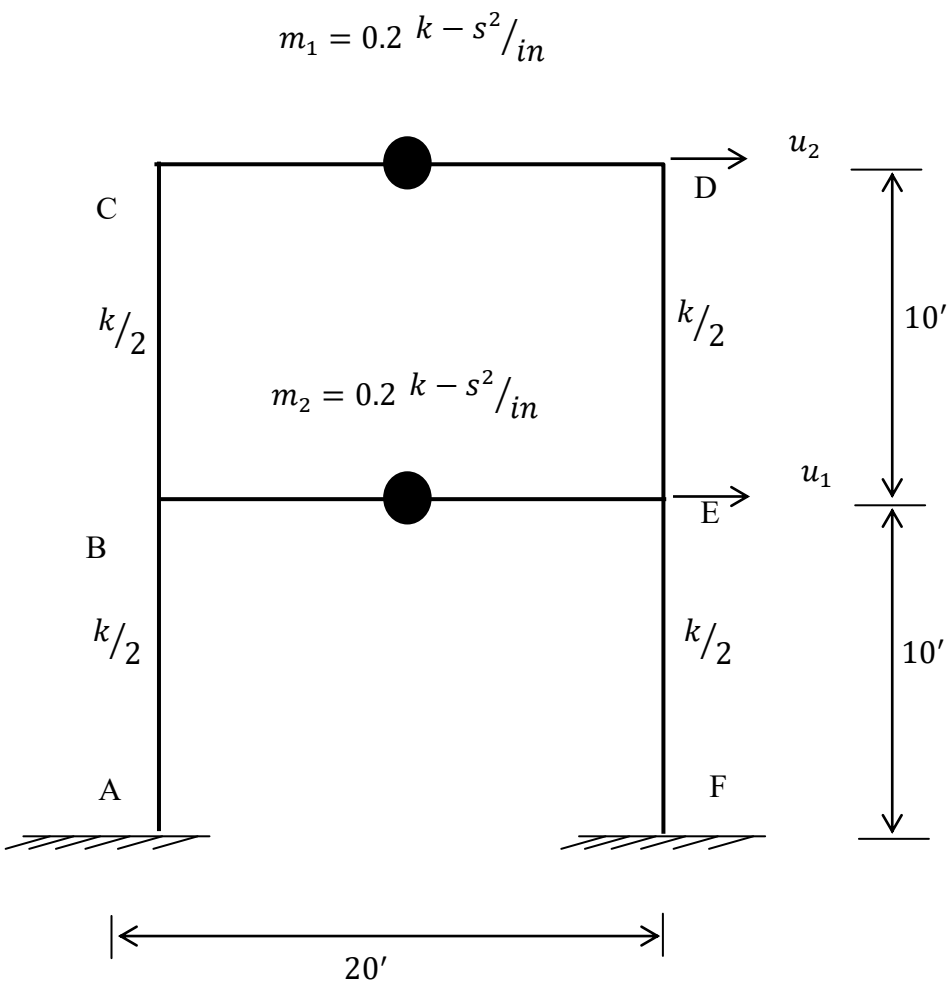

FigureA.10 Portal frame with mass and stiffness

Where,

$$[m] = \begin{bmatrix} 0.2 & 0 \\ 0 & 0.2 \end{bmatrix}$$

$$k_{tt} = \begin{bmatrix} 58.41 & -29.21 \\ -29.21 & 29.21 \end{bmatrix}$$

According to the Eigen value problem, we get: $[\underline{k} - \underline{m}\omega^2] = 0$

$$\begin{bmatrix} 58.41 & -29.21 \\ -29.21 & 29.21 \end{bmatrix} - \begin{bmatrix} 0.2\omega^2 & 0 \\ 0 & 0.2\omega^2 \end{bmatrix} = 0$$

$$58.41 \begin{bmatrix} 1 - \frac{\omega^2}{292.05} & -0.5 \\ -0.5 & 0.5 - \frac{\omega^2}{292.05} \end{bmatrix} = 0$$; Let us consider, $\frac{\omega^2}{292.05} = B$

$$\begin{bmatrix} 1 - B & -0.5 \\ -0.5 & 0.5 - B \end{bmatrix} = 0$$

$$\frac{{w_1}^2}{292.05} = 0.191 \ \ and \omega_1 = 7.47 \ {}^{rad}/_{sec}$$

$$\frac{{\omega_2}^2}{292.05} = 1.309 \ \ and \omega_2 = 19.55 \ {}^{rad}/_{sec}$$

Determination of modal coefficient and Eigen Vectors:

$$[\underline{k} - \underline{m}\omega^2] \begin{Bmatrix} \emptyset_{12} \\ \emptyset_{22} \end{Bmatrix} = \begin{Bmatrix} 0 \\ 0 \end{Bmatrix}$$

Mode 1: when $\omega_1 = 7.47 \, {}^{rad}/_{sec}$ than we get,

$$\begin{bmatrix} 1 - \frac{7.47^2}{292.05} & -0.5 \\ -0.5 & 0.5 - \frac{7.47^2}{292.05} \end{bmatrix} \begin{Bmatrix} \emptyset_{11} \\ \emptyset_{21} \end{Bmatrix} = \begin{Bmatrix} 0 \\ 0 \end{Bmatrix}$$

$$\begin{bmatrix} 0.809 & -0.5 \\ -0.5 & 0.309 \end{bmatrix} \begin{Bmatrix} \emptyset_{11} \\ \emptyset_{21} \end{Bmatrix} = \begin{Bmatrix} 0 \\ 0 \end{Bmatrix}$$

Modal pattern is obtained by considering top deflection to be 1. As such $\emptyset_{21} = 1$

$$\begin{bmatrix} 0.809 & -0.5 \\ -0.5 & 0.309 \end{bmatrix} \begin{Bmatrix} \emptyset_{11} \\ 1 \end{Bmatrix} = \begin{Bmatrix} 0 \\ 0 \end{Bmatrix}$$

$$\boldsymbol{\emptyset_{11}} = 0.62, \boldsymbol{\emptyset_{21}} = 1$$

Mode 2: when $\omega_2 = 19.55 \, {}^{rad}/_{sec}$ than we get,

$$\begin{bmatrix} 1-\dfrac{28.15^2}{292.05} & -0.5 \\ -0.5 & 0.5-\dfrac{28.15^2}{292.05} \end{bmatrix}\begin{Bmatrix} \emptyset_{12} \\ \emptyset_{22} \end{Bmatrix} = \begin{Bmatrix} 0 \\ 0 \end{Bmatrix}$$

$$\begin{bmatrix} -0.309 & -0.5 \\ -0.5 & -0.809 \end{bmatrix}\begin{Bmatrix} \emptyset_{12} \\ \emptyset_{22} \end{Bmatrix} = \begin{Bmatrix} 0 \\ 0 \end{Bmatrix}$$

Modal pattern is obtained by considering top deflection to be 1. As such $\emptyset_{22} = 1$

$$\begin{bmatrix} -0.309 & -0.5 \\ -0.5 & -0.809 \end{bmatrix}\begin{Bmatrix} \emptyset_{12} \\ 1 \end{Bmatrix} = \begin{Bmatrix} 0 \\ 0 \end{Bmatrix}$$

$\emptyset_{12} = -1.62\,,\ \emptyset_{22} = 1$

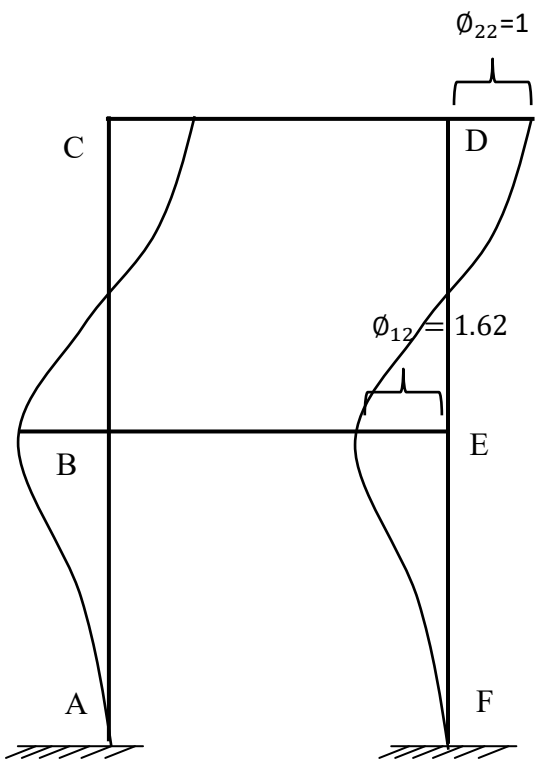

Figure A.11 Portal frame in mode2

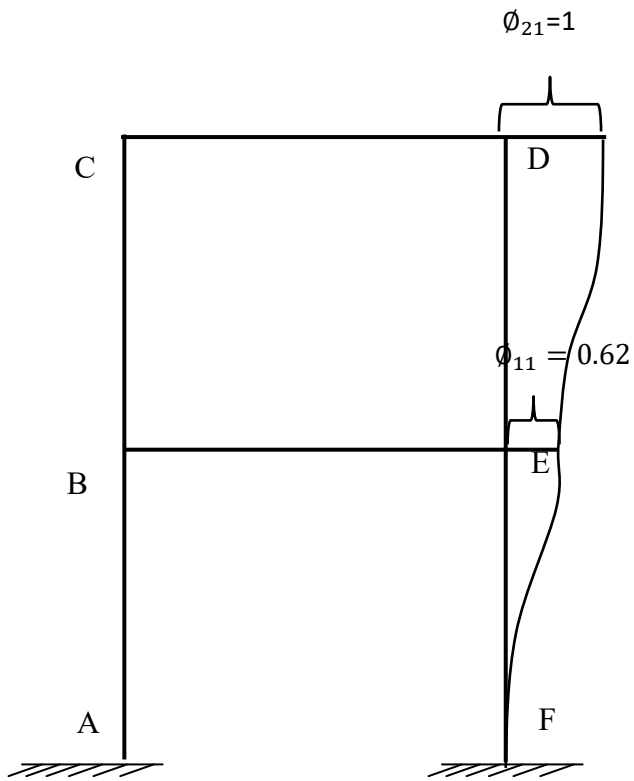

FigureA.12 Portal frame in mode 1

The modal coefficient of 1 mode shape is commonly known as the fundamental mode. Since the two storey building will be analyzed by pushover analysis thus our focus will remain with only the fundamental mode shape and modal coefficient in the subsequent study. The angular frequency and modal coefficients are

$$\begin{Bmatrix} \emptyset_{11} \\ \emptyset_{21} \end{Bmatrix} = \begin{Bmatrix} 0.62 \\ 1 \end{Bmatrix} \quad \text{and } \omega = 7.47\ {}^{rad}/_{sec} \quad \text{or} \quad \begin{Bmatrix} \emptyset_{21} \\ \emptyset_{11} \end{Bmatrix} = \begin{Bmatrix} 1 \\ 0.62 \end{Bmatrix}$$

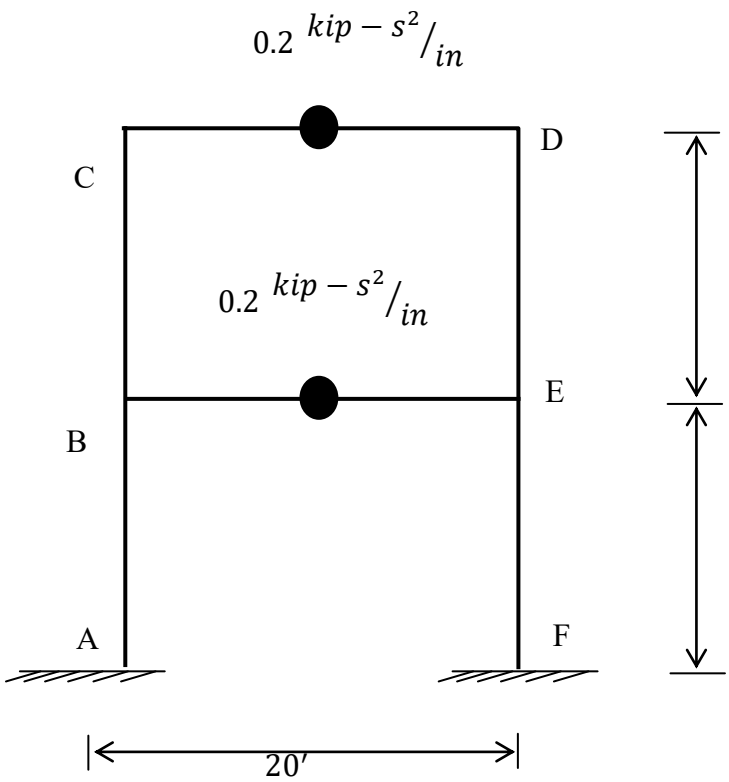

We Know,

$$\begin{Bmatrix}\omega_1\\ \omega_2\end{Bmatrix} = \begin{Bmatrix}7.47\\ 19.55\end{Bmatrix}$$

$$\begin{Bmatrix}\emptyset_{21}\\ \emptyset_{11}\end{Bmatrix} = \begin{Bmatrix}1\\ 0.62\end{Bmatrix}$$

$$[m] = \begin{bmatrix}0.2 & 0\\ 0 & 0.2\end{bmatrix}$$

$$k_{tt} = \begin{bmatrix}58.41 & -29.21\\ -29.21 & 29.21\end{bmatrix}$$

FigureA.13 Portal frame with lumped mass

We Know,

$$\begin{Bmatrix}\omega_1\\ \omega_2\end{Bmatrix} = \begin{Bmatrix}7.47\\ 19.55\end{Bmatrix}$$

$$\begin{Bmatrix}\emptyset_{21}\\ \emptyset_{11}\end{Bmatrix} = \begin{Bmatrix}1\\ 0.62\end{Bmatrix}$$

$$[m] = \begin{bmatrix}0.2 & 0\\ 0 & 0.2\end{bmatrix}$$

$$k_{tt} = \begin{bmatrix}58.41 & -29.21\\ -29.21 & 29.21\end{bmatrix}$$

The value of a_0 *and* a_1 can be derived from; $\frac{1}{2}\begin{bmatrix} 1/\omega_i & \omega_i \\ 1/\omega_j & \omega_j \end{bmatrix}\begin{bmatrix} a_0 \\ a_1 \end{bmatrix} = \begin{bmatrix} \zeta_i \\ \zeta_j \end{bmatrix}$

$$\begin{bmatrix} 1/7.47 & 7.47 \\ 1/19.55 & 19.55 \end{bmatrix}\begin{bmatrix} a_0 \\ a_1 \end{bmatrix} = 2\begin{bmatrix} 0.05 \\ 0.05 \end{bmatrix}$$

$0.093\ a_0 + 10.75\ a_1 = 0.1$

$0.0355\ a_0 + 28.15\ a_1 = 0.1$

Solving above equation we get, $a_0 = 0.54$ and $a_1 = 0.0037$

Damping matrix: $c = a_0\underline{m} + a_1\underline{k}$ $\therefore c = 0.54\begin{bmatrix} 0.2 & 0 \\ 0 & 0.2 \end{bmatrix} + 0.0037\begin{bmatrix} 58.41 & -29.21 \\ -29.21 & 29.21 \end{bmatrix}$

$$c = \begin{bmatrix} 0.108 & 0 \\ 0 & 0.108 \end{bmatrix} + \begin{bmatrix} 0.216 & -0.108 \\ -0.108 & 0.108 \end{bmatrix}$$

$$c = \begin{bmatrix} 0.324 & -0.108 \\ -0.108 & 0.216 \end{bmatrix}$$

A.5 Determination of Effective Stiffness

In case of effective stiffness, $\hat{k}$:

Derive the value of $k_{\theta\theta}$, $k_{\theta\theta} = \frac{2EI}{L}\begin{bmatrix} 6 & 1 & 1 & 0 \\ 1 & 6 & 0 & 1 \\ 1 & 0 & 4 & 1 \\ 0 & 1 & 1 & 4 \end{bmatrix}$

Determinant of $k_{\theta\theta} = 6 \times 86 - 1 \times 16 + 1 \times (-24) = 476$

Cofactor matrix of $k_{\theta\theta} = \begin{bmatrix} 86 & -16 & -24 & 10 \\ -16 & 86 & 10 & -24 \\ -24 & 10 & 134 & -36 \\ 10 & -24 & -36 & 134 \end{bmatrix}$

Inverse matrix of $k_{\theta\theta}, {k_{\theta\theta}}^{-1} = \frac{\mathrm{L}}{2\mathrm{EI}}\frac{1}{476}\begin{bmatrix} 86 & -16 & -24 & 10 \\ -16 & 86 & 10 & -24 \\ -24 & 10 & 134 & -36 \\ 10 & -24 & -36 & 134 \end{bmatrix}$

Multiplication of $k_{\theta\theta}{}^{-1}k_{\theta t} = \frac{L}{2EI}\frac{1}{476}\begin{bmatrix} 86 & -16 & -24 & 10 \\ -16 & 86 & 10 & -24 \\ -24 & 10 & 134 & -36 \\ 10 & -24 & -36 & 134 \end{bmatrix} \times \frac{2EI}{L^3}\begin{bmatrix} 0 & 3L \\ 0 & 3L \\ -3L & 3L \\ -3L & 3L \end{bmatrix}$

$$k_{\theta\theta}{}^{-1}k_{\theta t} = \frac{1}{L}\frac{1}{476}\begin{bmatrix} 86 & -16 & -24 & 10 \\ -16 & 86 & 10 & -24 \\ -24 & 10 & 134 & -36 \\ 10 & -24 & -36 & 134 \end{bmatrix} \times \begin{bmatrix} 0 & 3 \\ 0 & 3 \\ -3 & 3 \\ -3 & 3 \end{bmatrix}$$

$$k_{\theta\theta}{}^{-1}k_{\theta t} = \frac{1}{L \times 476}\begin{bmatrix} 86 & -16 & -24 & 10 \\ -16 & 86 & 10 & -24 \\ -24 & 10 & 134 & -36 \\ 10 & -24 & -36 & 134 \end{bmatrix}\begin{bmatrix} 0 & 3 \\ 0 & 3 \\ -3 & 3 \\ -3 & 3 \end{bmatrix}$$

$$k_{\theta\theta}{}^{-1}k_{\theta t} = \frac{1}{L \times 476}\begin{bmatrix} 42 & 168 \\ 42 & 168 \\ -294 & 252 \\ -294 & 252 \end{bmatrix}$$

Again, we get, $k_{t\theta}k_{\theta\theta}{}^{-1}k_{\theta t} = \frac{2EI}{L^3}\begin{bmatrix} 0 & 0 & -3L & -3L \\ 3L & 3L & 3L & 3L \end{bmatrix} \times \frac{1}{L\times 476}\begin{bmatrix} 42 & 168 \\ 42 & 168 \\ -294 & 252 \\ -294 & 252 \end{bmatrix}$

$$k_{t\theta}k_{\theta\theta}{}^{-1}k_{\theta t} = \frac{2EI}{L^3 \times 476}\begin{bmatrix} 0 & 0 & -3 & -3 \\ 3 & 3 & 3 & 3 \end{bmatrix} \times \begin{bmatrix} 42 & 168 \\ 42 & 168 \\ -294 & 252 \\ -294 & 252 \end{bmatrix}$$

$$k_{t\theta}k_{\theta\theta}{}^{-1}k_{\theta t} = \begin{bmatrix} 9 & -7.72 \\ -7.72 & 12.87 \end{bmatrix}$$

Effective Stiffness, $\hat{k} = k_{tt} - K_{t\theta}k_{\theta\theta}{}^{-1}K_{\theta t}$

$$\hat{k} = \begin{bmatrix} 58.41 & -29.21 \\ -29.21 & 29.21 \end{bmatrix} - \begin{bmatrix} 9 & -7.72 \\ -7.72 & 12.87 \end{bmatrix}$$

$$\hat{k} = \begin{bmatrix} 49.41 & -21.49 \\ -21.49 & 16.34 \end{bmatrix}$$

According to the Eigen value problem, we get: $[\underline{\hat{k}} - \underline{m}\omega^2] = 0$

$$\begin{bmatrix} 49.41 & -21.49 \\ -21.49 & 16.34 \end{bmatrix} - \begin{bmatrix} 0.2\omega^2 & 0 \\ 0 & 0.2\omega^2 \end{bmatrix} = 0$$

$$49.41\begin{bmatrix} 1-\frac{\omega^2}{247.05} & -0.435 \\ -0.435 & 0.33-\frac{\omega^2}{247.05} \end{bmatrix} = 0; \qquad \text{Let us consider, } \frac{\omega^2}{247.05} = B$$

$$\begin{bmatrix} 1-B & 0.435 \\ 0.435 & 0.33-B \end{bmatrix} = 0$$

$$\therefore\ B_1 = 0.115\ \ and\ B_2 = 1.215$$

$$\frac{{w_1}^2}{247.05} = 0.115\ \ and\ \omega_1 = 5.33\ {}^{rad}/_{sec}$$

$$\frac{{\omega_2}^2}{247.05} = 1.215\ \ and\ \omega_2 = 17.33\ {}^{rad}/_{sec}$$

Determination of modal coefficient and Eigen Vectors:

$$[\underline{k} - \underline{m}\omega^2]\begin{Bmatrix} \emptyset_{12} \\ \emptyset_{22} \end{Bmatrix} = \begin{Bmatrix} 0 \\ 0 \end{Bmatrix}$$

Mode 1: when $\omega_1 = 5.33\,{}^{rad}/_{sec}$than we get,

$$\begin{bmatrix} 1-\frac{5.33^2}{247.05} & -0.435 \\ -0.435 & 0.33-\frac{5.33^2}{247.05} \end{bmatrix}\begin{Bmatrix} \emptyset_{11} \\ \emptyset_{21} \end{Bmatrix} = \begin{Bmatrix} 0 \\ 0 \end{Bmatrix}$$

$$\begin{bmatrix} 0.885 & -0.435 \\ -0.435 & 0.215 \end{bmatrix}\begin{Bmatrix} \emptyset_{11} \\ \emptyset_{21} \end{Bmatrix} = \begin{Bmatrix} 0 \\ 0 \end{Bmatrix}$$

Modal pattern is obtained by considering top deflection to be 1. As such $\emptyset_{21} = 1$

$$\begin{bmatrix} 0.885 & -0.435 \\ -0.435 & 0.215 \end{bmatrix}\begin{Bmatrix} \emptyset_{11} \\ 1 \end{Bmatrix} = \begin{Bmatrix} 0 \\ 0 \end{Bmatrix}$$

$$\emptyset_{11} = 0.49\ \emptyset_{21} = 1$$

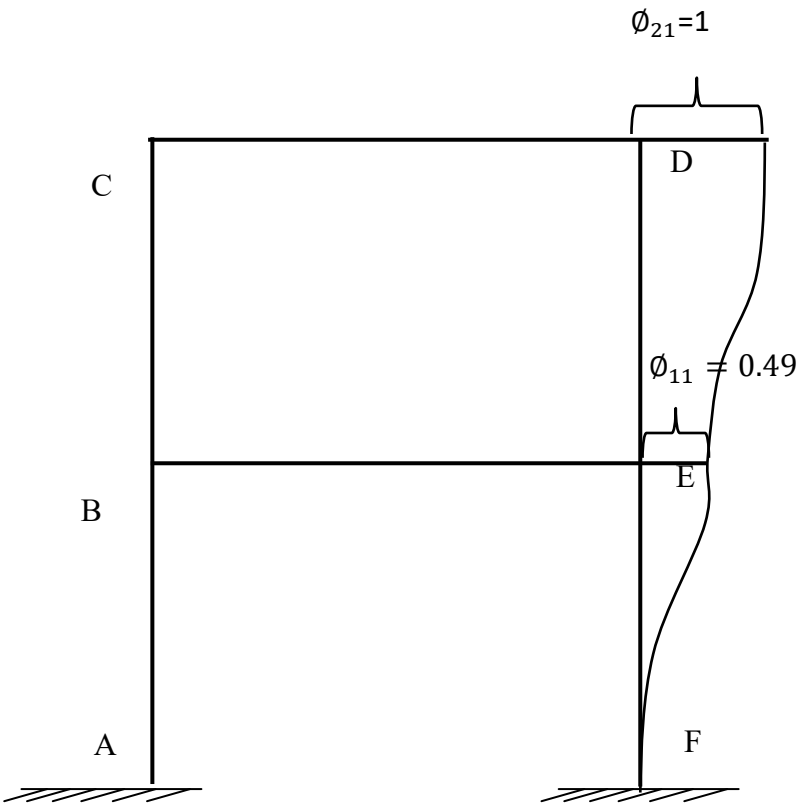

We Know,

$$\begin{Bmatrix}\omega_1\\ \omega_2\end{Bmatrix} = \begin{Bmatrix}5.33\\ 17.33\end{Bmatrix}$$

$$\begin{Bmatrix}\emptyset_{21}\\ \emptyset_{11}\end{Bmatrix} = \begin{Bmatrix}1\\ 0.49\end{Bmatrix}$$

$$[m] = \begin{bmatrix}0.2 & 0\\ 0 & 0.2\end{bmatrix}$$

$$k = \begin{bmatrix}49.41 & -21.49\\ -21.49 & 16.34\end{bmatrix}$$

Figure A.14 Portal frame mode shape in Mode 1

The value of a_0 *and* a_1 can be derived from $\frac{1}{2}\begin{bmatrix}1/\omega_i & \omega_i\\ 1/\omega_j & \omega_j\end{bmatrix}\begin{bmatrix}a_0\\ a_1\end{bmatrix} = \begin{bmatrix}\zeta_i\\ \zeta_j\end{bmatrix}$

$$\begin{bmatrix}1/5.33 & 5.33\\ 1/17.33 & 17.33\end{bmatrix}\begin{bmatrix}a_0\\ a_1\end{bmatrix} = 2\begin{bmatrix}0.05\\ 0.05\end{bmatrix}$$

$$0.1876\, a_0 + 5.33\, a_1 = 0.1$$

$$0.0577\, a_0 + 17.33\, a_1 = 0.1$$

Solving above equation we get, $a_0 = 0.41$ and $a_1 = 0.0041$

Damping matrix: $c = a_0\underline{m} + a_1\underline{k}$ $\therefore c = 0.41\begin{bmatrix}0.2 & 0\\ 0 & 0.2\end{bmatrix} + 0.0041\begin{bmatrix}49.41 & -21.49\\ -21.49 & 16.34\end{bmatrix}$

$$c = \begin{bmatrix}0.082 & 0\\ 0 & 0.082\end{bmatrix} + \begin{bmatrix}0.20 & -0.088\\ -0.088 & 0.067\end{bmatrix}$$

$$c = \begin{bmatrix}0.282 & -0.09\\ -0.09 & 0.15\end{bmatrix}$$

A.6 Conversion of MDOF to Equivalent SDOF System

A.6.1 Calculation of Data

Linear Stiffness of frame: $k_{tt} = \begin{bmatrix} 58.41 & -29.21 \\ -29.21 & 29.21 \end{bmatrix}$

Nonlinear effective stiffness of frame: $\hat{k}_{tt} = \begin{bmatrix} 49.41 & -21.49 \\ -21.49 & 16.34 \end{bmatrix}$

We Know,

$$\begin{Bmatrix} \omega_1 \\ \omega_2 \end{Bmatrix} = \begin{Bmatrix} 7.47 \\ 19.55 \end{Bmatrix}$$

$$\begin{Bmatrix} \emptyset_{21} \\ \emptyset_{11} \end{Bmatrix} = \begin{Bmatrix} 1 \\ 0.62 \end{Bmatrix}$$

$$[m] = \begin{bmatrix} 0.2 & 0 \\ 0 & 0.2 \end{bmatrix}$$

$$k_{tt} = \begin{bmatrix} 58.41 & -29.21 \\ -29.21 & 29.21 \end{bmatrix}$$

We Know,

$$\begin{Bmatrix} \omega_1 \\ \omega_2 \end{Bmatrix} = \begin{Bmatrix} 5.33 \\ 17.33 \end{Bmatrix}$$

$$\begin{Bmatrix} \emptyset_{21} \\ \emptyset_{11} \end{Bmatrix} = \begin{Bmatrix} 1 \\ 0.49 \end{Bmatrix}$$

$$[m] = \begin{bmatrix} 0.2 & 0 \\ 0 & 0.2 \end{bmatrix}$$

$$\hat{k} = \begin{bmatrix} 49.41 & -21.49 \\ -21.49 & 16.34 \end{bmatrix}$$

$$c_{tt} = \begin{bmatrix} 0.324 & -0.108 \\ -0.108 & 0.216 \end{bmatrix}$$

$$c_{\theta\theta} = \begin{bmatrix} 0.282 & -0.09 \\ -0.09 & 0.15 \end{bmatrix}$$

A.6.2 Modal Properties

- Normalized Mass, $M_1 = \phi_1^T \underline{M} \phi_1$

In case of linear analysis, $M_{1l} = \{0.62 \quad 1\} \begin{bmatrix} 0.2 & 0 \\ 0 & 0.2 \end{bmatrix} \begin{Bmatrix} 0.62 \\ 1 \end{Bmatrix}$

$$M_{1l} = \{0.124 \quad 0.2\} \begin{Bmatrix} 0.62 \\ 1 \end{Bmatrix}$$

$$M_{1l} = 0.28\ kips - sec^2/in$$

In case of nonlinear analysis, $M_{1nl} = \{0.49 \quad 1\} \begin{bmatrix} 0.2 & 0 \\ 0 & 0.2 \end{bmatrix} \begin{Bmatrix} 0.49 \\ 1 \end{Bmatrix}$

$$M_{1nl} = \{0.098 \quad 0.2\} \begin{Bmatrix} 0.49 \\ 1 \end{Bmatrix}$$

$$M_{1nl} = \mathbf{0.25}\ kips - sec^2/in$$

- Normalized Stiffness, $K_1 = \phi_1^T \underline{k} \phi_1$

  In case of linear analysis, $K_{1l} = \{0.62 \quad 1\}\begin{bmatrix} 58.41 & -29.21 \\ -29.21 & 29.21 \end{bmatrix}\begin{Bmatrix} 0.62 \\ 1 \end{Bmatrix}$

$$K_{1l} = \{7.0 \quad 11.1\}\begin{Bmatrix} 0.62 \\ 1 \end{Bmatrix}$$

$$K_{1l} = 15.44\ kips/in$$

  In case of nonlinear analysis, $K_{1nl} = \{0.49 \quad 1\}\begin{bmatrix} 49.41 & -21.49 \\ -21.49 & 16.34 \end{bmatrix}\begin{Bmatrix} 0.49 \\ 1 \end{Bmatrix}$

$$K_{1nl} = \{2.721 \quad 5.81\}\begin{Bmatrix} 0.49 \\ 1 \end{Bmatrix}$$

$$K_{1nl} = \mathbf{7.14}\ kips/in$$

- Normalized Stiffness, $C_1 = \phi_1^T \underline{c} \phi_1$

  In case of linear analysis, $C_{1l} = \{0.62 \quad 1\}\begin{bmatrix} 0.324 & -0.108 \\ -0.108 & 0.216 \end{bmatrix}\begin{Bmatrix} 0.62 \\ 1 \end{Bmatrix}$

$$C_{1l} = \{0.093 \quad 0.149\}\begin{Bmatrix} 0.62 \\ 1 \end{Bmatrix}$$

$$C_{1l} = 2.455\ kips/ft$$

$$C_{1l} = 0.21\ kips - sec/in$$

  In case of nonlinear analysis, $C_{1nl} = \{0.49 \quad 1\}\begin{bmatrix} 0.282 & -0.09 \\ -0.09 & 0.15 \end{bmatrix}\begin{Bmatrix} 0.49 \\ 1 \end{Bmatrix}$

$$C_{1nl} = \{0.048 \quad 0.106\}\begin{Bmatrix} 0.49 \\ 1 \end{Bmatrix}$$

$$C_{1nl} = \mathbf{0.13}\ kips - sec/in$$

A.6.3 Equivalent SDOF

- Earthquake excitation factor, $L_n^h = \sum_1^2 m_j \emptyset_{jn} = \begin{bmatrix} 0.2 & 0 \\ 0 & 0.2 \end{bmatrix}\begin{Bmatrix} 0.49 \\ 1 \end{Bmatrix}$

$$L_1^h = (0.2 \times 0.49 + 0.2 \times 1)$$

$$L_1^h = 0.30$$

- Coefficient of Modal Expansion of the Influence Vector, $\Gamma_1 = {L_1^h}/{M_1}$

$$\Gamma_{1l} = {0.30}/{0.25} = 1.2$$

- Effective mass of equivalent SDOF system, $M_{1l}^* = \frac{(L_n^h)^2}{M_1} = \frac{(0.30)^2}{0.25} = 0.36$ kip$-sec^2/in$
- Equivalent height of SDOF system, $L_1^\theta = \sum_1^2 h_j m_j \emptyset_{jn}$

$$L_1^\theta = \sum_1^2 \{10 \quad 20\} \begin{bmatrix} 0.2 & 0 \\ 0 & 0.2 \end{bmatrix} \begin{Bmatrix} 0.49 \\ 1 \end{Bmatrix}$$

$$L_1^\theta = \sum_1^2 [2 \quad 4] \begin{Bmatrix} 0.49 \\ 1 \end{Bmatrix}$$

$$L_1^\theta = 4.98$$

- Effective height of the equivalent SDOF system, $h_1^* = \frac{L_1^\theta}{L_1^h} = \frac{4.98}{0.30} = 16.6\ ft$

$$h_1^* = \frac{L_1^\theta}{L_1^h} = 16.6\ ft$$

- Natural period, $\omega_1 = 5.33\ rad/sec$; $T_n = \frac{2\times\pi}{{\omega_1}^2} = \frac{6.28}{5.33^2} = 0.22\ sec$
- % of damping, $\zeta = 0.05$

We need to determine the response u(t) of this system to P(t) defined by the response spectrum of Dhaka City(Table A.1). The factored lateral force on the effective modal mass is,

Table A.1: Equations of natural time period vs. spectral acceleration

Serial No.	T_i	S_{a_i}	S_{d_i}
1	0	0.372	0
2	0.88	0.372	2.82
3	1	0.3415	3.35
4	1.1	0.3112	3.69
5	1.2	0.2874	4.05
6	1.3	0.2674	4.43
7	1.4	0.2478	4.76
8	1.5	0.2292	5.05
9	1.6	0.2138	5.36
10	1.7	0.2	5.66
11	1.8	0.1891	6.00
12	1.9	0.1786	6.32
13	2	0.1686	6.61
14	2.1	0.1592	6.88
15	2.2	0.1509	7.16
16	2.3	0.1438	7.45
17	2.4	0.1376	7.77
18	2.5	0.1321	8.09
19	2.6	0.12632	8.37
20	2.7	0.12176	8.70
21	2.8	0.11792	9.06
22	2.9	0.1141	9.40
23	3	0.1126	9.93

Spatial distribution for mode 1 is, $S_1 = \Gamma_1 m \phi_1$

$$S_1 = 1.2 \begin{bmatrix} 0.2 & 0 \\ 0 & 0.2 \end{bmatrix} \begin{Bmatrix} 0.49 \\ 1 \end{Bmatrix}$$

$$S_1 = 1.2 \begin{bmatrix} 0.1 \\ 0.2 \end{bmatrix}$$

$$S_1 = \begin{bmatrix} 0.12 \\ 0.24 \end{bmatrix}$$

Total shear force acting on the effective mass, $V_1 = \sum_1^2 S_{jn} = (0.12 + 0.24)$

$$V_1 = 0.36\ kips\ {sec^2}/{in}$$

Properties of Equivalent SDOF Frame:

- Mass: 0.36kip-${sec^2}/{in}$
- k_i =7.14 Kips/in
- C_i = 0.123 Kips/in

Figure A.15 Model of Equivalent SDOF System

A.7 Development of Seismic Lateral Load, Ductility and Base Shear

A.7.1 Calculation of Shear Force by Equivalent Static Force Method

The total design base shear is; $V = \frac{ZIC}{R} W$

Where,

Z = Seismic zone coefficient = 0.15 (Dhaka)

I = Structure important coefficient = 1.0

R = Response modification coefficient = 8

C = Numerical coefficient

A.7.2Numerical Coefficient

$$C = \frac{1.25\ S}{T^{2/3}}$$

Where,

Z = Site Coefficient = 1.5 (Soft to medium clay and sand)

T = Fundamental period of vibration in sec

The value of C need not exceed 2.75 and this value may be used for any structure without regard to soil type of structure period. The minimum value of the ratio of C/R is 0.075

A.7.3 Calculation of Fundamental Period

$T = C_t h_n^{3/4}$

Where,

C_t = 0.073

h_n = Height in meters above the base to level n

$T = 0.073 \times 4.89^{3/4}$

$T = 0.24\ sec$

A.7.4 Calculation of C

$C = \frac{1.25 \times 1.5}{0.24^{2/3}} = 4.88$

Maximum value of C is 2.75. In our case, for the time period of 0.24 sec, the value of C is 2.5. Thus we will consider C as 2.5

A7.5 Base shear within nonlinear limit

$V = 0.15 \times 1 \times 2.5 = 0.375\ W$

A7.6 Allowable Drift

According to BNBC, let us consider storey drift of equivalent SDOF sys as 0.02 h_x

$u_a = 0.02 \times (16.6 \times 12) = 3.98\ in$

The plastic rotation acceptable at the base of the column is $\theta_p = 0.02\ rad$

$u_m = u_a + h\theta_p = 3.98 + (16.6 \times 12) \times 0.02 = 7.96\ in$

A.7.7 Ductility of the equivalent SDOF Sys

$$\mu = \frac{u_m}{u_y} = \frac{7.96}{3.98} = 2$$

A.7.8 Determination of required yield strength

$$f_y = ku_y = 7.14 * 3.98 = 34.11\ ksi$$

A.7.9 Base shear within yield limit

$$V_y = \frac{V_e}{2} = \frac{0.375}{2} W = 0.1875W$$

$$V_y = \frac{0.375}{2} W = 0.1875 \times 0.36 \times 386 = 26.06\ kip$$

$$0.6\ V_y = 0.6 \times 0.1875 = 0.1125$$

Base shear at 1st yield point is, $0.6\ V_y = 0.6 \times 26.06 = 15.63\ kips$

A.7.10 Development of Pushover Backbone Curve

Proposed Loading system for two storey frame is as follows:

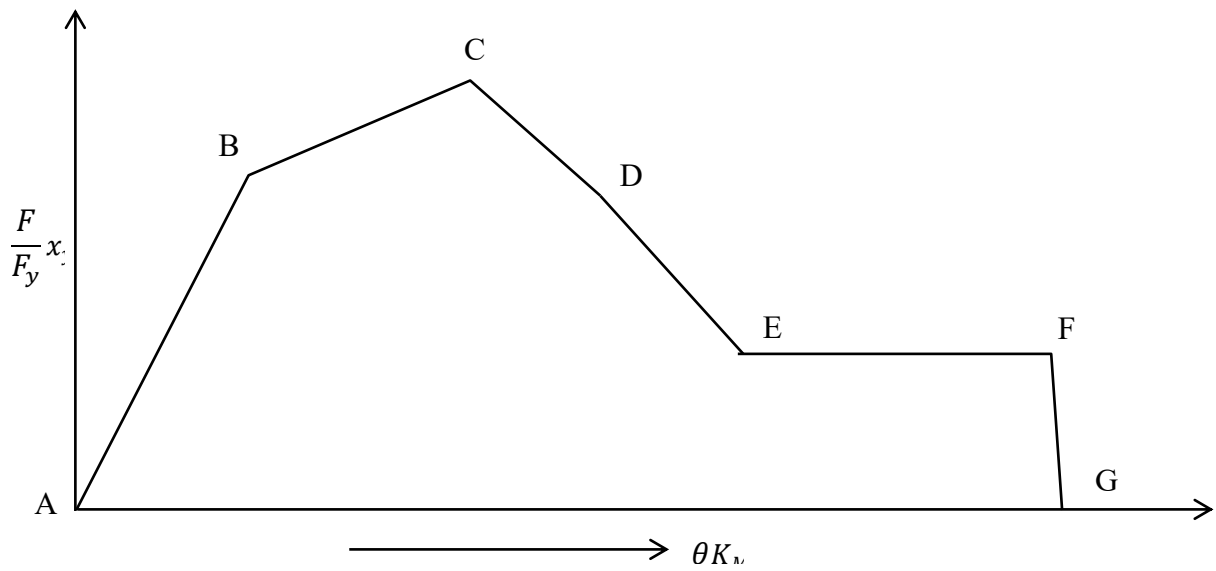

Figure A.16 Backbone curve for degrading

Table A.2: Force-Displacement Capacity Boundary Control Points for single-spring system

Prototype	Quantity	Point of the force deformation capacity boundary						
		A	B	C	D	E	F	G
Ductile Moment Frame	$\frac{F}{F_y}$	0	1	0.8	0.8	0.8	0.8	0
	θ	0	0.01	0.02	0.06	0.08	0.08	0.08

The initial stiffness is K_e. Once rotation is reached to 0.01 than the strain hardening will take place and stiffness will increase by 2 % positive slope i.e., $\alpha K_e = (1 + 0.02) = 1.02K_e$. Similarly when the rotation will be within 0.04 to 0.06 the stiffness will degrade at a rate of 13% as negative slope. Thus the degraded stiffness will be (1-0.13)K_e=0.87K_e.The stiffness will be zero when the rotation becomes 0.08 till it reaches to the point of collapse.

Table A.3: Monotonic loading table for pushover analysis

T_i	s_a	$\frac{F}{F_y}$	Modified s_a	Modified Load	Displacement	Allowable Displacement	Allowable θ_i	Modified Stiffness
0	0	1	0	0	0	u_y=16.6*12*0.01 =1.992	0.01	$K_e = 7.14$
0.1	0.02	1	0.02	2.782	0.01812			
0.2	0.04	1	0.04	5.564	0.10478			
0.3	0.06	1	0.06	8.346	0.31419			
0.4	0.08	1	0.08	11.128	0.67604			
0.5	0.10	1	0.10	13.91	1.19072			
0.6	0.12	1	0.12	16.692	1.8302			
0.7	0.14	1.05	0.147	20.448	2.5498	u_p=16.6*12*0.02 =3.984	0.02	$1.02K_e = 7.28$
0.8	0.16	1.05	0.168	23.369	3.3313			
0.9	0.18	1.05	0.189	26.291	4.1744			
1.0	0.2	0.8	0.16	22.257		u_m=16.6*12*0.08 =15.936	0.08	$0.87K_e = 6.21$
1.1	0.22	0.8	0.176	24.482				
1.2	0.24	0.8	0.192	26.708				
1.3	0.26	0.8	0.208	28.934				
1.4	0.28	0.8	0.224	31.159				
-	-	-	-	-	-	-	0.08	$0.87K_e = 6.21$
-	-	-	-	-	-	-	0.08	K=0.2

A.8 NEWMARK'S METHOD NONLINEAR ANALYSIS SYSTEMS

A.8.1 Time Step 1

Initial calculation

M=0.36 k=7.14 C=0.12, $f_y = 15.63$

$u_0 = 0$ $\dot{u}_0 = 0$ $p_0 = 0$ $p_1 = 2.782$

The restoring force-deformation relation is elasto-plastic with yield force and yield deformation as follows:

The analysis is done to determine the response $u\ (t)$ of the frame (starting from rest) to the monotonic loading as mentioned above using the constant average acceleration method with Δt sec and Newton-Raphson iteration.

1.1 State determination: $(f_s)_0\ and\ (k_T)_0$

1.2 $\ddot{u}_0 = \frac{p_0 - c\dot{u}_o - ku_0}{m} = 0$

1.3 Select $\Delta t = 0.1$

1.4 $a_1 = \frac{1}{\beta(\Delta t)^2} m + \frac{\gamma}{\beta(\Delta t)} c = \frac{4}{(0.1)^2} 0.36 + \frac{2}{(0.1)} 0.12 = 146.4$

$$a_2 = \frac{1}{\beta(\Delta t)} m + \left(\frac{\gamma}{\beta} - 1\right) c = \frac{4}{(0.1)} 0.36 + (2-1)0.12 = 14.52$$

$$a_3 = \left(\frac{1}{2\beta} - 1\right) m + (\Delta t)\left(\frac{\gamma}{2\beta} - 1\right) c = m = 0.36$$

A.8.2 Calculations for Each Time Instant, $i = 0$

a. Initialize, $j = 1;\ \ u^1{}_1 = u_0 = 0;\ \ (f_s)^1{}_1 = (f_s)_0 = 0$; and $(k_T)^1{}_1 = (k_T)_0 = k = 7.14$

b.$\hat{p}_1 = 2.782 + 146.4 \times 0 + 14.28 \times 0 + 0.36 \times 0 = 2.782\ kips$

A.8.3 ForEach Iteration, $j = 1$

a.$\hat{R}^j{}_{i+1} = \hat{p}_1 - (f_s)^1{}_1 - a_1 u^1{}_1 = 2.782 - 0 - 146.4 \times 0 = 2.782 > 0.001$

b. Check convergence; If the acceptance criteria are not met, implement steps 3.3 to 3.7; otherwise, skip these and go to step 4.0

c.$\left(\hat{k}_T\right)^1{}_1 = (k_T)^1{}_1 + a_1 = 7.14 + 146.4 = 153.54$

d.$(\Delta u)^1 = \hat{R}^1{}_1 \div \left(\hat{k}_T\right)^1{}_1 = 2.782 \div 153.54 = 0.01812$

e.$u^2{}_1 = u^1{}_1 + (\Delta u)^1 = 0 + 0.01812 = 0.01812$

f. State determination: $(f_s)^{j+1}{}_{i+1}$ and $(k_T)^{j+1}{}_{i+1}$

$$(f_s)^2{}_1 = (f_s)_0 + k(u^2{}_1 - u_0) = 0 + 7.14(0.01812 - 0) = 0.1294$$

$$(k_T)^2{}_1 = (k_T)_0 = k = 7.14$$

A.8.4 For Each Iteration, $j = 2$

a.$\hat{R}^2{}_1 = \hat{p}_1 - (f_s)^2{}_1 - a_1 u^2{}_1 = 2.782 - 0.12937 - 146.4 \times 0.01812$

$$= 8.4 \times 10^{-4} < 0.001$$

Therefore, the value of $u_1 = 0.01812$

A.8.5 Calculations for Velocity and Acceleration

a. $\dot{u}_1 = \frac{\gamma}{\beta(\Delta t)}(u_1 - u_0) + \left(1 - \frac{\gamma}{\beta}\right)\dot{u}_0 + (\Delta t)\left(1 - \frac{\gamma}{2\beta}\right)\ddot{u}_0$

$$\dot{u}_1 = \frac{2}{(0.1)}(0.01812 - 0) + \left(1 - \frac{\gamma}{\beta}\right) \times 0 + (\Delta t)\left(1 - \frac{\gamma}{2\beta}\right) \times 0$$

$$\dot{u}_1 = 0.3624$$

b. $\ddot{u}_1 = \frac{4}{(0.1)^2}(0.01812 - 0) - \frac{1}{\beta(\Delta t)} \times 0 - \left(\frac{1}{2\beta} - 1\right) \times 0$

$$\ddot{u}_1 = 7.248$$

A.8.2 Time Step 2

A.8.2.1 Initial Calculation

M=0.36 k=7.14 C=0.12

$u_1 = 0.01812$ $\dot{u}_1 = 0.3624$ $\ddot{u}_1 = 7.248$ $p_2 = 5.564$

1.5 State determination: $(f_s)_0$ *and* $(k_T)_0$

1.6 $\ddot{u}_0 = \frac{p_0 - c\dot{u}_o - ku_0}{m} = 0$

1.7 Select Δt

1.8 $a_1 = \frac{1}{\beta(\Delta t)^2}m + \frac{\gamma}{\beta(\Delta t)}c = \frac{4}{(0.1)^2}0.36 + \frac{2}{(0.1)}0.12 = 146.4$

$$a_2 = \frac{1}{\beta(\Delta t)}m + \left(\frac{\gamma}{\beta} - 1\right)c = \frac{4}{(0.1)}0.36 + (2 - 1)0.12 = 14.52$$

$$a_3 = \left(\frac{1}{2\beta} - 1\right)m + (\Delta t)\left(\frac{\gamma}{2\beta} - 1\right)c = m = 0.36$$

A.8.2.2 Calculations for Each Time Instant, $i = 1$

a. Initialize, $j = 1$; $u^1{}_2 = u_1 = 0.01812$; $(f_s)^1{}_2 = (f_s)_1 = 0.12937$ and $(k_T)^1{}_2 = (k_T)_1 = 7.14$

b. $\hat{p}_2 = p_2 + a_1u_1 + a_2\dot{u}_1 + a_3\ddot{u}_1$

$= 5.564 + 146.4 \times 0.01812 + 14.52 \times 0.3624 + 0.36 \times 7.248 = 19.088$

A.8.2.3 For Each Iteration, $j = 1$

a. $\hat{R}^1{}_2 = \hat{p}_2 - (f_s)^1{}_2 - a_1u^1{}_2 = 16.0881 - 0.12937 - 146.4 \times 0.01812$

$$=13.306 > 0.001$$

b. Check convergence; If the acceptance criteria are not met, implement steps 3.3 to 3.7; otherwise, skip these and go to step 4.0

c. $\left(\hat{k}_T\right)^1{}_2 = (k_T)^1{}_2 + a_1 = 7.14 + 146.4 = 153.54$

d. $(\Delta u)^1 = 13.306 \div 153.54 = 0.08666$

e. $u^2{}_2 = u^1{}_2 + (\Delta u)^1 = 0.01812 + 0.08666 = 0.10478$

f. State determination: $(f_s)^{j+1}{}_{i+1}$ and $(k_T)^{j+1}{}_{i+1}$

$$(f_s)^2{}_2 = (f_s)_1 + k(u^2{}_2 - u_1) = 0.12937 + 7.14(0.10478 - 0.01812) = 0.7481$$

$$(k_T)^2{}_2 = (k_T)_1 = k = 7.14$$

A.8.2.4 For Each Iteration, $j = 2$

a. $\hat{R}^2{}_2 = \hat{p}_2 - (f_s)^2{}_2 - a_1 u^2{}_2 = 16.0881 - 0.7481 - 146.4 \times 0.10478$

$$=2.08 \times 10^{-4} < 0.001$$

Therefore, $u_2 = 0.135$

A.4.3.2.5 Calculations for Velocity and Acceleration

$$\dot{u}_{i+1} = \frac{2}{(0.1)}(u_2 - u_1) + \left(1 - \frac{\gamma}{\beta}\right)\dot{u}_1 + (\Delta t)\left(1 - \frac{\gamma}{2\beta}\right)\ddot{u}_1$$

$$\dot{u}_2 = \frac{2}{(0.1)}(0.10478 - 0.011812) + (1 - 2)0.3624 + (\Delta t)(1 - 1)7.248$$

$$\dot{u}_2 = 1.3708$$

b. $\ddot{u}_2 = \frac{1}{\beta(0.1)^2}(u_2 - u_1) - \frac{1}{\beta(\Delta t)}\dot{u}_1 - \left(\frac{1}{2\beta} - 1\right)\ddot{u}_1$

$$\ddot{u}_2 = \frac{4}{(0.1)^2}(0.10478 - 0.011812) - \frac{4}{(0.1)}0.3624 - (2 - 1)7.248$$

$$\ddot{u}_2 = 12.92$$

The two storey building frame is applied with the lateral loaded monotonically increased with a time period of 0.1 second. The corresponding deflection, velocity, acceleration and shear forces are recorded. The nonlinear analysis of this building is carried out by the load given in the table 4.2. The calculation of first time step is given above. Summary of results is given below as Table 4.3.

Table A.4: Nonlinear displacement of two storey building by pushover analysis

t_i	P_i	$\hat{R}_i$	$(K_T)_i$	$(\hat{K}_T)_i$	$(\Delta u)^j{}_i$	u_i	$(f_s)_i$	$\dot{u}_i$	$\ddot{u}_i$
0.1	2.782	2.782	7.14	153.54	0.0181	0.0181	0.1294	0.3624	7.248
0.2	5.564	13.306	7.14	153.54	0.0866	0.135	0.7481	1.3708	12.92
0.3	8.346	32.153	7.14	153.54	0.2094	0.3142	2.243	2.8174	16.012
0.4	11.128	55.56	7.14	153.54	0.3618	0.676	4.8279	4.419	16.03
0.5	13.91	79.025	7.14	153.54	0.5147	1.1907	8.502	5.874	13.065
0.6	16.692	98.186	7.14	153.54	0.6395	1.8302	13.067	6.915	7.757
0.7	20.448	110.584	7.28	153.68	0.7196	2.5498	18.306	7.496	3.457
0.8	23.369	114.86	0	146.4	0.7845	3.331	18.757	8.1537	10.096
0.9	26.291	129.56	0	146.4	0.885	4.174	24.894	8.707	0.9704
1.0	29.212	131.093	0	146.4	0.8954	5.0273	31.104	8.353	-8.042
1.1	32.133	119.41	0	146.4	0.8157	5.8043	36.761	7.188	-15.253
1.2	35.054	97.167	0	146.4	0.6637	6.4366	41.364	5.458	-19.35

A.9 Development of Capacity Curve by Pushover Analysis

The lateral force acting on the roof of two storey building due to seismic load is V_{roof};

$$V_{roof} = M^* S_a\, g \tag{A.11}$$

Spectral acceleration in Mode 1, $$a_i = \frac{V_{roof}}{M^*} = S_a g \tag{A.12}$$

Spectral displacement in Mode 1, $$D_1 = \frac{u_i}{PF_1 \emptyset_{roof}} \tag{A.13}$$

Table A.5: Spectral acceleration and spectral displacement of capacity curve

Serial No.	Pushover Load S_a	V_{Roof}	$a_i = \frac{V_{roof}}{M^*}$	Nonlinear Displacement u_i	Spectral Displacement D_i
1	0	0	0	0	0
2	0.02	0.0072	0.02	0.01812	0.0151
3	0.04	0.0144	0.04	0.10478	0.087317
4	0.06	0.0216	0.06	0.31419	0.261825
5	0.08	0.0288	0.08	0.67604	0.563367
6	0.1	0.036	0.1	1.19072	0.992267
7	0.12	0.0432	0.12	1.8302	1.525167
8	0.14	0.0504	0.14	2.5498	2.124833
9	0.16	0.0576	0.16	3.3313	2.776083
10	0.18	0.0648	0.18	4.1744	3.478667
11	0.2	0.072	0.2	5.02732	4.189433
12	0.22	0.0792	0.22	5.80435	4.836958
13	0.24	0.0864	0.24	6.4366	5.363833

A.10 Development of Demand Curve from Design Response Spectrum of Dhaka City

A.10.1 Conversion of Dhaka Response Spectrum to ADRS

The response spectrum of Dhaka city of soft to medium clay and sand is taken from the BNBC 2006.

Table A.6: Natural period and spectral acceleration of Dhaka design response spectrum.

Ser. No.	Natural Time Period	Spectral Acceleration
1	0	0.372
2	0.88	0.372
3	1	0.3415
4	1.1	0.3112
5	1.2	0.2874
6	1.3	0.2674
7	1.4	0.2478
8	1.5	0.2292
9	1.6	0.2121
10	1.7	0.2
11	1.8	0.1891
12	1.9	0.1786
13	2	0.1686
14	2.1	0.1592
15	2.2	0.1509
16	2.3	0.1438
17	2.4	0.1376
18	2.5	0.1321
19	2.6	0.12632
20	2.7	0.12176
21	2.8	0.11792
22	2.9	0.1141
23	3	0.1126

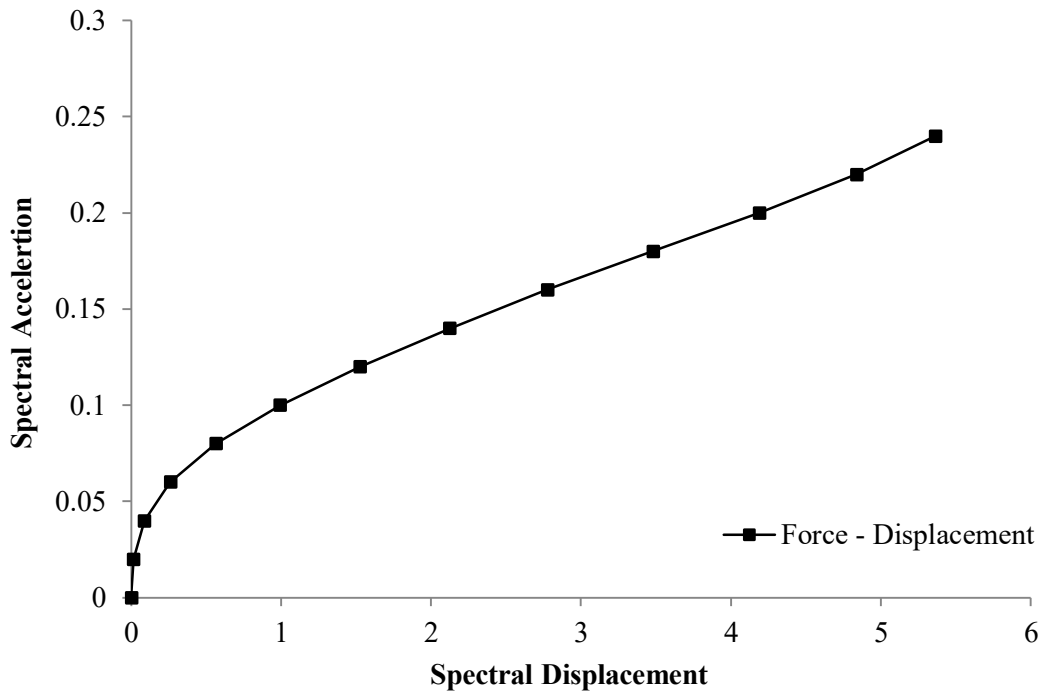

Figure A.18: Spectral acceleration vs. displacement (Capacity Curve) graph

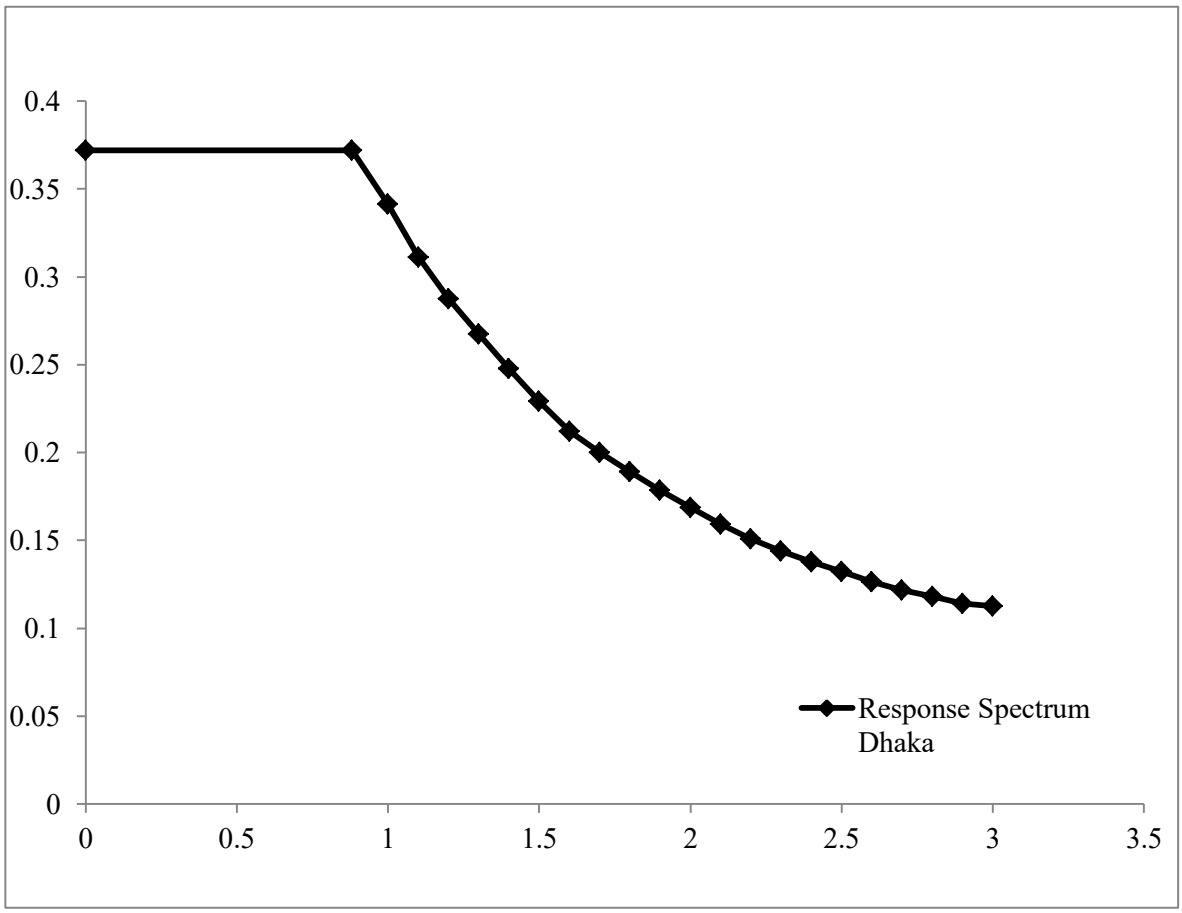

Figure A.19: Design response spectrum of Dhaka City

This response spectrum is converted to Acceleration Displacement Response Spectrum with equations given below:

$$S_{d_i} = \frac{{T_i}^2}{4 \times \pi^2} \times S_{a_i} g = \frac{{T_i}^2}{4 \times 3.14^2} \times S_{a_i} \times 386.4 = 9.798 S_{a_i} {T_i}^2$$

For any given time period and acceleration, the spectral displacement of Dhaka Response Spectrum was calculated. The conversion result is summarized in the table 11.

Table A.7: Spectral acceleration and displacement of two storey building for mode 1

Ser No.	Natural Time Period	Spectral Acceleration	Spectral Displacement
1	0	0.372	0
2	0.88	0.372	2.82
3	1	0.3415	3.35
4	1.1	0.3112	3.69
5	1.2	0.2874	4.05
6	1.3	0.2674	4.43
7	1.4	0.2478	4.76
8	1.5	0.2292	5.05
9	1.6	0.2121	5.36
10	1.7	0.2	5.66
11	1.8	0.1891	6.00
12	1.9	0.1786	6.32

Table A.8: Spectral acceleration and displacement of two storey building for mode 1 (continued)

Ser No.	Natural Time Period	Spectral Acceleration	Spectral Displacement
13	2	0.1686	6.61
14	2.1	0.1592	6.88
15	2.2	0.1509	7.16
16	2.3	0.1438	7.45
17	2.4	0.1376	7.77
18	2.5	0.1321	8.09
19	2.6	0.12632	8.37
20	2.7	0.12176	8.70
21	2.8	0.11792	9.06
22	2.9	0.1141	9.40
23	3	0.1126	9.93

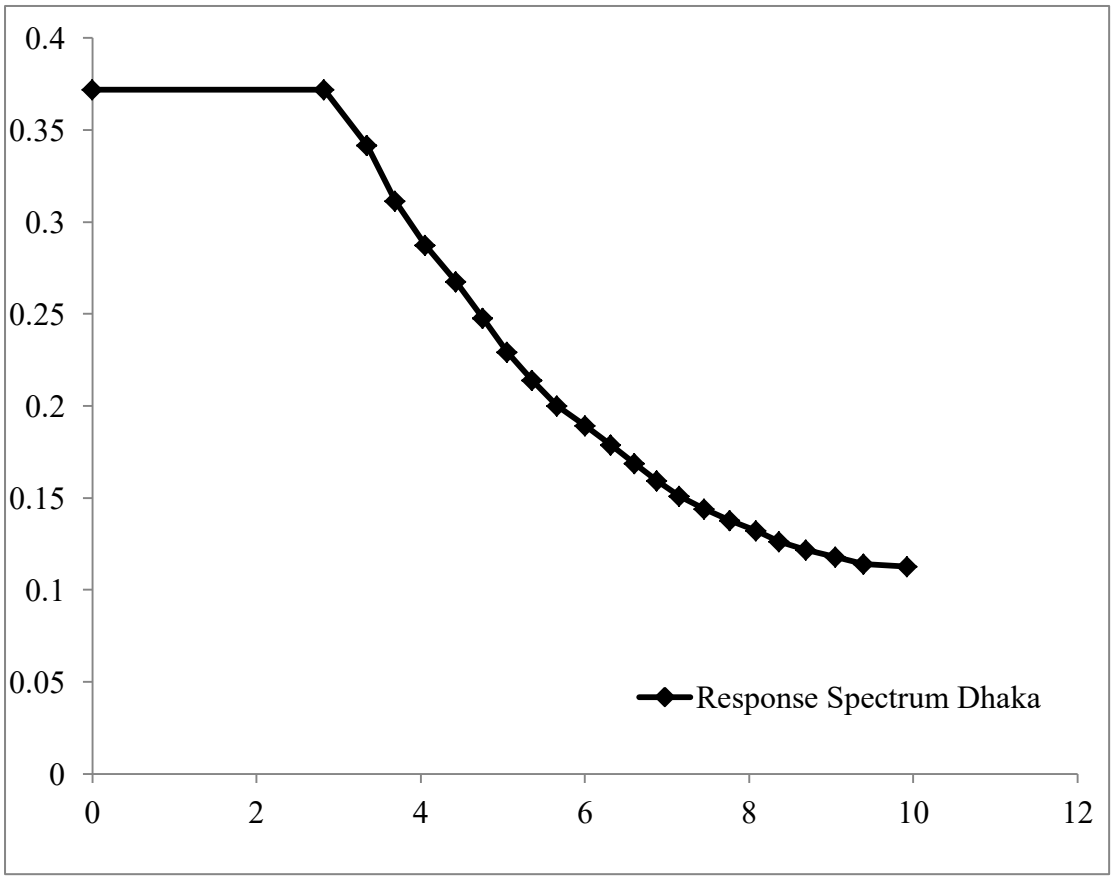

A.11 Determination of Performance Point

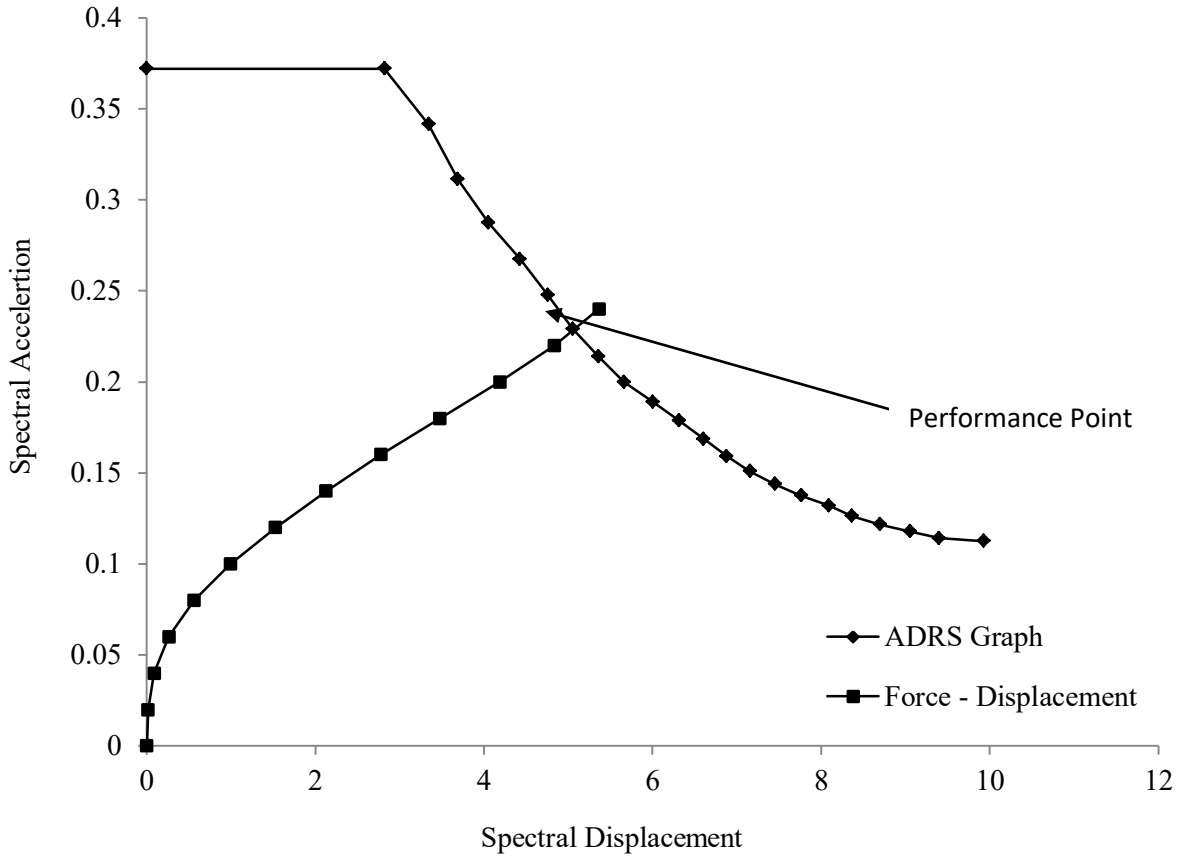

Figure 4.3 Demand curve of two storey building

A.12 Remarks

A two storey building has been designed by the conventional method nonlinearly. The backbone curve of RC frame building is used to modify monotonic incremental load as well as stiffness of the building with the progress of displacement. The capacity curve and demand curve are calculated for fundamental mode only. They are plotted together to determine the performance point. Thus, the two storey building under analysis will perform effectively till its spectral displacement of 4.6 inches for pushover analysis

APPENDIX B
MOMENT OF GROUND STOREY COLUMNS OF REFERENCE BUILDING

B.1 Moment of Ground Storey Column due to Bay Variation

Number of Bay	Moment at Base (KN.m)		
	Bare Frame	Bare Frame	Soft Storey Frame
	Linear (ESFM)	Nonlinear (POA)	Nonlinear (POA)
2	489.48	831.58	1261.43
4	546.98	871.97	1312.35
6	534.97	894.01	1343.06
8	540.06	893.5	1306.29
10	524.95	890.4	1296.95

B.2 Moment of Ground Storey Column due to Span Variation

Number of Storey	Moment at Base (KN.m)		
	Bare Frame	Bare Frame	Soft Storey
	Linear (ESFM)	Nonlinear (POA)	Nonlinear (POA)
2	526.48	735.54	1087.63
4	540.29	765.65	1128.91
6	534.97	812.60	1148.42
8	534.65	797.97	1206.41
10	517.58	796.78	1205.03

B.3 Moment of Ground Storey Column due to Percentage of Infill Variation

Percentage of Infill (%)	Moment of Ground Storey Column at Base (KN.m)		
	Bare Frame	Bare Frame	Soft Storey
	Linear (ESFM)	Nonlinear (POA)	Nonlinear (POA)
50	534.97	897.07	1072.62
60	534.97	897.07	1219.54
70	534.97	897.07	1343.06
80	534.97	897.07	1434.37
100	534.97	897.07	1490.78

APPENDIX C
SHEAR FORCE OF SOFT GROUND STOREY COLUMNS OF REFERENCE BUILDING

C.1 Shear Force of Ground Storey Column due to Bay Variation

Number of Bay	Shear Force (KN)		
	Bare Frame	Bare Frame	Soft Storey Frame
	Linear (ESFM)	Nonlinear (POA)	Nonlinear (POA)
2	152.57	217.38	404.5
4	170.79	228.73	415.98
6	165.51	234.82	422.92
8	166.68	233.37	408.71
10	162.96	231.81	403.94

C.2 Shear Force of Ground Storey Column due to Span Variation

Number of Span	Shear Force (KN)		
	Bare Frame	Bare Frame	Soft Storey
	Linear (ESFM)	Nonlinear (POA)	Nonlinear (POA)
2	159.5	188.33	338.27
4	166.64	199.22	355.86
6	165.51	214.66	371.86
8	165.59	210.74	386.90
10	161.51	210.26	386.09

C.3 Shear Force of Ground Storey Column due to Percentage of Infill Variation

Percentage of Infill (%)	Shear Force (KN)		
	Bare Frame	Bare Frame	Soft Storey
	Linear (ESFM)	Nonlinear (POA)	Nonlinear (POA)
50	165.51	235.62	333.91
60	165.51	235.62	382.06
70	165.51	235.62	422.92
80	165.51	235.62	456.62
100	165.51	235.62	502.16

APPENDIX D

MOMENT MAGNIFICATION FACTOR FOR SOFT STOREY COLUMN

D.1 Moment Magnification Factor for Bay Variation

Number of bays	Moment (KN.m)						MF (MF_{SSFP} / MF_{BFP})
	Bare Frame			Soft Story			
	Linear (BFL)	Nonlinear (BFP)	MF_{BFP} (BFP / BFL)	Linear (BFL)	Nonlinear (SSFP)	MF_{SSFP} (SSFP / BFL)	
2	489.48	831.58	1.70	489.48	1261.43	2.58	1.52
4	546.98	871.97	1.59	546.98	1312.35	2.40	1.51
6	534.97	894.01	1.67	534.97	1343.06	2.51	1.50
8	540.06	893.5	1.65	540.06	1306.29	2.42	1.46
10	524.95	890.4	1.70	524.95	1296.95	2.47	1.46

D.2 Moment Magnification Factor for Span Variation

Number of bays	Moment (KN.m)						MF (MF_{SSFP} / MF_{BFP})
	Bare Frame			Soft Story			
	Linear (BFL)	Nonlinear (BFP)	MF_{BFP} (BFP / BFL)	Linear (BFL)	Nonlinear (SSFP)	MF_{SSFP} (SSFP / BFL)	
2	526.48	735.54	1.40	526.48	1087.63	2.07	1.48
4	540.29	765.65	1.42	540.29	1128.91	2.09	1.47
6	534.97	894.01	1.67	534.97	1343.06	2.51	1.50
8	534.65	797.97	1.49	534.65	1206.41	2.26	1.51
10	517.58	796.78	1.54	517.58	1205.03	2.33	1.51

D.3 Moment Magnification Factor for Percentage of Infill Variation

Percentage of Infill (%)	Moment (KN.m)						MF (MF_{SSFP} / MF_{BFP})
	Bare Frame			Soft Story			
	Linear (BFL)	Nonlinear (BFP)	MF_{BFP} (BFP / BFL)	Linear (BFL)	Nonlinear (SSFP)	MF_{SSFP} (SSFP / BFL)	
50	534.97	897.07	1.68	534.97	1072.62	2.01	1.20
60	534.97	897.07	1.68	534.97	1219.54	2.28	1.36
70	534.97	897.07	1.68	534.97	1343.06	2.51	1.50
80	534.97	897.07	1.68	534.97	1434.37	2.68	1.60
100	534.97	897.07	1.68	534.97	1490.78	2.79	1.66

APPENDIX E

SHEAR FORCE MAGNIFICATION FACTOR FOR SOFT STOREY COLUMN

E.1 Shear Force Magnification Factor for Bay Variation

Number of bay	**Shear Force** (KN.m)						MF (MF_{SSFP} / MF_{BFP})
	Bare Frame			Soft Story			
	Linear (BFL)	Nonlinear (BFP)	MF_{BFP} (BFP / BFL)	Linear (BFL)	Nonlinear (SSFP)	MF_{SSFP} (SSFP / BFL)	
2	152.57	217.38	1.42	152.57	404.5	2.65	1.86
4	170.79	228.73	1.34	170.79	415.98	2.44	1.82
6	165.51	234.82	1.42	165.51	422.92	2.56	1.80
8	166.68	233.37	1.40	166.68	408.71	2.45	1.75
10	162.96	231.81	1.42	162.96	403.94	2.48	1.74

E.2 Shear Force Magnification Factor for Span Variation

Number of span	**Shear Force** (KN.m)						MF (MF_{SSFP} / MF_{BFP})
	Bare Frame			Soft Story			
	Linear (BFL)	Nonlinear (BFP)	MF_{BFP} (BFP / BFL)	Linear (BFL)	Nonlinear (SSFP)	MF_{SSFP} (SSFP / BFL)	
2	159.5	188.33	1.18	159.5	338.27	2.12	1.80
4	166.64	199.22	1.20	166.64	355.86	2.14	1.79
6	165.51	234.82	1.42	165.51	422.92	2.56	1.80
8	165.59	210.74	1.27	165.59	386.90	2.34	1.84
10	161.51	210.26	1.30	161.51	386.09	2.39	1.84

E.3 Shear Force Magnification Factor for Percentage of Infill Variation

Percentage of infill	**Shear Force** (KN.m)						MF (MF_{SSFP} / MF_{BFP})
	Bare Frame			Soft Story			
	Linear (BFL)	Nonlinear (BFP)	MF_{BFP} (BFP / BFL)	Linear (BFL)	Nonlinear (SSFP)	MF_{SSFP} (SSFP / BFL)	
50	165.51	235.62	1.42	165.51	333.91	2.02	1.42
60	165.51	235.62	1.42	165.51	382.06	2.31	1.62
70	165.51	235.62	1.42	165.51	422.92	2.56	1.79
80	165.51	235.62	1.42	165.51	456.62	2.76	1.94
100	165.51	235.62	1.42	165.51	502.16	3.03	2.13